Università degli Studi di Cagliari

PhD THESIS IN EARTH SCIENCE

XXIV Cycle

QUANTITATIVE STATUS, VULNERABILITY AND POLLUTION OF GROUNDWATER RESOURCES IN DIFFERENT ENVIRONMENTAL AND CLIMATIC CONTEXTS IN SARDINIA AND IN ETHIOPIA

GEO/05

Presented by: *Abdelwassie Hussien Bushra*

Dotoral Program Coordinator: *Prof. Rosa Cidu*

Tutor: *Prof. Giulio Barbieri*

Academic Year 2010 - 2011

ACKNOWLEDGEMENTS

I would like to express my sincere gratitude to the Government of Italy, through; the Ministry of Foreign Affairs' Cooperation Office for Developing Countries, for sponsoring me the pportunity to study my PhD in Cagliari. I am also grateful to my University , Mekele University, for granting me leave of absence to pursue further studies.

Above all, I would like to express my heartfelt gratitude and appreciation to my promoter, Professor Eng. Giulio Barbieri; without his scientific advice and guidance, constructive suggestions and all way round support; it would have been impossible to start and complete this thesis. So, thank you very much professor for everything you did to bring me to this level.

I am grateful to the Department of Earth Sciences of the University of Cagliari for allowing me all facilities to carry out my field work and use the hydrochemical laboratory. In this regard my special thanks go to Professor Rosa Cidu, Doctor Francesca Podda and Signor Conti for guiding me and carrying out the laboratory analysis. Similarly, I thank very much the staff at the Department of Territorial Engineering of the University of Cagliari for their collaboration and encouragement to this end.

I am thankful to Professor Eng. Antonio Vernier for his constructive comments and suggestions.

This research work would have not been successful without field data collection both in Sardinia and in Ethiopia. Therefore, I would like to thank Signor Mario Sitzia for his unlimited support both in the field and in the office and Haileslassie K. who accompanied me in my repeated field works in Ethiopia.

I am most thankful to all staff members of my department, Department of Earth Sciences of Mekele University, and my special thanks go to Dr. Tesfamicheal G., Dr. Solomon G., Dr. Kassa A. who continuously provided me important suggestion and encouragement.

I gratefully acknowledge all offices who have given me data for my study. My special thanks to Ethiopian Water Works Design and Supervision Enterprise, Tekeze Deep Water Wells Drilling Plc, Tigray Water Works Construction Enterprise, National Meteorological Agency and its Regional office in Mekele.

I am most thankful to Muuz Amare, Mohammedsultan Abdella, Kahsay, Yemane (enterprise), Daniel Hagos, Assefa Merssie, Afewerki Hailu, drilling crew member of Tekeze Deep Water Wells Drilling Plc, Sileshi Mamo and Ermias Hagos, who helped me a lot in the primary and secondary data collection during my fieldworks.

I would like to express my special gratitude to my friend Samuel Yehdego for the continuous back-up and for taking care after my family to this far.

I am thankful to my friends and colleagues: Paolo Cambuli, Marco Mura, Hajar Belghazal, Luigi, Tonio and Monica Casu for their unlimited support regarding both professional and accomdation matters through out my stay in Cagliari.

I cannot end without acknowledging the support and constructive suggestions I received from my colleagues Asmelash A. and Tesfaye A. I appreciate my stay with you and thanks for all what you have done.

Especially, I would like to give my special thanks to my wife Zebiba and my daughters Ekram, Sebah, Huda and Fewzia whose patient love enabled me to complete this work.

Finally, my deep gratitude and appreciation goes to my family members, specially to my beloved mother Saedia, Mohammedbrhan and his family, Znabu, Beyan M., Mustefa A. , Tuum K., Adem B. and Jemila S. for their unwavering support and love throughout my life.

For everything, the precious honour goes to Almighty ALLAH, Alhamdulillah.

This work is dedicated to my late father Hussien Bushra

ABSTRACT

The Raya Valley is located in the northern part of Ethiopia within the Regional State of Tigray. The valley is part of the series of grabens at the western margins of the Afar Depression. Rainfall in this area is erratic both in time and space; hence it has suffered from a number of severe droughts and associated famines, and is chronically food-insecure. The surface water resources are characterized by streams, which flow strongly during the short rainy season and no perennial flow of surface water there is during the dry period, except the minor seepages that die out within a short distance in the valley. Therefore, groundwater is the only source for both domestic and irrigational development. Previous studies were confined to developing these resources. Hence, the objective of this research, in the Raya Valley, is to understand and to characterize the groundwater system of Raya Valley, using hydrogeology, groundwater chemistry and isotope hydrology tools and to come up with different options that may help to monitor for efficient management of the groundwater. In the meantime, this work incorporated water balance evaluation and identification of the degree of vulnerability to contaminants of the Rio Mannu di Pabillonis Basin in the central part of Sardinia, Italy. Finally corresponding results were compared in relation to their climatic differences.

Field traverses have been undertaken to collect relevant information regarding geology, hydrology, and hydrogeology in the Raya Valley (in 2009, 2010 and 2011) and in the Rio Mannu di Pabillonis Basin (in 2010 and 2011). An inventory of groundwater levels of boreholes and springs was made. Land-use was also investigated during field visits to be used as ground truth for the verification of existing maps.

The isopiezometric/static water level contour maps show that the groundwater flow toward the centre and then all flow to the south in a similar fashion to the surface water, in the Raya Valley. In the Rio Mannu Basin, the groundwater flow direction is also to the centre of the basin and finally toward the north, following the topographic gradient.

Water samples, from Raya Valley and Rio Mannu Basin, were collected and analyzed and results were compared with Ethiopian and Italian drinking water standards, respectively. For most of the chemical constituents, water samples are within the safety standards with regard to the Raya Valley, whereas some elevated NO_3^- *values have been noticed in areas where the dominant activity is animal farming in Rio Mannu basin. In situ water temperature and electric conductivity measurements in the Raya Valley have shown distinct zonation along west to east, with the highest values recorded in the east. In the meantime,* $Ca\text{-}HCO_3$ *water type dominates the western boreholes and springs, while* $Na\text{-}Cl\text{-}SO_4$ *water type dominates the eastern boreholes and springs. The dominant water type is Na-Cl in Rio Mannu Basin.*

Rain water samples of two consecutive rainy seasons (2009 and 2010) from different elevations were analyzed for stable isotope (oxygen and hydrogen). The results were used to construct a Local Meteoric Water Line (LMWL) of the area. Additional 17 borehole and 3 spring samples were collected and analyzed for the same isotopes in the same laboratory. Correlation between $\delta^{18}O$ *and* $\delta^{2}H$ *(LMWL) is* $\delta^{2}H = 7.4756\ \delta^{18}O + 11.827$, $(r^2 = 0.9959)$ *and hence the later data were plotted alongside the meteoric water to define the possible sources of the groundwater recharge in the area of interest. Most of the borehole and spring samples plotted nearly along the local meteoric water line. But, the eastern boreholes and the hot spring, in the east, plotted away from the LMWL in the direction of higher water-rock interaction, with regression equation* $\delta^{18}O$ *and* $\delta^{2}H$ *(LMWL)* $\delta^{2}H = 6.7244\ \delta^{18}O - 0.0795$, $(r^2 = 0.998)$. *This indicates the existence of another source of water recharge to the Raya Valley.*

The Thornthwaite and WetSpass models were applied to simulate the hydrological water balance of both areas. In the Thornthwaite method the water balance was made using average, less than and greater than average precipitations in order to observe which of the water balance components are more affected positively or negatively. Thus the results signify that Cumulative Available Water is more sensitive to variation in precipitation and follows the same direction of precipitation, while Actual Evapotranspiration follows the reverse way, i.e. it decreases when precipitation increases and vice-versa. Thus, 86.5% of the average precipitation is lost as evapotranspiration, 4.3% becomes surface runoff~~,~~ and 9.2% is groundwater recharge in the Raya Valley. Meanwhile, it is 73.5% for evapotranspiration, 11.8% for surface runoff, and 14.7% for groundwater recharge in the Rio Mannu Basin.

Seasonal and annual evapotranspiration, surface runoff, and groundwater recharge are the main outputs of the WetSpass model. Accordingly, 81.1% of the precipitation in the basin is lost through evapotranspiration, 5.9% becomes surface runoff~~,~~ and 12.9% is groundwater recharge in the Raya Valley. And 54.4% of the precipitation in the basin is lost through evapotranspiration, 6.8% becomes surface runoff~~,~~ and 39.8% is groundwater recharge in the Rio Mannu Basin.

The intrinsic vulnerability map of the Raya Valley was prepared using SINTACS program with the help of ArcGIS. After running the model, the areas inherently vulnerable where rated as very low to high based on the results of the model. The alluvial deposit, including the Gerjalle swampy area, was rated as high vulnerable, demonstrating the higher risk in the main target area of the valley.

The Raya Valley is a graben running parallel to the western escarpment of the Afar Depression, in a north-south direction. Description of the local geology and cross-sections along different orientations elucidate that the valley floor is mainly composed of basin fill deposits underlain by moderately to highly fractured basalt. The thickness of the alluvial deposit is variable and ranges from about 18 to more than 311 meters. The minimum thickness is in the western and eastern flanks of the valley, whereas the maximum thickness is obtained towards the eastern part of the valley center. No significant impermeable layer that can act as a confining bed is observed. The gradient of the alluvial sediment is low (0.006 in a total length of over 60 kilometers along the flow direction) and the alluvial aquifer is inter-granular containing gravel, sand and with some intercalation of silt and clay. The groundwater recharge, as explained above, has two sources, precipitation and groundwater inflow. Therefore, the surface water divide does not coincide with the groundwater divide.

The hydraulic conductivity is variable both in lithology and space, thus it varies between 0.03-0.37 m/day in the volcanic rocks, and 0.11-26 m/day with mean value of 2.8 m/day~~,~~ in the alluvial sediments. Evidences from boreholes pierced in the volcanic rocks, beneath the alluvial sediments, show significant quantities of water. Therefore, an attempt to mathematically model the area should verify the groundwater inflow and consider the weathered and fractured part of the volcanic rocks as a second aquifer.

Key words: Recharge, Groundwater Temperature, Stable Isotopes, Vulnerability to pollution

TABLE OF CONTENTS

LIST OF FIGURES

LIST OF TABLES

LIST OF ABBREVIATIONS AND SYMBOLS

AAU	Addis Ababa University
Bare_area	Bare Area
Barecoef	Bare soil runoff coefficient
CSA	Central Statistical Agency
DEM	Digital Elevation Model
EC	Electrical Conductivity
EM-DAT	International Emergency Disaster Data base
EU	European Union
Evapodepth	Bare soil evaporation depth
FAO	Food and Agricultural Organization of the United Nations
Fieldcapa	Field capacity
FEWS-NET	Famine Early Warning Systems Network
GIS	Geographic Information Systems
GDP	Gross Domestic Product
GPS	Global Positioning System
ha	Hectare
IAEA	International Atomic Energy Agency
Imp_area	Impervious Area
Implusero	Impervious land-use runoff
Imrocoef	Runoff coefficient for impervious land-use type
IMWI	International Water Management Institute
Interc_per	Interception Percentage
ITCZ	Inter Tropical Convergence Zone
KAADP	Kobo Alamata Agricultural Development Project
Lai	Leaf Area Index
Landusenum	Number of runoff class for land-use
Landusero	Runoff class for land-use
Luse_type	Land Use Type
Min_stom	Minimum Stomatal Opening
MoWR	Ministry of Water Resources
Num_imp_Ro	Impervious Runoff class for impervious area types
Num_imp_ro	Impervious land-use runoff class
Num_veg_Ro	Runoff class for vegetation type
Openw_area	Open-water Area
P_frac_sum	Fraction of summer Precipitation contributing to Hortonian runoff
P_frac_win	Fraction of winter Precipitation contributing to Hortonian runoff
PAW	Plant available water content
PET	Potential Evapotranspiration
PPT	Precipitation
Residualwc	Residual water content
REST	Relief Society of Tigray
RMS	Root Mean square error
Root_depth	Root depth

Runoff_veg	Runoff Vegetation
Runoffcoef	Runoff coefficient
RVPIP	Raya Valley Pressurized Irrigation Project
SISS	Studio dell'Idrologia Superficiale della Sardegna
slope_[%]	Slope in percent
Slope_bare	Slope class of bare soil
Slope_imp	Slope class of impervious land-use type
Slopenum	Slope class
Soil_bare	Soil type (bare)
Soilnum	Soil class
TDS	Total Dissolved Solids
UNDP	United Nations Development Program
Tensionhht	Tension saturated height
Unique_num	Unique Number
Uniquebare	Unique Number
URS	United Registrar of System LTD
USDA	United States Department of Agriculture
USGS	United States Geological Survey
Veg_area	Vegetated Area
Veg_height	Vegetation Height
VSMOW	Vienna Standard Mean Oceanic Water
WGS84	World Geodetic System 1984
WHO	World Health Organization
Wiltingpnt	Wilting Point
WWDSE	Water Works Design and Supervision Enterprise
WetSpass	Water and Energy Transfer between Soil, Plants and Atmosphere under quasi-Steady Sate

PART ONE

RAYA VALLEY BASIN

1. CHAPTER I: GENERALITIES

1.1. INTRODUCTION

The availability of freshwater is one of the greatest issues facing mankind nowadays, because problems associated with water has been and are affecting the lives of many millions of people. Water scarcity is a critical issue because 1.1 billion of the world's 6 billion people lack access to safe drinking water [World Health Organization, 2003]. The rapid growth of population together with the steady increase in water requirements for agricultural and industrial development has imposed severe stress on the available water resources.

According to (R. Scanlon,Ian Jolly, Marios Sophocleous and Lu Zhang, 2007), water requirements for food production will increase to meet demands of the projected 50% increase in global population from _6 billion in 2000 to _9 billion in 2050. Meeting the United Nations Millennium Development Goal of reducing the proportion of people that suffer from hunger by 50% by 2015 is putting additional stress on limited water resources. Therefore, freshwater resources in terms of both the quantity and quality, requires consistent and careful assessment and management for its sustainable development.

Ethiopia is one of the economically fast growing countries with an estimated population of 74 million and annual growth rate of 2.6 % (Central Statistical Agency, 2008). Similar statistical data of the country depicts that more than 80% of its people depend on subsistence farming. . However, the agriculture is heavily dependent on rainfalls as the productivity and the production are strongly influenced by climatic and hydrological variability that often give rise to dry spells, droughts and floods. Droughts and floods are endemic, with significant events every 3 - 5 years, with increasing frequency compared to two or three decades ago. Droughts destroy watersheds, farmlands, and pastures, contributing to land degradation and causing crops to fail and livestock to perish (B. Awulachew S.; D. Yilma A.; M. Loulseged; Loiskandl W. Ayana M.; T. Alamirew, 2007).

To meet the food needs of its rapidly growing population, the country needs to double the production of cereals by 2025 (IWMI, 2007). Agriculture is the largest sector of the economy giving rise to about 50% of the country's GDP (Gross Domestic Product) and employing over 85% of the population.

On the other hand, Ethiopia has abundant water resources, with an estimated mean annual runoff of about 111 billion m^3 from its 12 major river basins (Figure1.1) and 2.6 billion m^3 groundwater potential ((MoWR, ETHIOPIAN WATER SECTOR STRATEGY, 2001), and (UNESCO, 2004)). The most important groundwater resources are confined in fractured and weathered volcanic trap series inter-bedded with paleosoils, river gravels in the highlands and in fractured volcanic formations covered with thick quaternary sediments in the rift. The rift and the intermountain valley fills have the best aquifers as a result of faulting and the occurrence of relatively permeable unconsolidated sediments (Ayenew T., 2008) which are regularly recharged by seasonal runoffs from the highlands and local rainfalls. Despite this large water resource, Ethiopia continues to receive food aid to about 10% of the population who are at risk annually.

Figure1.1 Major River Basins of Ethiopia

The challenge that Ethiopia faces in terms of food insecurity is associated with both inadequate food production for the ever population growing and natural events due to erratic rainfalls. Therefore, Ethiopia has to combine enhancing water availability for the more use of irrigation that can lead to better security in terms of getting a reliable harvest as well as intensification of cropping (producing more than one crop per year) (Awulachew S. B.; Merrey D. J.; Kamara A. B.; Van Koppen B.; Penning de Vries, F.; Boelee, E.; Makombe, G., 2005).

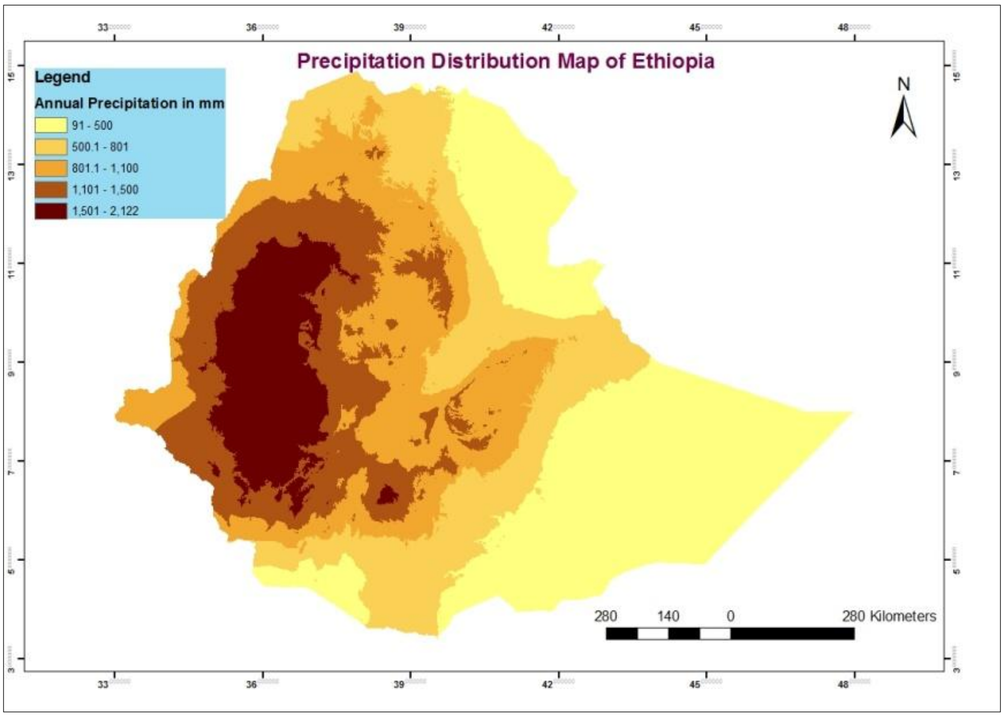

Figure 1.2 Rainfall Distribution of Ethiopia

Water resources and rainfalls are not evenly distributed in Ethiopia, both spatially (Figure 1.2) and temporally. The surface water resources come mainly from the highlands, while the major arable land is situated in the lowlands. Small scale irrigation is considered as one of the mechanisms to enhance the food productivity by harvesting at least twice a year. However, the availability of the surface water is not evenly distributed and the communities are urged to dig hand dug wells as supplementary water source at the end of the rainy season in order to get more food production where the well yield is adequate.

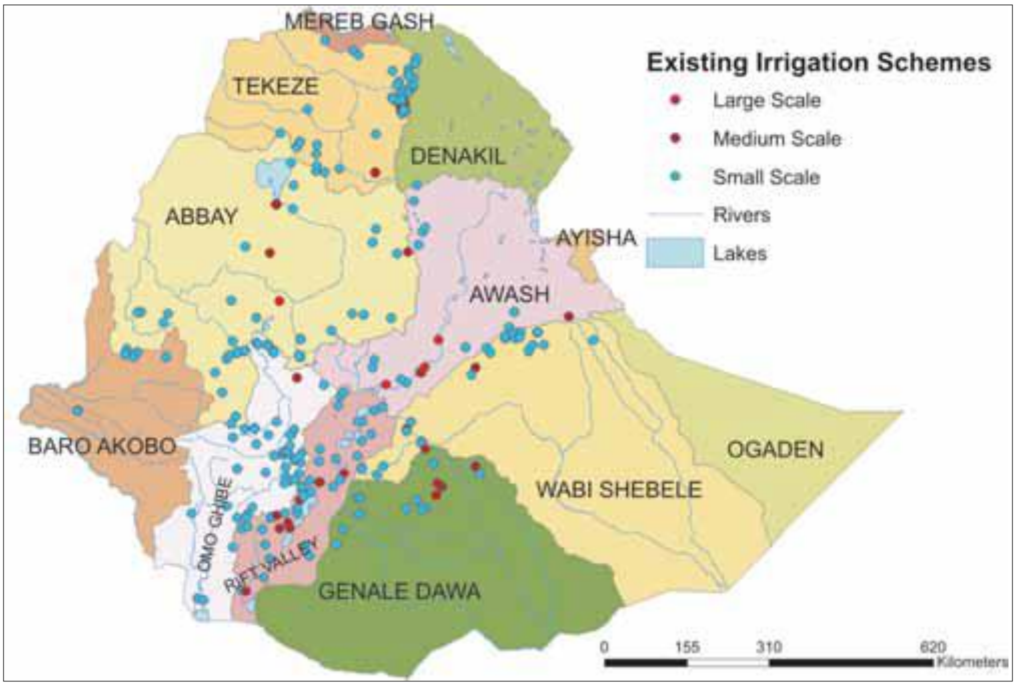

Figure 1.3 Distribution of Existing Irrigation Schemes, After IMWI,2007

The total irrigated area till 1991 was 176,015 hectares; this Figure had increased to 197,250 ha in 1998. According to data recently compiled by (MoWR, Irrigation (Potential) in Ethiopia, 2005) from different master plan studies and regions the area under irrigation in the country has increased to about 250,613 ha. This is due to the rapidly increasing irrigational areas under traditional irrigation (Figure 1.3).

Some estimations have shown that there is sufficient water in Ethiopia to develop about 3.73 million hectares of land under full irrigation (MoWRD, 2006). However, the irrigated agriculture has realized only 4.3% of its estimated potential and in terms of output it accounts for approximately 3% of the total food crop production (MoFED, 2006).

The Tigray Region, and in particular its southern zone, has suffered by a certain number of severe droughts and associated famines, so that is chronically food-insecure. It was the area of international attention in 1984, where thousand persons died due to drought and famine. Since then a number of drought periods has occurred but with less casualties. Below-averaged Belg rains (February-May) coupled with delayed and sporadic Kiremt/Summer rains (the main rainy season of June- September) have led to widespread food insecurity in the area. This lack of sufficient rainfalls during the Belg season failed to replenish the aquifers. In addition, the poor performance of the Kremt rainfalls has affected agricultural areas, particularly the lowlands and midlands of the Southern Zone. USAID's Famine Early Warning Systems Network (FEWS-NET) has estimated that the overall crop production in 1999-2000, 2002-2003 and 2008-2009 has been between 8-10% below average.

1.2. PREVIOUS WORKS and BACKGROUND

The intention of studying the Raya Valley for groundwater surveys dates back to the early 1970's. Since then some different appropriate water developmental studies have been carried out. Some of the previous works conducted were:

The study performed by Hunting Technical Services Ltd (M. Macdonald, and Partners, 1974-75), which covered 15,000 square kilometers of Tigray extending some 50 Km on each side of Addis Ababa – Adigrat road. The objective was an exploratory reconnaissance work to identify and describe the landforms and the soil resources of the studied area and to provide essential information on the land suitability for a rational planning of the agriculture in the region. This study provided also valuable highlights of the climatic and hydrologic characteristics of Mekele and its surroundings. It has covered parts of both the Tekeze and Danakil basin. The project time extent was only one year and within this limited time Hunting gauged the runoff of different streams and carried out solar radiation measurements around Mekele.

The study by the (German Agency for Technical Cooperation LTD., 1977), under the Kobo-Alamata Agricultural Development Program (KAADP), enclosed the area between Kobo and Alamata towns covering part of the Alamata sub basin. They prepared the geological and hydrogeological contour maps, the geo-electrical and seismic cross-sections and the lithological sections based on bore holes results which are posted on the http://eusoils.jrc.ec.europa.eu/esdb_archive/eudasm/africa/lists/k5_cet.htm web site. Some of their conclusions are:

- The groundwater table has a general east ward inclination and the average gradient is 0.01
- The depth of the groundwater table depends on the local morphology but it is shallower in the east

- The recharge is due to the stream flow and rainfall infiltration, the outflow is represented by evapotranspiration and overland flow
- The flattening of ground water level in the eastern part of the valley indicates wide-spread ground water losses by evapotranspiration in this part of the valley.

The other intensive and integrated study of the valley was started in 1996 by Relief Society of Tigray (REST) and the Tigray Regional Government. The overall goal of the study was to identify and to determine all potential means to enhance agricultural production in the area by means of an integrated and planned Valley development, thereby to sustain the well being of the people in the area and the region in general. The study has concluded that the groundwater, as the primary source of water supply for the community, may irrigate about 18,000 hectares of land in the Region. Very important and considerable geological and hydrogeological studies, supported by geophysical works, were carried out in the valley and these studies indicate that the valley has a good groundwater potential (Raya Valley Development Study Project , 1997).

This was followed by a feasibility study work of Raya Valley Agricultural Development Project (Raya Valley Agricultural Development Project , 1998). This study had come up with a feasibility report.

The feasibility report of the RVADP of 1998 was evaluated and verified by (Isaak Gervshanovich, 2000). He supposed the existence of large size fault of regional extent in the eastern part of the valley accompanied by ramified fracture systems that can be one possible groundwater regional drain of tectonic origin and potential zone for future development. As proposed in this report, the deep position of the aquifers in the fractured rocks will be compensated by significant discharge of wells. He estimated the exploitable groundwater potential of Raya Valley to be 130 Mm^3/year rather than 162 Mm^3/year (estimate of RVADP, 1998). His conceptual model for the Raya Valley was a fan-like field where water bearing layers extend to a large distance under the plain sinking deeper and deeper towards the central and eastern parts of the valley.

(Dessie Nedaw, 2003), has estimated the total amount of groundwater to be 129.3 MCM per year (similar to Isaak Gervhanovich). The majority of the boreholes drilled in the area were considered to be in moderate productivity (50-500 m^2/day). Groundwater flow in the valley converges to the centre. Unlike the most natural waters from the main Ethiopian rift system, the natural waters in Raya Valley are low in SAR value that makes them to be favorable for irrigation. The research has recommended a detailed investigation involving groundwater monitoring to identify the existence of groundwater outflow from the basin and to perform a complete three dimensional model to characterize the aquifer for better management.

Since 2007, the Raya Valley Pressurized Irrigation Project (RVPIP) study is under way by the Water Works Design and Supervision Enterprise (WWDSE). The draft final feasibility study report concluded that the drilled boreholes are insufficient to fully develop the Raya Valley by pressurized irrigation system. The report recommended to increase the number of wells to 610 whiles the average yield of each borehole to be 67l/s.

Geophysical resistivity surveys and recent drilling activities indicate that the thickness of the unconsolidated material (basin fill deposits) increased from west to east and attains its maximum (>250 m) in the central and eastern parts of the valley. The depth of water table varies according to the geological and morphological conditions. The ground water depth varies from less than one to 30 meters in the southern part of the valley (Alamata sub basin) and from 20 to 60 meters in the northern part of the basin (Mehoni sub basin).

However, most of the previous studies have been concerned more with resource development to meet users' need and alleviate the recurrent drought problem with low attention to the groundwater resource management. Besides, there is poor groundwater management and no valley based well monitoring system established. Such gaps can be seen even during the current field visit: the boreholes are not monitored and no surface water gauging stations over the area occur. On the other hand, safe groundwater abstraction and proper groundwater management is crucial for sustainability of the resource. At this time the demand of water for irrigation is increasing without developed controlling mechanism on its pumping rate. This uncontrolled pumping of wells will surely result in the depletion of the groundwater and well yield deterioration which in turn cause a total collapse of the groundwater irrigation projection before their design life.

The Ethiopian government formulated a water policy and sector strategy with the goal to enhance and promote all national efforts towards the efficient, equitable and optimum utilization of the available water resources for significant socio-economic development on sustainable basis. One of its five water management objectives is "development of the water resources of the country for economic and social benefits of the people, on equitable and sustainable basis" (MoWR, ETHIOPIAN WATER SECTOR STRATEGY, 2001).

Effective management of the country's water resources, including development of sustainable supplies, depends on sufficient and accurate information on which to build a scientifically sound management strategy.

So far over 250 boreholes have been drilled in the plain area of the valley. This number does not include the ever-increasing drilling activities going on, be it by the regional government or private sector in uncontrolled manner. As a result, the effects of borehole interference and degree of groundwater mining are not well addressed

Figure 1.4 Boreholes and their relative distribution at a radius of 500 meters. Besides, additional 610 boreholes are proposed by the RVPIP in their latest report of 2008.

Another aspect of the management is that: most of the boreholes that have been drilled are not used for the intended purpose yet. Most of them are sealed with metals, while their operational time is reducing and may require additional cost to rehabilitate them before being operative. Some attempts of pump installation and power supply activities are underway. However, the power supply is started, among some others, with the artesian wells which are pouring water to above 30 liters per second but not absolutely utilized (Figure 1.5).

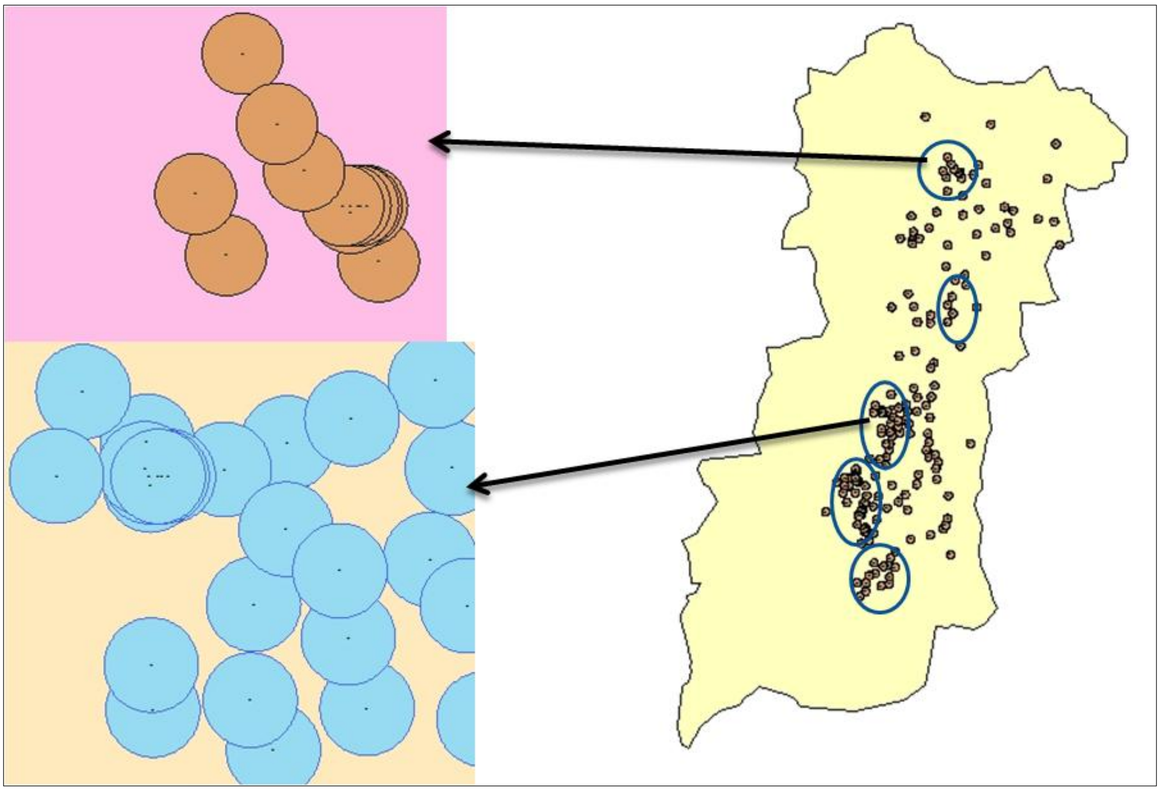

Figure 1.4 Boreholes and their relative distribution at a radius of 500 meters

Figure 1.5 Artesian well, RPW-060

In general it can be said that the 3D view of the Raya Valley is not conceptualized in terms of the groundwater system. That is, the hydrogeological investigation should include a complete characterization of the basin' aquifers together with the study of the hydrogeological boundary conditions, the hydraulic parameters of the aquifer and the confining units (if any), the horizontal and vertical distribution of the hydraulic head, the distribution and magnitude of groundwater recharge, and the best groundwater exploitation and the various groundwater management options.

1.3. OBJECTIVES

1.3.1. General Objective

The objective of this research is to understand and to characterize the groundwater system of Raya Valley, using hydrogeology, groundwater chemistry and isotope hydrology tools and to come up with different options that may help the monitoring and the most efficient management of the groundwater.

1.3.2. Specific Objectives

The specific objectives of this research will include:

- Describe the surface and subsurface extent of the different aquifer system(s) (their thickness, vertical &lateral variation, confining units, their boundary conditions)
- Determine and evaluate the various hydraulic parameters
- Define the distribution of groundwater recharge and discharge,
- define mechanisms of ground-water flow in the area,
- Describe the vertical and horizontal head distribution of the ground water system of the project area
- Develop the conceptual model of the basin that shows the subsurface geology, distribution of recharge, flow path and discharge

2. CHAPTER II: DESCRIPTION OF THE RAYA VALLEY

2.1. LOCATION

The Raya Valley is located in the northern part of Ethiopia within the Regional State of Tigray, between latitudes 12^0 30' and $12^0$55' north and longitudes $39^0$22' and $39^0$52' east. The valley is part of a series of depressions at the western margins of the Afar Depression. It is located at about 600 km north of Addis Ababa, the capital of Ethiopia (Figure 2.1).

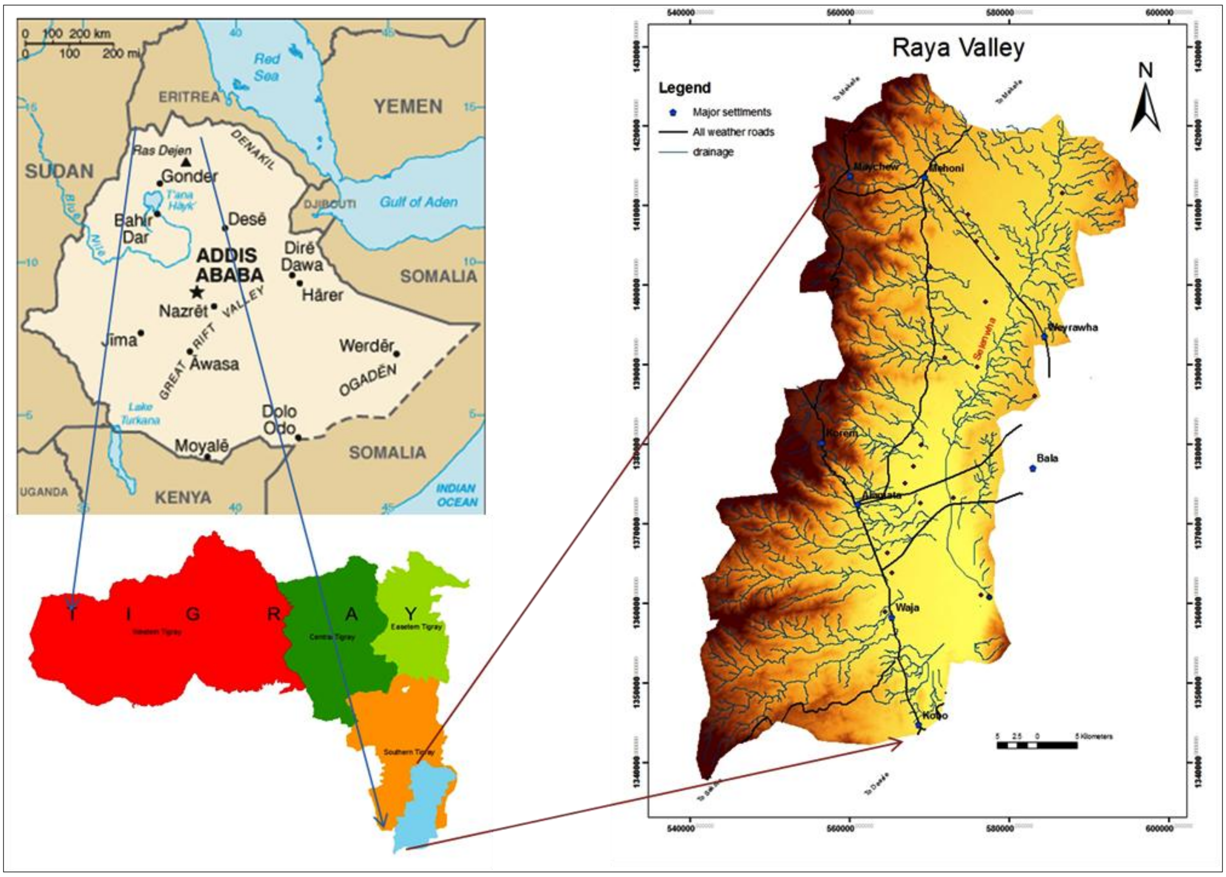

Figure 2.1 Location map of Raya Valley

2.2. REGIONAL GEOLOGICAL SETTING

The geological units in Ethiopia fall into one of the following four major categories; the Precambrian Basement, Late Paleozoic to Early Tertiary sediments, Tertiary volcanic rocks and the Cenozoic volcanic and associated sedimentary rocks. The Precambrian basement rocks are exposed in areas which are not intensively affected by Cenozoic volcanism and rifting and where the Phanerozoic and Mesozoic cover rocks have been eroded away. According to (Mengesha T.,Tadiwos C. and Workineh H., 1996), explanatory note of the geological map of Ethiopia, the litho-tectonic assemblages of the Precambrian basement in Ethiopia are similar to those recognized in the neighboring countries of northeast Africa and Arabian Peninsula. The Precambrian basements contain a wide variety of sedimentary, volcanic and intrusive rocks which have been metamorphosed to varying degrees. (Kazmin V., Alemu Shiferaw and Tilahun Balcha,, 1978) Classified the metamorphic complexes in Ethiopia into Lower, Middle, and Upper Complex. The Lower Complex is composed of high grade gneisses and is exposed in southern Ethiopia. The Middle Complex is identified in the southern, eastern and western parts of Ethiopia. The Upper Complex is the youngest metamorphic assemblage in Ethiopia consisting of low grade rock successions of ophiolictic rocks, andesitic metavolcanics, and associated metasediments.

Peneplanation of the metamorphic basement took place until Carboniferous and Permian (Kazmin V., 1972). Hence the late Paleozoic to Early Mesozoic sediments such as Enticho Sandstone, Edaga Arbi tilites in northern Ethiopia, Permian Sandstones in western and southern Ethiopia, Waju Sandstone in eastern Ethiopia (Kazmin V., 1972)& (Kazmin V., 1975) and Gum Sandstone in southern Ethiopia (Desta, 1978)accumulated- in shallow basins and narrow channels cut in the Precambrian basement.

This was followed by two major transgression-regression cycles during the Mesozoic era (Kazmin V., 1972). The first transgression started in the Early Jurassic or Late Triassic from the Ogaden region in the Southeast towards northwest. During this time Adigrat Formation consisting mainly of sandstone and minor lenses of siltstone and its equivalents in other parts of the country, such as Hamanilei Formation and Ebay Formation, were deposited. The regression of the sea started towards the end of Jurassic depositing lagoonal facies of the Agula Formation (Algae super sequence (Bosellini A., Russo A., Fantozzi P.L., Getaneh A., and Solomon T.,, 1977)) which consists of black shale, marl and claystone with beds of limestone, gypsum and dolomite in the Mekele area in northern Ethiopia. The Gabredare Formation, consisting of limestone and marl, marks the upper second regression event took place by depositing continental sediments predominantly composed of the most part of the Jurassic sedimentary succession in the Ogaden region, in eastern Ethiopia. In the Late Cretaceous the inter-bedded shale, siltstone and sandstone of the Amaba Aradom Formation occur.

In the Late Mesozoic-Early Tertiary, transgression of the sea from the south-east and an uplift of Afro-Arabia (East Africa together with Arabian Peninsula and the intervening regions now occupied by the Red sea and Gulf of Aden) occurred on an immense scale. According to (Mohr P.A., 1962)the magnitude of the uplift was such that nowhere in the world outside the orogenic belts have basement rocks been uplifted to such an elevation as that associated with the East African swell. The cause of the major uplift is related to a mantle plume whose decompression melting generated enormous quantities of basaltic magma in the lithosphere and resulted in the formation of a classic continental flood basalt province. The upraised and up arched crust fissuring under tension permitted the ascension of voluminous basaltic magma estimated as 300,000 km^3, (Mohr P. , 1983) to form the Trap Series of Ethiopia. Superimposed on the long uplifted swell of Afro-Arabia, whose axis approximately runs north-south, parts of the Great East African Rift System started to develop in the Miocene.

The pleistocene volcanic rocks outcropped within the Ethiopian rift, on the escarpment and nearby plateaus. The thickness of the unit increases away from the rift (Morton W.H., Rex D.C., Mitchell J.G., Mohr P.,, 1979). Acidic rocks dominate including acid tuffs, mostly ignimbrites, pantelleritic rhyolites and trachytes. They are inter-bedded with lavas and agglomerates of basaltic composition.

Tectonically the East African Rift System is one of the geologically exciting sites of the world, a place where the earth's tectonic forces are presently trying to create new plates by splitting apart the existing ones. Geologists are still debating and hypothesizing exactly how rifting come about, but the process is so well displayed in East Africa. The Nubian Plate that makes up most of Africa and the Somali plate are moving away from each other and also away from the Arabian plate in the north. The point where these three plates meet in the Afar region of Ethiopia and forms what is called a triple-junction.

Development of pre-rift domal uplifts and volcanism in East Africa is related to mantle plume (Kazmin V., 1975), but indicated these activities occurred during two (possibly three) stable periods in the plate motion: i.e. before 80 million years, at 60-35 million years, and at 20-14 million years. Volume and composition of volcanic depend on the length of the stable period. The general tendency of evolution in the pre-rift volcanic areas is from alkaline to transitional and then again to alkaline basalts.

After a $^{40}Ar/^{39}Ar$ dating of mineral separates and whole-rock (WR) samples analysis (Baker J., Snee J., Menzies L., 1996) established that basaltic continental flood volcanism began between 30.9 and 29.2 Ma. The sequence of events was surface uplift, flood magmatism and subsequent upper crustal extension both in Yemen and at the Afro-Arabian tripe junction.

(Tesfaye S., Harding D.J., Kusky T.M., 2003), described the western margins of the Afar Depression as a seismically active, right-stepping, en echelon system of discontinuous grabens that extend for about 500 km (Figure 2.2). The major marginal grabens from north to south are Maglala–Renda Coma, Dergaha- Sheket, Guf-Guf, Menebay-Hayk, and Borkena. The marginal grabens are interpreted to have been initiated during the early phase of Afar Rift tectonism (Chorowicz J., Collet B., Bonavia F., Korme T., 1999).

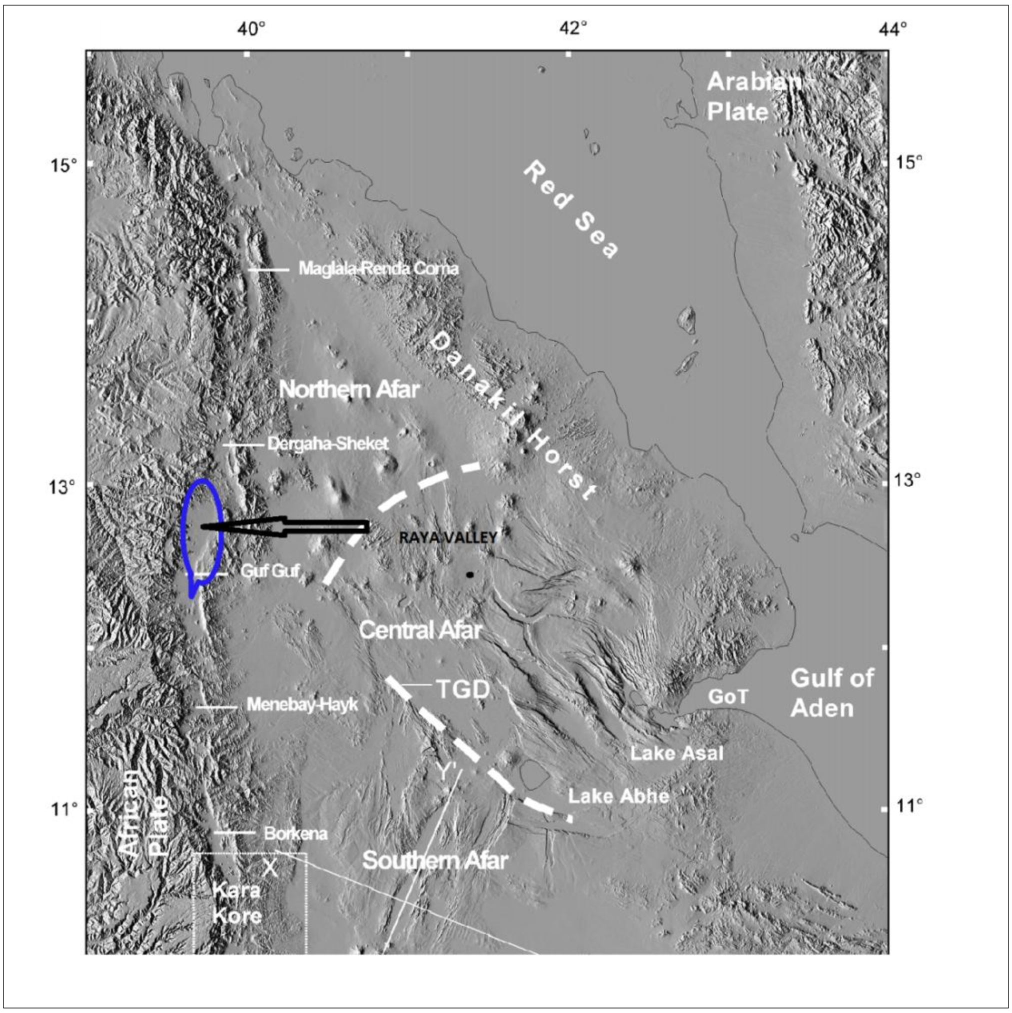

Figure 2.2 Shaded relief image of Afar and surroundings, pronounced from DTED, after Tesfaye et al., 2003

According to (Alebachew Beyene, Mohamed G. Abdelsalam, 2005) marginal basins with average 5 km wide and 30 km long were developed in regions dominated by extensional faulting related to the early phase in the development of the western margin of the Afar. The Main Ethiopian Rift is bounded by discontinuous boundary faults that give rise to major fault-escarpments separating the rift depression from the Ethiopian and Somalian plateaus. These faults are normally long, widely spaced and characterized by large vertical offsets (Figure 2.3).

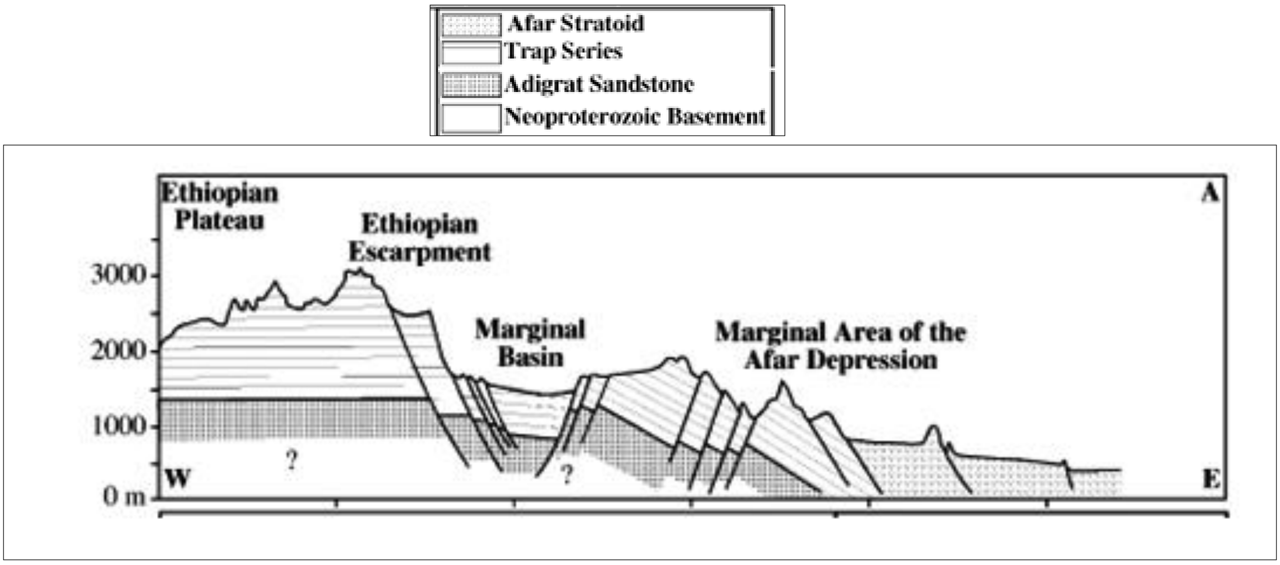

Figure 2.3 Stylized geological section illustrating the nature of crustal attenuation across the western Afar margin, After Alebachew B. et al, 2005

2.3. LOCAL GEOLOGICAL SETTING

2.3.1. Introduction

In the course of the development of parts of the Great East African Rift System in Ethiopia, a variety of continental sedimentary basins were developed since Miocene. In the Afar depression, sediments originating from the rapid erosion of the steep escarpments together with abundant volcanic products tended to fill the depression, but the tectonic deepening was more rapid than volcano-sedimentary infilling (Mengesha T.,Tadiwos C. and Workineh H., 1996)

Raya Valley, Guguf, as named by Tesfaye, S., Harding, D.J., Kusky, T.M., 2003, forms an intermountain depression of mainly north-south orientation directly related to the general N-S direction of the East African Rift system. The Raya Valley is believed to be formed at the time of the formation of the east African rift system. The asymmetric sedimentary fill graben structure configuration is vivid owing to the tectonic activities during its formation and subsequent regional tectonics. (Luigi Beccaluva, Gianluca Bianchini,Claudio Natali and Franca Siena, 2009) evidenced that dyke swarms that most probably fed continental flood basalt fissure eruptions (Me'ge D. & Korme T., 2004), are sub-parallel to sea - floor spreading axes in the Gulf of Aden and Red Sea, suggesting multiple rifting and spreading processes radiating from the still active Afar zone e.g. volcano-seismic crisis of autumn 2005; (Ayele A., Jacques E., Kassim M., Kidane T., Omar A., Tait S.,Nercessian, A., de Chabalier, J. B. & King, G., 2007).

The Raya Valley is boarded by Peak volcanic Mountains from the west, east and north with the highest elevation recorded in the western part. The valley floors infringed by scattered small volcanic hills at place, while the remaining vast area is gently sloping towards east and finally south sloping plain. Geological mapping of the local geologic units have been done by the Ethiopian Water Work Design and Supervision Enterprise in 2008. The main geological description was adopted from the above work and with modification from field observation is given below (Figure 2.4)

2.3.2. Quaternary alluvial sediments

Alluvial sediments are loose, eroded, transported and deposited in unconsolidated form by the action of water. Alluvium is typically made up of fine particles of silt and clay and larger particles of sand and gravel. An alluvial plain is a relatively flat landform created by the deposition of sediment over a long period of time by one or more rivers coming from highland regions, from which alluvial soil forms.

The alluvial sediments in the Raya Valley occupy the low lying plain where deposits of different size placed forming a fan like shape. Alluvial fans are cone-shaped deposits of fine to coarse stream sediments that are originated where a narrow canyon stream suddenly disgorges into a flat valley or where feeder channels release their solid load (Blair T. C., and McPherson J. G., 2009), (Leeder M. R., Harris T., and Kirkby M. J., 1998) and (Hartley A., Mather A. E., Jolley E., and Turner P., 2005). Alluvial fans consist of a variety of sediment types that gradually exhibit coarser materials near the apex of the streams and/or rivers to finer materials at distal areas. Weathering and subsequent erosion of the surrounding basaltic rocks by the west-east flowing streams that dominate the drainage pattern in the area, contribute the major role in the accumulation of these deposits. The alluvial deposits cover 51% of the total area of the Raya Valley. The thickness of these deposits increases towards the center of the valley and are not well developed at the foot of the eastern escarpment.

As it can be observed from lithologic logging of boreholes drilled at the foot of the western mountains, the major types of unconsolidated materials are colluvial deposits derived from the surrounding escarpments. The sediments are coarser on the west and get finer to the centre (RVDP, 1998). The maximum thickness drilled in the alluvial deposit, up to now, is 311m. It is mainly composed of medium to coarse sand with some silt, clay and gravel intercalations. The thickness of the alluvial sediments was anticipated to be greater than 250 meters by Geophysical exploration methods conducted by the German Consults in 1978, EIGS in 1996 and subsequent geophysical exploration works in the area. The lithological logs of boreholes drilled in the area show that the thickness of unconsolidated sediments ranges from 18 meters to over 311 meters at boreholes RPW-022 and PZ7 respectively.

2.3.3. Tertiary volcanic rocks

A first classification of the volcanic rocks of Ethiopia was introduced by (Blanford W.T, 1870). Considerable contribution to the study of volcanic rocks of Ethiopia was made by (Dainelli G., 1943), Mohr (1963), Kazmin (1972) and (Merla G., Abbate E., Canuti P.,Sagri M. and Tacconi P., 1973). Mohr (1963) attempted to divide the Cenozoic volcanic rocks of Ethiopia into the Trap and Aden Series. The term Trap Series is still widely used to represent the whole pile of Tertiary flood basalt sequences, which form the northwestern and southeastern plateau and attain a thickness of up to 3 Km. The term Aden Series was used for post-rift (Middle Miocene-Quaternary) volcanic rocks of the Main Ethiopian Rift, Afar Depression, and some parts of the Ethiopian Plateau.

The Ashange Formation represents the earliest fissural flood basalt volcanism on the northwestern plateau. These rock types occupy over 40.9% of the total area of the Raya Valley and contribute the major part of the sediments to the valley plain due to their areal coverage and the highly dissected relief. The western margin and a number of mountain ranges, such as Cheguara, Kara (in the north) and peaks within the alluvial basin are composed of Ashenge formation. The basalt flows are several hundreds of meters thick of strongly weathered, crushed, tilted basalts which lie below the major Pre-Oligocene unconformity (Zanettin B., Justin-Visentin, E.Nicoletti M., Piccirillo E.M., 1980). The Ashenge Formation consists of predominantly mildly alkaline basalts with inter-bedded pyroclastics and rare rhyolites and is commonly injected by dolerite sills and dykes.

The degree of weathering is related to the kind of basalt in the Ashange formation. The weathering in the aphanatic basalt penetrates along the vertical, polygonal and columnar jointing. Calcareous materials or rarely siliceous materials fill the fissures in the aphanatic basalt.

2.3.4. Quaternary basic volcanic rocks

These fresh basaltic volcanic rocks are expected to be much younger than Ashange basaltic formation (Tertiary Volcanic Rocks) in the west. These rock types occupy over 5.4% of the study area. The basalts are mainly distributed nearly N-S direction in the eastern escarpment and probably lies unconformably on the Ashange formation. They possess a less degree of tectonic crushing, dark-gray, fine grained, compact and homogeneous, and exist in relatively thin flows.

2.3.5. Quaternary acidic volcanic rocks

The rhyolites are located along N-S and NE-SW running fault controlled directions in the eastern escarpment and some exist as isolated hills in the Kilto and Weyra Wiha areas. They also occur as very steep peak in the Aba Hali area. These rocks are gray, compact, consisting of oriented array of feldspar phnocrysts. (Ayalew D., Ebinger C., Bourdon E., Wolfenden E., Yirgu G., & Grassineau N., 2006)interpreted the rhyolitic volcanic rocks on the eastern margin of the north western plateau, neighboring the Afar escarpment, as the differentiated products of basaltic magmas that mark the start of continental rifting.

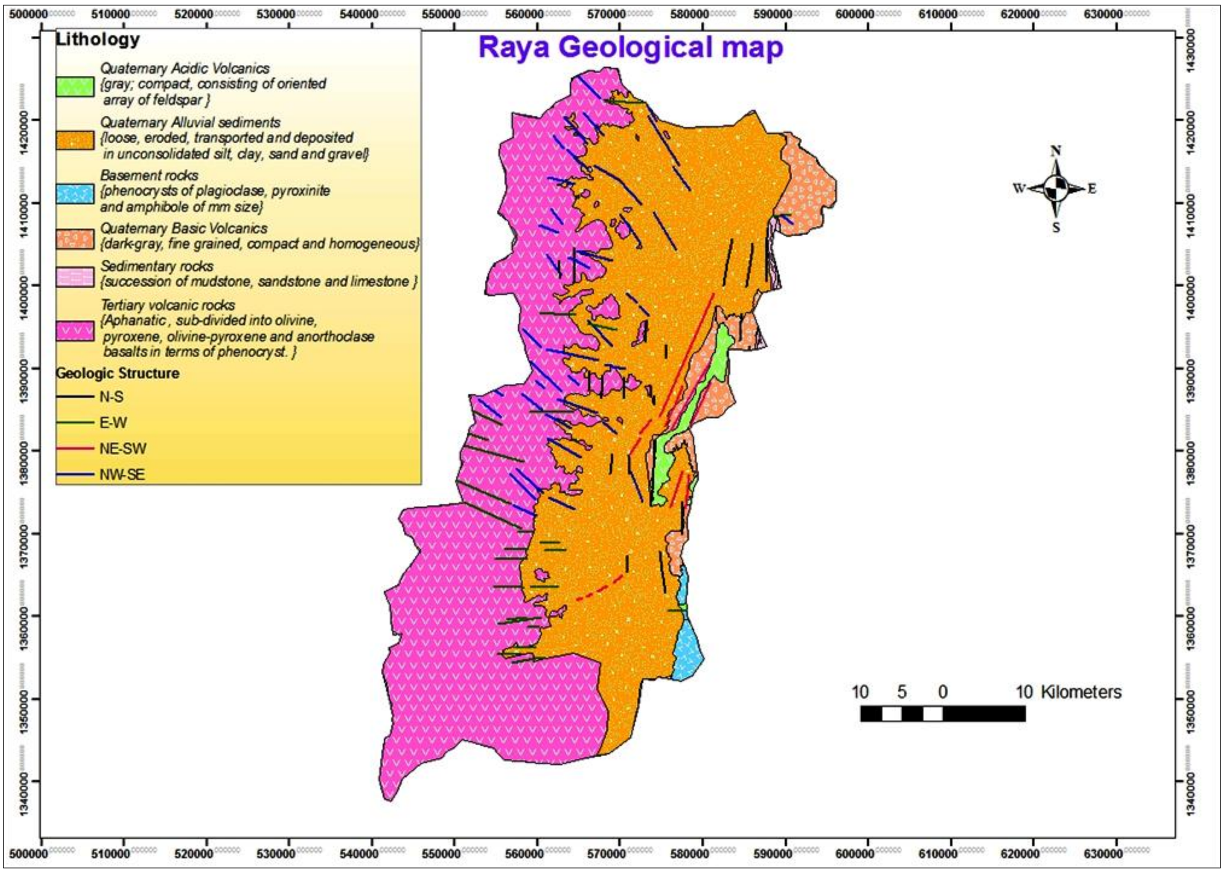

Figure 2.4 Geological map of the Raya Valley

2.3.6. Sedimentary rocks

These rocks are found as patches at about 5 kilometers from Mehoni, along the road to Maichew and on the eastern highlands. On the eastern highlands extending from Adibedera to Hade Alga they form a sedimentary rock succession of mudstone, sandstone and limestone from top to bottom respectively. Their sedimentary beds dip 26^0 towards NE and strike N100W in the highlands. The mudstone and sandstone formations exhibit variegated colors including reddish, yellowish and whitish. The sandstone is more or less equi-granular medium sand. The limestone is siliceous type. It exists in form of beds or thin tabular sheets (Muuz Amare 2007, Msc. thesis). They occupy less than 0.36 % of the studied area.

2.3.7. Basement rocks

Three rock units of metamorphic origin are identified in the south eastern part of the valley near the outlet. These are Pyroxenite, Gabbro and Anorthosite. They are coarse grained with phenocrysts of pyroxene 3-5 mm in size (for pyroxinite), plagioclase and pyroxene crystals in case of gabbros (1-2 mm) and 90-95% of 1-5mm size plagioclase and amphibole crystal 2-3mm for Anorthosite. These rocks cover about 0.91% of the total studied area.

2.3.8. Geologic structures

There are 4 major structural orientations which dominate the structural make up of the area. Most lineaments that were traced are oriented nearly in the N–S, NE-SW, NW-SW and E–W directions (Figure 2.4). The N-S striking faults are probably responsible of the creation of the Raya Valley and for the easterly tilting and throw of block in that direction. The major direction of flow of most streams, draining the western highland and those streams draining the eastern mountains, are governed by the E-W faults. However the major seasonal river in the area, Sullula, is oriented N-S along the lineament. In general, the structural patterns are congruent to the major structures of the rift.

2.4. GEOMORPHOLOGY and DRAINAGE

2.4.1. Geomorphology

The four widely known major physiographic regions in Ethiopia are the western plateau, southeastern plateau, the main Ethiopian Rift and Afar Depression. The Raya Valley is located at the western margin of the Afar rift and the escarpment of the western plateau. Therefore, the area exhibits physiographic features of the adjacent major physiographic regions.

The physiographic features that dominate the area are the valley plain, chain of mountains and their sloping sides, and small portion of plateau. The elevation of the mountains ranges from about 1800 to over 3680 above mean sea level (a.m.s.l.). The plain areas are situated between 1353 and 1800 m.a.s.l and the plateaus are mainly found in the high altitude between 2000 and over 2500 above mean sea level. The study area approximately covers a total land of 2558 km^2. Of these total areal coverage of the valley, the area of the mountain and plateaus part is about 1253 km^2 (49%), while that of the plain area is about 1302 km^2 (51%). Warm temperature and tropical rainy climates prevail in the mountain and plateau areas while hot dry climate characterizes a large part of the project area which is the lowland part. The mountains are serving as sources of sediment load (due to high erosion) and recharge to the valley while the floor of the valley has relatively low rainfall, but with potential fertile land (Figure 2.5).

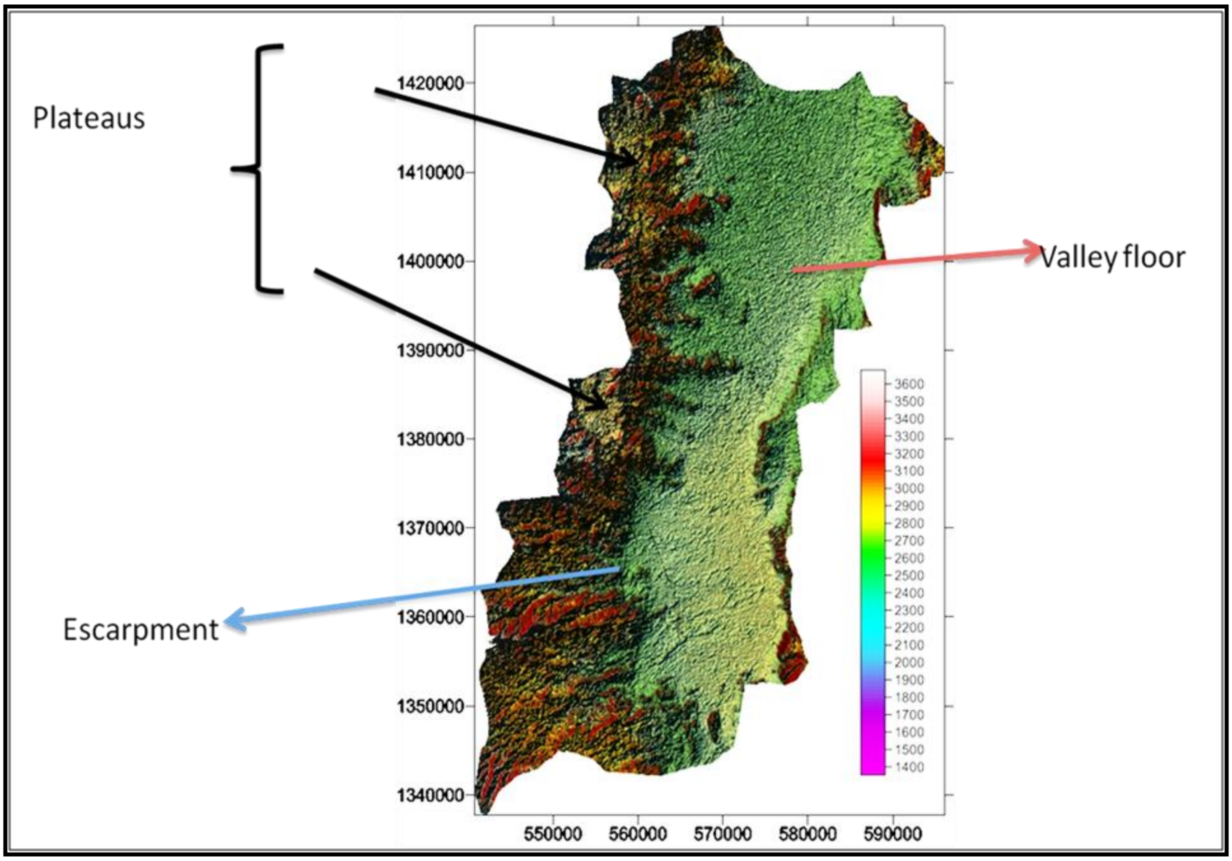

Figure 2.5 Land forms of the Raya Valley

2.4.2. Drainage

The surface water resources are characterized by streams, which flow strongly during the short rainy season. Flash floods are common during the rainy season due to the high intensity storms and the denuded landscape which has little vegetation left to retard runoff. Erosion and desertification is also common on these uplands. There exist no hydrological gauging stations in the area. However, the seasonal variability in these streams reflects the rainfall variation with minimum or no flow occurring from October to June, until the beginning of Kremt. The main streams in the area tend to have no perennial flows and most of them die out in the valley floor (Figure 2.6). Therefore, it can be concluded that there is not any perennial flow of surface water during the dry period in all parts of the valley, except the minor seepages from Waja springs that vanish within a short distance in the valley and another hot spring at the outlet in Selenber. Even in this latter case, springs may supply a perennial source of water for small irrigation schemes at their vicinity.

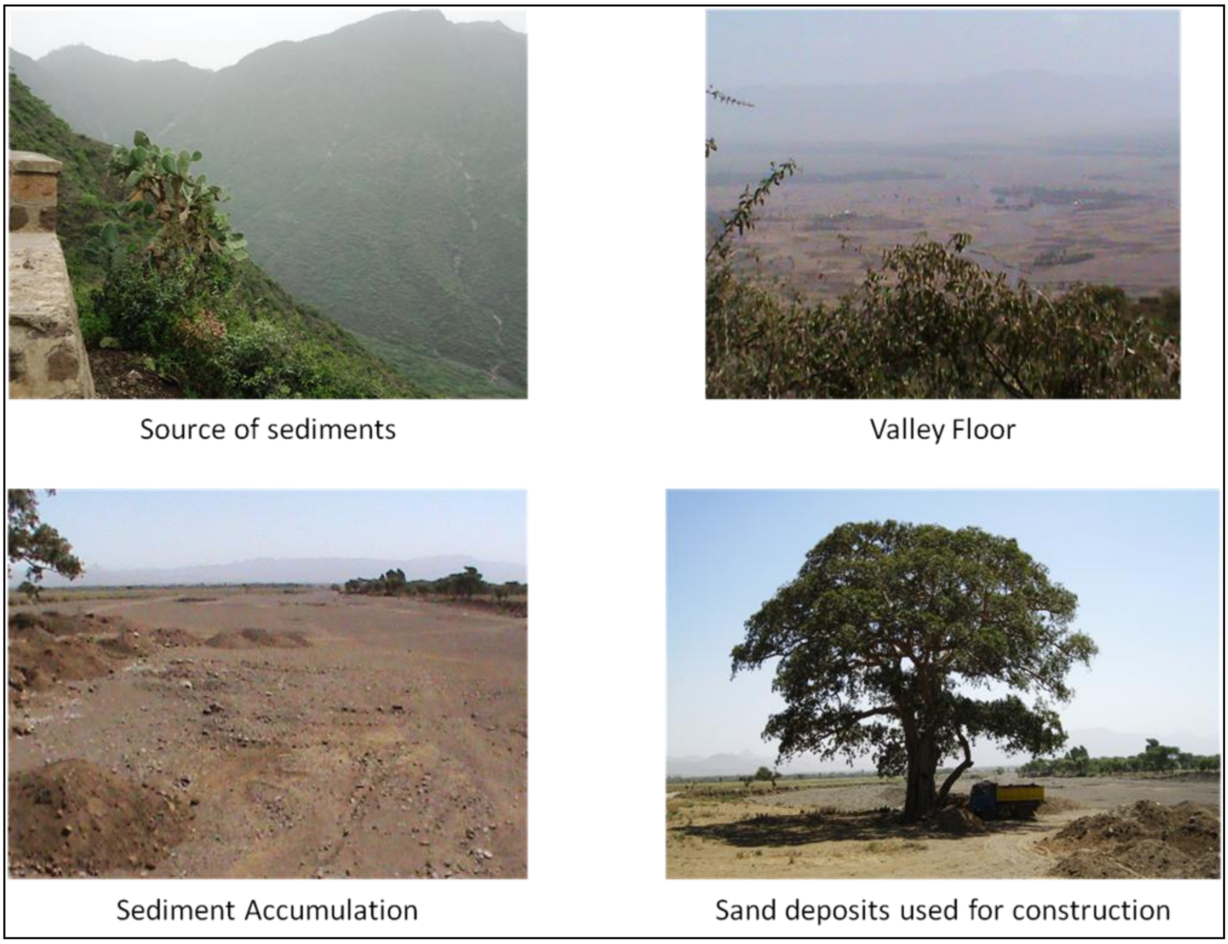

Figure 2.6 Photos showing how sediments deposit in the valley floor and transported as construction materials

Sulula is the main river in the area that crosses the catchment dividing the basin asymmetrically into two halves (Figure 2.7). The river drains in a north-south direction almost parallel or following the major regional structure. Many seasonal tributaries feed the main stream both from the west and east with substantial amounts of water during the rainy season. The streams coming from the western highlands are characterized by dendritic drainage pattern with separate and nearly parallel flow patterns. They follow a nearly W-E flow direction, in concordance with one of the dominant geological structures. The streams tend to be dispersed as they encounter the flat area and hence no visible drainage path is observed due to loss of energy. These behaviors of the streams determine the type and the amount of sediment deposition in the plain area. During the heavy rains, flood storms may reach the out let; otherwise settle within the valley floor exposed to evaporation or join the groundwater. On the other hand the E-W draining streams from the eastern margin of the valley are directly connected to Sulula River, the major drainage system in the area, and follow a nearly NNE-SSW flow direction and drain out of the valley through the only outlet in Selember (Figure 2.7).

Within the plain area, an approximately 100 square kilometer depression exists at which the runoff draining from all parts of the basin remains for long periods beyond the rainy season. The runoff to the Danakil depression, through the outlet, is supposed to begin after inundating the depression and bringing it to the required level. The moisture content of the soil remains for longer period and local people use it to grow cereals without supplemental water

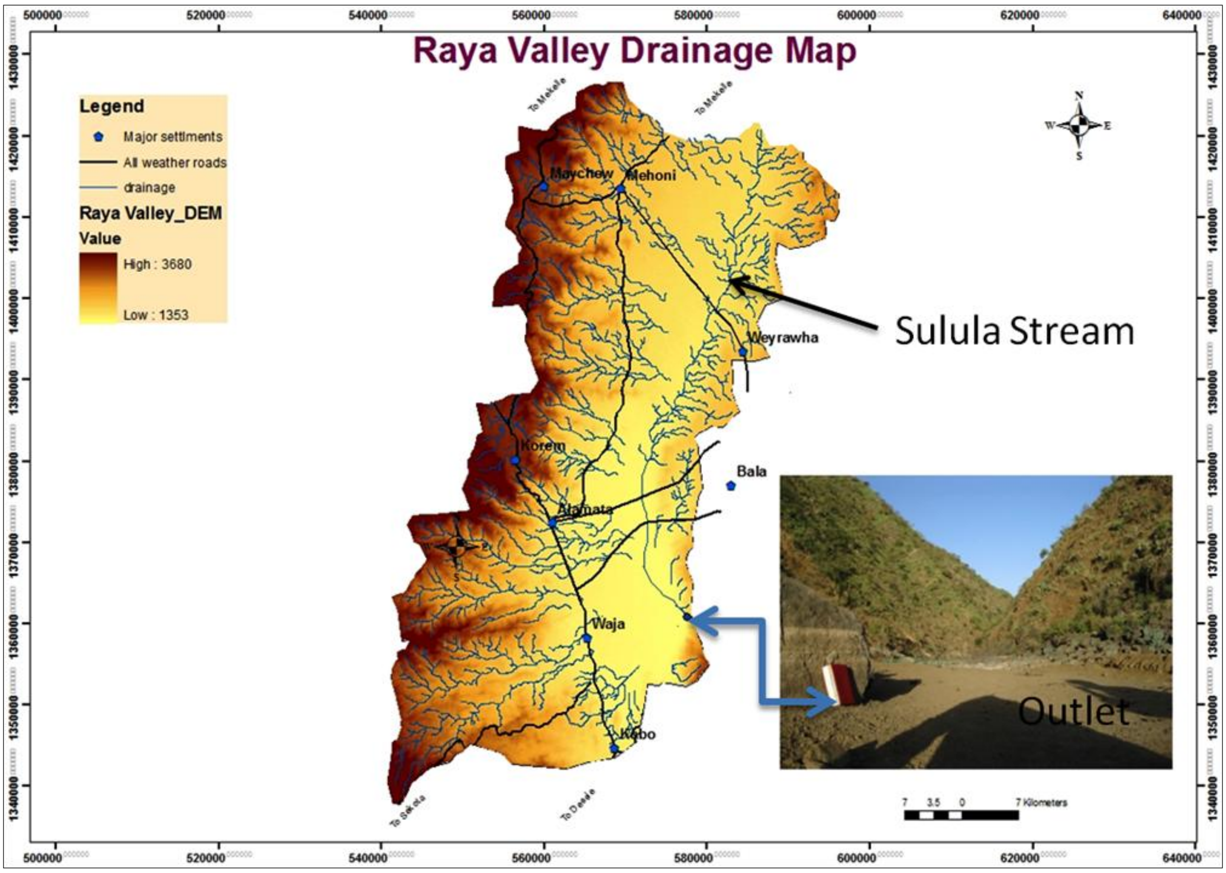

Figure 2.7 Drainage map of the Raya Valley

2.5. METEOROLOGY

Meteorological data have been collected from National Meteorological Agency of Ethiopia main office at Addis Ababa and from the Mekele branch. These data include (47, 39, 18, 16, 12, 13 and 3 years) of records for Maichew, Alamata, Korem, Mehoni, Waja, Kobo and Chercher respectively. The data of Maichew suffered major interruptions in the late 1980's and early 1990's. The other stations also faced the same problem of data record break. Therefore, the consecutive records (1996-2007) were utilized for water balance, trend and seasonal variation analysis.

2.5.1. Precipitation

The climate Ethiopia is dominated by combined effects of the Inter-tropical Convergence Zone (ITCZ) and the complex topography (Tesfaye, 2003). This gives rise to wide rainfall spatial variations, with certain areas of the west receiving more than 1000 mm per year, and parts of the east receiving between 500- 600 mm per year.

According to the UNDP country profiles (http://country-profiles.geog.ox.ac.uk) the seasonal rainfall in Ethiopia is driven mainly by the migration of the Inter-Tropical Convergence Zone (ITCZ). The exact position of the ITCZ changes over the course of the year, oscillating across the equator from its northern most position over northern Ethiopia in July and August, to its southern most position over southern Kenya in January and February. The movements of the ITCZ are sensitive to variations in

Indian Ocean sea-surface temperatures and vary from year to year, hence the onset and duration of the rainfall seasons vary considerably inter-annually, causing frequent drought.

(Gemechu, 1977), has classified the rainfall distribution in Ethiopia into western and eastern halves, where the Raya Valley is part of the western half of the country, which receives bi-modal rainfall. Figure 2.8 points out that the rainfall of all the stations is characterized by bimodal seasonal rainfall type. The months of June-September, major rainy season (Kiremt) account for the 59% of the total precipitation, while the small rainy season, March-May (Belg), accounts 22%. Even in the months of highest rainfall the precipitation is rather of great intensity.

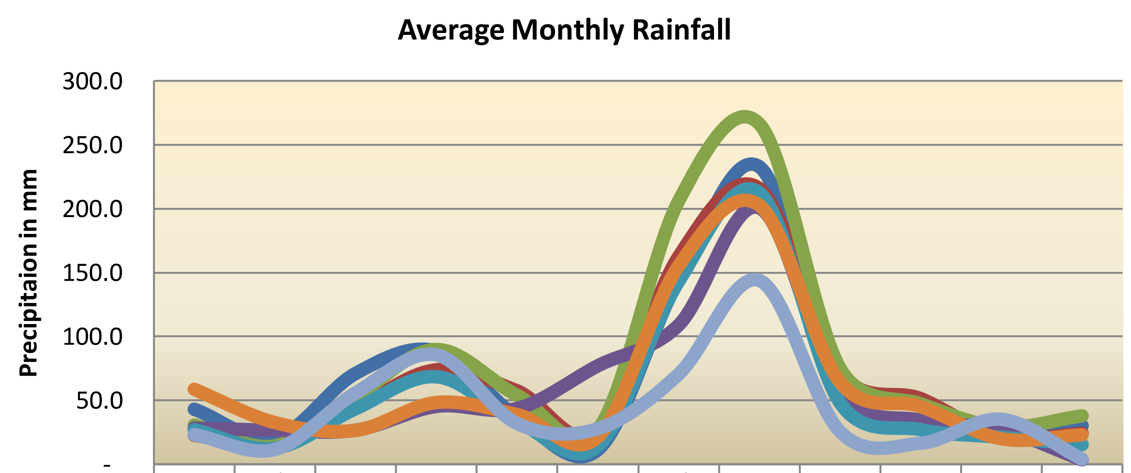

	Jan	Feb	Mar	Apr	May	Jun	Jul	Aug	Sep	Oct	Nov	Dec
Alamata	43.0	20.5	71.1	88.6	37.1	11.3	144.3	232.9	56.6	27.1	29.0	30.1
Maichew	22.5	13.2	44.0	73.7	57.2	24.8	162.3	215.9	71.8	51.2	21.1	23.8
Korem	30.7	14.5	53.0	89.9	54.1	27.4	206.0	266.6	75.4	47.4	29.2	38.0
Chercher	28.1	26.5	26.5	45.1	43.5	76.9	108.7	200.5	56.2	34.3	26.9	3.4
Waja	26.9	12.4	43.4	68.4	33.6	14.1	143.0	212.8	48.1	27.0	21.0	15.2
Kobbo	58.4	32.3	26.2	48.1	38.7	21.1	155.1	202.8	64.1	44.9	19.7	22.8
Mehoni	23.0	11.4	55.7	85.5	31.6	27.6	70.2	143.8	25.4	16.2	35.0	3.8

Figure 2.8 Average monthly precipitation

The weighted average maximum and minimum precipitation was calculated using the Thiessen polygons (Figure 2.9) as a method of interpolating rainfall depths using the following equation:

$$P = \frac{A_1P_1 + A_2P_2 + A_3P_3 + \ldots\ldots + A_iP_i\ldots\ldots A_nP_n}{A_t}$$

where: - P = Basin weighted mean precipitation

A_t = Total area of the basin

A_i = Area of the i^{th} Thiessen polygon

P_i = Precipitation on the i^{th} meteorological station

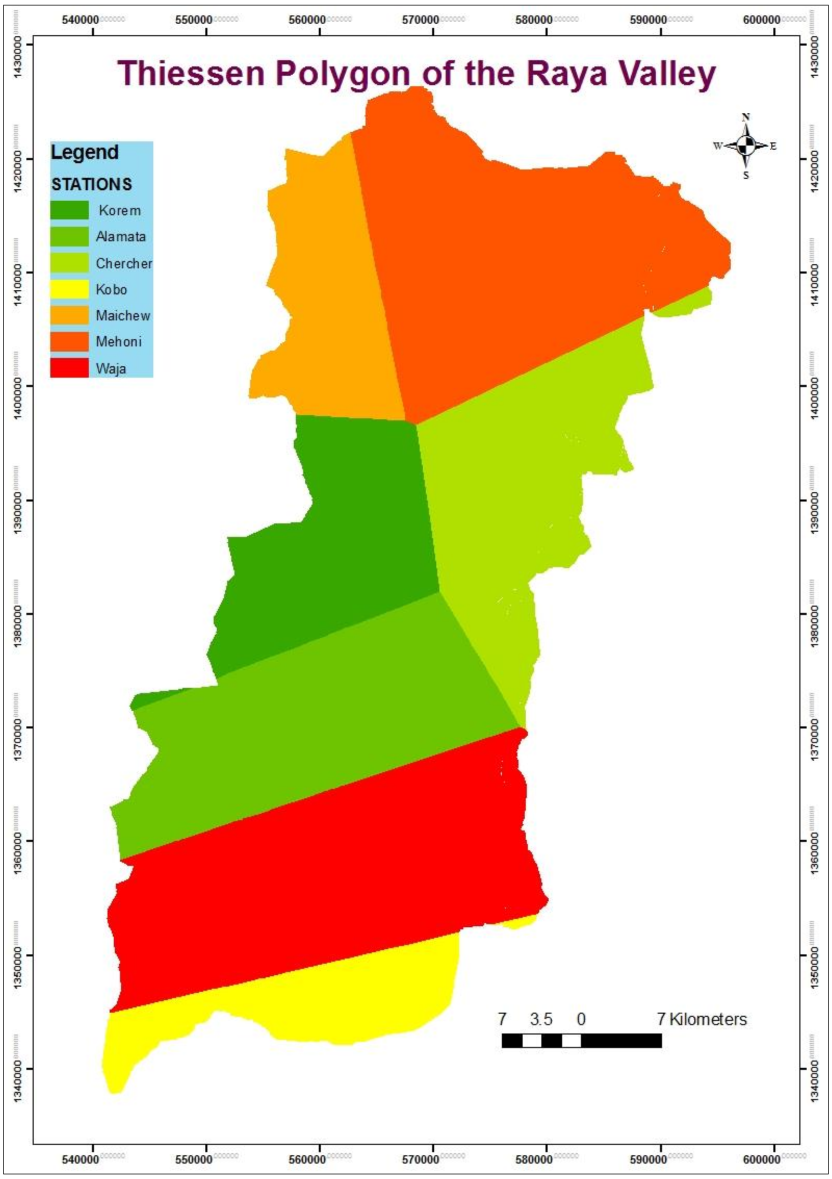

Figure 2.9 Thiessen Polygons

Hence the amount of precipitation at highest precipitation period is 942mm per year while at the lowest precipitation period is 577mm per year. The highest annual precipitation recorded so far is 1357mm at Korem in 1998, while the minimum was 357mm in the same year but in the station at Mehoni. Though these stations are within the same basin, the local altitudinal difference may have contributed to the wetness or dryness of each station. The average precipitation of the valley is 733.6 mm per year.

(Dessie Nedaw, 2003) has investigated the variation of rainfall with altitude, verifying that the highest rainfall is related to the highest elevations and vice versa on the basis of the data analyses from rainfall stations located at different altitudes within the Raya Valley boundary using the data of 1993 to 1995. Analysis of the data of 1996-2007 showed very poor correlation, but however a clear variability of rainfall from the west to the east is observed as depicted in the Figure 2.10.

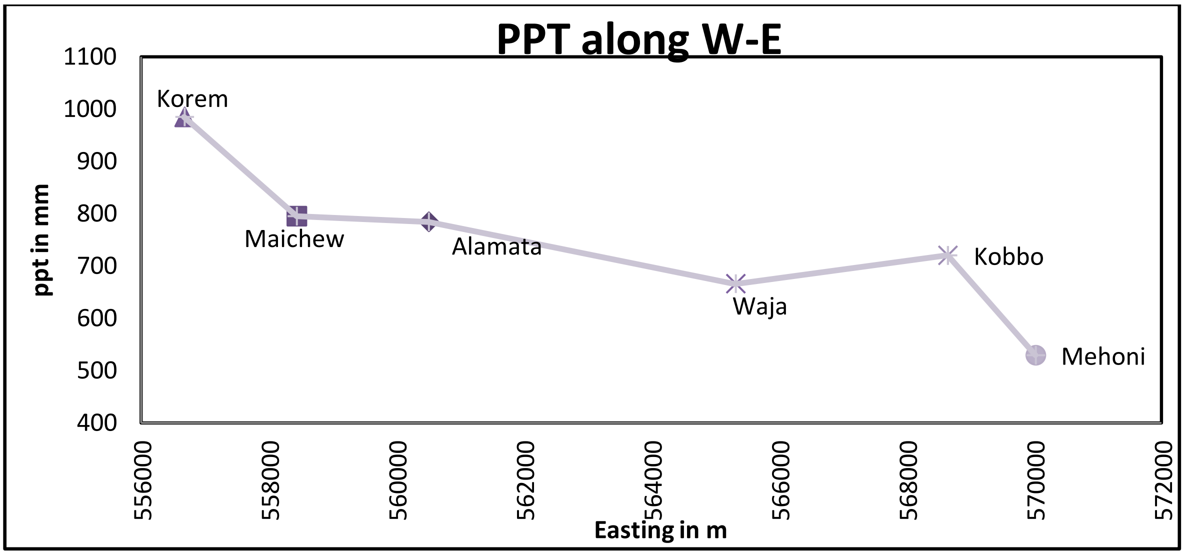

Figure 2.10 Variation of precipitation from west to east, toward the Afar depression

2.5.2. Temperature, Relative Humidity and Wind Speed

2.5.2.1. Temperature

Temperature is an important variable in calculating the evapotranspiration of a basin. There are seven meteorological stations in the basin and its surroundings with temperature recordings. The mean monthly minimum temperature ranges from 4.1°C at Korem (highland) to 12.2°C at Kobo (lowland) while the mean monthly maximum temperature ranges from 25.5°C in Maichew (highland) to 34.7°C in Waja (lowland). Mean annual temperature is also subject to variation depending on the altitude difference, from 12.1°C in Korem, highland to 26.2°C in Kobo lowland (Figure 2.12). Data plot of average temperature versus altitude showed a strong correlation i.e. 0.73°C for every 100 meters of altitudinal increment or vice versa as observed in the Figure 2.11.

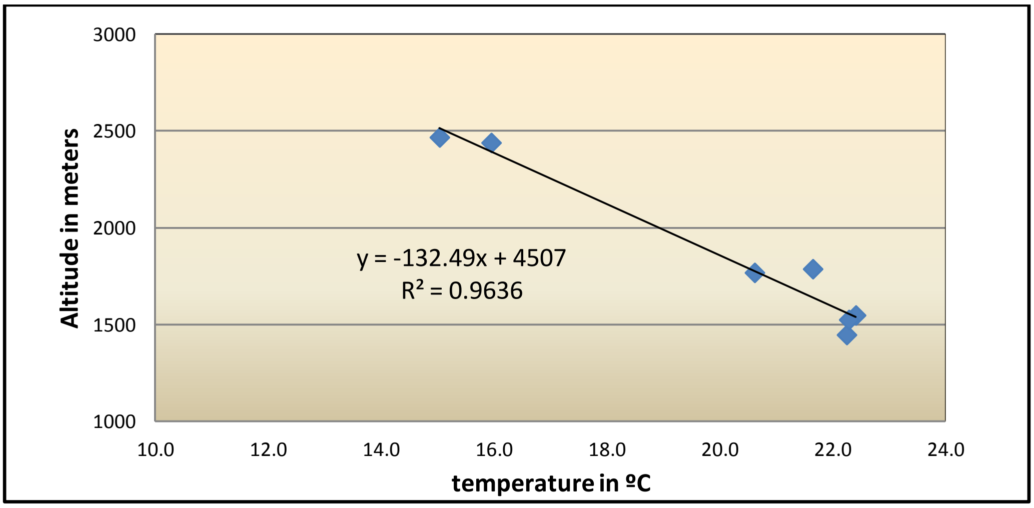

Figure 2.11 Temperature variation with altitude

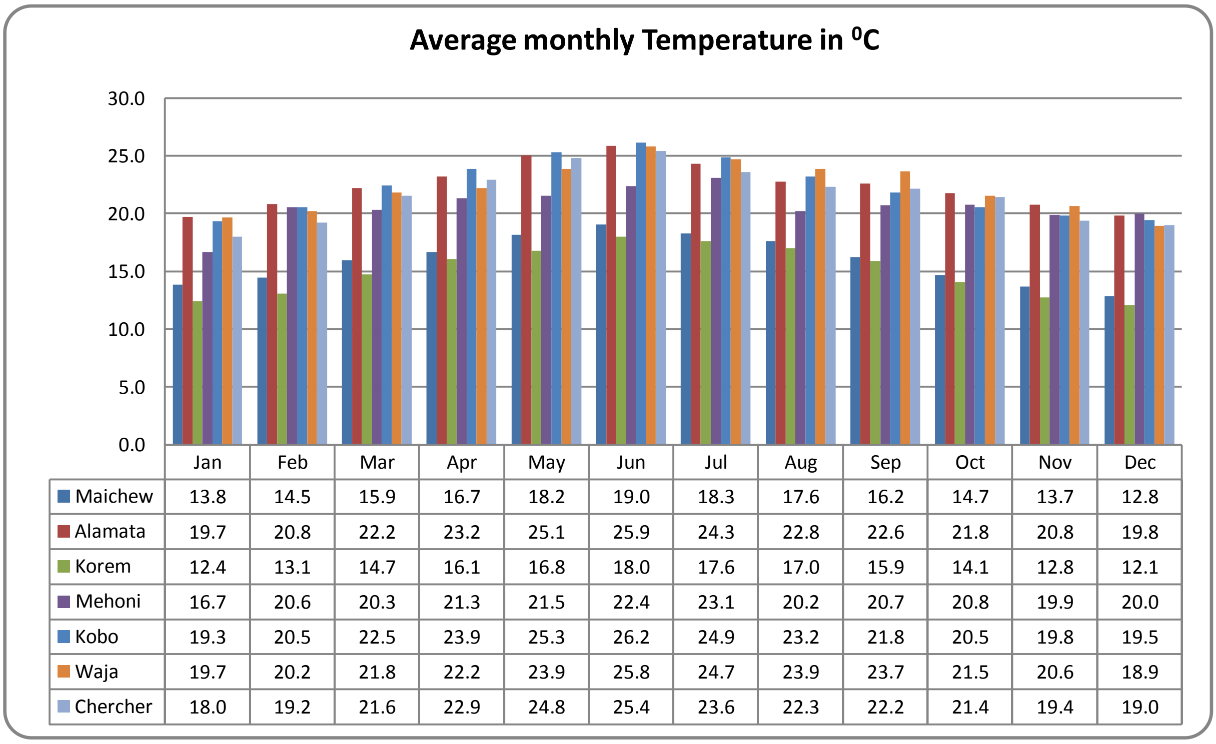

	Jan	Feb	Mar	Apr	May	Jun	Jul	Aug	Sep	Oct	Nov	Dec
Maichew	13.8	14.5	15.9	16.7	18.2	19.0	18.3	17.6	16.2	14.7	13.7	12.8
Alamata	19.7	20.8	22.2	23.2	25.1	25.9	24.3	22.8	22.6	21.8	20.8	19.8
Korem	12.4	13.1	14.7	16.1	16.8	18.0	17.6	17.0	15.9	14.1	12.8	12.1
Mehoni	16.7	20.6	20.3	21.3	21.5	22.4	23.1	20.2	20.7	20.8	19.9	20.0
Kobo	19.3	20.5	22.5	23.9	25.3	26.2	24.9	23.2	21.8	20.5	19.8	19.5
Waja	19.7	20.2	21.8	22.2	23.9	25.8	24.7	23.9	23.7	21.5	20.6	18.9
Chercher	18.0	19.2	21.6	22.9	24.8	25.4	23.6	22.3	22.2	21.4	19.4	19.0

Figure 2.12 Average monthly temperature

2.5.2.2. Relative humidity

Is the amount of water vapor in the air at any given time, being usually less than that required to saturate the air. The relative humidity is the percent of saturation humidity, generally calculated in relation to the saturated vapor density.

The average monthly relative humidity varies between 33% and 68%. The highest humidity values correspond to the wettest months of the year (July, August & September), and the lowest to the driest months of March, April, May & June (Figure 2.13).

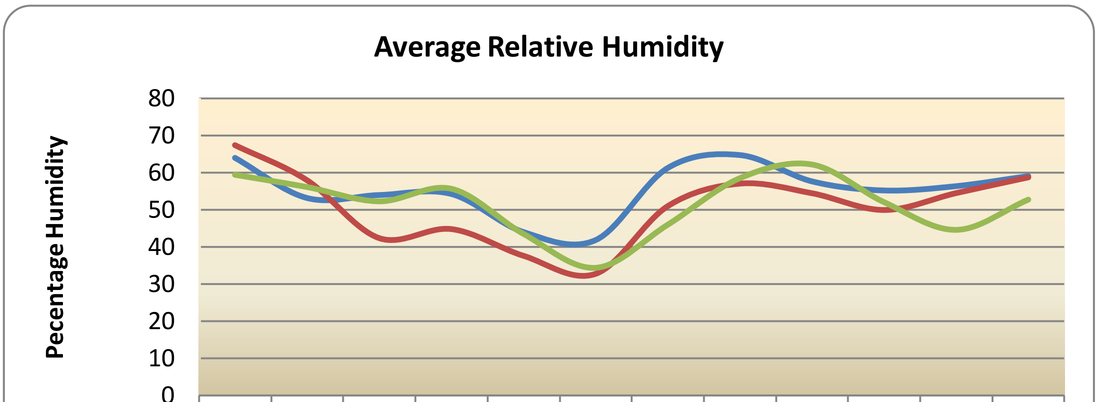

	Jan	Feb	Mar	Apr	May	Jun	Jul	Aug	Sep	Oct	Nov	Dec
maichew	64	53	54	54	44	42	61	65	58	55	56	59
chercher	68	58	42	45	38	33	51	57	55	50	55	59
kobo	60	56	52	56	44	34	46	59	62	52	45	53

Figure 2.13 Average monthly relative humidity

For practical purposes the weighted mean relative humidity of the three stations is taken into consideration. Those stations without recorded data of relative humidity were filled with data of the nearest station and of similar altitude when necessary.

2.5.2.3. Wind speed and Sun shine hours

Monthly wind speed measured at two meters above the ground surface, at Maichew, Kobo and Mehoni are available for the years 1996-2007. The monthly mean wind speed in m/s is indicated in Figure 2.14. The data shows that there is high wind speed in the months of June, July and August. The lowest record is that of December and January.

Wind speed has a strong influence on the principal hydrological elements such as evapotranspiration. The mean data are used for the calculation of evapotranspiration while using methods that make use of wind speed such as radiation based method. The average wind speed at Maichew shows a decreasing trend(s) in the last 18 years, which could be attributed to the regional climatological variation.

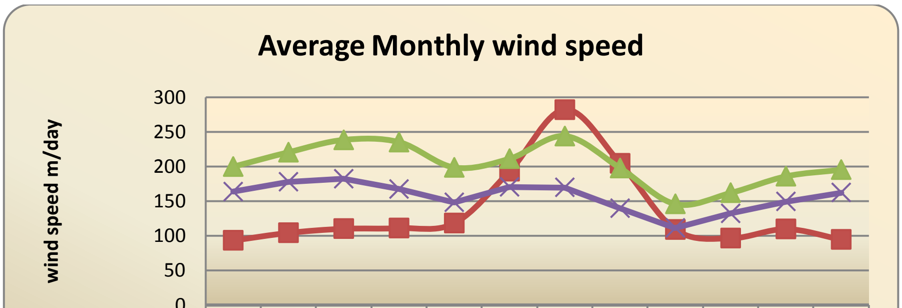

	Jan	Feb	Mar	Apr	May	Jun	Jul	Aug	Sep	Oct	Nov	Dec
Maichew	93	104	110	111	118	193	282	204	109	96	110	94
Chercher	200	220	238	235	198	211	244	198	146	162	186	195
Kobo	164	178	182	167	148	170	170	140	111	132	149	162

Figure 2.14 Average monthly wind speed

3. CHAPTER III: AQUIFER GEOMETRY

Raya Valley is an important alluvial graben running parallel to the western escarpment in a north-south direction. As there are no perennial rivers and streams in the area, groundwater is considered to be the primary source of water for both domestic water supply and for irrigation. On the other hand, the government considers Raya Valley to be one of the development corridors in the region. In line with the government plan, intensive groundwater investigation and development activities have been going on since 1996. The proposed groundwater-based irrigation is one of the main and the largest projects (>18000 hectares) in the country (Ministry of water &energy 2010), which is designed to ensure food security in the region.

According to the aforementioned situation, hydrogeological investigations were carried out in some parts of the valley and considerable number of boreholes has been drilled. Besides, some drip and sprinkler irrigations have been carried out as a pilot and still others are on the design process.

Descriptions of the local geology and cross-sections along different orientations show that the valley is mainly composed of basin fill deposits characterized by various degree of groundwater potential. This variation is attributed to the variation in thickness, proportion of the soil types in the alluvial deposit and their sorting. Drilling in areas with high proportion of very fine alluvial deposits (silt and clay) and thinly weathered and fractured basaltic rocks are supposed to encounter low yielding aquifers. Borehole data depict that the main aquifer in Raya Valley is the alluvial deposit. The thickness of the alluvial deposit is variable and ranges from about 18 to more than 311m. The minimum thickness is in the western and eastern flanks of the valley, whereas the maximum thickness is obtained towards the central eastern part of the valley (Figure 3.1 and Figure 3.2a-e).

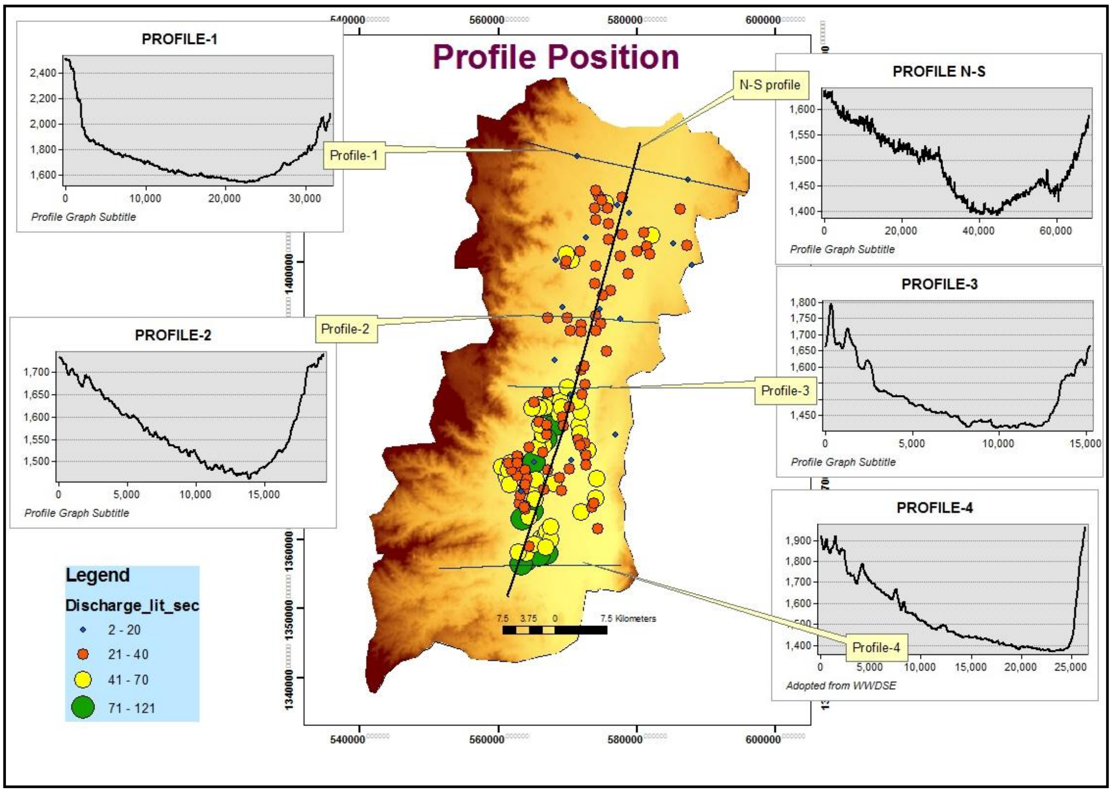

Figure 3.1 The position of the profiles & the distribution of discharge from wells

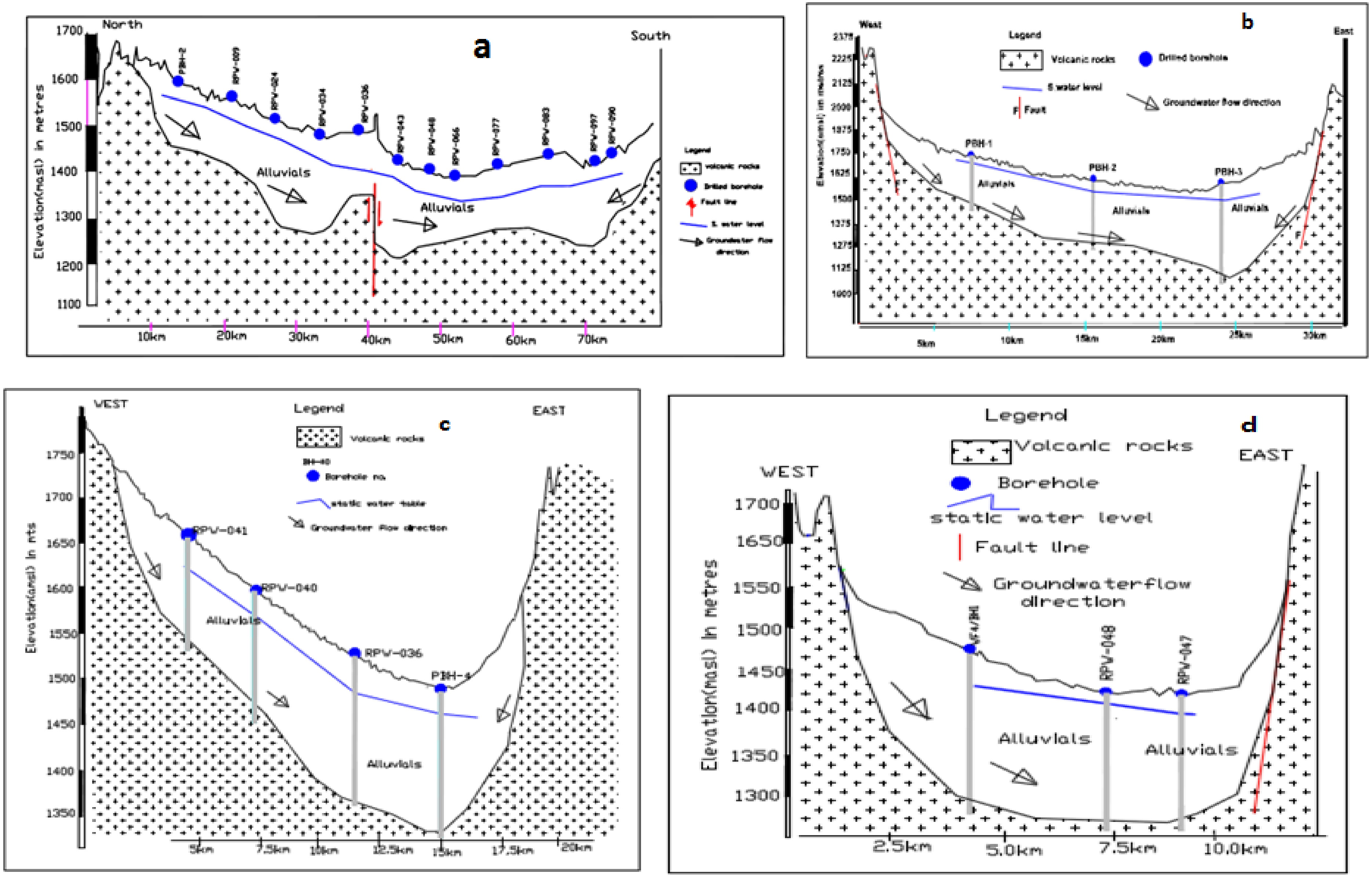
a
North
South
Elevation(masl) in metres
1700
1600
1500
1400
1300
1200
1100
PBH-2
RPV-009
RPV-024
RPV-034
RPV-036
RPV-043
RPV-048
RPV-066
RPV-077
RPV-083
RPV-097
RPV-090
Alluvials
Alluvials
10km
20km
30km
40km
50km
60km
70km
Legend
volcanic rocks
Drilled borehole
Fault line
S. water level
Groundwater flow direction
b
West
East
Legend
Volcanic rocks
Drilled borehole
S water level
Groundwater flow direction
F Fault
PBH-1
PBH 2
PBH-3
Alluvials
Alluvials
Alluvials
5km
10km
15km
20km
25km
30km
c
WEST
EAST
Legend
Volcanic rocks
Borehole no.
static water table
Groundwater flow direction
Elevation(masl) in mts
1750
1700
1650
1600
1550
1500
1450
1400
1350
RPV-041
RPV-040
RPV-036
PBH-4
Alluvials
Alluvials
5km
7.5km
10km
12.5km
15km
17.5km
20km
d
Legend
Volcanic rocks
Borehole
static water level
Fault line
Groundwaterflow direction
WEST
EAST
Elevation(masl) in metres
1700
1650
1550
1500
1450
1400
1350
1300
RPV-048
RPV-047
Alluvials
Alluvials
2.5km
5.0km
7.5km
10.0km

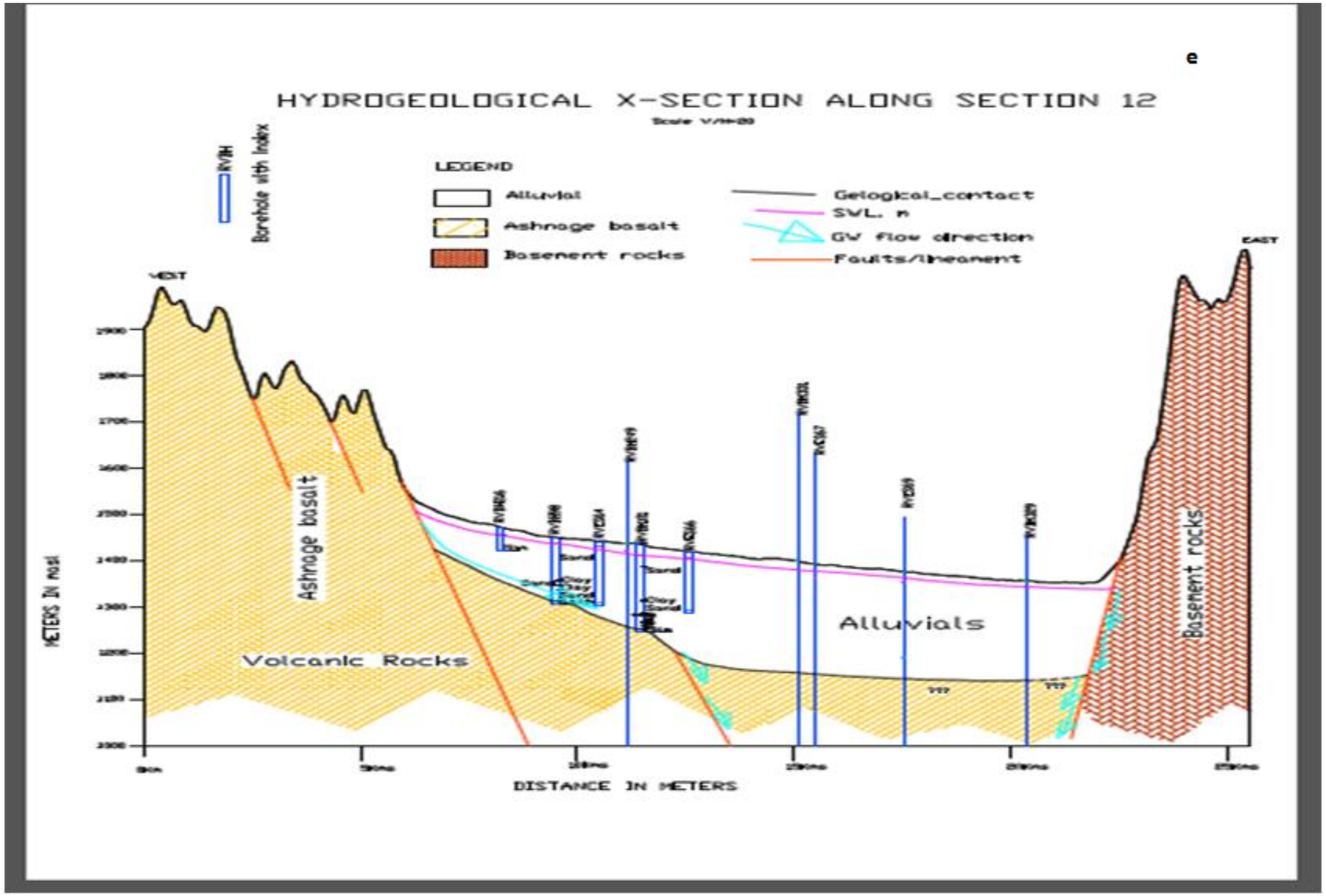

Figure 3.2 a) N-S profile b) West-East profile-1 c) West-East profile-2 d) West-East Profile-3 and e) West-East profile-4

The slope of the valley floor decreases from north toward south. However, the thickness of the deposits increases significantly in the central part of the valley (Fig. 3.2. a) where it attains its maximum, east of Alamata town. The western part of the aquifer has generally unconfined groundwater condition, whereas the south-eastern part is characterized mostly by semi-confined and at places by confined conditions. This can be related to the local topographic differences, because borehole logs of almost all artesian wells are devoid of any considerable thickness of confining bed, such as clay (Figure 3.3).

Pumping test data analyses show that the hydraulic conductivity values of the aquifer ranges from about 0.03 to 26 md^{-1}. The source of groundwater recharge of Raya Valley is mainly due to seasonal floods and subsurface runoff from adjacent highlands of the western, northern and eastern sides of the valley and in situ precipitations. In addition to the alluvial deposits the volcanic rocks are acting as aquifers when fractured. But the volcanic aquifers don't have such high potential as the alluvial deposits.

The depth of the groundwater varies from 0 to about 50m below ground level in Alamata sub-basin (south) and from 20 to about 90m in Mohoni sub-basin (north). As Alamata sub-basin has more recharge area and thick alluvial deposits, it has more groundwater potential than Mohoni sub-basin. Currently, in both sub-basins there are more deep well drilling activities for the implementation of modern pressurized irrigation systems.

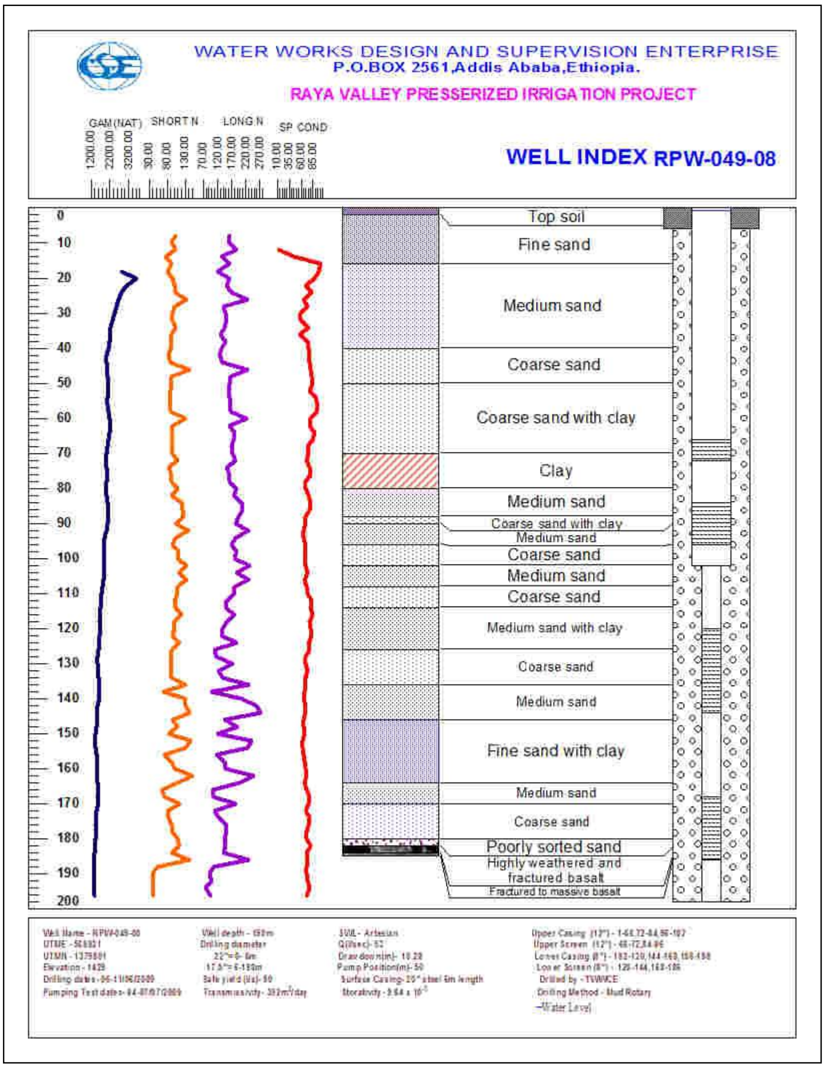

Figure 3.3 An artesian well without considerable thickness of clay

4. CHAPTER IV: HYDROGEOLOGICAL SURVEYS

4.1. GROUND WATER LEVEL AND FLOW DIRECTION

The groundwater levels in the Raya wells are not well monitored. Most of the wells in the well fields are not accessible to measure the water level because either they are sealed with metal sheets or are constructed without observation pipes or with clogged ones. No monitoring records of wells except for the two wells that were installed in the 2001 -2004 and the measuring ceased after that time. An attempt was made to measure the SWL of the boreholes during field visits of 2009 and 2011; however it was not possible to measure all or the major part of the production wells due to the above reasons. The measured data are given in Table 4-1. These own measured data were used to compare and verify the fitness of the previously collected water level measurements for analysis before utilizing them in the determination of the groundwater flow direction.

Figure 4.1 Shows field static water level measurements

The 2001-2004 monitored wells show no groundwater level variation record in areas of little irrigational activities (Chelekot), and a variation of 2.7m under conditions where there is significant abstraction (Figure 4.2 and Figure 4.3) Since most of the boreholes in the area are not exploited yet and the recently collected data also show similar trend, it is safe to take previous measurements and contour the potentiometric surface of the area.

Table 4-1 Static water level measurements of 2009 & 2011

SAMPLE_ID	x	y	SWL,2009	SWL,2011	SWL-Differences
MECHARE	586590	1411414	61.02	62.5	-1.48
DALETI	585461	1399571	30.2	31.1	-0.9
KM	584142	1402059	18.2	19.1	-0.9
Chercher	583164	1385941	39.2	40.3	-1.1
FRIATNA	578489	1403273	57.8	57.5	0.3
shame	577218	1419056	57		
ABERA4	576495	1390580	37.2	38.59	-1.39
DEJENA	576057	1403655	40.2	40.38	-0.18
ABERA3	575933	1389658	37.5		
SAFRON	575903	1405382	43.75	42.13	1.62
MINORA	574849	1408723	41.27	45.3	-4.03
ALEMWRGA	574513	1409306	41.8	42.3	-0.5
HAFTEMARIAM	571942	1390761	39.03	39.8	-0.77
HAFTU	571786	1401449	15.2		
REST2	570301	1402654	11.6	10.8	0.8
Galika	570242	1369977	28.4	27.2	1.2
REST1	570052	1402112	15.98	15.2	0.78
ARTESIAN	568921	1379804	-1	-1	0
TAFIE	568801	1372527	3.2	3.21	-0.01
GANDAGORO	568041	1378056	3.2	3.2	
ARTESIAN2	568006	1377084	-1	-1	
WAEKELE	567368	1412826	66.51	67.36	-0.85
AGAMTIE	566956	1376678	2.1	2.3	-0.2
ARTESIAN1	566917	1374984	-2	-2	0
Domestic2	566873	1356900	5.23	5.3	-0.07
Gebru	565322	1369341	11.89	11.88	0.01
Domestic3	565261	1378278	12.88		
HARLE	565244	1363696	4.3	4.3	
ADISHEHASHIM	565213	1378211	12.63		
rpw-89	565016	1360341	0	0	
Alamata Agro	564719	1366258	12.3	19	-6.7
DRAR	564408	1358785	5.7	4.3	1.4
BELAY TELA	564250	1363445	18.35		

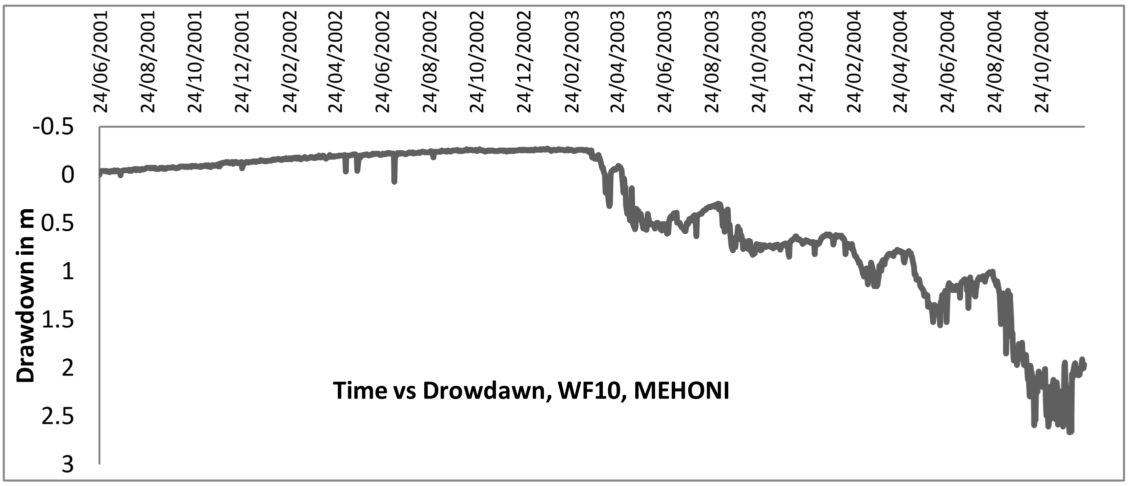

Figure 4.2 Monitored static water level measurements (Kara Adishihu), after RVADP

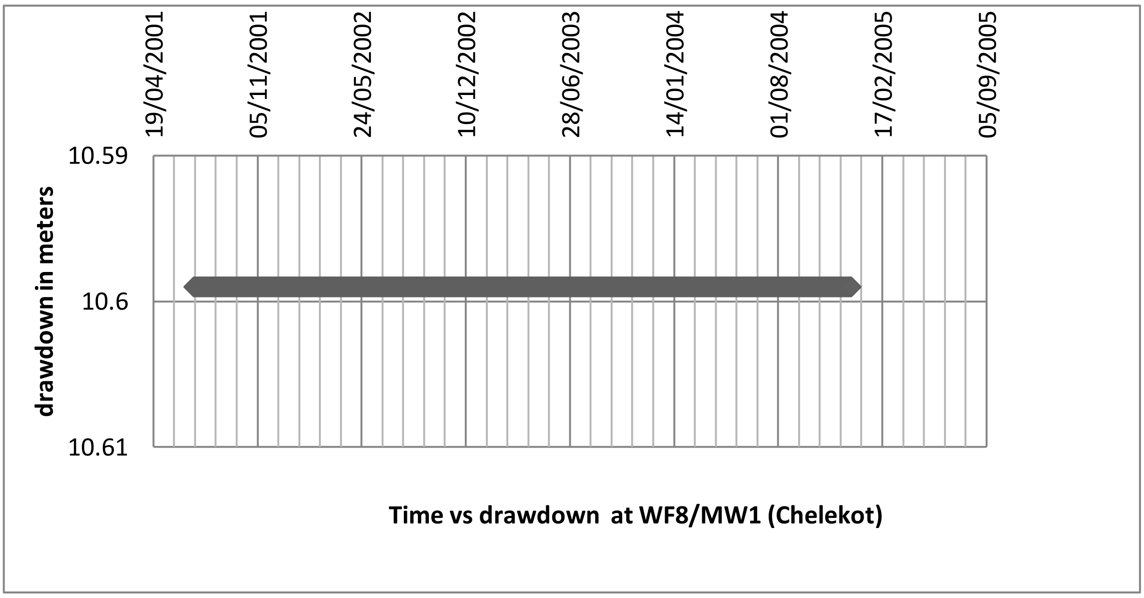

Figure 4.3 Monitored static water level measurements (Chelekot), after RVADP

4.2. GRAIN SIZE ANALYSIS OF THE ALLUVIAL SEDIMENTS

The Raya Valley is one of the highly drought prone area in the region. Owing to the developmental plan of federal and regional states, this area is supposed to be the developmental corridor for huge irrigation projects. In line with that and to combat the effect of drought, additional wells were drilled in the area. Nine borehole samples were collected for grain size analyses. Being obvious that during drilling, rocks will be crushed and soils may not maintain their original property, in order to minimize this effect, samples of boreholes drilled from a reverse circulation drilling were collected. The samples were analyzed for grain size distribution in the laboratory of Mekele University, department of Civil Engineering in 2010. Figure 4.4 shows a plot of one of the results. Then the results were used in estimating the porosity and hydraulic conductivity of the borehole samples using empirical relationship.

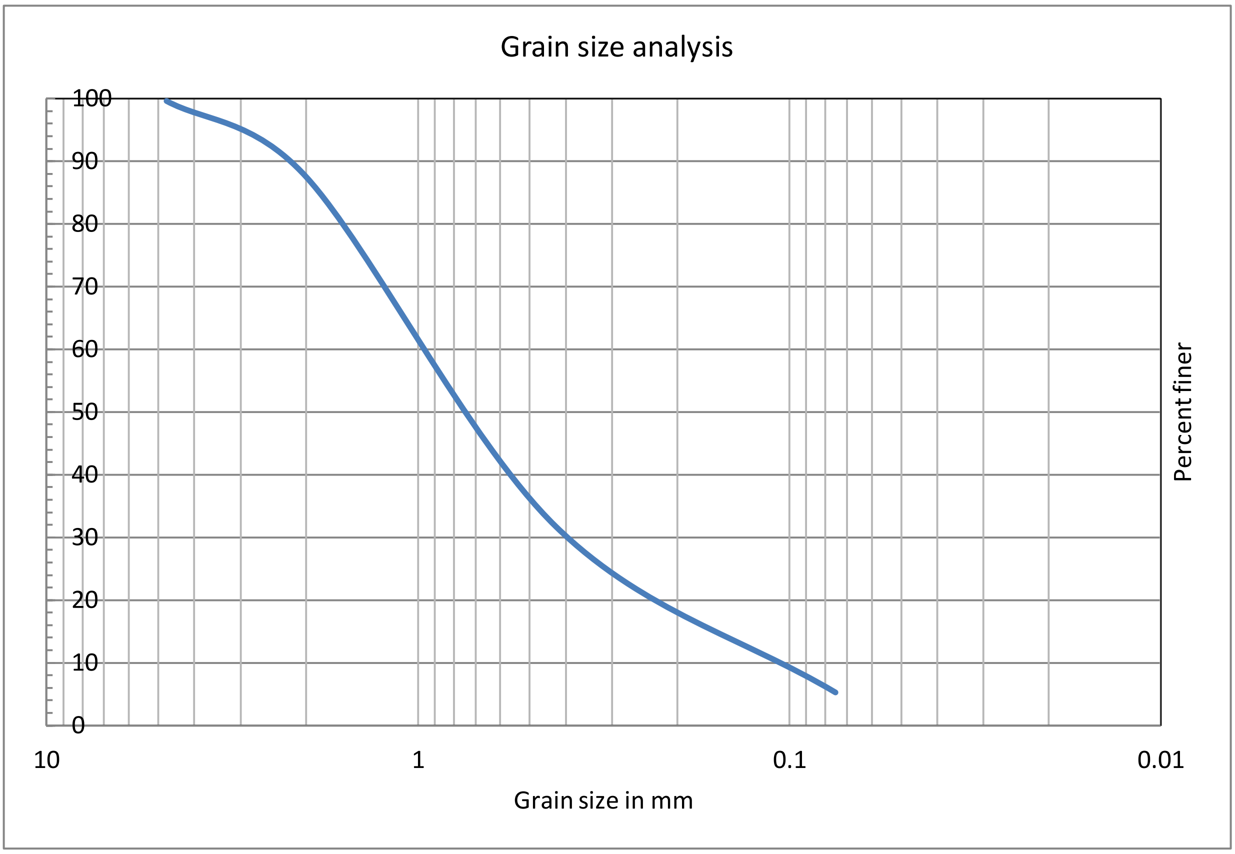

Figure 4.4 Grain size analysis plot

4.3. PUMPING TEST DATA

A pumping test consists of pumping a well, or an observation one, usually at a constant rate, and measuring the change in water level decline. Existing data of pumping tests and borehole logs were collected from Water Works Design and Supervision Enterprise (WWDSE), Tekeze Deep water well drilling and Tigray Water Works Construction Enterprise. These data were analyzed to extract important hydrogeological information such as aquifer thickness and variability, discharge rate, static and dynamic water levels. A total of 189 borehole data were collected from the respective institutions.

4.4. WATER QUALITY

4.4.1. Sampling site selection

Water samples points were selected from the existing boreholes and spring locations, in a manner that they could give clue in the groundwater flow direction in agreement with previous static water level measurements. While the selected water points were not accessible because of either they are sealed with metal sheets and not under production, alternatives points in the nearest areas were sampled for both chemical and isotopic analyses, Figure 4.5.

Once on the sites, the location of a sampling point was recorded using the Global Positioning System (GPS) (WGS-84 datum, Adindan). The date and time of sampling was also noted. The measurement of static water level of the wells, using deep meters, was made before the well is purged to remove stagnant water. Nevertheless in most cases the boreholes were found to be under continuous pumping because of the need of water either for irrigation or domestic water supply. After recording the water level, when needed, the stagnated water was removed by pumping except for artesian wells.

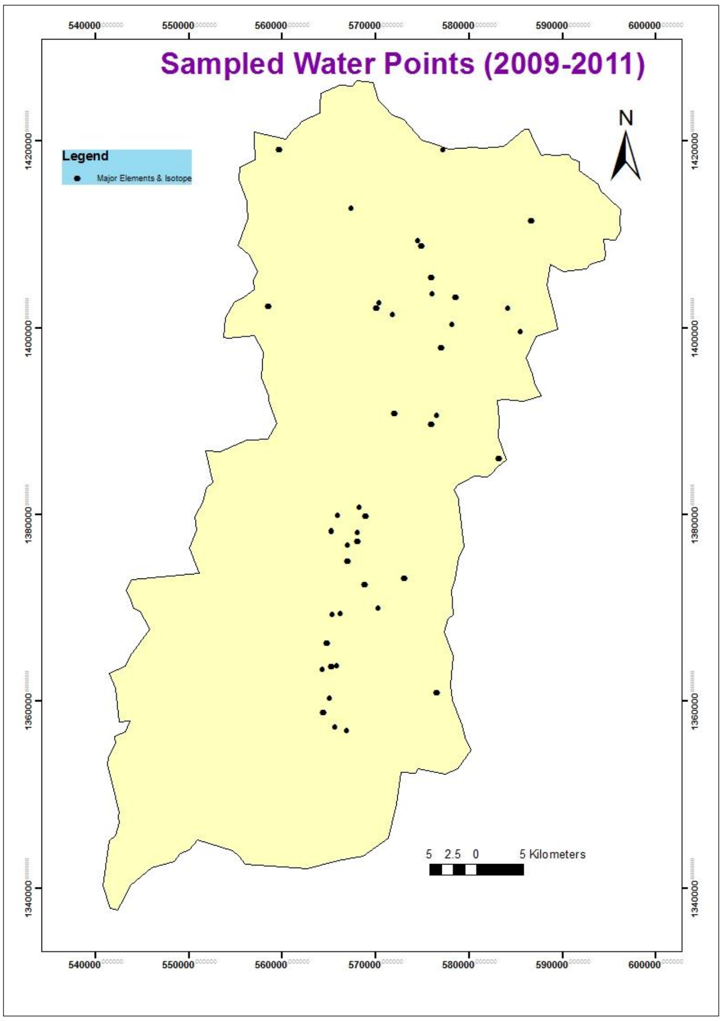

Figure 4.5 Water sampling and measurement points

4.4.2. In situ measurements

4.4.2.1. pH measurements

pH is the most common measure of acidity/alkalinity balance in a solution. It is defined as the negative logarithm (to base 10) of the hydrogen ion activity (in moles/liter) in water at 25°C. pH 7 is termed as neutral. The values above and below this values indicate the alkalinity and acidity of the water respectively. In practice few water have a pH of precisely equal to 7, and therefore refer to waters with a pH in the range between 6.5 and 8.5 as being circum-neutral (Paul L. Younger, 2007).

Before the measurement the pH meter was calibrated according to the manufacturer's requirements, using a two point calibration with buffers of known concentration. The selection of the calibration standard was dependent on the anticipated nature of the water to be sampled and calibrated with standards appropriate to the anticipated range (pH 7 and 10). Calibration standards were stored appropriately to ensure their accuracy.

The pH of borehole samples ranges between 6.6 and 8.25 and for stream samples it ranges between 7.8 and 8.5. Generally the results are within the permissible limit of the drinking water quality according to the World Health Organization (WHO) drinking water standards (1984). Therefore, the pH values of water samples of the study area indicate that there is no danger of extreme acidity or alkalinity of the water.

4.4.2.2. Temperature measurements

The temperature of the water to be sampled will generally be the mean temperature of the region that the monitored borehole is located. Temperature will move toward ambient upon sampling, so it should be recorded as soon as a stable reading is obtained after collection.

Purposes for which groundwater-temperature measurements may range from quality considerations for domestic, municipal, and industrial uses to problem solving in geology and hydrology. Groundwater temperature data may be used to study rates and directions of ground-water movement, identify areas of recharge and discharge (zones), prospect for and evaluate geothermal resources etc. In addition, temperature data can be used in modeling ground-water flow systems.

- Temperature affects chemical reactions. Generally, the rate of a chemical change is approximately doubled for each 10°C rise in temperature (Parker F. L., and Krenkel P. A., 1969);
- Because of heat conduction from the land surface, very shallow groundwater will show diurnal and seasonal temperature variations of about the same magnitude as those observed for surface-water bodies.
- Ground-water temperatures also vary with depth, owing to the geothermal gradient. Consequently, groundwater occurring 10 to 20 meters below land surface generally exceed the local mean annual air temperature by l° to 2°C. Moreover, at depths greater than 20 meters, ground-water temperatures generally reflect the geothermal gradient and, hence, usually increase by 2° to 3°C per 100 meters of depth (Collins W. D., 1925).

The groundwater temperature of the boreholes and springs of the Raya Valley was measured three times in this work. Besides, a groundwater temperature measurement that has been carried out during the construction of the boreholes was collected from respective organizations. In the analysis of the two sets of samples the trend was found to be the same, that is the temperature increases to the east and the maximum temperature was recorded in the spring near the outlet of the basin, which is above the limit of measuring instrument 50^0C. The lowest temperature is recorded in the springs of the highlands at Emba Hatsi (16.4^0C). The similarities of the trend of the results of samples collected at different periods enhance the dependability of the previously collected data and use these data as secondary source (Figure 4.6).

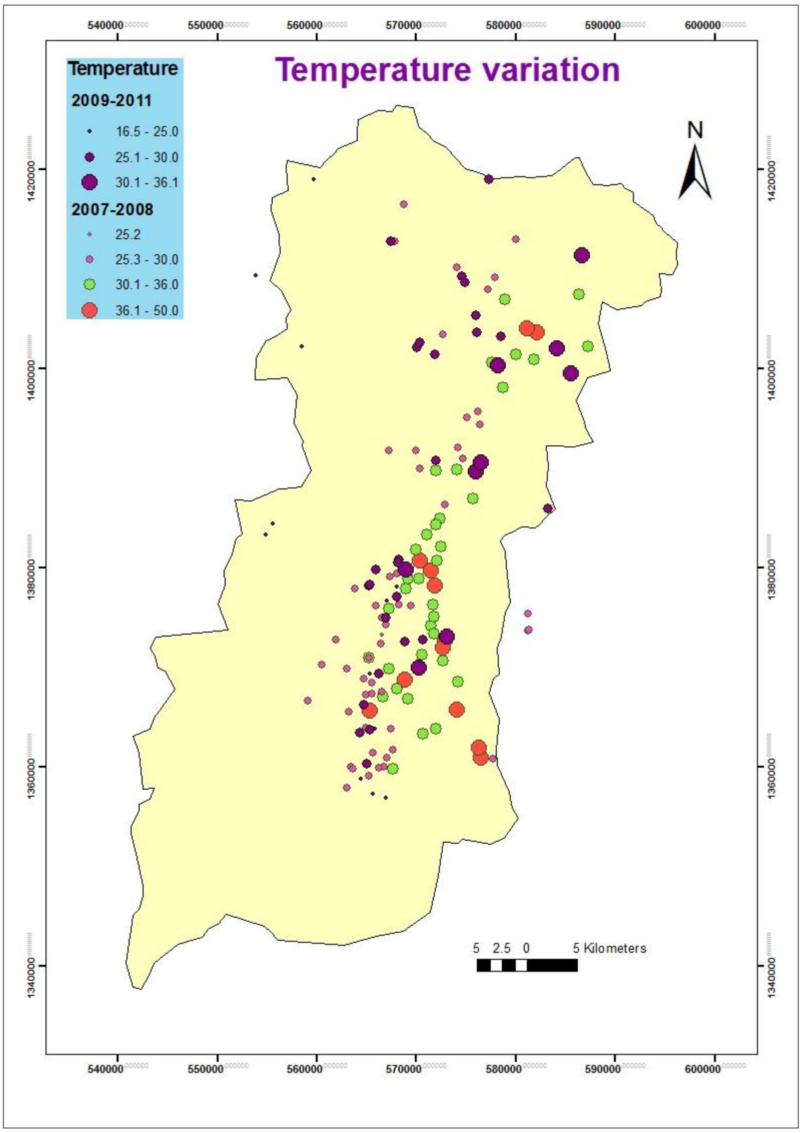

Figure 4.6 Groundwater temperature measurement points

4.4.2.3. Electrical Conductivity Measurements

It is the ability of given water to conduct electricity and it is directly proportional to the amount of dissolved substances, charged species (ions) in the water that is, the higher the concentration the higher the conductivity. The relationship between ionic content and conductivity is direct: the sum of meq/l cation or anion concentrations in the water, multiplied by 100, the resulting number should approximately very close (±10%) the conductivity of that water expressed in µS/cm (Paul L. Younger, 2007). While taking the measurements, as with pH measurement, calibration of conductivity meters was performed using standards of a known concentration.

The electrical conductivity (EC) measured during the field work vary from 503 to 1260 and from 406 to 860 µS/cm for boreholes and spring samples respectively. The springs are located up stream of the catchment and Ec values indicate that there is low residence time in which the sustained flow comes from. However, the Ec values of borehole samples vary significantly: those of the artesian wells have lower values as compared to the other samples. The boreholes at the south eastern part of the valley, near the stream out let, have records greater than 800μS/cm. This indicates that the groundwater quality with respect to the electrical conductivity decrease along the groundwater flow. The hot spring has the highest value, 2080 μS/cm.

4.4.3. Filtration, acidification and labeling of samples for chemical analysis

Filtration of samples in the field is required for laboratory measurement of cations and anions. After disassembling the two-chamber filtering unit, a 0.45 μm membrane filter was placed onto the filter holder on the lower chamber of the filtration unit. After refitting the chamber units, water was injected through the upper opening of the chamber, using a 50ml syringe, slowly. Meanwhile the filtered water is collected in plastic bottle placed at the bottom end of the filtration unit. For cations, the filtered water sample was acidified using a few drops of concentrated nitric acid. Then was closed by double plastic lids and shacked for proper mixing. For anions, no need to add any chemicals. The bottles were labeled carefully with the relevant information about the sample.

4.4.4. Stable isotope sampling

Sampling for oxygen-18 and deuterium is simple. No sample filtration or preservation is required. A 50 ml, double capped, polyethylene bottle was filled directly from the source or from a secondary container. The sample clearly labeled with all details.. Maximum care was taken to avoid evaporation of the samples during sampling, storage and transportation to the laboratory. The bottles were tightly capped with lids.

5. CHAPTER V: HYDRAULIC PROPERTIES

5.1. INTRODUCTION

Ground waters are stored in the open spaces and fractures within geologic materials such as soils and rocks occurring beneath the land surface. Pumping tests (or aquifer tests) are in situ methods that can be used to determine hydraulic parameters such as transmissivity, hydraulic conductivity, storage coefficient, specific capacity and well efficiency. Hydraulic values derived from pumping tests are averaged over the spatial zone of influence of the test.

There are 188 boreholes with important, but sometimes insufficient well test data; all of them have been utilized in the analyses, when the necessary data exist. Only five boreholes have been pump tested by means of observation wells, while the remaining are single wells without observation wells. The five boreholes with observation wells have been pumped for continuous 15 days in order to understand the hydrogeological characteristics of the aquifers. Most of the single boreholes have been pump tested for one to three days.

Calculating hydraulic characteristics would be easy if the aquifer system is precisely known. However this is not generally the case; so interpreting pumping test is primarily a matter of identifying an unknown system. System identification relies on models, the characteristics of which are assumed to represent the behavior of the aquifer system. Selection of a theoretical model is crucial step in the interpretation of pumping tests. If a wrong model is chosen the hydraulic characteristics calculated for the real aquifer will not be correct (Kruseman G.P. and de Ridder N.A., 1994).

Hence, to overcome this crucial issue, in addition to the established knowhow of the area, the following operations have been done:

firstly a systematic observation and evaluation of borehole logs was carried out: (for example the amount of clay in the lithological logging of the phreatic borehole RPW-025, is much more when compared to RPW-56 and RPW-44, artesian boreholes, and hence the clay has no determinant factor whether the borehole is artesian or not);

Secondly, a log-log and some semi-log plots of the drawdown versus time were compared to the type graphs indicated in Kruseman and de Ridder, 1994, p. 48. The semi-log and log-log plots of wells have been similar to an unconfined aquifer type (Figure 5.1). The artesian wells in the Raya Valley do not correspond to typical type curves of confined aquifers;

Thirdly, because over 80% of the screen positions were determined after granulometic analysis of the borehole samples, especially the latest 100 boreholes, their granulometic graphs illustrate that the grain size is basically well sorted and coarse grained with some intercalations of silt and clay.

In addition to the above observations, the best fit method was applied during the pumping test analysis; i.e. most of the boreholes have shown a best fit with Neumann type curve (unconfined aquifer). Those boreholes which were tested with observation wells were also considered as references during analysis.

Based on the above factors the single well pumping tests were classified as 70% with a trend of an unconfined aquifer and as 30% of confined or leaky confined aquifer. In the meantime the specific discharge of all available boreholes data of step drawdown was analyzed which enabled to identify the boreholes that could be accounted safely in the analysis because of their efficiency. Evaluating inefficient wells to estimate the aquifer properties may lead to erroneous conclusions. According to

(Walton W.C., 1962) cited in (Todd, 2005), Table 5-1, the range of values of well loss coefficient, C, can be used to differentiate boreholes that have been affected by improper construction from those with proper construction. 102 step drawdown tests have been utilized in this research where 25% are wells values less than 0.5 min2/m5, indicating properly designed and developed boreholes, 26% have less than 1 min2/m5, indicating mild deterioration or clogging, 40 % with sever deterioration and 12% are in irreversible condition.

Table 5-1 relation of well loss coefficient, C, to well conditions (after Walton)

Well loss coefficient (min^2/m^5)	Well Condition
<0.5	Properly designed and developed
0.5 to 1.0	Mild deterioration or clogging
1.0 to 4.0	Sever deterioration or clogging
>4.0	Difficult to restore well to original capacity

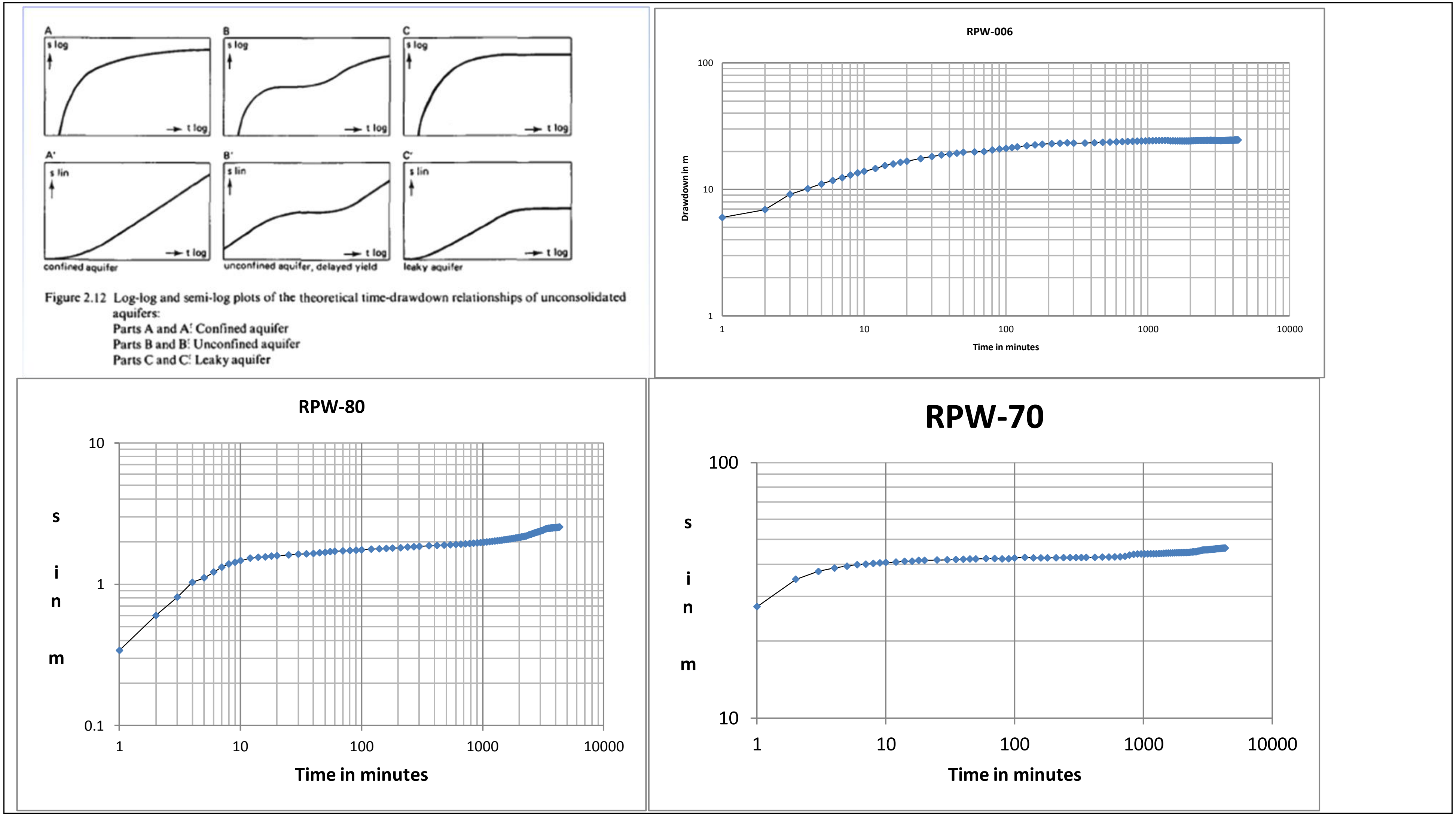

Figure 5.1 Comparison of Type Curves with borehole analysis

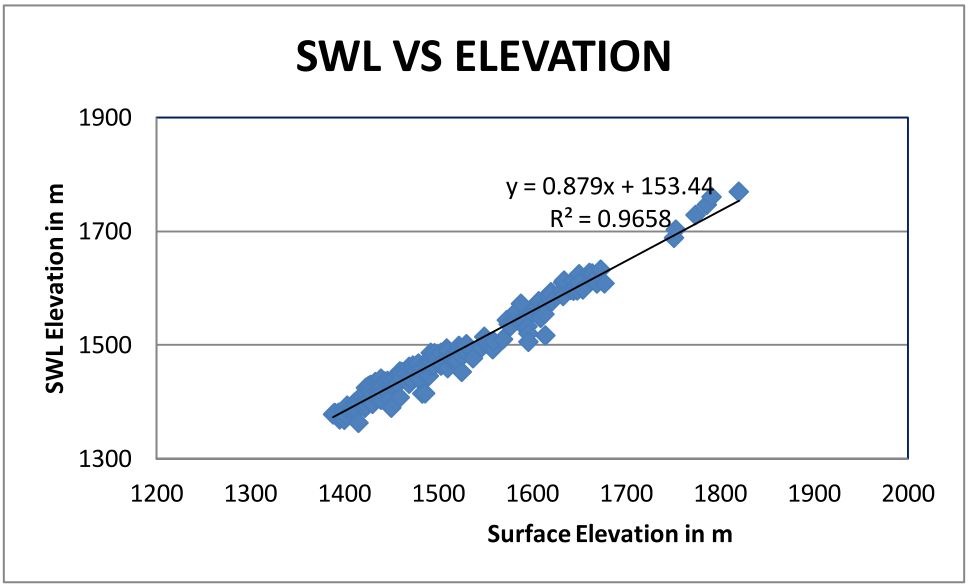

Figure 5.2 Correlation between static water level and surface elevation

5.2. ANALYTICAL METHODS

Groundwater flow is treated as flow of fluids in a porous media. It has been seen that in addition to the continuity equation and the state equation, the equation of motion should be considered in any hydrodynamic problem. However, for the fluid flow through porous media, the equation of motion is replaced by Darcy's law to obtain groundwater flow equation. All the theoretical backgrounds rely on the pumping tests carried out in extensive confined and phreatic aquifers whereby groundwater flow to the pumped well is either in steady state or unsteady state (Paul L. Younger, 2007)

5.2.1. Steady state flow in aquifers

(Dupuit. J., 1863) was the first who combined Darcy's law with the continuity equation to derive an equation for well discharge. He stated the following assumptions 1) the velocity of flow has to be proportional to the tangent of the hydraulic gradient instead of the sine as defined by Darcy's law 2) the flow has to be horizontal and uniform everywhere in the vertical section.

(Thiem G., 1906) was the first to use two or more piezometers to determine the aquifer transmissivity. He showed that the well discharge for confined aquifers can be expressed as:

For an unconfined aquifer:

where kD is aquifer transmissivity (L^2/T), Q is pumping rate (L^3/T), h_2 and h_w are the head levels above the impervious bed at distance r_2 and r_w (L) from the pumping well.

Equation (2) can be used if the following assumptions and conditions are satisfied:

- The aquifer has seemingly infinite areal extent.
- The aquifer is homogeneous and of uniform thickness over the area influenced by the test.
- Prior to pumping, the water table is horizontal over the area influenced by the test.
- The aquifer is isotropic.
- The aquifer is pumped at a constant discharge rate
- The aquifer is unconfined
- The flow to the well is in an unsteady state.
- The well penetrates the entire aquifer and thus receives water from the entire saturated thickness of the aquifer
- The flow to the well is in a steady state
- Should fulfill Dupuit's assumptions

5.2.2. Unsteady state flow in aquifers

5.2.2.1. Newman, non radial flow in unconfined aquifers

A graphical method for analysis of aquifer test in unconfined aquifers has been developed by Newman, 1975. This method is based on the following assumptions:

The aquifer is unconfined, the vadose zone has no influence on the drawdown, water comes from the instantaneous release of water from elastic storage, eventually water comes from storage due to gravity drainage of interconnected pores, the drawdown is negligible as compared to the saturated aquifer thickness, and the aquifer may be anisotropic. Hence the solution is given by:

where the well function for water table aquifer and found in tabulated form.

where

= drawdown (L; m or ft)

Q = Rate of discharge in (L^3/t; m^3 or ft^3/day)

r = Radial distance from well (L; m or ft) (Placeholder1)

T = Transmissivity of the aquifer in (L^2/t; m^2 or ft^2/day)

S_y = Specific yield, dimensionless

S = Storativity, dimensionless

t = time in days

k_v = Vertical hydraulic conductivity(L/t; m or ft/day)

k_h = Horizontal hydraulic conductivity(L/t; m or ft/day)

b = Initial saturated thickness of the aquifer (L; m or ft)

5.2.2.2. Hantush-Jacob method for leaky confined aquifers

Most confined aquifers are not totally isolated from sources of vertical recharge. Less permeable layers, either above or below the aquifer, can leak water into the aquifer under pumping conditions. Walton developed a method of solution for pumping tests (based on Hantush-Jacob, 1955) in leaky-confined aquifers with unsteady-state flow. The flow equation for a confined aquifer with leakage is:

Where:

K' is the vertical hydraulic conductivity of the leaky aquitard

b' is the thickness of the leaky aquitard

The Walton solution to the above equation is given by

where:

where W(u,r/B) is known as the Leaky well function (Freeze, R.A and Cherry, J.A., 1979)

The well function is a function of both u and r/B, which are defined as:

The leakage factor, B, and the hydraulic resistance, c, are defined as:

If K' = 0 (non-leaky aquitard) then r/B = 0 and the solution reduces to the Theis solution for a confined system.

A log/log scale plot of the relationship W(u,r/B) along the Y axis versus 1/u along the X axis is used as the type curve as with the Theis method. The field measurements are plotted as t along the X axis and s along the Y axis. The data analysis is done by curve matching.

The Hantush-Jacob solution has the following assumptions:

- The aquifer is leaky and has an "apparent" infinite extent
- The aquifer and the confining layer are homogeneous, isotropic, and of uniform thickness over the area influenced by pumping
- The piezometric surface was horizontal prior to pumping

- The well is pumped at a constant rate
- The well is fully penetrating
- Water removed from storage is discharged instantaneously with decline in head
- The well diameter is small, so well storage is negligible
- Leakage through the confining layer is vertical and proportional to the drawdown
- The head in any un-pumped aquifer(s) remains constant
- Storage in the confining layer is negligible
- Flow is unsteady

The data requirements for the Hantush-Jacob (no aquitard storage) solution are:

- Drawdown vs. time data at an observation well
- Distance from the pumping well to the observation well
- Pumping rate (constant)

5.2.3. Theis recovery method

In a classic paper, (Theis C.V., 1935) applied the principle of superposition to derive an exact solution for the recovering water levels in a well by summing two draw downs: one (s'), caused by imaginary continuation of the original pumping and the other (s), due to an imaginary injection at the same constant rate. Since then, many have developed simplified methods for estimating T and S from recovery data by approximating the exact Theis solution:

where

When u and u' are sufficiently small for u<0.01. The above equations can be approximated by

where

s' residual drawdown

r distance in m from well to piezometers

KD (T) transmissivity of the aquifer in m^2/day

S' Storativity during recovery, dimensionless

S Storativity during pumping, dimensionless t time in days since the start of pumping

t' time in days since the cessation of pumping

Q rate of recharge = rate of discharge in m^3 per day

The method is strictly applied to confined aquifers which are fully penetrated by a well that is pumped at a constant rate. However this method may also be applied for unconfined aquifers where the residual drawdown is much less than the aquifer thickness and for late time recovery data. The Theis recovery method is applicable to data from single well recovery tests conducted in confined, leaky or unconfined aquifers (Kruseman G.P. and de Ridder N.A., 1994). Since the residual drawdown of the wells in the Raya Valley is much less than the aquifer thickness this method was applied in the estimation of hydraulic properties of the aquifer.

5.3. PUMPING TEST DATA PRESENTATION AND ANALYSIS

5.3.1. Introduction

From the data and the explanation that has been discussed previously, it is evident that the aquifer in the Raya Valley is considered to be mainly unconfined aquifer. Thus pumping test analysis was carried out in line with this assumption. Therefore, using the aquifer test analysis software (aquifer test v3.02), the values of the hydraulic properties has been estimated. In this regard the boreholes with observation wells were used as reference for the interpretation because they basically fulfill the required assumption to carry out the analysis.

The Raya Valley is sub divided into a total of 14 well fields (WF0 to WF13) distributed along different parts of the valley. However, pumping test with observation wells is carried out only on five of these well fields (Figure 5.2). The aquifer test of these well fields included five production wells (central wells) with five observation wells each. The configuration of the central and observation wells is given in Figure 5.4. The lithological logs of these boreholes do not indicate the presence of any significant confining layer within the Sand and Gravel aquifer at the sites.

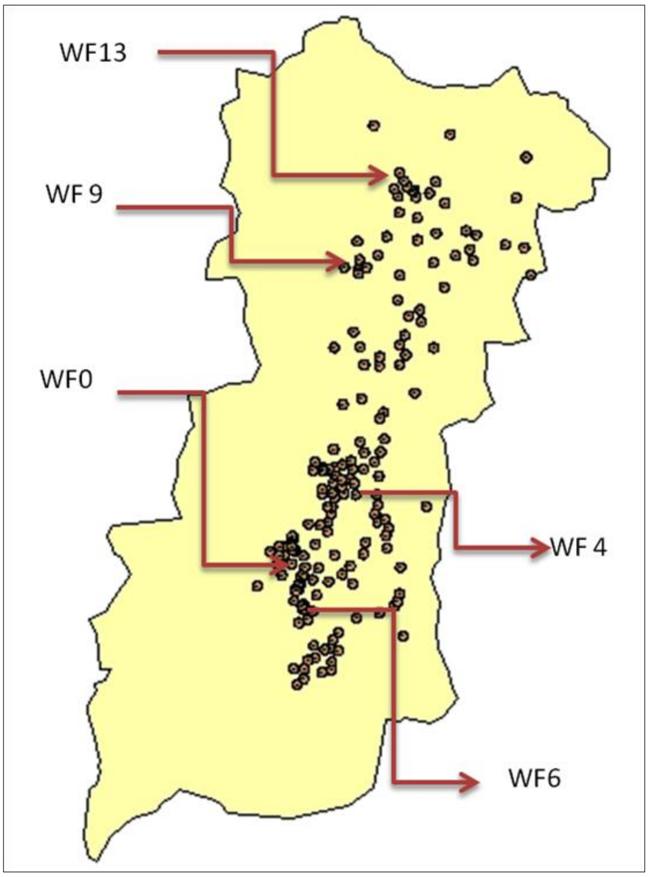

Figure 5.3 Location of some of the well field in the Raya Valley

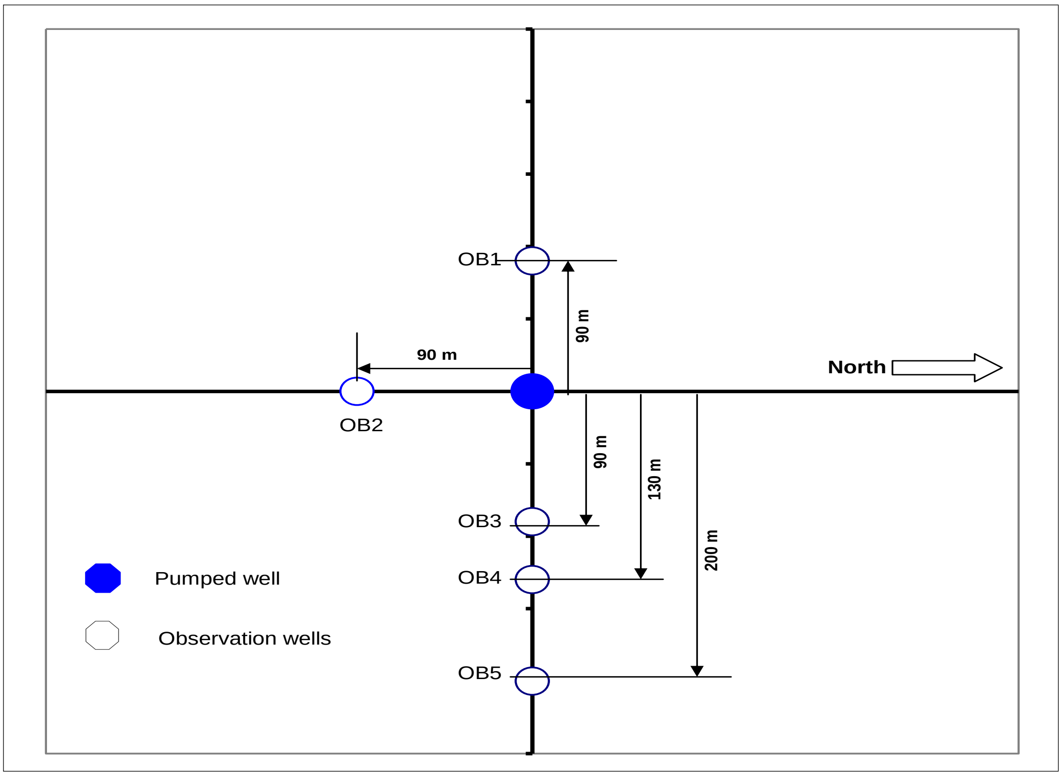

Figure 5.4 configuration of central and observation wells, after WWDSE 2008

The central wells were pumped for 15 days of continuous pumping with discharges determined from previous measurements. Accordingly WF9BH3, WF13BH5, WF6BH3, WF4BH2 and WF0BH2 were pumped at 30l/s, 49.7 l/s, 30l/s, 49.7 l/s and 33.8 l/s respectively. Meanwhile water Level measurement of the central wells and of the observation wells was carried out at a specified time interval (Table 5-2).

Table 5-2 Dynamic water level measurement intervals

Frequency of water level	From	To
1 min	1 min	**10 min**
2 min	10 min	**20 min**
5 min	20 min	**50 min**
10 min	50 min	**100 min**
20 min	100 min	**180 min**
30 min	180 min	**360 min**
1 hour	360 min	**18 hrs**
2 hour	18 hrs	**168 hrs**
4 hour	**168 hrs**	**360 hrs**

A brief description of the observations from the data of WWDSE, 2008 are stated below:

The central wells in **Well Field 13 (Wargeba)** and **Well field 9 (Wara Abaye)** were pumped for 15 days with a discharge of 49.7 l/s and 30 l/s respectively. During the test a certain number of rainy days occurs, however the water level measurements versus time on central well and observation wells were smooth (Figure 5.5 a & b).

The central well in **WF0** was pumped for 15 days with a discharge of 33.6 l/s. The test was carried out in a dry season and the water level measurements versus time on central well and observation wells were smooth except fluctuations attributed to power supply interruptions (Figure 5.5c).

Well Field 6 the dynamic water level measurements of observation wells 1 (OB1), 90 meter west of the central well, showed different static water level than the other observation wells (Figure 5.5d).The drawdown in OB1 was insignificant and recovered 100% while the others observation well recovered only about 80% in fixed time interval (800minutes), indicating that the central well and OB-2 to OB-5 are found in the same aquifer while OB-1 is found in different aquifer.

Well field 4 (Gerjele) The water Level measurement on central well first declined for 3.81 meters, which is the maximum, up to the 1080th minutes (the first day) after which it started rising up gradually. Hence pumping the well, for the remaining 14 days, has shown a rise of 0.41 meters and the final dynamic water level was 3.4 meters. The observation wells have also responded in a similar pattern to the central well (Figure 5.5e).

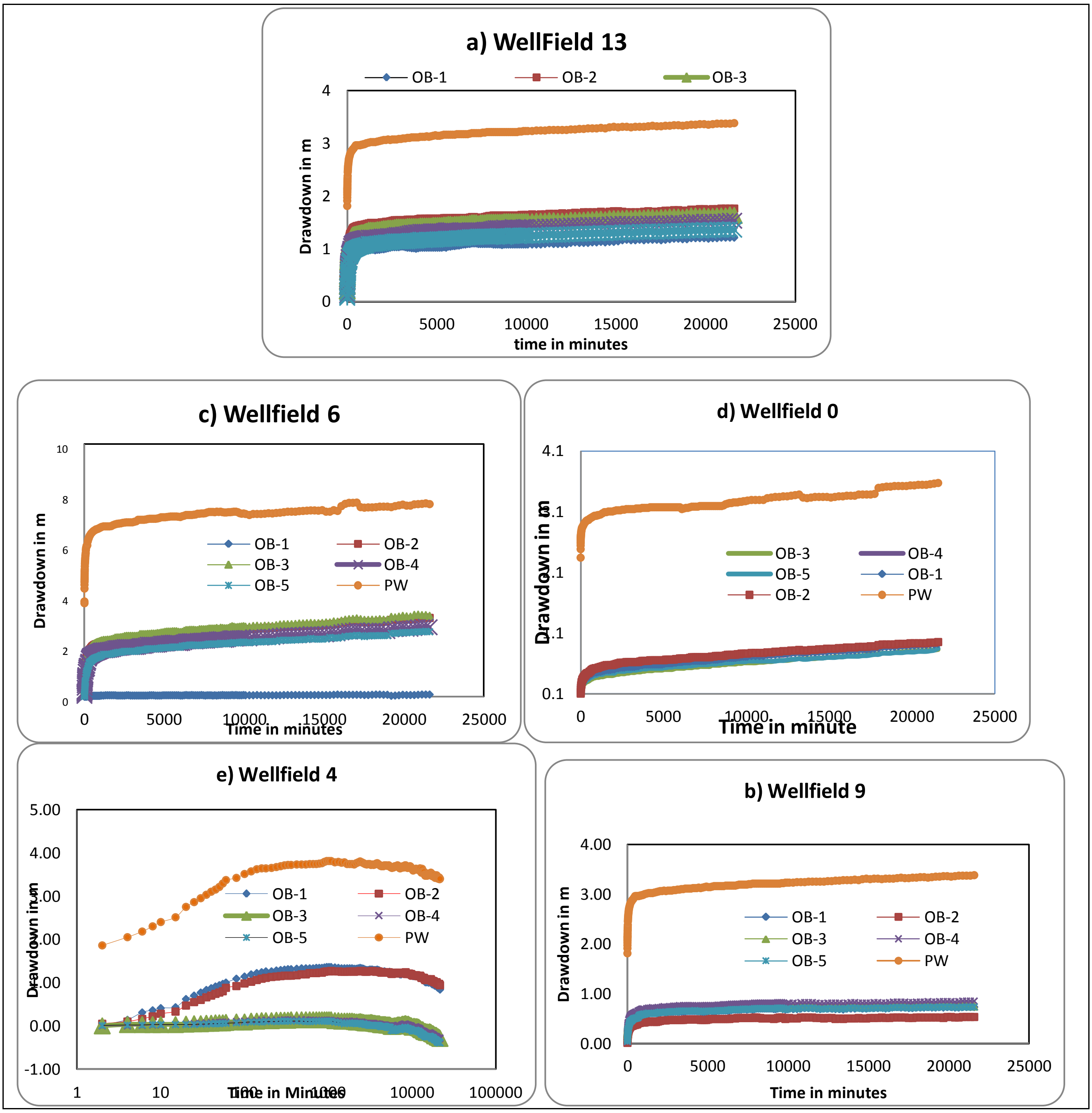

Figure 5.5 Log-Semi Log plots of well fields

The central wells were drilled by REST (Relief Society of Tigray) from the end of 2004 to the beginning of 2006. Step drawdown and constant test pumping was carried out on each borehole to evaluate the hydraulic characteristics of the aquifer. The duration of step drawdown test was uniform for every borehole: i.e. four steps of 90 minutes each. The continuous test periods differ from one well to the other and range between 1.3-2.5 days of pumping. The dynamic water level measured, the discharge and the duration were documented and have been used to compare with the results of the continuous pumping test carried out for 15 days (Table 5-3).

These boreholes were tested under different discharge rates, except WF9/BH3 (Table 5.3), time and pumping periods. However a plot of the dynamic water levels and the specific yield of the two periods in each well showed a strong correlation of r^2=0.9922 and r^2=0.9871 respectively (Figure 5.6). It is important to note that these well fields cover important parts of the valley and the regression equation hence could be utilized for initial estimation of the possible drawdown by assuming different discharge rate or drawdown of wells drilled in the vicinity.

Table 5-3 Summary of data of well fields

	Single well test			With observation wells		
Well fields	**Time (minutes)**	**Discharge (l/s)**	**Drawdown (m)**	**Time (minutes)**	**Discharge (l/s)**	**Drawdown(m)**
WF9/BH3	3120	30	11.44	21600	30	13.74
WF13/BH5	2880	43.8	2.44	21600	49.7	3.38
WF6/BH3	3120	35	6.43	21600	30	7.61
WF4/BH2	1920	46	3.38	21600	49.7	3.4

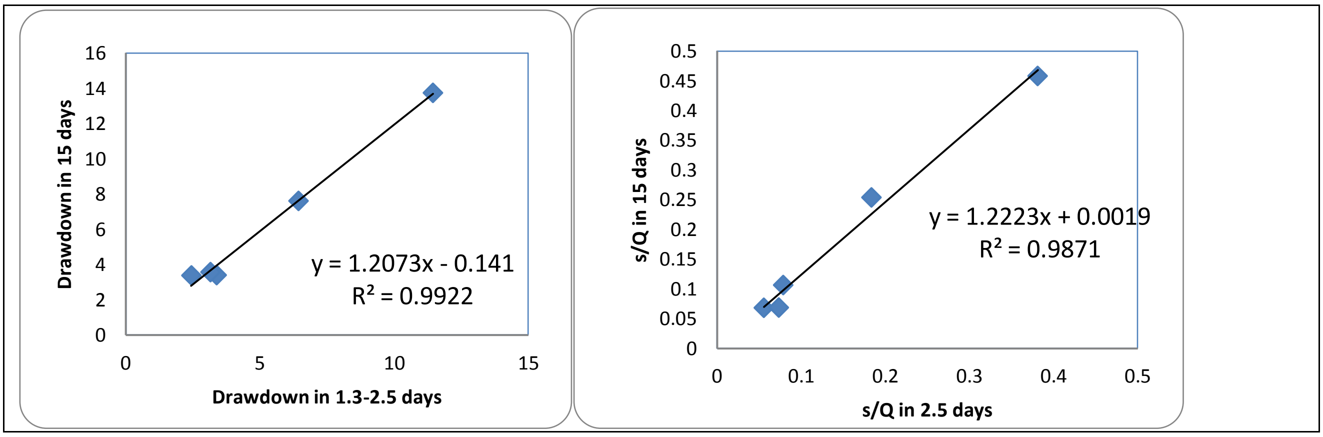

Figure 5.6 Comparison of drawdown & specific yield for different lengths of pumping time

5.3.2. Boreholes with observation wells

5.3.2.1. Continuous test

Pump test data analysis of the 3 boreholes with observation wells, located at different parts of the valley, and their borehole lithological description is given below. For the other wells, only the results of the analysis and a sample lithologic log are indicated.

WF -13 is located in the northern part of the Raya Valley and is 132m deep, with a static water level at 36.2 m below the ground surface. The borehole lithologic log (Figure 5.8) indicates that the main water bearing formation is an alternating fine to coarse sand, gravel, pebbles and cobles without significant clay layer. After 15 days of pumping at 49.7 l/s, the drawdown in the pumped well and observation wells 1 to 5 was 3.38, 1.21, 1.76, 1.63, 1.53 and 1.36 m respectively. The Newmann method (Figure 5.7) was applied to evaluate the hydraulic properties: the transmissivity of the aquifer is 1500 m^2/day when observation well 1 is considered. Considering a saturated thickness of 95.8 m, the hydraulic conductivity is calculated to be 15.7 m/d. The specific storage is estimated to be 0.14.

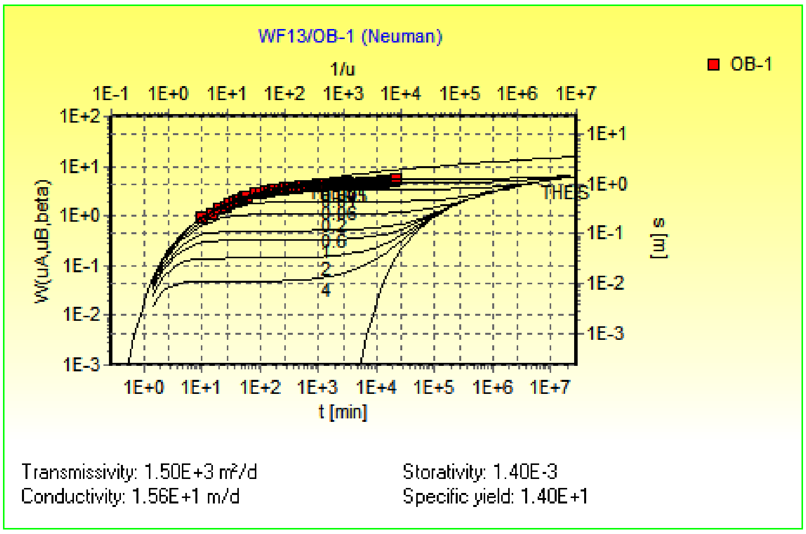

Figure 5.7 Graph showing pumping test data analysis of well field 13, Neuman method

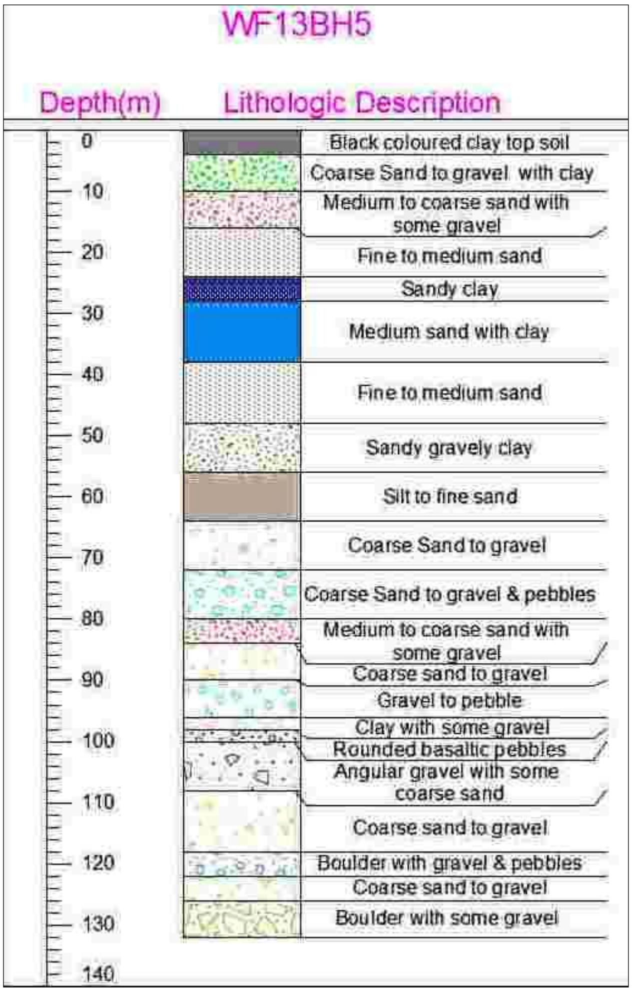

Figure 5.8 Lithologic log of the central well in well field- 13

WF -9 is located in the central western part of the Raya Valley and the well is 128m deep, with a static water level at 20.66 m below the ground surface. The borehole lithologic log (Figure 5.10) indicates that the main water bearing formation is an alternating medium to coarse sand, gravel, pebbles and cobles without significant clay layer. After 15 days of pumping at 30 l/s, the drawdown in the pumped well and observation wells 1 to 5 was 13.74, 0.73, 0.53, 0.74, 0.85 and 0.73 m respectively. The Newmann method (Figure 5.9) was applied to evaluate the hydraulic property and the transmissivity of the aquifer is 2060 m^2/day when observation well 2 is considered. Considering a saturated thickness of 107.34 m, the hydraulic conductivity is calculated to be 19.19 m/d. The specific storage is estimated to be 0.23.

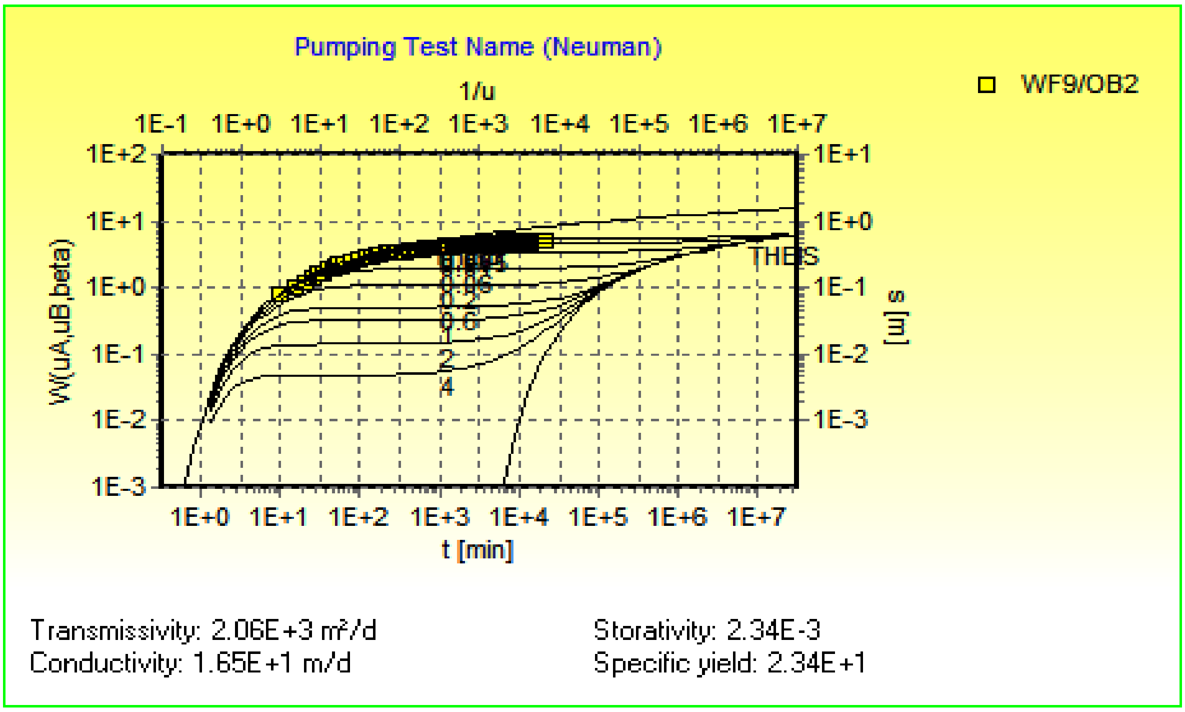

Figure 5.9 Graph showing pumping test data analysis of well field 9, Neuman method

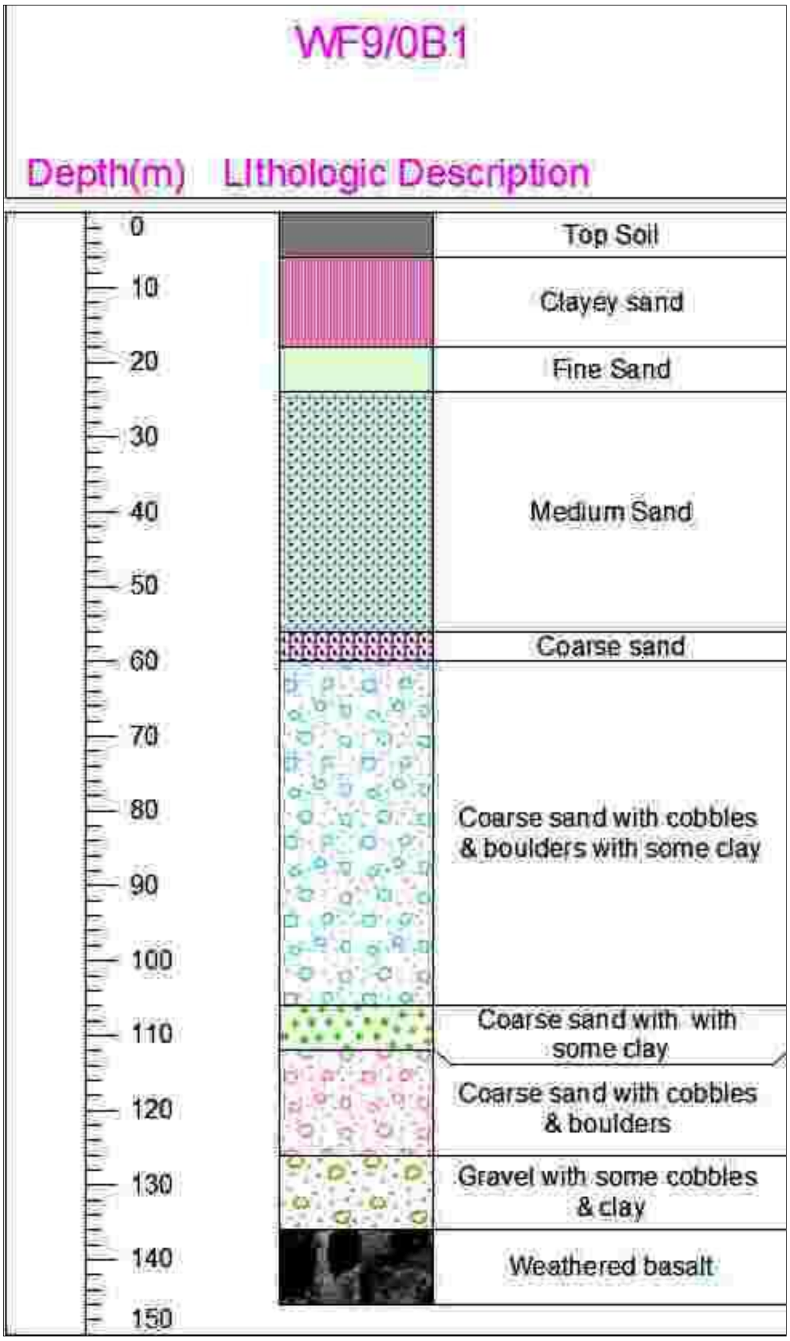

Figure 5.10 lithologic log of the observation well-1 in well field -9

WF -0 is located in the southern part of the Raya Valley and the well is 88m deep, with a static water level at 10.37 m below the ground surface. The borehole lithologic log (Figure 5.12) indicates that the main water bearing formation is an alternating fine, medium to coarse sand without significant clay layer. After 15 days of pumping at 30 l/s, the drawdown in the pumped well and observation wells 1 to 5 was 3.57, 0.92, 0.95, 0.83, 0.91and 0.85 m respectively. The Newmann method (Figure 5.11) was applied to evaluate the hydraulic property and the transmissivity of the aquifer is 1600 m^2/day when observation well 2 is considered. Considering a saturated thickness of 77.63 m, the hydraulic conductivity is calculated to be 20.6 m/d. The specific storage is estimated to be 0.21.

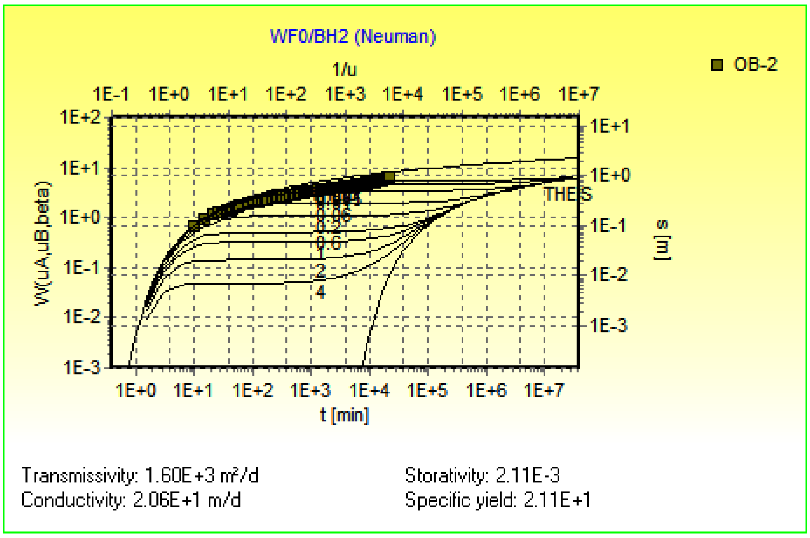

Figure 5.11 Graph showing pumping test data analysis of well field -0, Neuman method

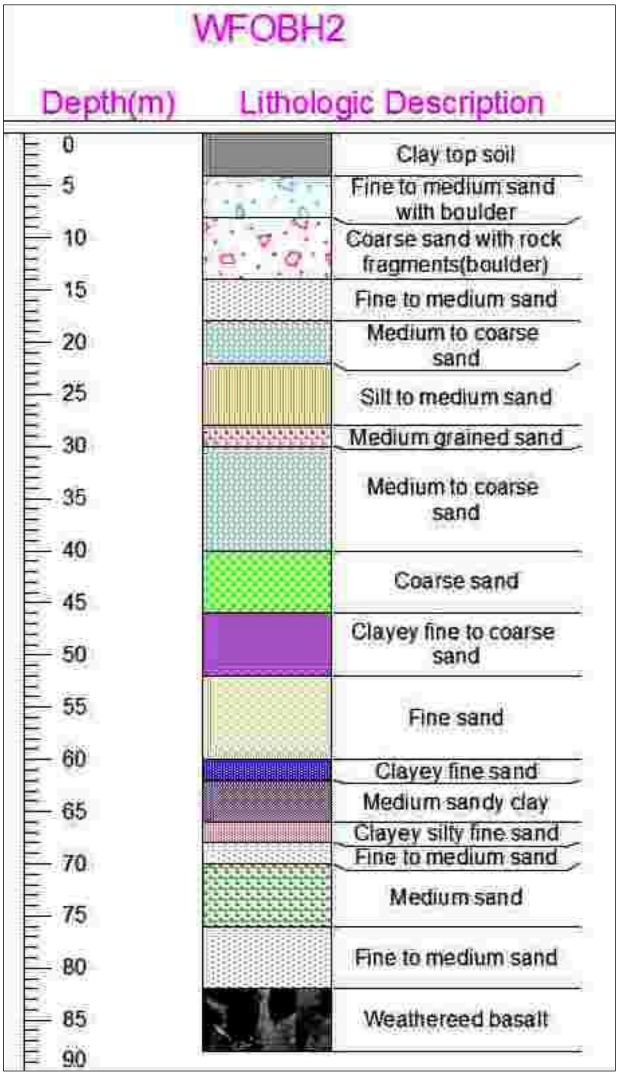

Figure 5.12 Lithologic log of the central well in well field -0

Regarding well field 4, the artificial gradient created by pumping in the first day (1080 minutes) is 3.81 meters and tends to rise up indicating the recharge is greater than the discharged water. There could be three possibilities which should be ruled out; these are either

- The borehole is taping a coarse grained buried channel with higher hydraulic conductivity to compensate the discharged water or
- The gradient created is high enough to encounter a fault zone which could supply enough amount of water or
- The pumping rate was higher in the beginning and the rate of discharge was reduced because of efficiency or other technical problems or
- a mixture two or more reasons

The lithologic log of the pumped well indicates high proportion of permeable zones of gravel and mixture of gravel and boulder which are devoid of significant clay material. In the meantime, the lithologic logs of the observation wells, those with similar response to pumping, have considerable proportion of gravel and sand (Figure 5.13). Therefore, the area is of high permeability zone. This means when a borehole is pumped in the area under consideration there is an immediate replenishment from the surrounding to compensate the created artificial gradient. But highly permeable aquifer gives water back proportional to flow of water from the aquifer. Hence the possibility of rise of the water level due to high permeability is unacceptable.

The Raya Valley, in response to its location in the rift margin, is affected by different regional and local geological structures. However, there is no visible geological structure crossing the well field under consideration different from the other well fields.

Therefore, the reason for the rise of dynamic water level in the well field is due efficiency drop of the pump or other technical problems related to it. To understand the behavior of the aquifer in this area it is necessary to overcome the rate of replenishment and create the gradient required for estimating hydraulic properties of the aquifer.

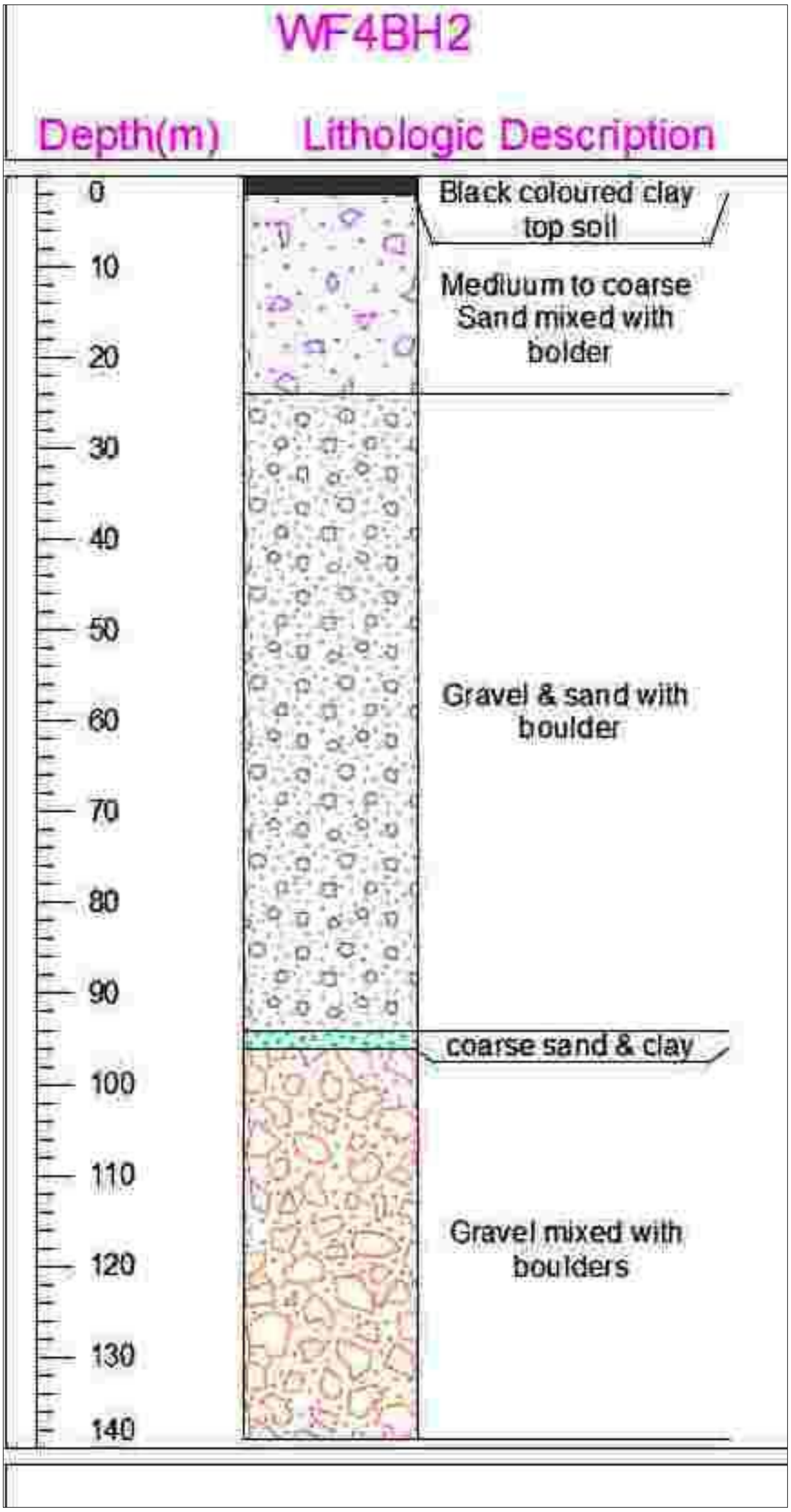

Figure 5.13 Lithologic log of the central well in well field - 4

5.3.3. Single well analysis

5.3.3.1. Continuous tests

The measurements are made in the pumping well itself, only the transmissivity can be calculated from the time drawdown graph, and not the storage coefficient. The hydraulic conductivity can be obtained by dividing the transmissivity by the saturated thickness of the water bearing layers tapped by the well screen. The saturated aquifer thickness is calculated based on whether the well is artesian, leaky or phreatic. For leaky and artesian wells, the thickness is estimated based on the level at which water was struck during the drilling of the well (in this case below the first screen position because the water struck is not know due to the drilling method, Mud system) and the cumulative thickness of the water bearing layers below the water strike level. For phreatic wells, the saturated thickness is calculated by taking the thickness of all water bearing layers below the static water level. Most boreholes in the Raya Valley, tape an unconfined aquifer and hence were analyzed using the mathematical models of Neumann, Jacob and Theis . The drawdown was adjusted before applying the Jacob and Theis methods because these methods, originally designed for confined aquifer tests, can be applied after correction factor set by Jacob. The measured drawdown in wells pumping unconfined aquifers were corrected for decreasing saturated thickness using the relation established by (Jacob, 1944).

where: Swcor is the corrected drawdown, Sw the measured drawdown and H the original saturated thickness of the aquifer. The software applied in calculating the hydraulic properties, WHI Aquifer test version 3.02 of Waterloo Hydrogeologic, Inc.2001, has the ability to carry out the correction if pumping test for an unconfined aquifer is selected by the user. Hydraulic conductivity varies from 0.03- 25.47m/day and transmissivity 7.5 -3117.1m^2/d. The water bearing horizons of each borehole were extracted from lithologic logs and subtracted from the total depth before estimating the hydraulic conductivity. An example of the analyzed boreholes is Figure 5.14 and the results of each analyzed borehole is given in Table 5-4

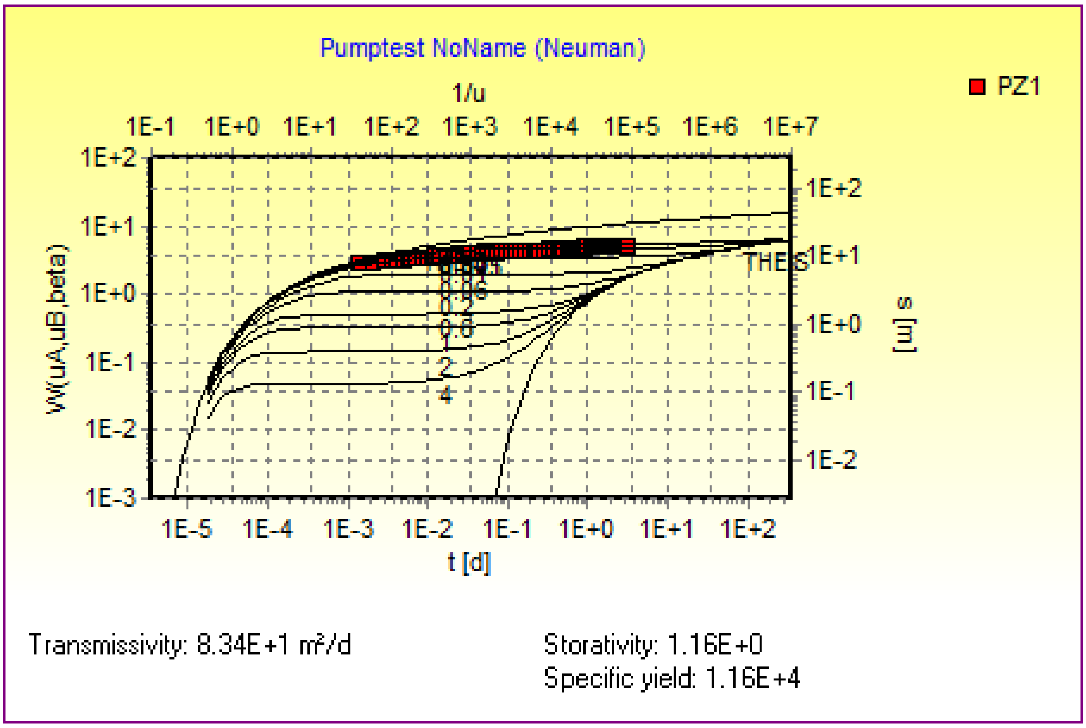

Figure 5.14 Pumping test data analysis of PZ1, Neuman method

5.3.3.2. Artesian wells

In the valley floor five artesian wells occur. These boreholes are clustered in the swampy area, locally known as Gerjalle. The estimated level above ground level of these boreholes is between 1 and 2 meters. Most of these boreholes have yield exceeding 50 liters per second. Their lithological logs do not show any significant confining unit having much less clay content than the phreatic boreholes in the area. However their location is directly related to local depressions as shown in Figure 5.15

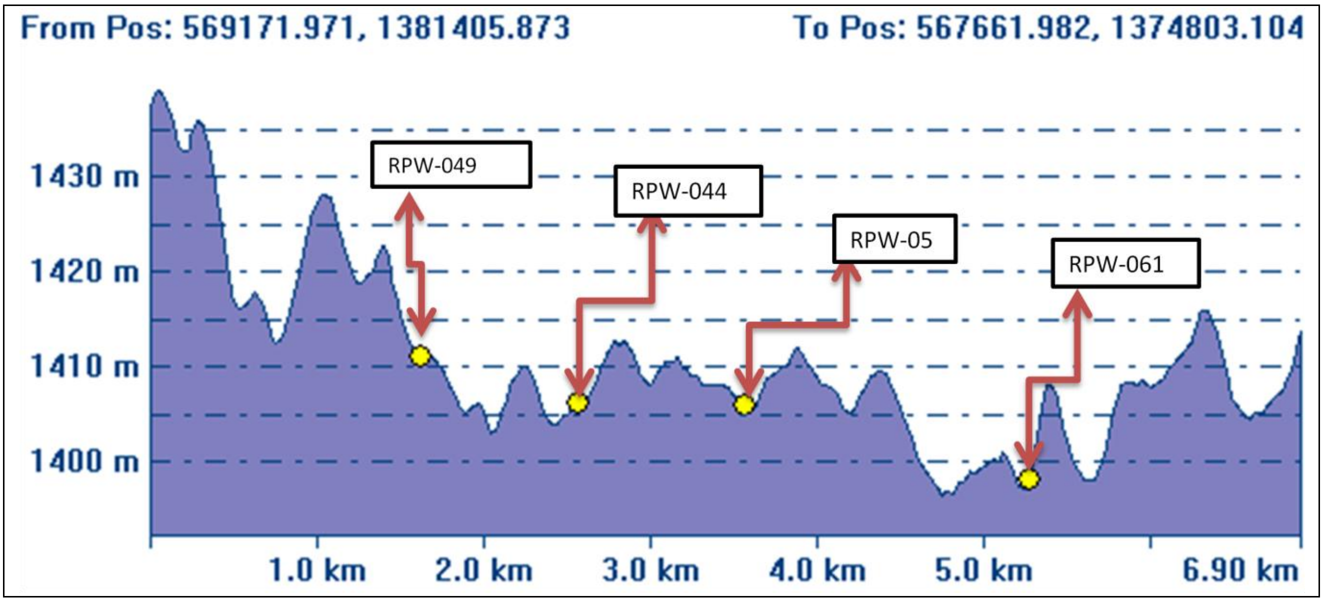

Figure 5.15 Position of the artesian wells along the flow line

5.3.3.3. Recovery test

This method is mainly used to counter check the reliability of aquifer parameter results calculated from pumping test data. When the pump is shut down after a pumping test, the water levels in the well will start to rise. This rise in water level is known as residual drawdown, s', Where s' is the drawdown expressed as the difference between the original water level before the start of pumping and the water level measured at a time t' after the cessation of pumping. Residual draw down data are more reliable than pumping test data because recovery occurs at a constant rate, where as a constant discharge during pumping is often difficult to achieve in the field. The Theis and Jacob recovery method is applied by using the Aquifer Test program in all wells which have recovery data; after the constant pumping test, the recovery data were analyzed to estimate the hydraulic properties (Figure 5.16).

The Transmissivity values estimated by continuous pumping and those obtained from recovery test have fair correlation as shown by the Figure 5.17; Table 5-4 contains the borehole data and results of the analysis carried out on each borehole.

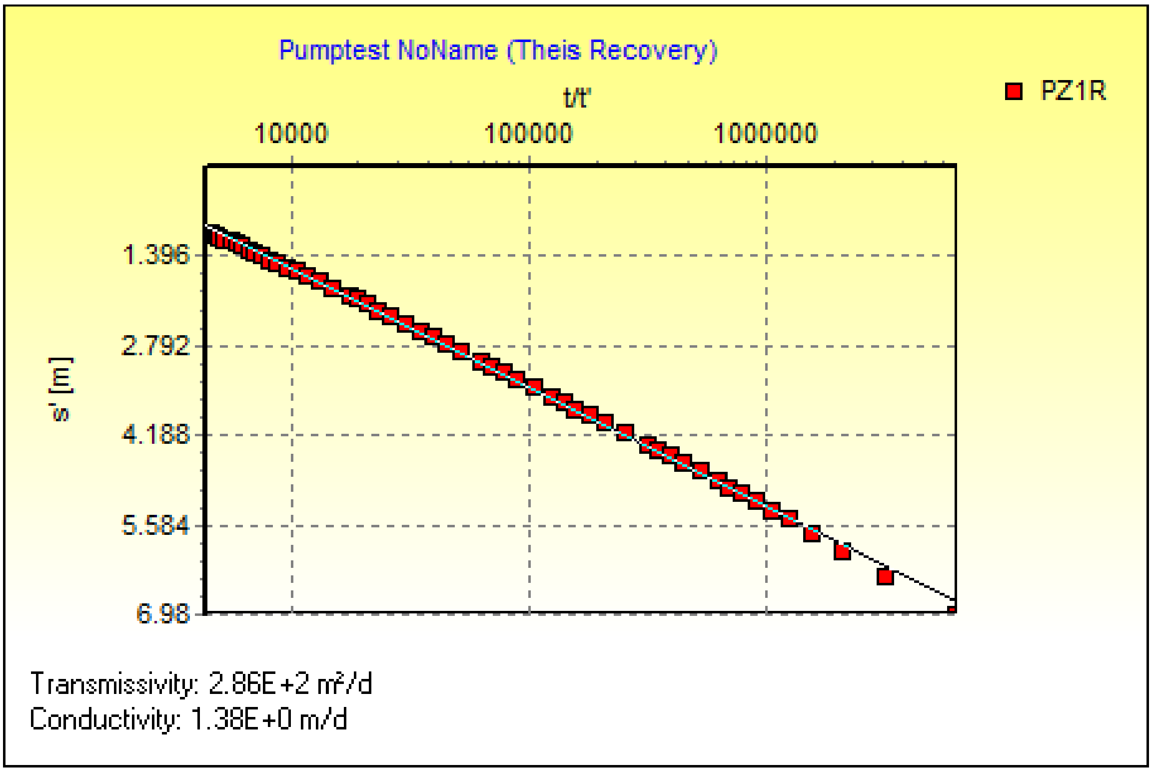

Figure 5.16 Plot of recovery test data analysis PZ1

Hydraulic conductivity varies from 0.078 to 25.8 m/day and transmissivity from 7.8 to 3156 m^2/d. The water bearing horizons of each borehole were extracted from lithological logs and subtracted from the total depth, before estimating the hydraulic conductivity.

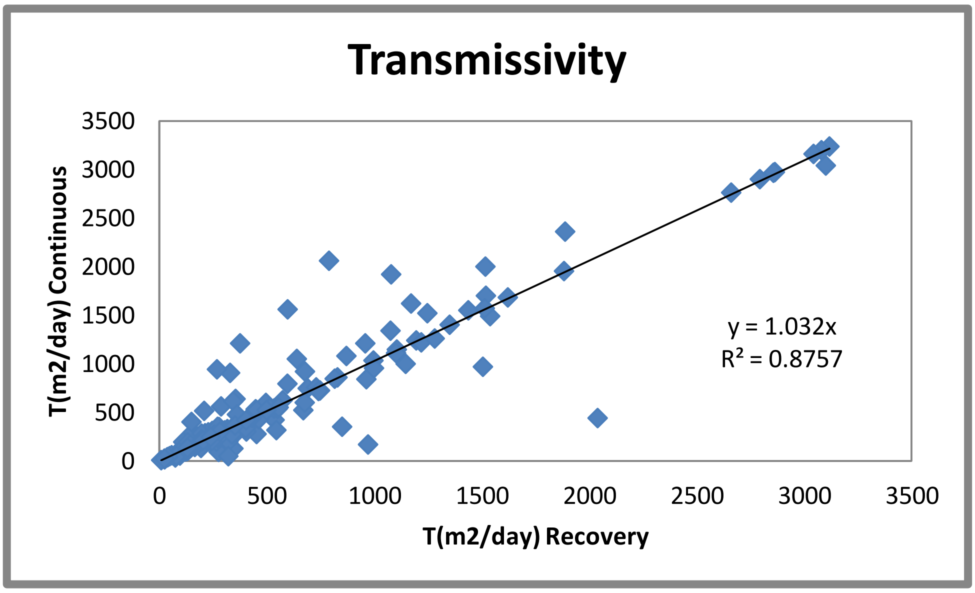

Figure 5.17 Correlation between transmissivity values of continuous pumping and recovery tests

Table 5-4 Summary of pumping test results of transmissivity and head loss

Well index	X	Y	Elevation, m	Well depth, m	saturated thickness (of alluvial only)	SWL, m	Q, l/s	DD, m	Average T,m^2/day	Recovery T,m^2/day	Head Losses	
											B	C
RPW-001-08	566503	1373320	1442.7	120	112.5	7.5	66.5	58.3	302.8	314.7	5.95E-04	9.98E-07
PW-002-08	574080	1410165	1661.1	144	63	49	30	6.5	438.1	455	3.34E-03	3.94E-07
RPW-005-08	577889	1409202	1608	128	54.1	60	25	7.4	292	303.4		
RPW-006-08	577182	1408010	1609.9	148	99.5	46.5	10	24.6	34.4	36.1	1.39E-03	6.22E-08
RPW-007-08	573877	1407677	1642.4	154	101.7	48.3	30	3.5	1349.8	1401.4		
RPW-008-08	559048	1366594	1594.1	186	103.4	76.6	8.5	63	7.5	8.1		
RPW-009-08	578838	1406957	1583.2	152	78.6	65.4	6.2	8.5	81.8	85.2		
RPW-010-08	568193	1376340	1424.4	243	90.5	37.5	99.3	62.8	224.4	233.3		
RPW-011-08	563281	1356231	1498.3	190	160.6	15.4	105.8	28.6	315.5	327.8	1.84E-03	6.10E-07
RPW-012-08	581052	1404035	1542	220	181.6	34.4	31.8	9.7	312.6	177	5.94E-03	2.22E-06
RPW-013-08	572677	1403437	1609	116	55.4	58.6	17	12.2	110	195	9.33E-04	2.11E-07
RPW-014-08	582104	1403603	1533.5	184	139.4	40.6	48.3	6.6	827.9	859.7	9.39E-04	2.91E-07
RPW-016-08	586277	1407519	1566.6	270	198.5	59.5	38.8	9	420.3	436.6	3.44E-03	7.53E-07
RPW-018-08	579972	1401424	1534.2	216	170	36	38.7	17	268.5	279	1.44E-03	1.41E-06
RPW-019-08	581768	1400964	1520.6	215	181	29	31.8	12.7	286.3	561	1.32E-03	1.09E-06
RPW-020-08	577596	1400661	1541.8	235	187.7	42.3	31.8	10	328.1	906	7.17E-04	1.62E-07
RPW-021-08	571906	1363793	1404.1	159	131.8	22.2	60.7	5.4	1194.4	1240.1		
RPW-023-08	568247	1400186	1656.9	111	68	34	13	35.4	73.3	35.5	1.23E-03	2.20E-07
RPW-024-08	574055	1399330	1568.4	140	97.7	38.3	28	4.1	668.9	522	0.00175	3.31E-07
RPW-025-08	574144	1368595	1396.6	270	252	18	41.3	12.2	361.1	375.2	4.93E-06	3.10E-11
RPW-026-08	570329	1389923	1575.1	105	79	26	39.5	4	814.9	846.1	4.23E-03	6.15E-07
RPW-027-08	566871	1374240	1435.3	188	182.7	3.3	80	59.5	210.2	218.5	6.98E-04	2.84E-07
RPW-028-08	578718	1398109	1513.7	226	186.4	33.6	25	5	689.2	747	1.57E-05	2.43E-11
RPW-029-08	567346	1379142	1444.1	214	197.7	12.3	98.2	24.8	494.9	514.1	2.58E-03	4.86E-07
RPW-030-08	573856	1396696	1556.1	174	126.6	47.5	24	5.3	244.7	308	5.07E-04	4.22E-08
RPW-031-08	566678	1378864	1453.3	220	190	20	55.5	3	1620.7	1682.6	3.20E-03	8.85E-07
RPW-032-08	576189	1395698	1521.6	182	148.7	31.3	32	17.9	343.6	128	2.93E-03	1.22E-06
RPW-033-08	575022	1395075	1530.8	162	120.8	33.2	30.2	14.3	276.7	348	4.77E-03	4.44E-07
RPW-034-08	576332	1394432	1514.4	224	183.8	36.2	23.2	11.6	155	227	4.47E-04	2.06E-07
RPW-035-08	566991	1377439	1438.8	203	194.7	7.3	107.6	31.2	277.6	233	6.16E-04	4.10E-07

RPW-036-08	574094	1392035	1523.9	160	112.3	39.8	31.3	3.5	957.3	1210	9.75E-04	3.05E-07
RPW-037-08	574690	1390976	1509.5	160	120.3	33.7	30.5	9.6	211.6	285	2.84E-03	2.18E-06
RPW-038-08	574039	1389891	1512.6	182	140.8	39.2	25.3	20	85.4	72.1	4.29E-03	6.76E-07
RPW-039-08	571901	1389798	1547.3	127	68.4	49.6	30	13.7	250.7	260.6	1.85E-03	2.08E-06
RPW-040-08	569910	1391794	1598.6	142	100	40	31.8	25.5	47.1	49.2	1.32E-03	5.24E-07
RPW-041-08	567155	1391738	1658.9	128	87.9	38.2	30	5.5	728.7	756.7	1.00E+00	7.21E-07
RPW-042-08	572853	1372716	1401.8	184	166.1	13.9	52.3	15.3	346.5	360	8.63E-03	1.33E-06
RPW-043-08	572369	1384905	1459.1	202	149	51	30	29	94.9	55.4	2.53E-03	6.40E-07
RPW-044-08	569097	1378878	1425	209	209	-1	50.6	23.7	192.8	134	3.22E-03	7.07E-07
RPW-045-08	572436	1382113	1433.3	178	146.7	29.3	37.7	28.1	120.6	98.1	5.57E-03	4.25E-07
RPW-046-08	569905	1381800	1446	180	145.7	28.3	40.8	32	82.6	80.7	4.29E-03	5.60E-07
RPW-047-08	572052	1380755	1425.7	136	109	25	37	23.2	131.4	136.7	5.81E-03	1.21E-05
RPW-048-08	570343	1380681	1428.6	150	130.8	17.2	15	58.7	23.6	16.3	2.35E-04	1.08E-06
RPW-049-08	568921	1379801	1429	198	186	-2	53	15.3	224.5	202	6.79E-04	4.58E-07
RPW-050-08	571429	1379689	1421	166	145.8	18.2	43.8	10.6	364.8	306	8.85E-04	4.66E-07
RPW-051-08	568031	1379400	1437	200	191.7	8.3	63.4	17.7	261	216	1.58E-01	2.47E-06
RPW-052-08	570263	1378912	1420.4	136	124.1	9.9	35	39	91.9	80.8		
RPW-053-08	568862	1377910	1427.3	218	219	-2	55.5	16.9	274.7	92.7	3.05E-05	1.48E-07
RPW-054-08	567333	1378232	1442.1	186	172.6	12.4	121.1	21.2	447	532	1.37E-03	5.84E-07
RPW-055-08	571864	1378166	1417.1	216	195	17	46	17.2	264.8	200	3.81E-04	1.81E-07
RPW-057-08	569431	1376222	1417.6	142	129.2	8.8	31	19.9	138.2	147	5.98E-04	1.29E-06
RPW-058-08	571642	1376249	1409.1	186	170.1	12	65	15.3	327.4	290	2.38E-04	8.92E-07
RPW-059-08	565861	1379159	1464.6	174	139.8	24.3	58.1	5.3	1504.5	969	5.26E-04	1.45E-07
RPW-060-08	566917	1374980	1430	198	192	-2	37	4	238.4	247.8	1.10E-03	1.86E-07
RPW-061-08	567200	1375899	1439	156	155	-1	113.3	40.5	320.1	198	2.21E-03	7.60E-07
RPW-062-08	566450	1374975	1436	143	134.7	3.3	50.6	14.7	347.8	361.3	7.91E-04	8.88E-07
RPW-063-08	571462	1374198	1404.3	224	205.3	14.8	34	11.4	186	195	2.36E-03	4.05E-07
RPW-064-08	564467	1373141	1475.8	112	84.3	21.7	35	8.4	267	943	1.08E-03	1.28E-07
RPW-065-08	565658	1373049	1455.1	126	102.8	17.2	54.5	6.9	2038.4	441	1.64E-03	3.80E-07
RPW-066-08	566444	1372391	1444.5	146	134.9	9.1	38.8	9.6	451.3	277	5.02E-04	2.02E-06
RPW-067-08	571726	1373354	1400.5	218	200.6	13.4	31.3	15.5	535.2	422	2.93E-03	3.51E-07
RPW-068-08	572613	1371922	1400.5	264	244.5	15.5	36	10.6	403.9	303	1.64E-03	6.32E-08
RPW-069-08	565204	1371005	1459	154	140.1	12.9	106.2	29.1	319.9	48.8	2.17E-02	9.51E-06

RPW-070-08	570481	1371229	1408	144	117.3	22.7	16	47.1	56.2	58.6	8.63E-04	1.47E-07
RPW-071-08	565483	1368490	1465	160	146.7	11.4	54.5	6.4	970.2	169	2.55E-03	9.69E-07
RPW-072-08	572671	1370616	1400	262	236.5	17.5	31.3	15.6	185.5	192.9	2.08E-03	3.09E-07
RPW-073-08	560422	1370267	1558	120	53.1	64.9	44	8	995.2	1033.3	1.94E-03	4.30E-07
RPW-074-08	564898	1367281	1474.1	176	156.2	15.8	54	21.1	249.7	259.5	2.20E-04	7.01E-07
RPW-075-08	561215	1368924	1528.8	130	97.5	28.5	48	8.3	494.8	597	1.10E-03	2.81E-07
RPW-076-08	567162	1369865	1438.4	232	213.7	14.3	38.8	8	400.4	336	6.73E-03	4.08E-07
RPW-077-08	565483	1368490	1465	137	118.7	15.4	41.6	4.6	1145.1	999	2.03E-03	2.19E-06
RPW-078-08	569076	1366877	1424	96	62	30.1	31.8	15.1	154.5	294	7.78E-04	1.20E-07
RPW-079-08	568008	1367866	1436	210	183.4	20.6	44.5	6	675.3	601		
RPW-080-08	565204	1371005	1459	138	108.4	25.6	13	2.5	461.6	429	4.07E-03	4.82E-07
RPW-081-08	566566	1367059	1452.2	190	169.3	16.7	40	22.7	125.3	99.9	2.51E-03	5.37E-07
RPW-082-08	574045	1365777	1388.2	276	264.5	9.5	40.9	13.6	353.6	638	5.72E-04	4.28E-07
RPW-083-08	565271	1365661	1469.1	160	142.6	11.4	50	8.7	532.3	539	2.17E-03	1.56E-06
RPW-084-08	568850	1368728	1424	146	116.4	21.6	30.3	28.2	108.4	93.5		
RPW-085-08	564906	1363929	1478.8	120	100.7	17.3	110	16.8	962.2	841	3.12E-03	1.26E-06
RPW-086-08	563445	1362750	1502	118	80.9	35.1	93.2	45.8	1077.7	1920	1.60E-03	7.37E-07
RPW-087-08	567591	1361714	1434	170	159.6	6.4	41.6	6.3	572.6	623	9.33E-04	2.99E-07
RPW-088-08	567019	1360930	1436.5	176	159	7	50	15.3	239.6	206	1.69E-03	1.19E-07
RPW-090-08	563934	1356825	1485	182	173	9	116	19.5	638.6	1050	8.47E-04	2.91E-07
RPW-091-08	566689	1360036	1438.2	166	161.3	2.7	59.5	12.9	429.1	445.7	1.11E-03	2.22E-07
RPW-092-08	571968	1384297	1455	194	149.1	42.9	33.6	4.9	849.3	352	2.00E-03	2.77E-07
RPW-093-09	567588	1359766	1435.3	288	280.1	5.9	46	15.7	226.5	294	5.34E-03	4.36E-07
RPW-094-08	566164	1359929	1440.7	182	171.6	8.4	70	57.2	95	98.9	2.20E-03	4.92E-07
RPW-095-08	565153	1359042	1455	196	188.6	5.4	43.8	17.4	145.3	136	1.20E-03	6.56E-07
RPW-096-08	566902	1358605	1459	186	168.6	15.4	43.8	12.2	270.9	236	3.05E-03	1.58E-07
RPW-097-08	564016	1357876	1475	144	128.3	13.7	46	16.9	207.5	515	1.59E-03	2.23E-07
RPW-098-08	562933	1357904	1487.3	154	144.4	5.6	41.6	8	676.5	920	1.60E-04	1.58E-07
RPW-099-08	566904	1357791	1453	230	206.6	19.4	112	18.6	549.1	536	7.43E-04	7.71E-08
RPW-100-08	565838	1357528	1463.3	190	163.5	24.5	108	22.2	452.2	523		
PBH1	571313	1415112	1751	96	166	2		8.9	78.8	51.7		
PBH3	587384	1411774	1595.9	204	94.3	2.7	34	3.7	139	139	9.02E-04	3.78E-06
PBH4	577642	1391710	1488	180	103	5	34.8		163.9	144		

PBH7	568084	1385736	1524.9	139	71.4	8.1	38.7		343.1	613	1.47E-03	4.94E-06
PBH8	574586	1393040	1518.2	152	301.1	8.9	34.8	17.8	136	118	7.45E-04	3.66E-05
PBH9	569200	1393395	1618.3	67	81.1	9	7	5.6	131.4	191	3.20E-03	1.52E-06
PZ1	581458	1402058	1527.3	240	76.9	9.1		14.3	195.5	281		
PZ2	585168	1402537	1541	90	137.1	9.4	39.5	6.3	39.4	40.4	2.35E-04	6.80E-07
PZ3	569257	1377425	1427.9	170	148.4	9.6	36.3	9.6	869.3	1080	1.72E-03	1.04E-07
PZ4	565181	1379685	1480	90	80.3	9.7		5.5	1246	1520	2.28E-04	4.05E-08
PZ5	572491	1373604	1403	184	174.3	9.8	28.7	1.6	1217.7	1220	3.08E-03	7.55E-06
PZ7	574387	1361357	1389	311	300.6	10.4	40	16.9	148.5	401		
PZ9	562943	1365069	1509.7	146	133.6	12.4	33.6		997.8	955	6.35E-04	1.07E-07
WF13/BH1	574502	1409298	1649.1	137.5	111	15	40	2.6	1538.2	1490		
WF13/BH2	575754	1407602	1620.5	168	166.2	15.8	32	4.3	746.6	725		
WF13/BH4	574837	1408721	1640.9	144	68.1	15.9	30	3.8	1516.3	2000		
WF11/BH4	577896	1403786	1568.3	198	74.8	17.2	35	7.8	543.5	317		
WF9/BH1	569813	1400983	1643.9	151	42.3	17.7	35	5.1	1518.6	1700		
WF9/BH2	569708	1399528	1632.8	150	68.3	17.8	35	13	374.7	1210	2.46E-03	7.89E-07
WF9/BH3	569798	1400023	1634.1	128	101.5	18.5		13.7	270	351		
WF9/BH4	570553	1400160	1620.4	150	65.2	18.8	35	3.4	1887.3	2360		
WF2/V9	565921	1376322	1435	78	83.2	18.8		6.2	1104	1146.2		
WF4/BH1	567110	1381023	1475.6	172	145.8	19.2		7.1	512	545		
WF4/BH3	564899	1378795	1490.5	132	120.8	19.5		6.3	1074.7	1340		
WF0/BH1	562709	1370793	1499.7	98	119.3	19.7	49.7	5.1	595	794	6.07E-04	1.54E-07
WF0/BH2	562905	1370393	1492.1	88	106.1	19.9		3.2	3117.1	3235.9	3.96E-03	8.37E-07
WF0/BH3	563923	1369802	1477	80	120	20		16	232.7	248		
WF0/BH4	562697	1368978	1496	106	120.2	20.1		14.5	195.7	221		
WF0/BH5	561903	1369790	1508.9	136	73.5	20.5	25	5.3	595.9	1560		
WF0/BH6	561399	1370777	1521	93	107.3	20.7	30	4.8	788.4	2060		
WF0/BH7	561796	1370780	1511.3	102	99.2	20.8		1.8	3100.3	3040	5.43E-03	6.60E-07
WF0/BH8	561409	1369799	1523.3	132	73.2	20.8	44	6	1170.3	1620	4.99E-03	8.13E-07
WF1/V1	562872	1371640	1498.4	78	56.7	21.3		16.4	254.3	271		
WF1/V9	562713	1371855	1499.4	73	51.3	21.7		3.1	739.4	720	1.25E-03	1.88E-07
WF1/V10	562681	1371183	1499.5	102	79.7	22.3		4.6	1280.3	1260		
WF5/BH1	563690	1366993	1487.6	96	73.3	22.7		14.6	243.9	209		

WF5/BH2	564103	1368593	1484	108	85.1	22.9	35	6.1	554.2	551		
WF5/BH3	563673	1367565	1490.9	84	63	23	5	6.2	497.8	523		
WF5/BH4	563905	1367793	1485.5	101	54.6	23.5	43.8	16.2	130.6	104	1.36E-03	3.23E-07
WF6/BH3	563156	1366192	1499.2	96	77.2	24.8	35	7.6	337	273		
WF6/BH4	563912	1364685	1491.2	122	10.7	25.3	*	3	1100.5	1110		
WF7/BH1	564378	1363098	1490.9	137	143.6	26.4	20	1.7	1882	1953.8		
WF7/BH2	563863	1364133	1494.5	162	118.9	27.1	44	2.5	1436.7	1550		
WF11/BH1	573995	1405945	1632.7	129.5	102.2	27.8	44	15.8	143.3	167	3.01E-03	8.72E-07
WF3/BH1	565904	1376796	1438.7	114	62.8	30.2	40	14.3	360	478	2.70E-03	7.42E-07
WF3/BH2	566954	1376426	1435.5	97	127.7	30.3	37.5	12.3	280.7	300	1.03E-02	4.25E-05
WF6/BH2	563355	1366693	1492.7	96	49.3	30.8	31.6	20.2	22.6	23.8		
WF11/BH3	574905	1404793	1603.5	82	47.9	34.1	7		129.7	134.9		
Habtemariam	571950	1390760	1554.3	138	80.7	57.4	31.8	12.9	219	227.7		
Galika Trading	570245	1369978	1412.5	100	71.5	28.5	34	15.8	194.4	202.1		
Safron plc	575879	1405388	1594.9	138	97.1	40.9	34.8	5.5	351.4	365.1		
Kalibso plc	571787	1401448	1602.6	146.5	107.4	39.1	35.5	11	203	211		
GOBU	564404	1358786	1460.8	79.5	71.4	8.1	38.7	3.1	1513.1	1570.9		
Balambaras	573832	1365003	1388	60	50.3	9.8	28.7	13.6	237.2	246.6		

5.3.3.4. Step drawdown test

A step drawdown test is a single well test in which the well is pumped at a low constant discharge rate until the drawdown in the well stabilizes. The pumping rate is then abruptly increased to a higher constant discharge rate and the well is pumped until the drawdown stabilizes once again. This process is repeated through at least three steps which should be of equal duration. Step-drawdown tests is commonly used to quantify well loss which are extremely useful in aquifer modeling exercises, since they allow observed water levels in production wells to be compared on like-for –like bases with numerically simulated heads (Gholam H. Karami, & Paul L. Younger, 2002).

The total drawdown in a pumped well consists of aquifer losses and well losses. Well performance analysis is conducted to determine these losses. Aquifer losses are the head losses that occur in an aquifer where the flow is laminar. Well losses are linear or non-linear and caused by aquifer damage during drilling and completion of the well. All these losses cause that the drawdown inside the well is much larger than one would expect on theoretical grounds. The step drawdown test data for Raya Valley were analyzed based on Hanthush-Bierschenk well loss techniques. To obtain the information on the condition or efficiencies of the well, the relation between calculated aquifer loss (BQ) and well loss (CQ^2) has been applied:

where:
BQ: represents the drawdown due to formation loss
$CQ^{2:}$ represents the drawdown due to well loss.

The efficiency of a well is governed largely by the magnitude of the well loss and thus falls off rapidly as discharge is increased. The efficiency of a well in an aquifer having a high Transmissivity is affected by well loss to a greater degree than the efficiency of a well in an aquifer having a low Transmissivity, and it is least affected by partial penetration of aquifers having a large Transmissivity.

In addition, the safe yield and permissible drawdown was analyzed from the step drawdown tests. On the other hand this estimation may lead to erroneous conclusion because it does not account the interferences between neighboring boreholes, boundary condition that may exist due to long pumping period. It obvious that drawdown in an unconfined aquifer will continue to drop if pumping continues and this will directly affect the primarily (previously) set aquifer thickness in any of the aquifer models stated above. However, it is also recommended to carry out this preliminary analysis which could be used to monitor the changes that could result from wells interferences caused by group pumping.

Therefore, analysis of 52 boreholes with proper data were selected and analyzed as shown in Figure 5.18a, b, c ,d. and the results are given in Table 5-5.

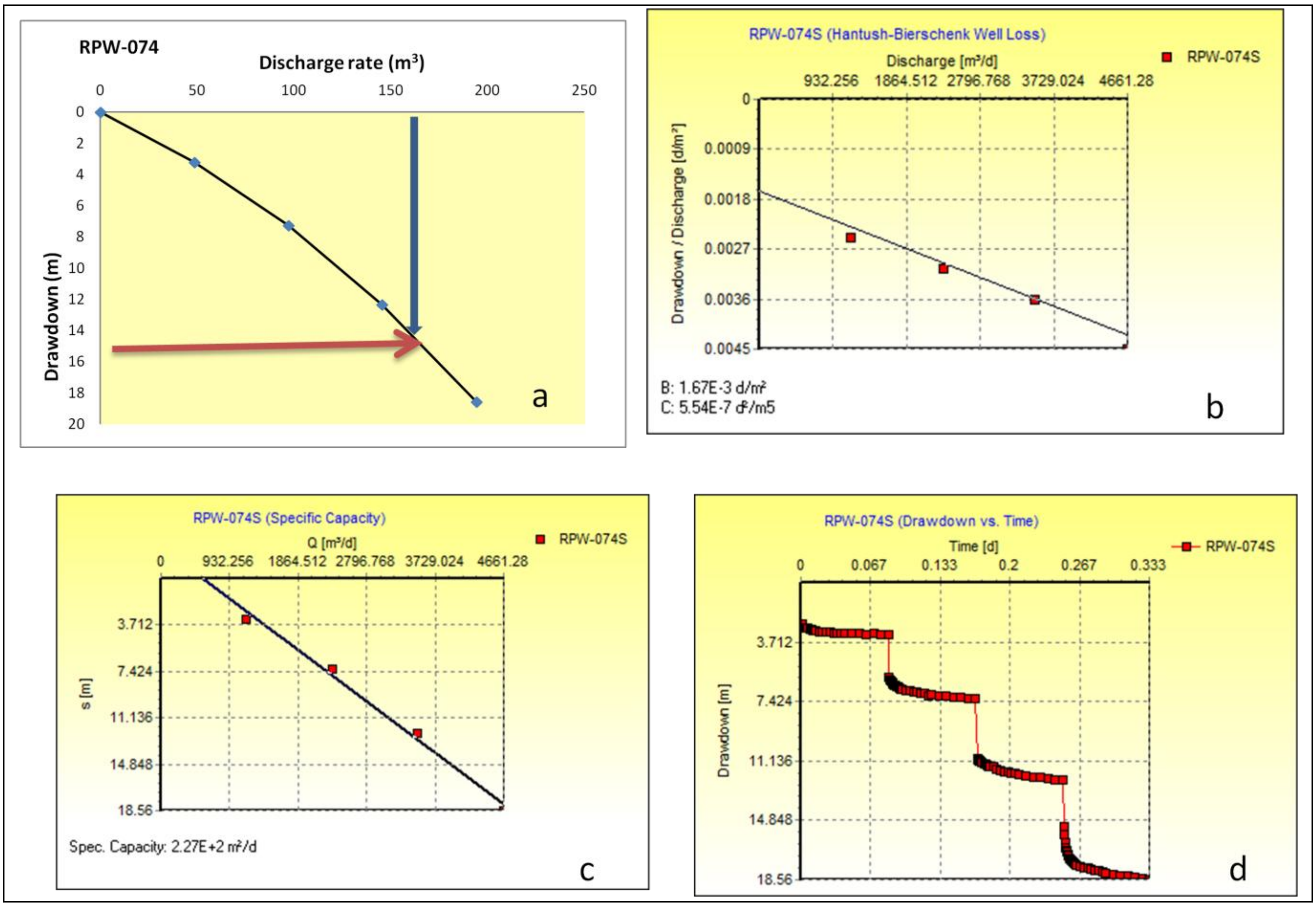

Figure 5.18 a) Safe yield estimation b) Coefficients of head loss estimation c) Specific Capacity estimation

Table 5-5 Summary of safe yield, permissible drawdown and allowable discharge estimation results

Well index	X	Y	Z	Well depth, m	SWL,m	Q,l/s	DD,m	T,m^2/day	Recovery T, m^2/day	safe yield m^3/d	Permissible drawdown	Q, l/s
RPW-001-08	566503	1373320	1443	120	7.54	66.52	58.26	39		208	40	57.8
RPW-003-08	587171	1402249	1588	260	90.52	32.25	8.68	168		96	3.3	26.7
RPW-004-08	587866	1399382	1607	260	72.56	6	42.34	4.71		76	6	21.1
RPW-012-08	581052	1404035	1542	220	34.4	31.8	9.7	113	177	105	7.5	29.2
RPW-013-08	572677	1403437	1609	116	58.57	17	12.19	40.3	195	46	8.8	12.8
RPW-014-08	582104	1403603	1534	184	40.6	48.3	6.55	536		150	5.6	41.7
RPW-015-08	575651	1386962	1478	166	36.66	35	42.16	26.6		112	36	31.1
RPW-016-08	586277	1407519	1567	270	59.5	38.8	9.04	462		116	5	32.2
RPW-017-08	571732	1375106	1406	209	12.4	48.7	51.95	29.8		150	38	41.7
RPW-018-08	579972	1401424	1534	216	36	38.7	17.01	368		116	14	32.2
RPW-023-08	568247	1400186	1657	111	34	13	35.4	11.9	35.5	39	26	10.8
RPW-025-08	574144	1368595	1397	270	18	41.3	12.17	496		124	9	34.4
RPW-026-08	570329	1389923	1575	105	26	39.5	3.98	1430		122	3	33.9
RPW-027-08	566871	1374240	1435	188	3.3	80	59.47	435		240	46	66.7
RPW-028-08	578718	1398109	1514	226	33.58	25	4.95	753	747	70	2	19.4
RPW-029-08	567346	1379142	1444	214	12.27	98.21	24.82	873		300	16	83.3
RPW-032-08	576189	1395698	1522	182	31.27	32	17.87	151	128	96	12	26.7
RPW-033-08	575022	1395075	1531	162	33.2	30.23	14.32	405	348	92	11	25.6
RPW-035-08	566991	1377439	1439	203	7.3	107.61	31.23	304	233	340	18	94.4
RPW-037-08	574690	1390976	1509	160	33.72	30.5	9.56	126	285	90	4	25.0
RPW-038-08	574039	1389891	1513	182	39.2	25.3	20	93.4	72.1	76	13	21.1
RPW-040-08	569910	1391794	1599	142	30	31.8	25.49			98	14	27.2
RPW-043-08	572369	1384905	1459	202	51	30	29	174	55.4	90	21	25.0
RPW-045-08	572436	1382113	1433	178	29.34	37.7	28.08	50.2	98.1	128	13	35.6
RPW-048-08	570343	1380681	1429	150	17.22	15	58.69	16.8	16.3	60	43	16.7
RPW-049-08	568921	1379801	1429	198	-2	53	15.28	217	202	124	8	34.4
RPW-050-08	571429	1379689	1421	166	18.17	43.8	10.59	306	306	124	6	34.4

RPW-051-08	568031	1379400	1437	200	8.28	63.4	17.73	207	216	160	12	44.4
RPW-052-08	570263	1378912	1420	136	9.92	35	39	147	80.8	120	25	33.3
RPW-054-08	567333	1378232	1442	186	12.4	121.06	21.15	226	852	346	10	96.1
RPW-056-08	567995	1377085	1428	200	-2	113.25	22.54		587	315	13	87.5
RPW-057-08	569431	1376222	1418	142	8.8	31	19.9	66	147	130	14	36.1
RPW-058-08	571642	1376249	1409	186	11.95	65	15.32	344	290	125	9	34.7
RPW-059-08	565861	1379159	1465	174	24.25	58.1	5.26	393	969	170	5	47.2
RPW-061-08	567200	1375899	1439	156	-1	113.25	40.5	95.6	198	340	22	94.4
RPW-063-08	571462	1374198	1404	224	14.75	34	11.38	223	195	102	8	28.3
RPW-065-08	565658	1373049	1455	126	17.2	54.45	6.92	516		165	6	45.8
RPW-067-08	571726	1373354	1400	218	13.39	31.28	15.48	275	277	93	9	25.8
RPW-070-08	570481	1371229	1408	144	22.72	16	47.09	11.8	48.8	47	35	13.1
RPW-071-08	565483	1368490	1465	160	11.35	54.45	6.4	291		165	5	45.8
RPW-072-08	572671	1370616	1400	262	17.5	31.3	15.64	199	169	96	11	26.7
RPW-074-08	564898	1367281	1474	176	15.78	53.95	21.13	85.7		165	15	45.8
RPW-085-08	564906	1363929	1479	120	17.26	110	16.81	242	560	330	16	91.7
RPW-088-08	567019	1360930	1437	176	7.01	50	15.29	136	206	150	7	41.7
RPW-091-08	566689	1360036	1438	166	2.7	59.53	12.85	471		175	9	48.6
RPW-094-08	566164	1359929	1441	182	8.44	70	57.15	41.9		225	45	62.5
RPW-096-08	566902	1358605	1459	186	15.41	43.8	12.21	276	236	135	11	37.5
RPW-097-08	564016	1357876	1475	144	13.74	46	16.89	91.2	515	145	11	40.3
RPW-099-08	566904	1357791	1453	230	19.42	112	18.62	644	536	340	12	94.4
RPW-100-08	565838	1357528	1463	190	24.53	108	22.2	242	523	330	10	91.7
PZ3	569257	1377425	1428	170	9.58	36.3	9.58	1050	1080	104		28.9
PZ7	574387	1361357	1389	311	8.93	34.8	16.9	223	401	108		30.0

5.4. STATIC WATER LEVEL AND GROUNDWATER FLOW DIRECTION

The data collected by this research work and those obtained from previous works were plotted with help of ArcGIS 9.3. The contours show that the groundwater flows from the west, east and north toward the centre of the valley, following the topography of the area. Then groundwater flows to the south in a similar fashion to the surface water flow (Fig. 5.19).

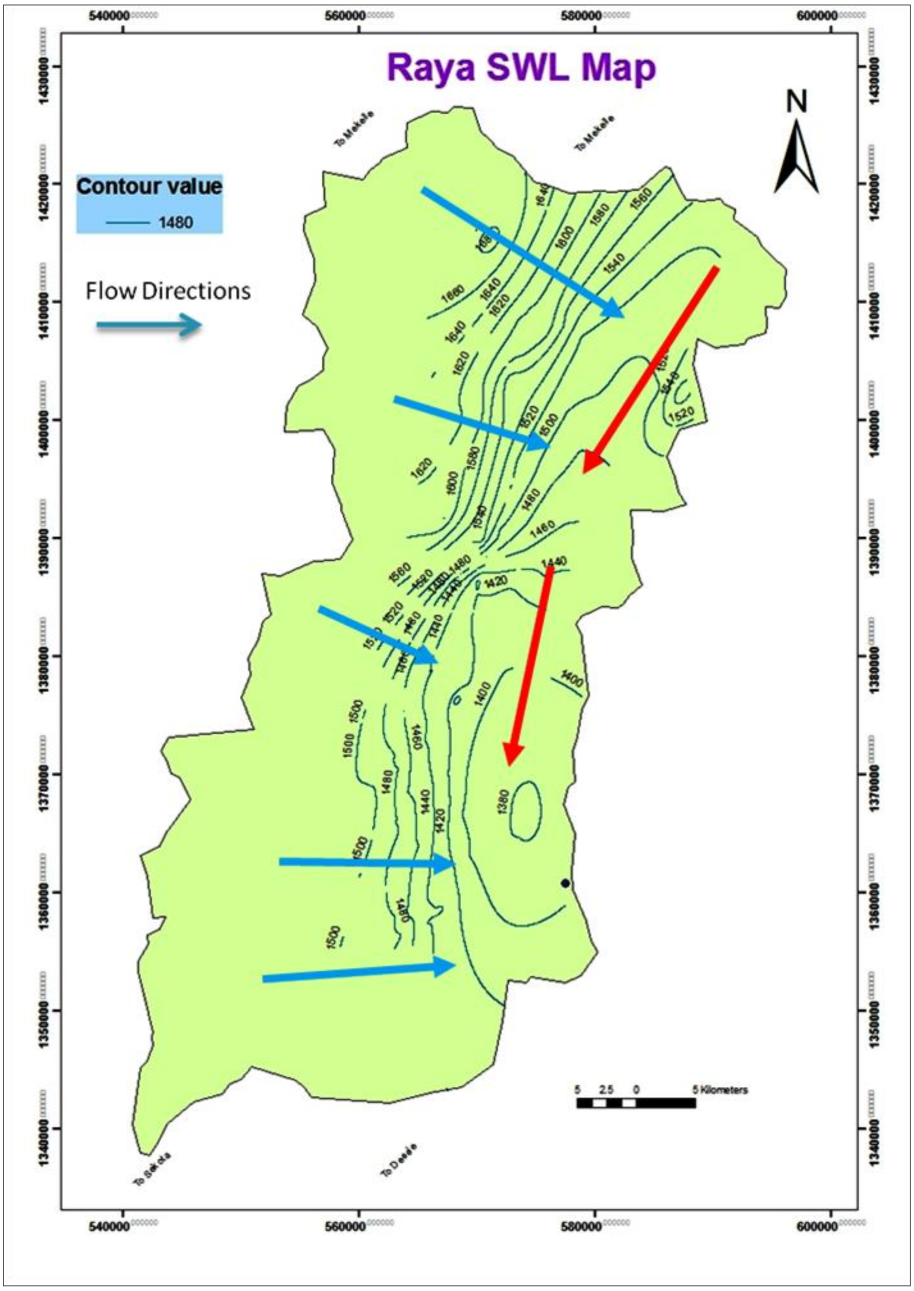

Fig. 5.19 Groundwater flow direction

5.5. SIEVE ANALYSIS RESULTS

Through the nine borehole samples analyzed for grain size analysis do not represent the whole studied area, but can give clue on how the sediments deposited in the valley seem to be. The location of these samples is confined to the central northern part of the study area because the boreholes in other parts have been drilled before the initiation of this research work. The samples were analyzed for porosity estimation. According to (Vukovic M., and Soro A., 1992), porosity (n) may be derived from the empirical relationship with the coefficient of grain uniformity (U) as:

$$n = 0.255\left(+0.83^{U}\right) \qquad (1)$$

where U is the coefficient of grain uniformity and is given by:

$$U = \left(\frac{d_{60}}{d_{10}}\right) \qquad (2)$$

Here, d_{60} and d_{10} in the formula represent the grain diameter in (mm) for which, 60% and 10% of the sample respectively, are finer than.

From these sieve analysis results the hydraulic conductivity was calculated based on the equation:

—

where

c : is a constant that ranges between 1 and 1.5. (BRAJA M. DAS, 2006)

d_{10} : is the diameter, in cm, corresponding to 10 percent finer of the grain size curve.

The results are given in Table 5.6.

Table 5.6 grain size analysis results

	X	Y	K (m/d)	Porosity
1	576459	1405949	77.76	
2	575001	1405548	12.98	25.7
3	578592	1404061	37.45	43.2
4	576755	1405254	11.7	25.7
5	**577500**	**1403255**	15.68	30.1
6	578396	1404634	12.98	
7	579585	1401210	12.98	25.6

6. CHAPTER VI: CHEMICAL AND ISOTOPE ANALYSIS

6.1. CHEMICAL COMPOSITION OF WATER SAMPLES

Groundwater in unconsolidated aquifers is usually of excellent quality; being naturally filtered. The water is normally clear, colorless, and free from microbial contamination and thus requires minimal treatment. As a consequence of the slow travel times in the flat plains and due to the long contact time with the sediment, the groundwater often contains significant quantities of minerals in solution. The solute content varies and depends on the residence time of water in the aquifer and the mineral composition of the aquifer itself.

Thirty water samples were collected for chemical analysis from boreholes and springs. The major constituents contained in the chemical analysis results include cations such as calcium, magnesium, sodium & potassium, and anions such as bicarbonate, sulfate, chloride & nitrate and both expressed in ionic form. The chemical composition of the waters from the area is variable, but Ca and Mg dominate the cations and bicarbonate and chloride dominate the anions (Table 6-1).

6.1.1. Cations

Calcium (Ca^{++}) and Magnesium (Mg^{++}) are the most dominant cations and are followed by relatively low amounts of Sodium and Potassium (Na^{+}, K^{+}). However, sodium has a significant concentration in the wells located in the eastern part of the Raya Valley, in which the value goes up to 18 meq/l in the hot spring near the out let. The concentration of calcium varies between 0.91 to 3.74 meq/l and that of magnesium varies between 0.56 and 6.96 meq/l for borehole samples. The sodium & potassium value vary between 0.44 to 18 and 0.02 to 0.86 meq/l respectively. In most cases the lower values correspond to the western spring while the higher values are related to the eastern escarpment and the hot spring (Figure 6.1 and 6.2).

The variability in the concentration of the cations and anions will be explained by correlating the results of isotope analysis in the summary.

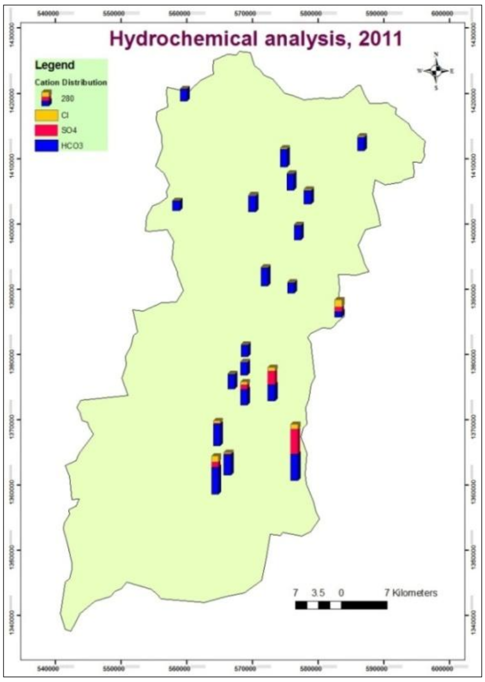

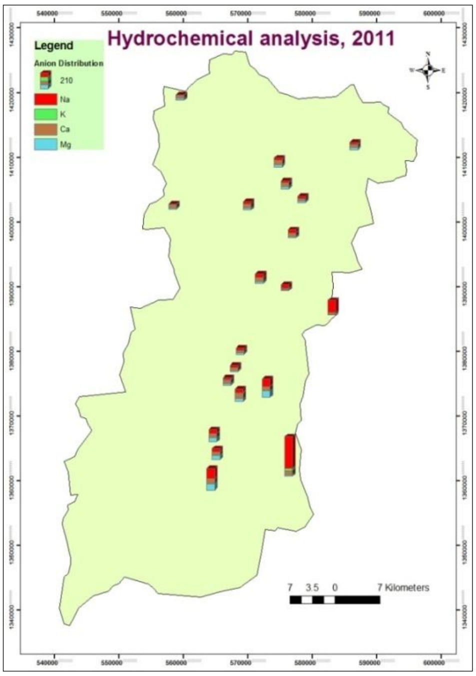

Figure 6.1 Cation distribution of chemical analysis 2009-2011   6.2 Anion distribution of chemical analysis 2009-2011

Table 6-1 Results of water sample analysis 2009-2010

S/N0	SampleID	Site	Lithology	X	Y	Z	pH	Cond	TDS	Na	K	Mg	Ca	F	Cl	SO4	No2	NO3	HCO3	Water type
1	ADISHEHASHIM	raya	Alluvial deposit	565213	1378211	1489	8.5	530	260	26.3	1.8	30	59	0.2	12.4	13.7	3.2	0	365	Ca-Mg-HCO3
2	ALEMWRGA	raya	Alluvial deposit	574513	1409306	1647	8.4	590	300	31.3	1.7	30.3	63.9	0.2	26.3	18.6	4.1	0.5	363.9	Ca-Mg-HCO3
3	MINORA1	raya	Alluvial deposit	574849	1408723	1645	8.4	570	290	27.5	2.3	30.6	65.7	0.2	19.2	13.2	4.2	0	381.2	Ca-Mg-HCO3
4	SAFRON1	raya	Alluvial deposit	575903	1405382	1602	8.3	530	270	28.8	1.8	30.8	53.9	0.3	13.8	12.2	3.2	0	359.8	Ca-Mg-HCO3
5	Cinque maggio	raya	W. basalt	558497	1402251	2419	7.5	860	430	12.7	0.6	16.8	39.8	0.1	4.5	7	15.1	0	207.3	Ca-Mg-HCO3
6	EMBAHASTI	raya	W. basalt	559651	1419070	2900	7.9	406	203	10.1	1.2	22.8	40.8	0.1	2.4	4.8	7.8	0	249.3	Ca-Mg-HCO3
7	TAFIE1	raya	Alluvial deposit	568801	1372527	1431	8.4	830	420	44.9	3.3	43.8	82.4	0.2	79.4	10.8	4.1	0	445.5	Ca-Mg-HCO3-Cl
8	ABU	raya	Alluvial deposit	573517	1422733	1824	8.3	1050	550	61.3	2.7	54.5	95.9	0.2	71	73.7	4.4	0	514.7	Ca-Mg-Na-HCO3
9	artesian3	raya	Alluvial deposit	568920	1379807	1428	7.5	560	280	31.1	1.6	17.7	31.1	0.3	11.7	9.9	1.5	0	235.9	Ca-Mg-Na-HCO3
10	ARTESIAN11	raya	Alluvial deposit	566917	1374984	1417	8.5	450	230	28	2	21.8	48.4	0.2	12.9	15.1	3.9	0	293.5	Ca-Mg-Na-HCO3
11	ARTESIAN2	raya	Alluvial deposit	568006	1377084	1431	8	448	224	29.5	1.2	19.4	36.1	0.3	6	4.5	2.1	0	268.6	Ca-Mg-Na-HCO3
12	HAFTEMARIAM1	raya	Alluvial deposit	571942	1390761	1558	8.4	590	300	45.8	1.2	28	54.8	0.3	21.8	18.6	6.4	0.9	370.2	Ca-Mg-Na-HCO3
13	HAFTU	raya	Alluvial deposit	571786	1401449	1617	8.3	530	260	31.2	1.2	23.8	59	0.3	16.6	13.7	3.2	0	338.4	Ca-Mg-Na-HCO3
14	REST11	raya	Alluvial deposit	570052	1402112	1666	8.4	520	270	31.2	1	24.5	59.7	0.3	13.2	13	3.2	0	351.1	Ca-Mg-Na-HCO3
15	REST21	raya	Alluvial deposit	570301	1402654	1660	8.3	690	350	42.1	1.2	30.5	76.9	0.3	26.2	19.4	4.4	0	431.8	Ca-Mg-Na-HCO3
16	WAEKELE	raya	Alluvial deposit	567368	1412826	1800	8.5	890	440	49.6	2.4	39.3	85.1	0.3	99.4	49.1	5.1	0	356.4	Ca-Mg-Na-HCO3-Cl
17	china	raya	Alluvial deposit	576993	1397808	1526	7.9	543	272	43.1	2.7	20.5	41.3	0.3	16	8.7	10.6	0.1	296.4	Ca-Na-Mg-HCO3
18	MECHARE1	raya	Alluvial deposit	586590	1411414	1591	8	470	230	25.4	3.3	27	43.1	0.4	17.7	10.7	4.2	0	296.3	Mg-Ca-HCO3
19	AGAMTIE	raya	Alluvial deposit	566956	1376678	1434	8.5	740	370	47.2	1.2	51.6	59.8	0.4	25.4	20.2	3.9	0.8	500.9	Mg-Ca-Na-HCO3
20	BELAY Tella	raya	Alluvial deposit	564250	1363445	1477	8.4	680	340	38.9	1.7	44.3	57.7	0.3	28.2	31.3	6.4	0	416.3	Mg-Ca-Na-HCO3
21	DEJENA	raya	Alluvial deposit	576057	1403655	1584	8.4	560	280	37	2.1	33.5	42.5	0.3	12.4	12.3	3.2	0.4	363.5	Mg-Ca-Na-HCO3
22	FRIATNA1	raya	Alluvial deposit	578489	1403273	1558	8.4	520	260	38.6	2.7	30.2	37.3	0.3	14.1	16.9	3.3	0	327	Mg-Ca-Na-HCO3
23	G.TSADKAN1	raya	Alluvial deposit	564719	1366258	1487	8.4	730	370	53.8	2.9	48.2	47.1	0.2	42.9	22.9	4.2	0	430.6	Mg-Ca-Na-HCO3
24	HARLE1	raya	Alluvial deposit	565244	1363696	1471	8.3	750	370	45	1.5	57.5	49.6	0.3	32.2	28.8	6.5	0	470.9	Mg-Ca-Na-HCO3
25	DRAR1	raya	Alluvial deposit	564408	1358785	1464	8.2	1410	710	122.4	1.8	90.3	76.9	0.3	15.6	130	8.7	0	821.6	Mg-Na-Ca-HCO3

26	KARSOLE1	raya	Alluvial deposit	573002	1373117	1405	8.2	1160	590	91.8	3.8	69.8	40.9	0.3	63.9	233	4.3	0	308.6	Mg-Na-HCO3-SO4
27	ABERA31	raya	Alluvial deposit	575933	1389658	1495	8.3	460	230	51.6	2.4	16.9	35.9	0.3	11.3	22.5	6.5	0.6	286.2	Na-Ca-Mg-HCO3
28	ABERA41	raya	Alluvial deposit	576495	1390580	1498	8.4	470	230	49.5	2.3	15.8	36.6	0.4	10.6	31.6	3.9	0	266.4	Na-Ca-Mg-HCO3
29	Chercher	raya	Alluvial deposit	580537	1374029	1534	8.6	900	450	161.5	1.3	6.8	18.3	0.2	148.4	96.3	9.4	0.1	119	Na-Cl-SO4-HCO3
30	hot spring	raya	Alluvial deposit	576480	1360918	1379	7.6			414.7	33.7	23.1	50.8	0.8	90.1	522.6	6.1	0	543.1	Na-SO4-HCO3

6.1.2. Anions

The dominant anions are bicarbonates in most borehole samples and in the cold spring samples. The range of variation of bicarbonates in borehole samples is from 1.95 to 9.17 milliequivalents per liter. The chlorides and sulfates are with values ranging from 0.07 to 3.67 and 0.1 to 5.77 milliequivalents per liter in the western spring and central boreholes and up to 10.88 and 4.19 milliequivalents per liter in the eastern boreholes and the hot spring of the Raya Valley, respectively. The nitrate concentration is low in the valley, indicating less anthropogenic rural pollution so far. The nitrate level is pretty below the (WHO, 2011) drinking water standards (50 milligrams per liter) except public borehole at Karsole, 50 mg/ l, where a number of animals drop their secretion in the nearby cattle trough.

6.1.3. Other parameters

6.1.3.1. Sodium Adsorption Ratio (SAR)

Sodium concentration is an important factor in classifying water for irrigation. Because sodium reacts with soils and reduce its permeability which makes cultivation difficult. The salinity laboratory of the United States Department of Agriculture recommended the SAR as an index (Table 6-2) for sodium hazard and defined it as:

$$SAR = \frac{Na}{\sqrt{\frac{Ca + Mg}{2}}}$$

Where, the concentrations of the constituents are expressed in milliequivalent per liter.

Table 6-2 sodium adsorption ration classification , after (Todd, 2005)

Water class	**Alkali Hazard (SAR)**
Excellent	*up to 10*
Good	10-18
Fair	18-26
Poor	>26

Ninety percent of the water samples have SAR less than 2.3. Therefore, there is no much danger of sodium hazard.

6.1.3.2. Hardness

Hardness results from the presence of divalent metallic cations, of which calcium and magnesium are the most important once. Because of their adverse action with soap, hard waters are unsatisfactory for household cleaning purposes.

Accordingly Hardness (H) is expressed as:

$$H = 2.5\,Ca + 4.1\,Mg$$

where: Ca and Mg are measured in milligram per liter as the equivalent of calcium carbonate. In the present work this method has been used to determine the total hardness of the water samples. For classification of range of hardness concentrations, (Todd, 2005)used the following classification (Table 6-3).

Table 6-3 Classification of hardness values, after Todd 2005

Hardness, (mg/l as $CaCO_3$)	water class
0-75	Soft
75-150	moderately soft
150-300	Hard
>300	Very hard

Based on the above classification, 5% are soft, 20% are moderately soft and the remaining 65% fall in the very hard water class. Springs, are within the moderately soft to hard category with a similar manner to the boreholes.

6.1.3.3. Water type classification

An important task in groundwater investigation is the compilation and presentation of chemical data in a convenient manner for visual interpretation. Thus, the Pipers tri-linear diagram (Fig. 6.3 and 6.4) and chemical variation stiff plots (Fig. 6.5) are used.

a) Pipers Tri-linear Plot

Here cations are expressed as percentages of total cations (Mg, Ca, Na , and K) and similarly anions are expressed as percentages of the total anions. These two points are then projected into the central diamond-shaped area parallel to the upper edges of the central area. This single point is thus uniquely related to the total ionic distributions. This diagram conveniently reveals similarities and differences among water samples because those with similar quantities will tend to plot together as groups.

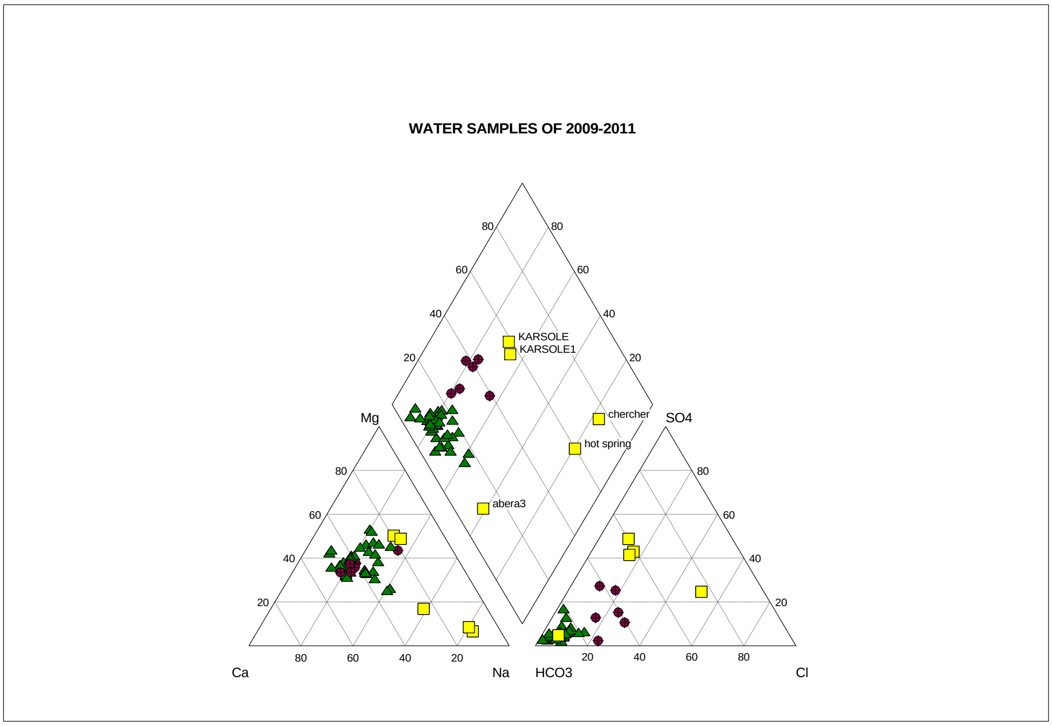

Figure 6.3 Piper trilinear diagram of water samples of 2009 & 2010

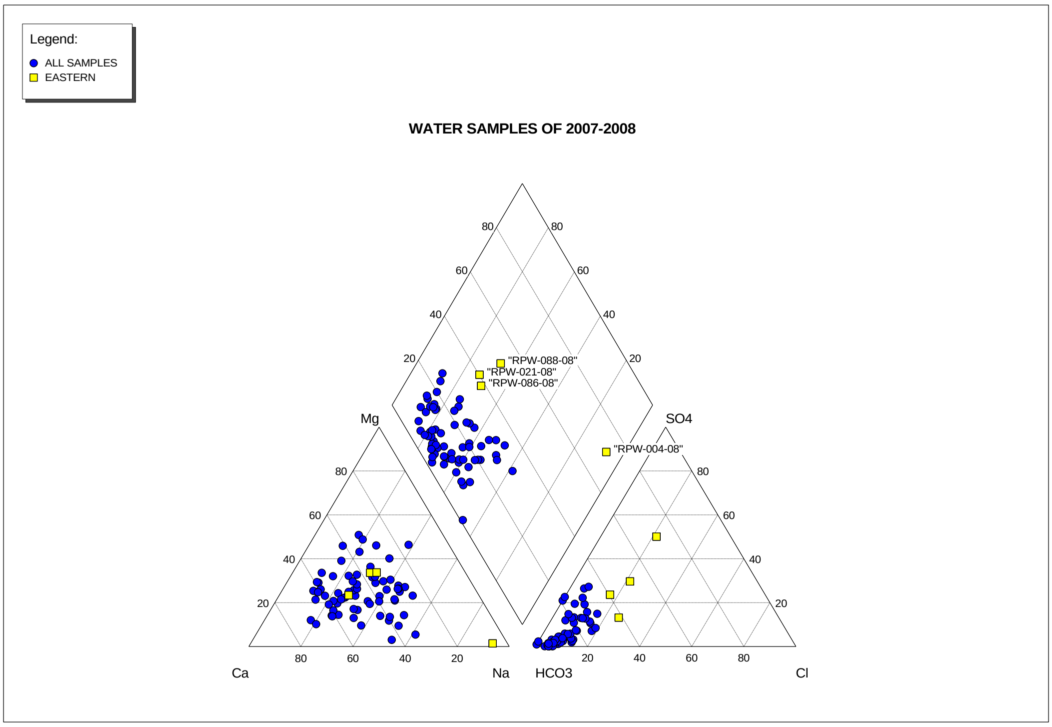

Figure 6.4 Piper trilinear diagram of water sample collected in 2007-2008, after WWDSE

From the Figure 6.3 and Figure 6.4, at least two types of waters can be distinguished. These are the *Ca-HCO$_3$, and* Na-*Cl-SO$_4$* types. Highland spring samples and most of the western borehole samples, from the Raya Valley, plot in the *Ca-HCO$_3$* type field, while the eastern boreholes and the hot spring are grouped in the second category. The remaining central valley boreholes basically have a mixture of the major types of water with considerable amount of magnesium.

b) Chemical Variation Plots

Chemical variation diagrams have been constructed in order to understand the evolution in groundwater chemistry, Figure 6.5.

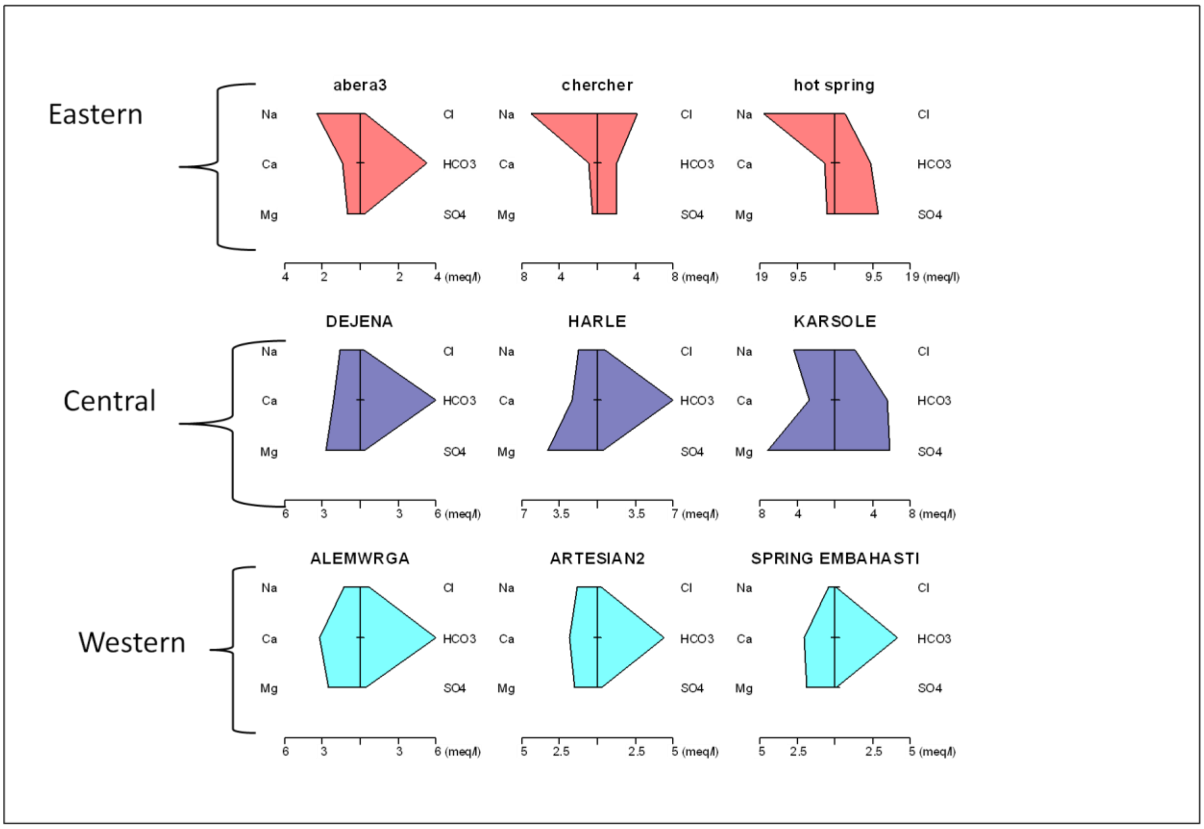

Figure 6.5 Stiff diagram of water samples of 2009 & 2011

6.2. STABLE ISOTOPE ANALYSIS:

Stable isotope studies are based on the tendency of pairs of isotopes to fractionate. This fractionation occurs during some geologic processes like evaporation or heating. Stable isotopes readily fractionate because have relatively large difference in mass between the two isotopes and have one isotope that is more abundant than the other. If R is the ratio of the heavy isotope to the light one, then the relative fractionation is expressed in δ notation as:

Results are expressed as deviation in parts per thousand (‰). If the value of δ is positive then the sample is enriched with heavy isotopes relative to the standard; a negative sample is isotopically light. Oxygen and Hydrogen isotope data are reported in the standard delta (δ) notation in parts per thousands (‰) to Vienna Standard Mean Ocean Water (VSMOW). During the sampling period, in the rainy seasons of 2009 and 2010, two samples each from selected site of Korem, Alamata and Kisadgudo were collected to observe the variability which could exist in the western half of the valley. This area is considered the main source of groundwater recharge for the low land and the plateau. In the mean time isotopic data of the eastern side of the valley, isotope precipitation record at Checher (Weyrawha), was obtained from a Hydrogeology, Hydro geochemistry and Isotope Hydrology of Raya and Kobo Valleys, Adjacent Plateau, Escarpment and Part of Afar Rift, (Sileshi, 2007).

The data from Sileshi, 2007 are part of the technical cooperation project carried out between the International Atomic Energy Agency (IAEA) and the then Ministry of Mines and Energy of Ethiopia. The project focused on conducting isotope hydrological studies in Ethiopian Rift and Adjacent plateaus in which over 200 samples for ^{18}O, , δ^2H, ^{13}C, ^3H and hydrochemistry were gathered and analyzed. These were used to produce a local meteoric water line of the area.

In this work, additional 17 boreholes and 3 spring samples (Table 6-4)were collected and analyzed for the same isotope in the same laboratory of the AAU. Hence the later data were plotted against the meteoric water to define the possible sources of the groundwater recharge in the area of interest.

The following stable isotope indices of precipitation in Raya Valley were, therefore, used for interpretation purposes, correlating $\delta^{18}O$ and δ^2H (LMWL):

$\delta^2H = 7.4756\ \delta^{18}O + 11.827$ $(r^2= 0.9959)$ (Figure 6.7)

Most of the boreholes and springs and borehole samples plotted nearly along the local meteoric water line. But, the eastern boreholes and the hot spring (Figure 6.6) plotted away from the LMWL in the direction of major rock-water interaction with the following regression equation between $\delta^{18}O$ and δ^2H .

$\delta^2H = 6.7244\ \delta^{18}O - 0.0795$ $(r^2= 0.998)$ (Figure 6.8)

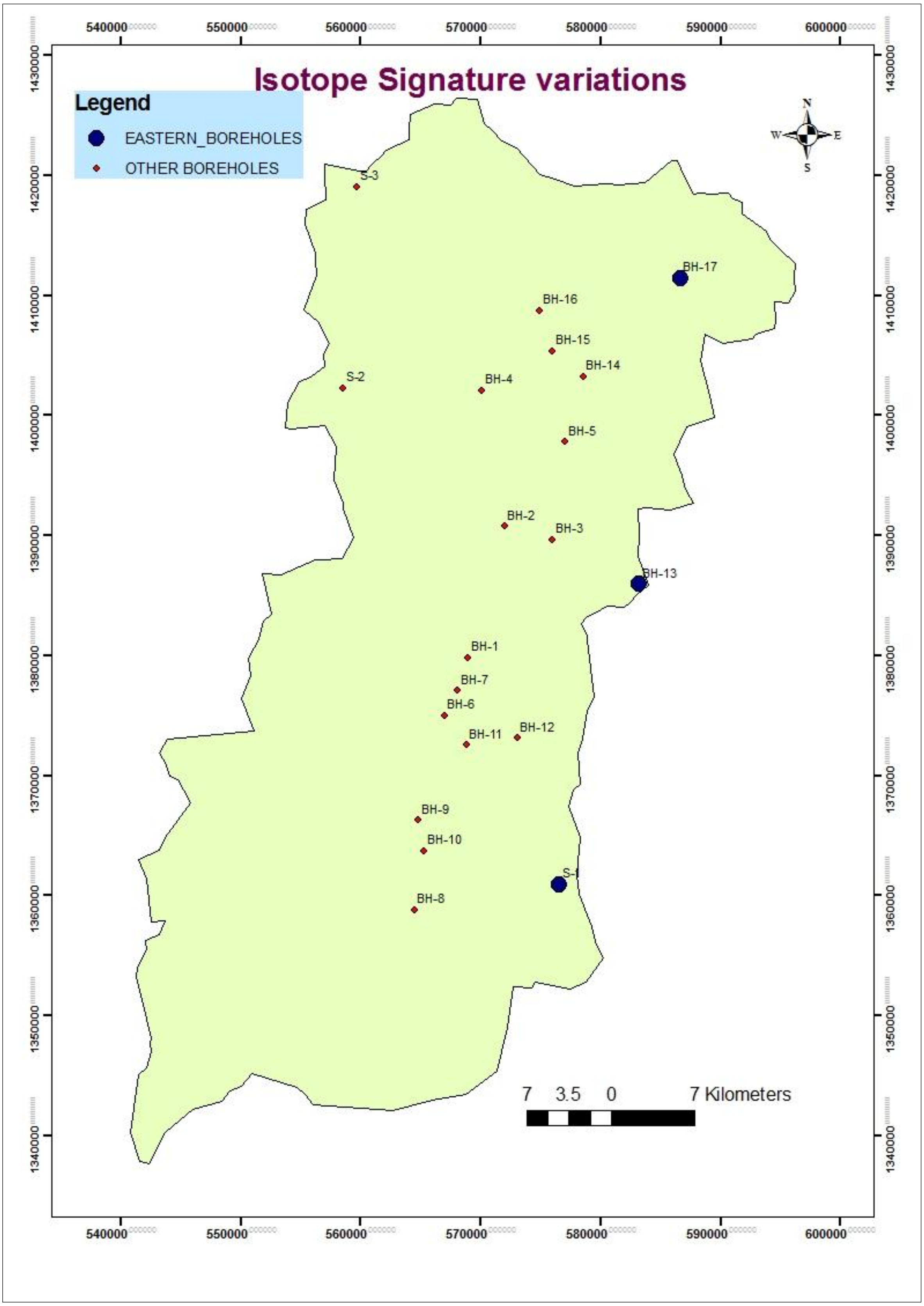

Figure 6.6 Isotopic spatial variation

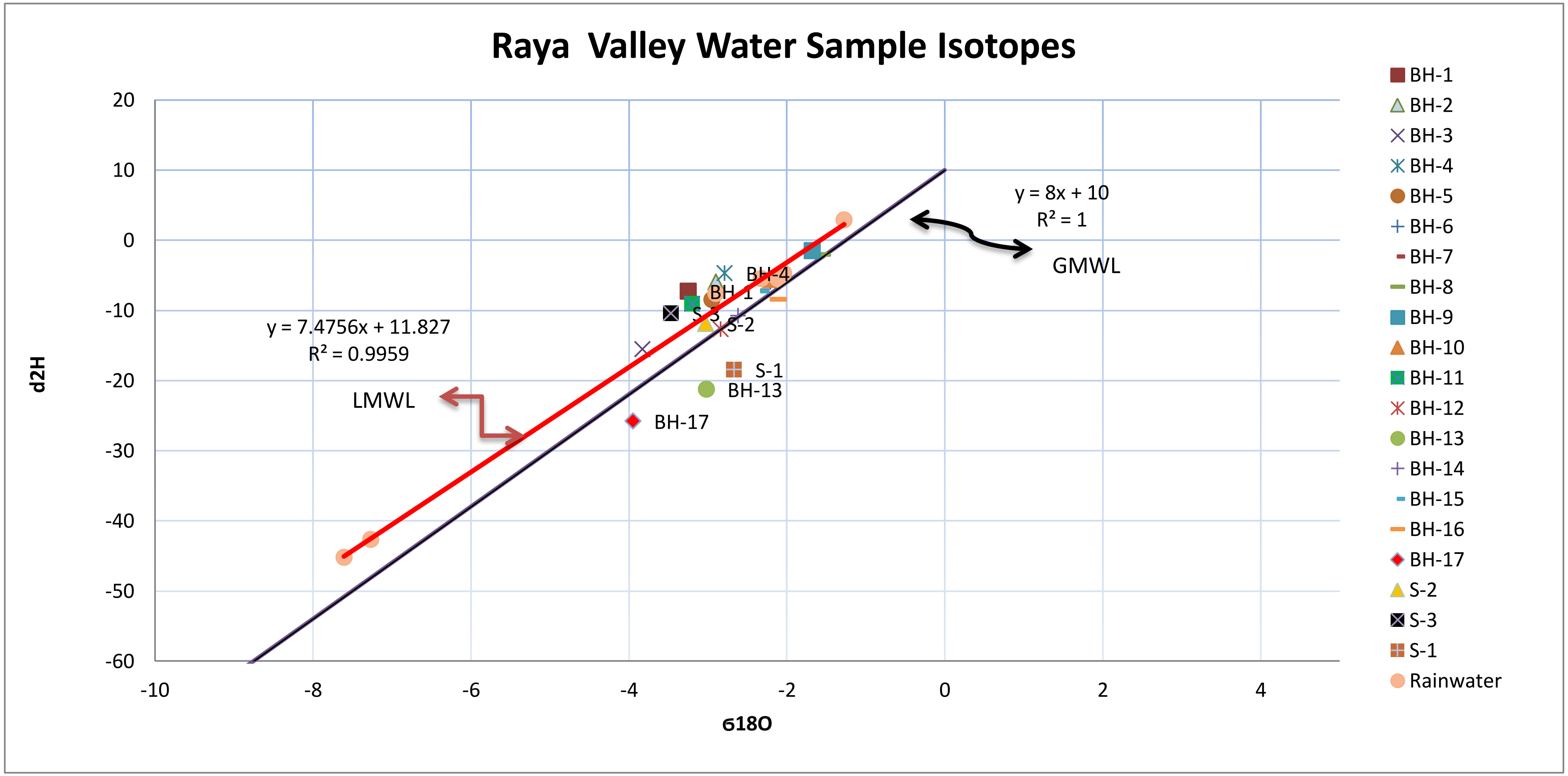

Figure 6.7 Isotope analysis of water samples in relation to GMWL and LMWL

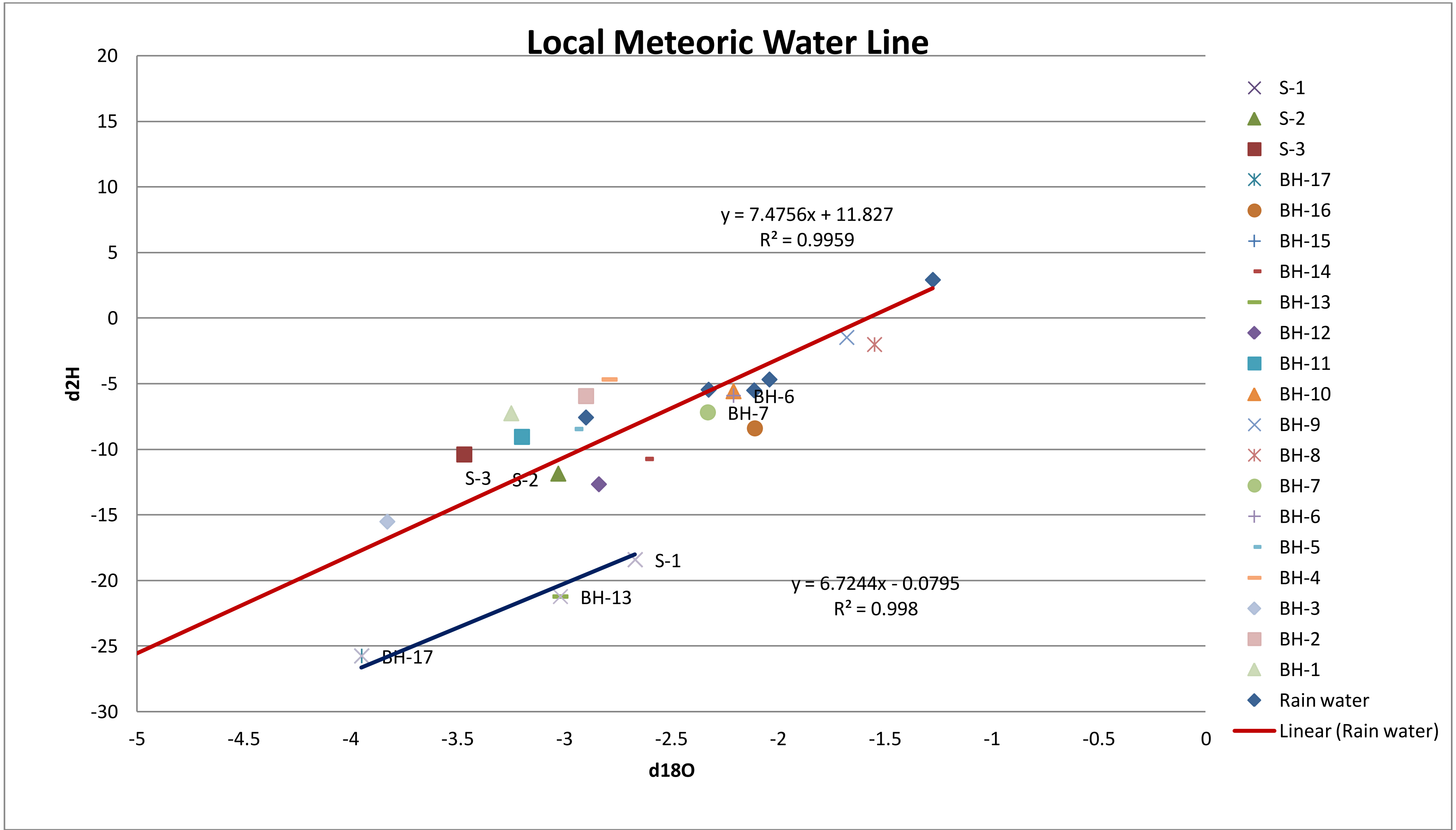

Figure 6.8 Isotope analysis of water samples in relation to LMWL

Table 6-4 Isotope analysis results

Lab. Sample Number	Sample Code	δ^{2}H Reportable Value (Permil)	δ^{18}O Reportable Value (Permil)
001 – 11	BH – 1	-7.25	-3.25
002 – 11	BH – 2	-5.94	-2.90
003 – 11	BH – 3	-15.51	-3.83
004 – 11	BH – 4	-4.67	-2.79
005 – 11	BH – 5	-8.45	-2.95
006 – 11	BH – 6	-5.90	-2.21
007 – 11	BH – 7	-7.18	-2.33
008 – 11	BH – 8	-2.01	-1.55
009 – 11	BH – 9	-1.47	-1.68
010 – 11	BH – 10	-5.57	-2.21
011 – 11	BH – 11	-9.05	-3.20
012 – 11	BH – 12	-12.66	-2.84
013 – 11	BH – 13	-21.22	-3.02
014 – 11	BH – 14	-10.73	-2.62
015 – 11	BH – 15	-7.23	-2.33
016 – 11	BH – 16	-8.40	-2.11
017 – 11	BH – 17	-25.75	-3.95
018 – 11	S – 1	-18.41	-2.67
019 – 11	S – 2	-11.85	-3.03
020 – 11	S – 3	-10.39	-3.47

7. CHAPTER VII GROUNDWATER RECHARGE EVALUATION

7.1. INTRODUCTION

Quantification of the rate of natural groundwater recharge is a basic pre-requisite for efficient groundwater resource management. It is particularly important in regions with large demands for ground water supplies, where such resources are the key to economic development. However, the rate of aquifer recharge is one of the most difficult factors to measure in the evaluation of groundwater resources. The main techniques used to estimate ground water recharge rates are the Soil Water Balance approach, WetSpass, Chloride Mass Balance and the Groundwater Level Fluctuation approach etc. Estimation of recharge, by whatever method, is normally subject to large uncertainties and errors. The Thornthwaite, WetSpass and Chloride Mass Balance methods are employed in this research work and are presented as follows:

7.2. THORNTHWAITE AND MATHER METHOD

Water balance calculations are required to know the amount of water available for ground water recharge and to indicate proper management of groundwater utilization. The water balance calculation is made using the following equation:

where

P = Precipitation

AET = Actual evapotranspiration

Runoff = Overland flow

I = Infiltration

The estimation of the different hydrologic parameters involves different important considerations and assumptions. Water balance is done for the data of the years 1996-2007. (Thornthwaite and Mather, 1955) developed a simple "bookkeeping" model, which estimates the balance between the inflow and outflow of water. When applying this method, to estimate the recharge for a catchment area, the calculation should be repeated for areas with different precipitation, evapotranspiration, crop type and soil type.

The input parameters are mean monthly effective precipitation, mean monthly potential evapotranspiration of the considered months and water holding capacity of the soils. In addition to calculating the actual evapotranspiration of the catchment the model has been used to estimate the soil moisture deficit, detention, and runoff .The inputs of this model were derived as follows:

7.2.1 Raya Valley soil map

The Raya Valley Pressurized Irrigation Project (RVPIP, 2008) had studied the water holding capacity of soils in the Valley using a total of 1270 auger observations and 91 profile pits, and 14 hydraulic conductivity and infiltration measurements, core sampling and deep boring. Soil samples were collected from 47 profile pits for full laboratory analysis. The result of their analysis confers the average soil moisture content and the rooting depth, up to which evapotranspiration is effective, for each soil type.

In this work the soil types were classified and mapped into six groups (Figure 7.1). Accordingly the areal coverage of each soil type is calculated using ArcGIS 9.3. The root depth of all soil types and the water holding capacity of each soil were adopted from the data of (RVPIP, 2008) and FAO soil classification in running the model. An overlay of the soil map with the Thiessen polygons made it possible to get the proportion of each soil type in each polygon. Finally, the weighted average of each polygon was used in calculating the inputs to the method (Table 7-1). And hence, the maximum available water content is considered to 140mm as weighted average of the Raya Valley.

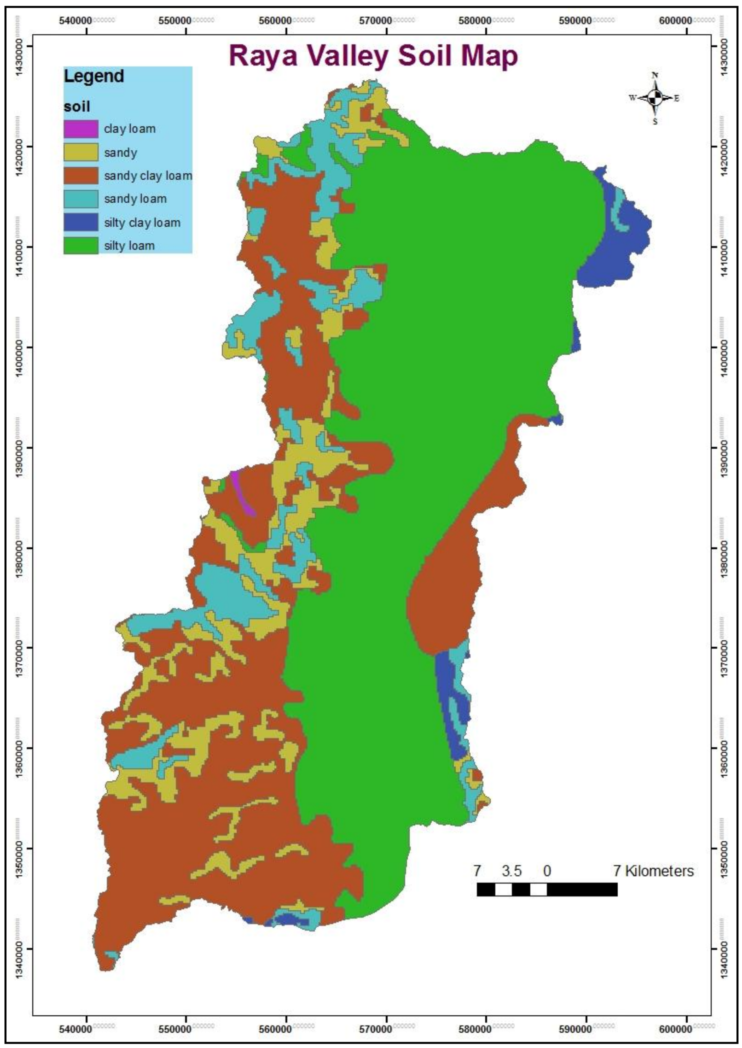

Figure 7.1 Soil classification map

Table 7-1 Frequency of occurrence and field capacity of soil types, after WWDSE and FAO 1988

Soil type	Field capacity	Frequency of a Soil type in each Thiessen Polygon in %							
		Alamata	Chercher	Kobo	Korem	Maichew	Mehoni	Wajja	Sum
SANDY	110	14.11	0	3.63	23.33	13.52	4.38	11.41	70.38
SANDY CLAY LOAM	130	38.71	20.91	66.99	38.31	53.51	2.24	39.8	260.47
SANDY LOAM	120	9.27	0.2	3.83	13.89	22.72	7.77	4.04	61.72
SILTY LOAM	140	37.9	76	23.47	23.39	0	80.04	41.53	282.33
SILTY CLAY LOAM	160	0	2.89	2.09	0	10.24	5.57	3.22	24.01
CLAY LOAM	190	0	0	0	1.07	0	0	0	1.07

7.2.2 Potential evapotranspiration

Potential evapotranspiration is defined as the amount of water that would be removed from the land surface by evaporation and transpiration processes if sufficient water were available in the soil to meet the demand. In order to calculate the potential evapotranspiration of the Raya Valley various methods have been employed. The potential evapotranspiration (PET) was estimated using Modified Penman - Montheith method in the Cropwat package, however the results were found to be much higher than pan evaporation estimates recorded at Maichew, the only class A station in the area. Therefore this method is considered as inappropriate method to estimate the evapotranspiration of the area.

Therefore, methods such as radiation based and temperature based approaches were utilized. The objective of calculating the potential evapotranspiration is to extract the actual evapotranspiration values using methods that make use of potential evapotranspiration.

The meteorological data required in estimating evapotranspiration using radiation based methods are summarized below.

Solar short wave radiation (K)

There are no direct short wave and long wave radiation measurements of the Raya Valley. Hence measurements carried out in the periods 1974-1975 by Macdonald et al, 1975 at Mekele 100Km, away from the center of the valley, were adopted. The record includes ten days average values of each month . The incoming solar radiation values are corrected for albedo allowance and are given in mm/ day. This mass of water is converted to energy by multiplying it by the latent heat of vaporization and the results are given in Table 7-2. It can be observed from the table that the highest values are recorded for the months of March, April, May & October and the lowest values for July & August. This variation could be attributed to the cloud cover variation in the area which has a direct effect on the incoming radiation. The values obtained were used to calculate the potential evapotranspiration using radiation based and combination approach methods.

Solar long wave radiation (L)

The recorded long wave radiation data is treated in a similar fashion to that of the short wave radiation before applying it in the evapotranspiration calculations. The lower magnitude of the long wave radiation corresponds to that of the short wave radiation. The result of the long wave radiation is presented in Table 7-2.

Sensible heat exchange (H)

It is a none radiant heat transfer which occurs between the ground surface and the air in the form of latent heat whenever there is a difference in vapor pressure between the surface and the overlying air. The upward rate of sensible heat exchange by turbulent transfer is also measured in the same time and the values are given in mm/day. The result shows lowest values in June, July & August having a similar trend with the short wave and long wave radiation. The monthly sensible heat exchange rate is given in Table 7-2**.**

The monthly mean temperature is given in Table 7-2. The highest temperature is recorded for the months of May, June & July, which coincides with the period when the sun is over head on the area. The lowest temperature is recorded in the months between November and January.

The average monthly relative humidity varies between 0.35 and 0.63. The highest humidity values recorded are for the months of January, February, August & September and the lowest to the months of May & June.

In all cases the available data are averaged and utilized in the calculation of Potential and actual evapotranspiration using the radiation based methods and combination approaches (Dingman, 2002).

Table 7-2 Summary of meteorological data, short wave radiation (K) in cal/cm2/day, long wave radiation (L) in cal/cm2/day, sensible heat (H) in cal/cm2/day, wind speed (va) in m/s, fraction cloud cover (C), temperature in 0C and relative humidity (Wa) in percentage.

Variables	Jan	Feb	Mar	Apr	May	Jun	Jul	Aug	Sep	Oct	Nov	Dec
K	338	343	426	440	436	330	312	270	326	399	362	343
L	-134	-114	-125	-132	-137	-76	-59	-49	-76	-133	-145	-135
H	-98	-96	-99	-120	-48	-11	-20	-66	-93	-85	-96	-96
C	8.0	8.2	8.9	8.5	8.7	6.6	5.4	6.1	6.4	8.5	8.8	8.4
va	162.5	178.4	187.9	180.4	160.2	189.6	218.8	173.4	123.2	135.7	154.5	160.6
Wa	0.63	0.56	0.49	0.52	0.42	0.35	0.51	0.59	0.59	0.52	0.51	0.56
Temp	17.0	19.1	20.3	21.2	22.6	23.8	22.9	21.2	20.9	20.0	19.0	18.4

Radiation based methods

This approach requires data on net radiation, air temperature and pressure. It is a modified Penman's method by (Priestely C.H.B., and Taylor R.J., 1972).

The equation is written as:-

PET is Potential evapotranspiration in cm/ day

The Empirical constants are given as:.

α_{PT} is a constant that depends on the height at which wind speed and air vapor pressure are measured and is equal to 1.26.

γ Is psychometric constant, which is a function of temperature and saturation vapor pressure

ρ_w is mass density of water, 1g/cm^3

λ_v latent heat of vaporization of water, 590cal/g

s(Ta) is slope of saturation vapor pressure vs. air temperature (T in °C) and is given by:-

Temperature Based Methods

a) (Malmstrom V.H.,, 1969)

PET = Potential Evapotranspiration

$e_{sat}(Ta)$ = Saturated vapor pressure of the atmosphere.

b) Thornthwaite Method (1948)

The Thornthwaite methods requires only temperature data and the equation is given

ET_0 = Potential evapotranspiration in mm per month.

t = mean monthly temperature in ^{0}C .

i = monthly heat index

I = annual heat index obtained by summing the 12 monthly heat indices,

$$i = \left(\frac{t}{5}\right)^{1.514}$$

$$a = 675*10^{-9}I^3 - 771*10^{-7}I^2 + 1792*10^{-5}I + 0.49239$$

Meanwhile, the correction factor k, which is the day light length proportion as given by the equation

was utilized to correct the input of Thornthwaite method for calculating potential evapotranspiration as defined by (COMISIÓN DOCENTE CURSO INTERNACIONAL DI HIDROLOGÌA SUBTERRÁNEA, 2009)

Manipulation of the above equations resulted in the following monthly potential evapotranspiration values and is given in Table 7-3.

Table 7-3 Calculated potential evapotranspiration using different methods

Stations	Methods	Jan	Feb	Mar	Apr	May	Jun	Jul	Aug	Sep	Oct	Nov	Dec	Total
Maichew	Radiation	43	56	87	81	109	109	102	68	68	75	58	44	898
	Malmstrom	57	63	66	68	68	73	69	71	68	60	56	54	773
	Thornthwaite	47	47	62	66	81	85	82	76	63	54	45	41	747
Chercher	Radiation	47	54	95	87	123	116	112	74	72	85	52	50	965
	Malmstrom	73	78	89	95	105	109	99	92	91	88	79	77	1075
	Thornthwaite	61	64	92	103	129	133	117	103	95	89	69	67	1123
Kobo	Radiation	49	55	96	88	125	117	115	76	73	85	54	51	984
	Malmstrom	86	86	96	104	109	109	104	104	96	88	86	73	1140
	Thornthwaite	59	64	92	107	132	140	127	104	84	72	62	60	1102
Alamata	Radiation	45	54	94	86	122	116	114	73	71	84	53	50	962
	Malmstrom	65	75	80	86	94	101	93	81	79	75	72	67	968
	Thornthwaite	59	64	92	107	132	140	127	104	84	72	62	60	1102
Waja	Radiation	50	55	95	85	123	118	113	75	73	85	55	52	977
	Malmstrom	91	84	88	88	104	118	101	98	98	88	91	86	1135
	Thornthwaite	63	61	86	89	113	136	125	112	103	81	69	56	1093
Korem	Radiation	43	48	84	78	109	103	102	67	64	73	45	43	859
	Malmstrom	53	55	61	62	67	73	71	69	64	58	54	52	737
	Thornthwaite	43	42	58	66	74	81	80	74	64	53	43	40	720
Mehoni	Radiation	44	55	92	85	118	111	114	71	69	84	52	51	946
	Malmstrom	67	84	83	87	88	93	96	82	85	85	81	81	1012
	Thornthwaite	47	70	77	85	93	99	109	79	79	80	68	70	955

As it is observed in table above, there are similarities of the results obtained from the temperature based methods. However, the results of the radiation based method, almost in all areas are within a limit range, sometimes greater than the temperature methods.

After preparation of the input parameters, the Thornthwaite method requires constructing a table that consists of rows of: Precipitation (PPT), potential evapotranspiration (PET), the difference between PPT and PET, and accumulated potential water loss (ACPWL) as the summation of the excessive potential evapotranspiration for the dry months; and soil moisture storage, which can be derived from maximum available water capacity (MAWC) and the ACPWL using the following equation . Then the change in soil moisture content was calculated for consecutive months, while the difference between PPT and the change in soil moisture storage will give rise to Actual Evapotranspiration (AET). This value will be equal to PET during excess rain and never is greater than PET. The deficit D is the difference between potential and actual evapotranspiration and the surplus (which is the available water for both infiltration and runoff) is the excess water in the wet seasons beyond the field capacity (Leopold, Thomas Dunne and Luna B., 1998)

To observe the effect of precipitation on the amount of water available for both infiltration and runoff, analysis of the year of highest precipitation(Table 7-5), lowest precipitation(Table 7-7) and average precipitation (Table 7-6)where employed in performing the water balance using Thornthwaite method. The outputs are presented in tables (7.5-7.7) and the summary is given in Table 7-4.

Table 7-4 comparison of outputs of Thornthwaite method at different amount of precipitation

RAYA VALLEY BASIN									
Average PPT				High PPT 1999			Low PPT 2003		
PPT	733.6			753.4		3% incremnt of average PPT	688.0		6% reduction of average PPT
PET	926.2			926.2			926.2		
AET	634.5	86.5% of PPT		631.6	84% of PPT	0.5% reduction than average AET	654.3	95% of PPT	3% increment than average AET
CAW	99.1	13.5% of PPT		121.8	16.16% of PPT increased from average	23% increment of Average CAW	34.3	5% of PPT decreased from average	65% reduction of average CAW
Runoff, R	31.7	4.3% of PPT	32% of CAW	39.0	5.2% of PPT increase from average	23% increment of Average R	11.0	1.6% of PPT decreased from average	65% reduction of average R
Infiltration (I)	**67.4**	**9.2% of PPT**	**68% of CAW**	**82.8**	**11% of PPT increased**	**23% increment of Average(I)**	**23.3**	**3.4% ofPPT decreased from average**	**65% reduction of average I**

where PPT is Precipitation, PET is Potential Evapotranspiration, AET is Actual Evapotranspiration and CAW is Cumulative Available Water that can be divided into both runoff and infiltration.

The following observations can drawn from the results in Table 7-4:

- The Actual Evapotranspiration does not change even when there is an increment in the amount of rainfall but when there is a decrease in precipitation there is an increment of AET. This could be due the relatively extended daily sunshine hours caused by lack of cloud cover which exposed a drop of water for evaporation.
- The cumulative available water shows an increment of 23%, from that of the average precipitation period, in response to 3% rainfall increment in precipitation. While 65% reduction is observed in response of 6% reduction in precipitation.

- The runoff and infiltration are affected by rainfall variability in a similar trend of CAW. Therefore it can be concluded that the CAW and its components are highly affected by rainfall variability than the actual evapotranspiration.

Table 7-5 Results of Thornthwaite method at higher precipitation

						1999 higher PPT							
	JAN	**FEB**	**MAR**	**APR**	**MAY**	**JUNE**	**JULY**	**AUG**	**SEP**	**OCT**	**NOV**	**DEC**	
PPT	59.3	41.0	43.2	26.8	22.0	15.8	117.5	323.4	62.6	32.0	0.5	9.4	753.37
PET	51.9	56.0	75.5	83.3	100.9	109.0	102.7	88.1	78.5	69.3	57.4	53.6	926.18
PPT-PET	7.4	-15.0	-32.3	-56.5	-79.0	-93.2	14.8	235.4	-16.0	-37.3	-56.9	-44.2	
Acc pwl	-147.0	-162.1	-194.4	-250.9	-329.8	-423.0	-408.2		-16.0	-53.3	-110.2	-154.4	
SM retained	48.7	43.7	34.6	23.1	13.1	6.7	7.4	140.0	124.0	86.7	63.4	46.1	
ΔSM	2.5	-5.0	-9.1	-11.6	-10.0	-6.4	0.8	132.6	-16.0	-37.3	-23.3	-17.3	
AET	51.9	46.0	52.3	38.3	31.9	22.2	102.7	88.1	78.5	69.3	23.8	26.6	631.62
Deficit	0.0	10.0	23.3	45.0	69.0	86.8	0.0	0.0	0.0	0.0	33.6	26.9	294.56
Surplus	4.9	0.0	0.0	0.0	0.0	0.0	14.1	102.8	0.0	0.0	0.0	0.0	121.76
Availa. water	0.0	0.0	0.0	0.0	0.0	0.0	0.0	102.8	0.0	0.0	0.0	0.0	
Runoff	0.0	0.0	0.0	0.0	0.0	0.0	0.0	32.9	0.0	0.0	0.0	0.0	
Detention	0.0	0.0	0.0	0.0	0.0	0.0	0.0	69.9	0.0	0.0	0.0	0.0	

Table 7-6 Results of Thornthwaite method at average precipitation

Average Precipitation in mm													
	JAN	FEB	MAR	APR	MAY	JUNE	JULY	AUG	SEP	OCT	NOV	DEC	
PPT	30.9	10.3	30.0	58.5	49.3	24.0	169.0	254.2	51.1	12.3	30.6	13.5	733.61
PET	51.9	56.0	75.5	83.3	100.9	109.0	102.7	88.1	78.5	69.3	57.4	53.6	926.18
PPT-PET	-21.0	-45.7	-45.5	-24.8	-51.7	-85.0	66.3	166.2	-27.5	-57.0	-26.8	-40.1	
Acc pwl	- 172.4	-218.1	-263.6	-288.4	-340.1	-425.1			-27.5	-84.4	- 111.2	- 151.3	
SM retained	40.5	29.2	21.0	17.6	12.1	6.6	72.9	140.0	112.5	55.6	62.9	47.2	
ΔSM	-6.6	-11.4	-8.1	-3.4	-5.5	-5.6	66.3	67.1	-27.5	-57.0	7.4	-15.8	
AET	37.5	21.7	38.1	62.0	54.7	29.6	102.7	88.1	78.5	69.3	23.2	29.3	634.53
Deficit	14.4	34.4	37.4	21.3	46.2	79.4	0.0	0.0	0.0	0.0	34.2	24.3	291.65
Surplus	0.0	0.0	0.0	0.0	0.0	0.0	0.0	99.1	0.0	0.0	0.0	0.0	99.08
Availa. water	0.0	0.0	0.0	0.0	0.0	0.0	0.0	99.1	0.0	0.0	0.0	0.0	
Runoff	0.0	0.0	0.0	0.0	0.0	0.0	0.0	31.7	0.0	0.0	0.0	0.0	
Detention	0.0	0.0	0.0	0.0	0.0	0.0	0.0	67.4	0.0	0.0	0.0	0.0	

Table 7-7 Results of Thornthwaite method at lower precipitation

2003 lower PPT in mm													
	JAN	FEB	MAR	APR	MAY	JUNE	JULY	AUG	SEP	OCT	NOV	DEC	
PPT	**35.5**	**40.4**	**45.1**	**82.5**	**19.8**	**21.9**	**102.1**	**254.7**	**56.5**	**0.6**	**0.8**	**27.9**	**688.04**
PET	**51.9**	**56.0**	**75.5**	**83.3**	**100.9**	**109.0**	**102.7**	**88.1**	**78.5**	**69.3**	**57.4**	**53.6**	**926.18**
PPT-PET	**-16.4**	**-15.6**	**-30.4**	**-0.8**	**-81.2**	**-87.1**	**-0.6**	**166.6**	**-22.0**	**-68.6**	**-56.6**	**-25.7**	
Acc pwl	**-189.3**	**-204.9**	**-235.3**	**-236.0**	**-317.2**	**-404.2**	**-404.8**		**-22.0**	**-90.6**	**-147.2**	**-172.9**	
SM retained	**35.9**	**32.1**	**25.8**	**25.7**	**14.3**	**7.7**	**7.6**	**140.0**	**119.5**	**73.0**	**48.6**	**40.4**	
ΔSM	**-4.5**	**-3.8**	**-6.3**	**-0.1**	**-11.3**	**-6.7**	**0.0**	**132.4**	**-20.5**	**-46.5**	**-24.4**	**-8.2**	
AET	**40.0**	**44.2**	**51.4**	**82.7**	**31.1**	**28.6**	**102.7**	**88.1**	**77.0**	**47.2**	**25.2**	**36.1**	**654.29**
Deficit	**11.9**	**11.8**	**24.1**	**0.6**	**69.8**	**80.4**	**0.0**	**0.0**	**1.5**	**22.1**	**32.2**	**17.5**	**271.89**
Surplus	**0.0**	**0.0**	**0.0**	**0.0**	**0.0**	**0.0**	**0.0**	**34.3**	**0.0**	**0.0**	**0.0**	**0.0**	**34.28**
Availa. water	**0.0**	**0.0**	**0.0**	**0.0**	**0.0**	**0.0**	**0.0**	**34.3**	**0.0**	**0.0**	**0.0**	**0.0**	
Runoff	**0.0**	**0.0**	**0.0**	**0.0**	**0.0**	**0.0**	**0.0**	**11.0**	**0.0**	**0.0**	**0.0**	**0.0**	
Detention	**0.0**	**0.0**	**0.0**	**0.0**	**0.0**	**0.0**	**0.0**	**23.3**	**0.0**	**0.0**	**0.0**	**0.0**	

Table 7-8 Weighted average precipitation

Basin weighted Precipitation in mm													
YEAR	JAN	FEB	MAR	APR	MAY	JUNE	JULY	AUG	SEP	OCT	NOV	DEC	
1996	61.7	5.1	63.7	129.7	119	82.7	83.7	188.2	47.5	10.3	68.1	4.6	864.3
1997	49.8	1.5	84.1	36.3	39.2	36.4	126.8	68.8	32.3	188.4	74.2	1.4	739.2
1998	76.3	32.5	28	30.4	47	40.3	216.8	276.9	90.7	12.6	1.3	2.8	855.6
1999	59.3	41	43.2	26.8	22	15.8	117.5	323.4	62.6	32	0.5	9.4	753.5
2000	17.1	3.7	11.3	52.7	54.4	9.7	217.4	305.5	46.3	53.3	79.1	42.8	893.3
2001	8.1	2.7	75	16	24.2	31.5	188.2	236.3	55.9	9.9	10.8	4.7	663.3
2002	43	1.8	21.4	62.8	13.7	6.3	73.6	178.5	58.9	12.2	1.6	52.6	526.4
2003	35.5	40.9	45.2	82.5	19.8	21.9	102.1	254.7	56.5	0.6	0.8	27.9	688.4
2004	29.8	15.4	49.4	116.7	9.9	43.4	81.8	169.6	47.8	36.7	23.2	10.2	633.9
2005	18.4	12	55	124.5	84.3	28.6	138.6	180.1	28.9	13.8	16.5	3.1	703.8
2006	6	5.6	127.6	110.1	25.1	28.8	113.3	217.2	46.6	25.3	27.9	39.7	773.2
2007	23.9	35	25.3	88.6	14.3	36	212.4	219.6	37.6	7.9	7.3	1.3	709.2
WEIGHTED AVERAGE													733.675

7.3. WETSPASS MODEL

7.3.1 Concepts of WetSpass

The model is described by (Batelaan O. and De Smedt F., 2001) as follows: The WetSpass term stands for Water and Energy Transfer between Soil, Plants and Atmosphere under quasi-Steady State (Batelaan and De Smedt, 2001). It is a physically based model for the estimation of the long term average spatial patterns of groundwater recharge, surface runoff and evapotranspiration performed by means of long term average meteorological data together with land use, soil, and groundwater level grid maps by employing physical and empirical relationships. The model treats a basin or a region as a regular pattern of grid cells. Every grid cell may be subdivided in a vegetated and a non-vegetated part. For every grid cell a water balance will be maintained.

Regional groundwater models used for analyzing recharge-discharge relations are often quasi-steady state and need long term average recharge input that accounts for the spatial variability of the recharge. Thus, the recharge output from WetSpass can be used for these computations. Among the water cycle components, evapotranspiration is the determining factor in the water balance. Therefore, the WetSpass approach aims at describing the evapotranspiration processes in a physically based way while other processes in the determination of the water balance are treated more empirically.

In general, WetSpass gives various hydrologic outputs on yearly and seasonal (summer and winter) basis. Even though the model is originally developed mainly to compute the long-term average spatially distributed recharge of a basin, it also computes the spatially distributed surface runoff, evapotranspiration, interception, transpiration, soil evaporation and error in water balance.

The model is entirely integrated with GIS Arc View (3.x) as a raster model coded in Avenue, the programming language of Arc View. Parameters such as land use and soil types are connected to the model as attribute tables of the land use and soil raster maps. This makes it handy in that it allows easy new definitions of climatic as well as land use and soil types (Batelaan O. and Woldeamlak S.T., 2003).

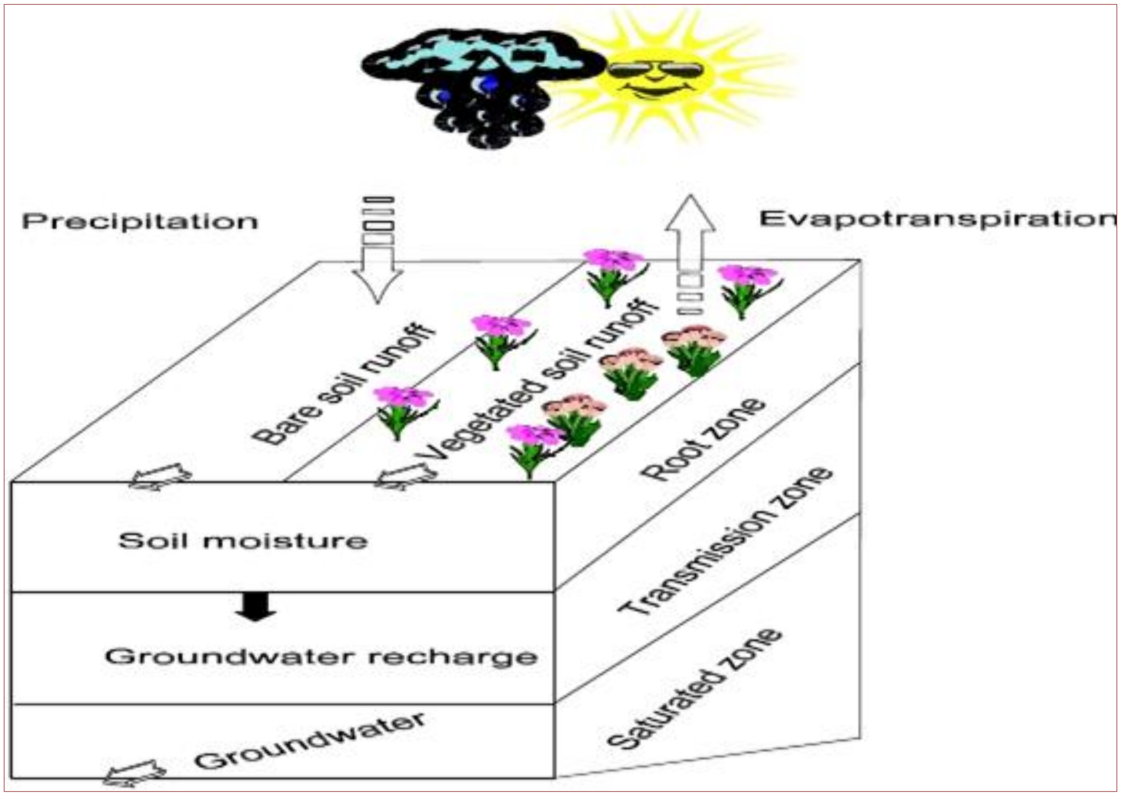

Figure 7.2 Schematic water balance in typical grid cell, (Asefa T, Wang Z, Batelaan O, De Smedt F, 1999)

It uses long-term average precipitation, potential evaporation from free water surface and wind speed as inputs, to simulate average spatial patterns of surface runoff, actual evapotranspiration and groundwater recharge in a basin or a region. It is a simplified version of the time dependent spatial distributed water balance model 'WetSpa' (Batelaan O., Wang Z. M. & de Smedt F., 1996). The model treats a basin or a region as a regular pattern of grid cells. Every grid cell can be subdivided in a vegetated and a non-vegetated part. For every grid cell a water balance will be maintained.

Water balance components

Since WetSpass model is a distributed water balance model, the water balance computation is performed at raster cell level. Individual raster water balance is obtained by summing up independent water balances for the vegetated, bare soil, open water and impervious fractions of a raster cell. This allows, depending on the resolution of the raster cell, to account for the non-uniformity of the land-use per cell and soil type per cell (Figure 7.2).

In general the total water balance components, per raster cell and season, can be calculated using the water balance components for vegetated, bare soil, open water and impervious parts of the raster cell (Batelaan O. and De Smedt F., 2001) as follows:

$$ET_{raster} = a_v ET_v + a_s E_s + a_o E_o + a_i E_i \quad 2.1$$

$$S_{raster} = a_v S_v + a_s S_s + a_o S_o + a_i S_i \quad 2.2$$

$$R_{raster} = a_v R_v + a_s R_s + a_o R_o + a_i R_i \quad 2.3$$

Where ET_{raster}, S_{raster} and R_{raster} are the total evapotranspiration, surface runoff, and groundwater recharge of a raster cell respectively, each having **v**egetated, bare **s**oil, **o**pen water and **i**mpervious area components denoted by a_v, a_s, a_o, and a_i respectively.

Precipitation is taken as the starting point for the computation of the water balance of each of the above mentioned components of a raster cell, the rest of the processes (interception, runoff, evapotranspiration, & recharge) follow in an orderly manner. This order becomes a prerequisite for the seasonal time scale with which the processes will be quantified.

The water balance for vegetated surfaces is given by:

(1)

where P is the average seasonal precipitation [LT^{-1}], I, is the interception by vegetation [LT^{-1}], is runoff over land surface beneath vegetation [LT^{-1}], is the actual transpiration [LT^{-1}] and is groundwater recharge [LT^{-1}].

The **interception** fraction has been shown to be reasonably constant at a given annual precipitation value and exhibits a consistent decrease with increasing annual rainfall total (Roberts J., 1983). Therefore, the intercepted value is parameterized as a constant percentage from precipitation, dependent on the vegetation type .

The **surface runoff**, , is calculated in two stages. In the first the potential surface runoff is calculated as a coefficient times the precipitation minus the interception:

where is a surface runoff coefficient for vegetated infiltration areas, based on the rational formula (Smedema L. K. & Rycroft D. W., 1988). is a function of vegetation type, soil type and slope. In groundwater discharge areas, saturated surface runoff is occurring. Here, the surface runoff coefficient is very high and assumed to be constant, due to its reduced dependency on soil and vegetation type and the generally near to river position of the runoff producing areas. In the second stage, the potential surface runoff is actualized by taking into account differences in precipitation intensities in relation to soil infiltration capacities. (Rubin J., 1966) showed that in this case Hortonian overland flow is rare.

Is a coefficient that parameterizes the part of the seasonal precipitation which is actually contributing to the Hortonian surface runoff. In groundwater discharge areas all intensities of precipitation contribute to surface runoff, i.e. is 1. In infiltration areas only with high intensity storms will generate surface runoff.

In order to obtain a seasonal distributed **evapotranspiration** value, WetSpass proposes to convert the open-water evaporation value, as commonly available from the Penman equation, to a reference transpiration (Federer C. A., 1979) value based on a vegetation coefficient:

where is the reference transpiration of a vegetated surface [LT^{-1}], is the potential evaporation of open water [LT^{-1}] and *c* is the vegetation coefficient. The vegetation coefficient can be determined as the quotient of the reference vegetation transpiration and the potential open-water evaporation, as given by the Penman equation, resulting in:

where the proportionality constant Δ is the slope of the first derivative of the saturated vapor pressure curve [$ML^{-1}T^{-2}C^{-1}$], is the psychrometric constant [$ML^{-1}T^{-2}C^{-1}$], is the canopy resistance [TL^{-1}] and is the aerodynamic resistance [TL^{-1}]. is calculated as follows:

)

Where k is the Von Kármán constant, is the wind speed on the measurement level , d is the zero-plane displacement length and is the roughness length for the vegetation or soil, is the slope of the saturation vapor pressure at the prevailing air temperature. The value of indicates the Penman coefficient, and can be obtained according to the following table(Table 7-9):

Table 7-9 γ/Δ variation with temperature

	-20	-10	0	5	10	15	20	25	30	35	40
	5.864	2.829	1.456	1.067	0.793	0.597	0.445	0.351	0.273	0.215	0.171

In vegetated groundwater discharge areas, the actual transpiration, , is equal to the reference transpiration, since soil water availability is not limiting:

where, is the groundwater depth [L], h_t is the tension saturated height [L] and R_d is the rooting depth [L]. The actual transpiration for vegetated areas where the groundwater level is below the root zone is calculated as:

where f (Ø) is a function of the water content. In WetSpass, for a time invariant situation; the methodology developed by (Vandewiele G. L., Xu C.-Y. & Ni-Lar-Win, 1991)is used for defining f (Ø):

where a_1 is a calibrated parameter related to the sand content of a soil type (Van der Beken & Huybrechts, 1990), w is the available water for transpiration [LT^{-1}], and is the plant available water content.

Water balance for non-vegetated surfaces

The same procedure as for the vegetated surfaces can be applied for the non-vegetated surfaces. The water balance for non-vegetated surfaces is given by:

where P is the precipitation, E_s is the actual evapotranspiration of the non-vegetated surfaces, S_s is the surface runoff and R_s is the groundwater recharge. The potential evapotranspiration is given by:

In the model the coefficient c is 1, because it is assumed that the surface resistance of water and non-vegetated soils are equal. The actual evapotranspiration is calculated as (Vandewiele G.L., Xu C-Y. and Ni-Lar-Win,, 1993):

Where is a factor determined by:

Where is the potential evapotranspiration calculated according to Equation12, a_1 is a factor which is determined by the sand content in a soil type (Van der Beken, A. and Huybrechts, W., 1990), and w is the available water for evapotranspiration, coming from the precipitation and the water in the soil.

The available water for evapotranspiration is calculated, on monthly basis, as:

where P_m is the average monthly precipitation, θ_{vc} the water content in the soil at field capacity, θ_{vw} the water content in the soil at permanent wilting point, and L_w the extinction depth of the evaporation in the soil, here taken as 1 m.

For groundwater discharge areas f in Equation 13 is 1 because on the saturated non-vegetated soil the evapotranspiration is potential. Ss, the surface runoff is calculated as a coefficient times the net-precipitation

where CSs is a surface runoff coefficient for non-vegetated surfaces, adjusted after Mallants and Feyen (1990).

Groundwater recharge can be calculated as a residual term, from the water balance:

The methodology described here will result in the estimation of spatially distributed recharge as a function of vegetation, soil type, slope, groundwater depth, precipitation regime and other climatic variables. Even in groundwater discharge areas some recharge will be calculated, in agreement with the conceptual picture that a thin unsaturated zone is also present in discharge areas, allowing some recharge.

7.3.2 Input data preparation

WetSpass model requires inputs that can be classified as input grid maps and parameter tables. The grids maps are topographic, slope, groundwater level, soil, land use and seasonally classified meteorological maps of precipitation, potential evapotranspiration, temperature and wind speed. These grid files are prepared with the help of ArcGIS 9.3 and Arc view 3.2 softwares. The grid maps and their brief description are given below:

7.3.2.1 Topographic map

Topography of a catchment has a major impact on the hydrological and geomorphological processes active in the landscape. The spatial distribution of topographic features can often be used as an indirect measure of the spatial variability of these processes. Many geographic information systems are being developed that store topographic information as the primary data for analyzing water resource. Besides, topography can be used to develop more physically realistic structures for hydrologic and water resource models that directly account for the impact of topography on the hydrology. The topography grid map of the Raya Valley produced from the Shuttle Radar Topography Mission (SRTM) dataset of the National Aeronautics and Space Administration (NASA) is shown in (Figure 7.3a)

Elevation in the Valley decreases from both north to south and west to east. The minimum which is 1353m above mean sea level is within the depression at the south eastern part of the valley. While the maximum elevation 3680 m is the highest peak in the area around Maichew.

The slope grid map (Figure 7.3b) of the Raya Valley is extracted from the digital elevation model using ArcGIS 9.3 special analyst tool. The slope ranges from 0 to 74.16% with a mean of 10.6% and standard deviation of 10.3%.

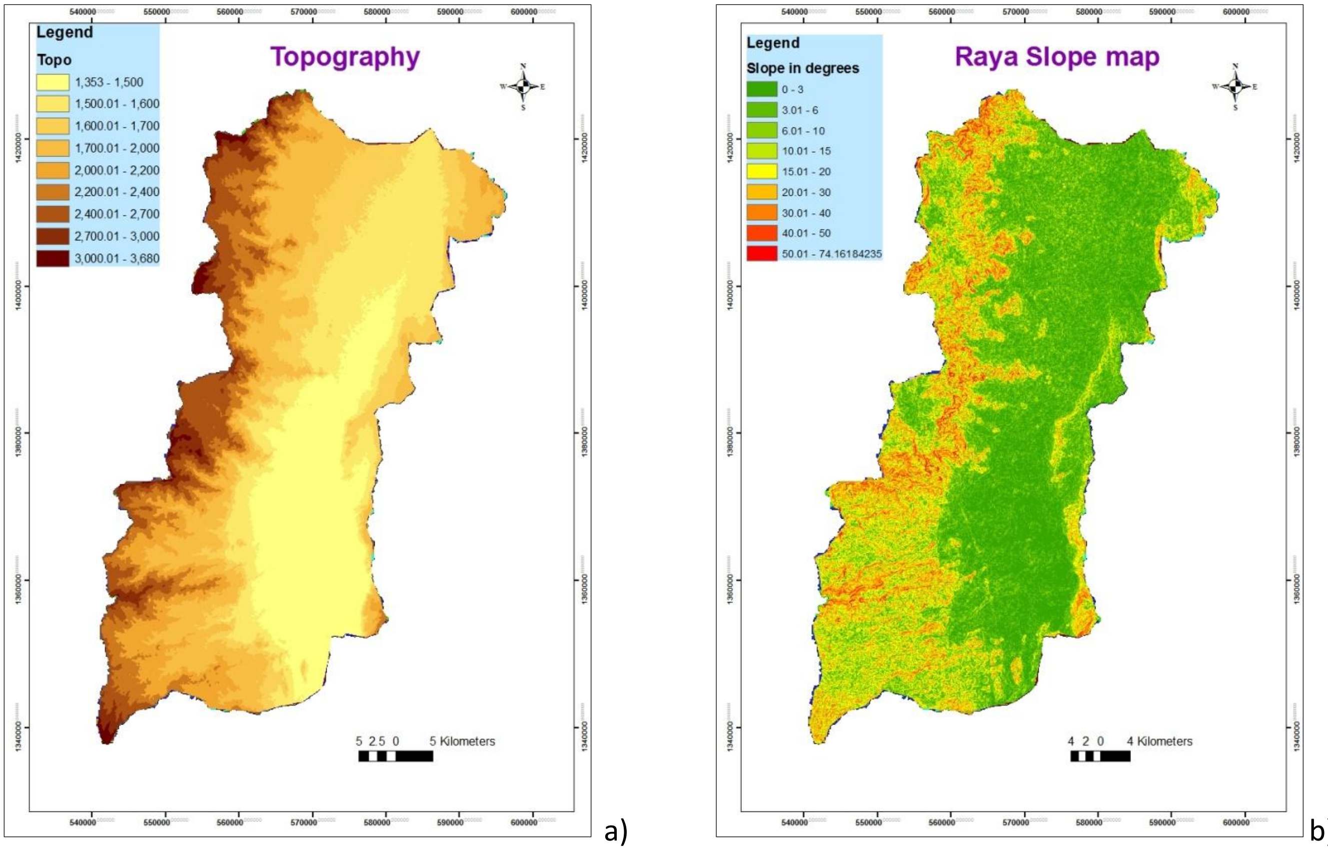

Figure 7.3 a) Topographic b) Slope maps

7.3.2.2 Land Use and Soil grid maps

Land-cover denotes the surface cover over land, including vegetation, rock and human-modified surfaces such as buildings. Land-cover is a characteristic of the land that can be observed physically, as by remote sensing. This is different than land-use, because a single land-cover type can be used in various ways by humans (Encyclopedia of Earth. Eds. Cutler J.)

Up-to-date land-use information is indispensable for water resources monitoring, management and planning. Hence, a land-use map is derived from the land use database map of Ethiopia, using ArcGIS 9.3 software. The land use pattern of the Raya Valley is shown in (Figure 7.4) below. The proportion of each land use unit with respect to the total area is; the bushes and shrubs cover (52%), farmland (41%), wet land (1%), forest (4.9%), and settlements (1%) of the surface area. The soil distribution map described in Figure 7.1, and this land use maps were used as an input after converting them to grids.

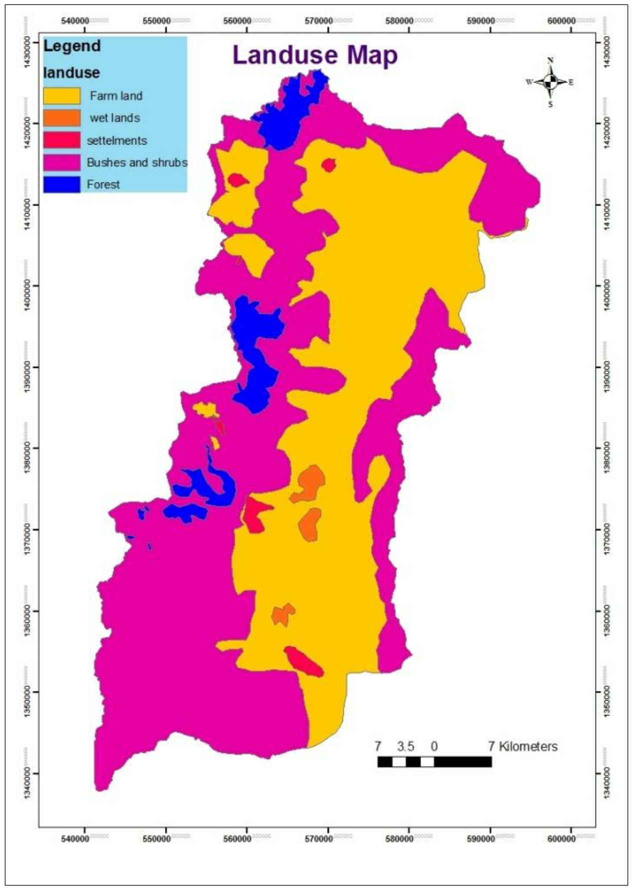

Figure 7.4 Land use map

7.3.2.3 Groundwater level grid map

Groundwater level (grid map) is one input to the WetSpass model. Hence, the groundwater table values of the measured boreholes and springs were interpolated to prepare the groundwater level grid map (Figure 7.5) by exporting them in data base file format.

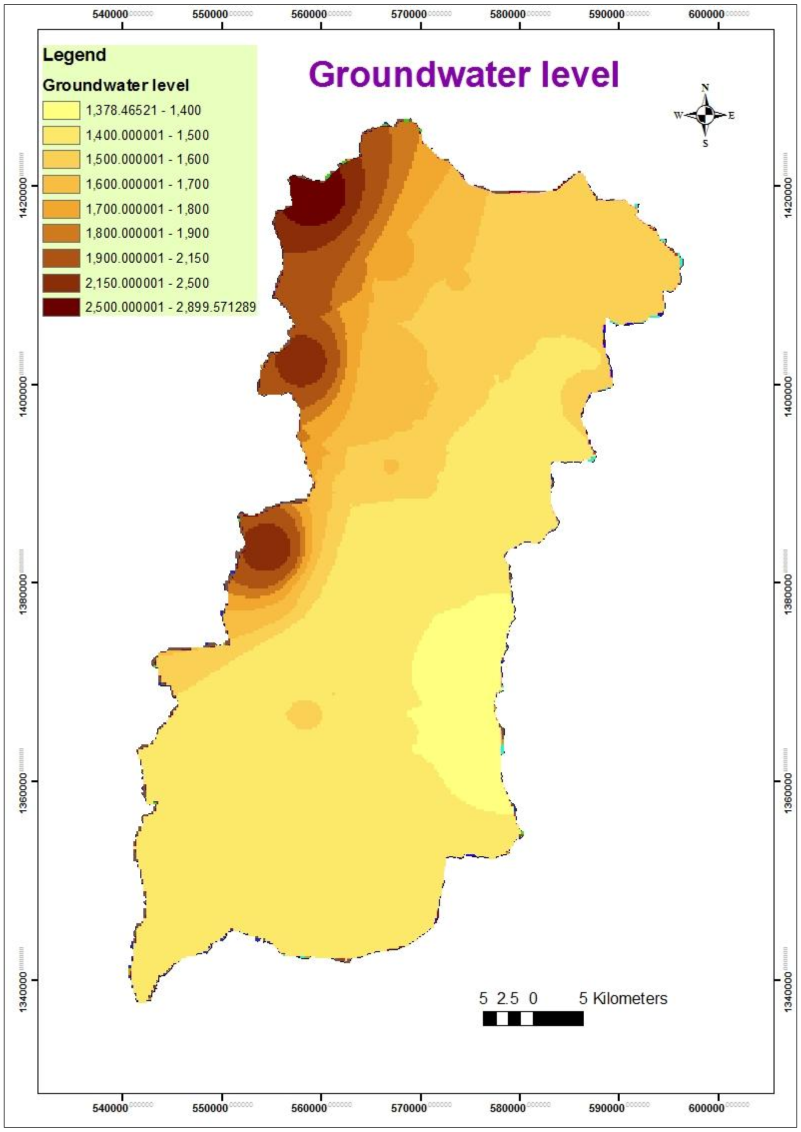

Figure 7.5 Groundwater level map

7.3.2.4 Other grid maps

The calculated winter and summer potential evapotranspiration values, the seasonal mean temperature, the recorded wind speed of the stations at Maichew, Kobo and Chercher, the precipitation in all the stations within the basin are given in (Table 7-10).

Interpolation of the data in Table 7-10 in Arc View was carried out in the preparation of seasonal grid maps as input grids in running the WetSpass model. These grid maps are presented in (Figure 7.6 a & b, Figure 7.7 a & b) below (for both the summer and winter seasons).

Table 7-10 Summarized mean meteorological values exported to data base file format of WetSpass

STATION	X	Y	PPT-S	PPT-W	T-S	T-W	W-S	W-W	PET-S	PET-W
Alamata	560502	1372456	445	346	24	22	0.000	0.000	374	589
Maichew	558432	1412871	475	307	18	15	2.280	1.210	347	552
Korem	556673	1382295	575	357	17	14	0.000	0.000	336	521
Chercher	583164	1385941	442	234	23	21	2.310	2.370	374	591
Waja	565315	1357995	418	248	25	21	0.000	0.000	383	592
Kobo	568641	1343604	443	291	24	21	1.710	1.860	379	602
Raya	570019	1415122	267	262	22	20	0.000	0.000	366	579

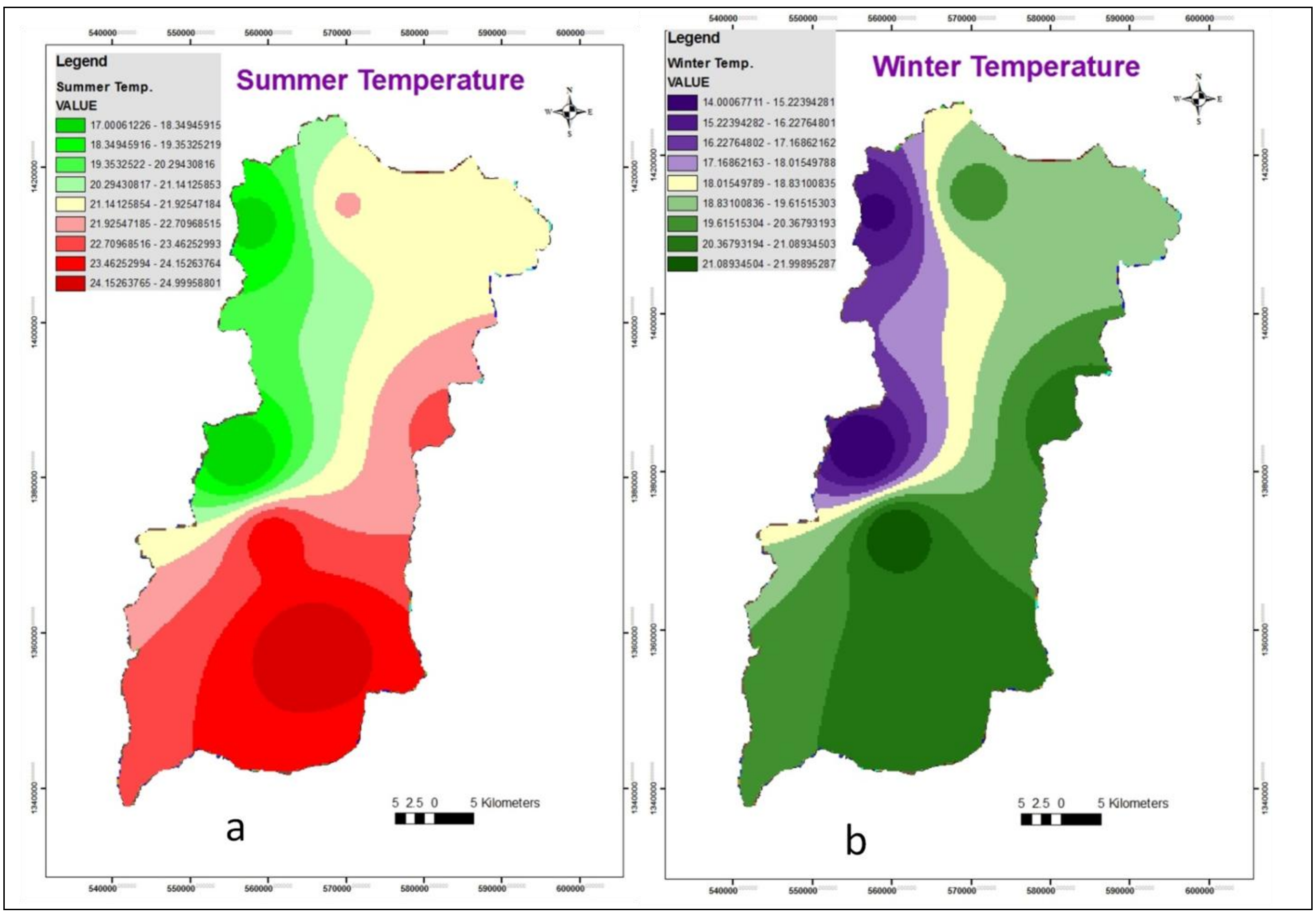

Figure 7.6 a) mean summer (June to September) b) Mean winter (October to May) temperature grids

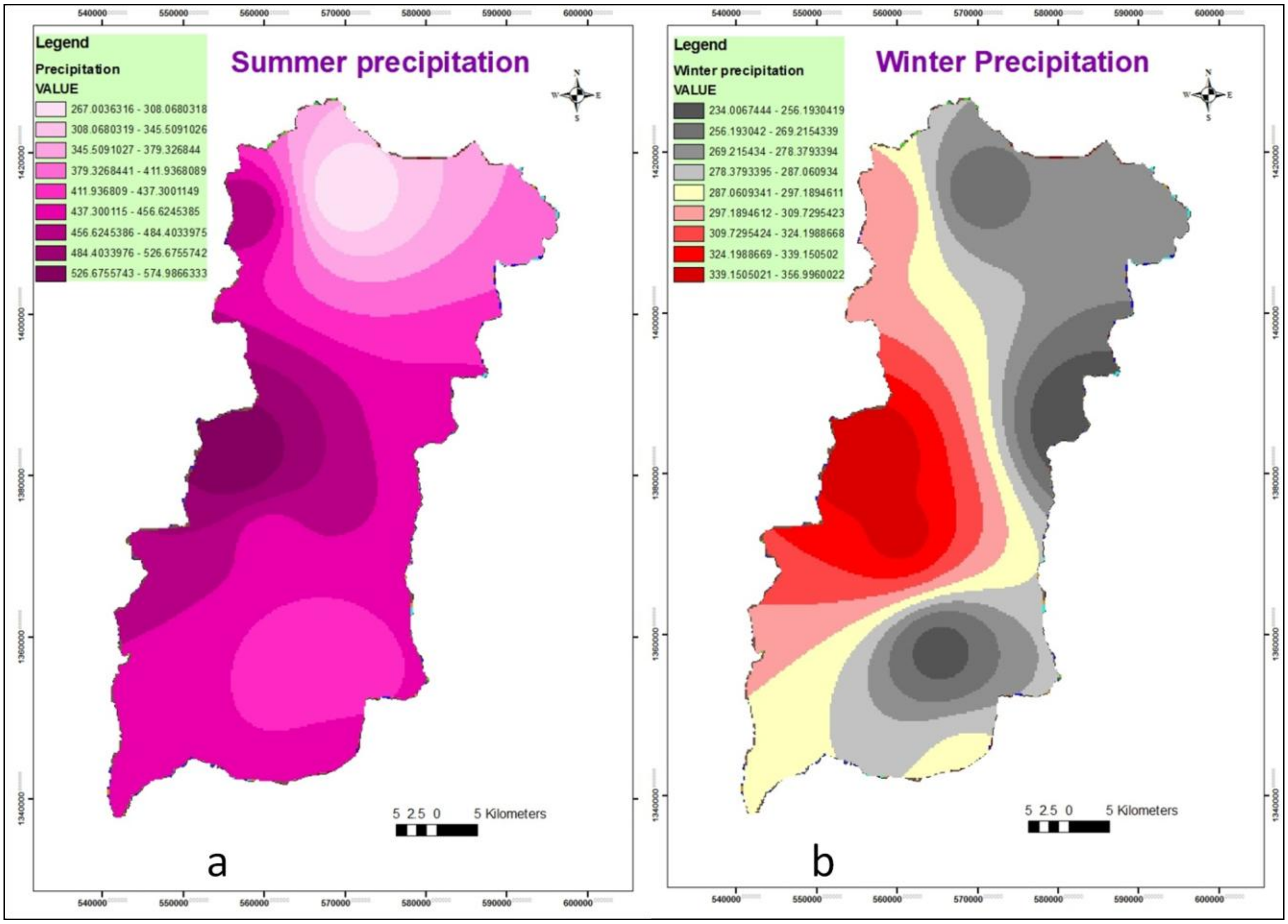

Figure 7.7 a) Summer (June to September) b) Winter (October to May) precipitation grid maps

7.3.2.5 Parameter tables

There are four parameter tables that are linked to the previously described model inputs through their attribute. Summer and winter land-use, soil and runoff coefficient parameters are the four parameters tables used by WetSpass. The land-use attribute tables include fields such as land-use type, rooting depth, leaf area index, vegetation height etc. The soil parameter table fields contain soil parameters such as textural soil class, plant available water contents and proportion of the soil type. The runoff coefficient attribute tables contain parameters for runoff classes of various land-uses, slope, runoff coefficient etc. These attributes tables allow for easy definition of new land-use and soil type as well as changes to each parameter value.

This land-use parameter tables originally were developed to fit the land use types and characteristics from temperate regions, Europe in particular. Thus Kahsay, 2010, has modified these input values to fit the Ethiopian condition, especially to the Raya Valley after his Msc research work in the area. The modified parameters were adopted from his work. The significant modification has been done on the land-use parameters such as leaf area index, crop height and interception percentage of the land use types. The summer and winter land-use parameter tables are presented in

Table 7-11 and Table 7-12 , respectively.

In the meantime, the seasonal variation was adjusted to fit the wet and dry months of Ethiopia before running the model. Hence the number of months that fall in winter are eight (October to May) and four for summer (June to September). In this respect winter is the dry season while summer is the main rainy season in Ethiopia. Therefore, modification of the model inputs was necessary before running the model.

After the above preparation of the input maps and parameter tables, an Arc View 3.2 Avenue script has been used for running WetSpass.

Table 7-11 Modified summer land-use parameter table

NUMBER	LUSE_ TYPE	RUNOFF_ VEG	NUM_ VEG_RO	NUM_I MP_RO	VEG_ AREA	BARE_ AREA	IMP_ AREA	OPENW_ AREA	ROOT_ DEPTH	LAI	MIN_ STOM	INTERC_ PER	VEG_ HEIGHT
21	Cultivation	Crop	1.000	0.000	0.800	0.000	0.200	0.000	0.400	0.200	180.000	35.000	0.700
36	shrub land	Grass	2.000	0.000	0.800	0.000	0.200	0.000	0.600	0.600	110.000	42.000	2.500
11	Forest	forest	3.000	0.000	0.800	0.000	0.200	0.000	2.500	3.500	310.000	50.000	10.000
15	Bare land	bare soil	4.000	0.000	0.700	0.000	0.300	0.000	0.100	0.080	110.000	27.000	0.120
12	Grass land	Grass	2.000	0.000	1.000	0.000	0.000	0.000	0.300	2.000	140.000	10.000	0.120
31	Wood land	forest	3.000	0.000	1.000	0.000	0.000	0.000	2.000	5.000	250.000	25.000	18.000

Table 7-12 Modified winter land-use parameter table

NUMBER	LUSE_ TYPE	RUNOFF_ VEG	NUM_ VEG_RO	NUM_ IMP_RO	VEG_ AREA	BARE_ AREA	IMP_ AREA	OPEW_ AREA	ROOT_ DEPTH	LAI	MIN_ STOM	INTEC_ PER	VEG_ HEIGHT
21	Cultivation	Crop	1	0	0.2000	0.4000	0.4000	0.0000	0.3500	2.00	180.00	22.00	0.6000
36	shrub land	grass	2	0	0.6500	0.3000	0.0500	0.0000	0.6000	3.00	110.00	30.00	2.0000
11	Forest	forest	3	0	0.8000	0.1000	0.1000	0.0000	2.0000	4.00	340.00	42.00	10.0000
15	Bare land	bare soil	4	0	0.2000	0.4000	0.4000	0.0000	0.0500	0.00	110.00	0.00	0.0010
12	Grass land	grass	2	0	0.6000	0.3000	0.1000	0.0000	0.3000	1.00	140.00	10.00	0.1200
31	Wood land	forest	3	0	0.2000	0.8000	0.0000	0.0000	2.0000	0.00	250.00	10.00	18.0000

7.3.2. 6. *WetSpass model results*

The outputs of WetSpass model are displayed on yearly and seasonal (summer and winter) basis. The total water balance per grid cell is calculated with the previous described water balance components for vegetated and non-vegetated parts of a grid cell.

Evapotranspiration

The simulated annual evapotranspiration of the Raya Valley is 713 mm and 471 mm as maximum and minimum values respectively. The mean and standard deviation of this distribution are 594mm and 58.91 mm respectively. The average evapotranspiration is the largest portion of the mean annual rainfall accounting 81% of the precipitation. This shows that evapotranspiration is the main processes by which water is lost in the valley, Figure 7.8. This is attributed to the high rates of solar radiation and extended dry periods.

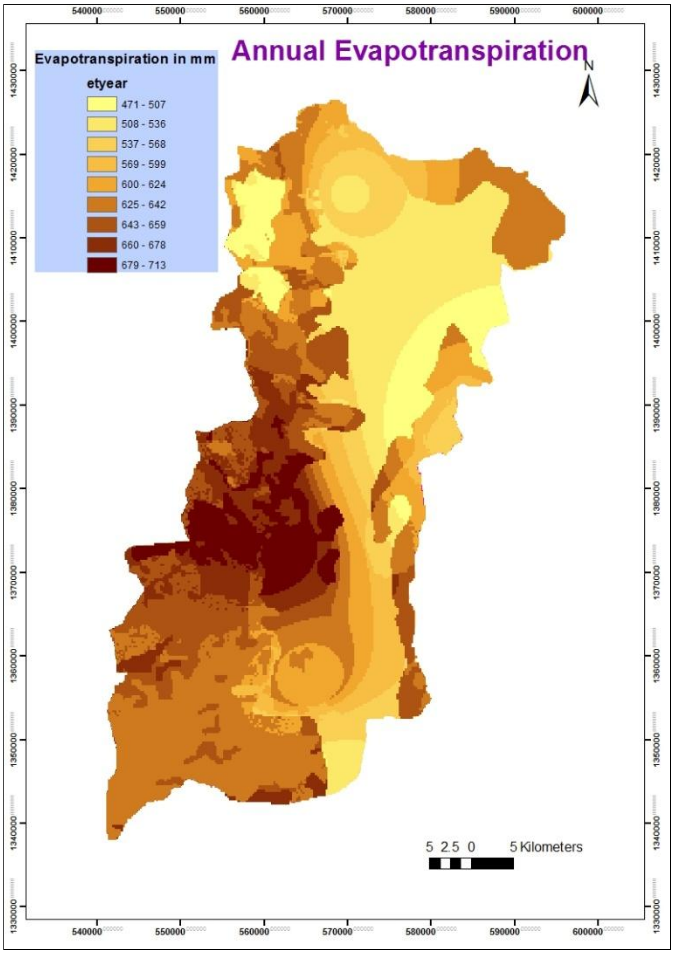

Figure 7.8 WetSpass simulated annual evapotranspiration of the Raya Valley

Surface runoff

The WetSpass model uses the runoff coefficient method for the estimation of surface runoff. The surface runoff coefficient on the other hand is a function of vegetation type, soil texture and slope. Hence it is apparent that the surface runoff in Raya Valley does also vary spatially with topography and other catchment characteristics, Figure 7.9. The simulated runoff varies from less than a mm to a maximum of 137 mm with a mean and standard deviation of 44 mm and 31.97 mm respectively.

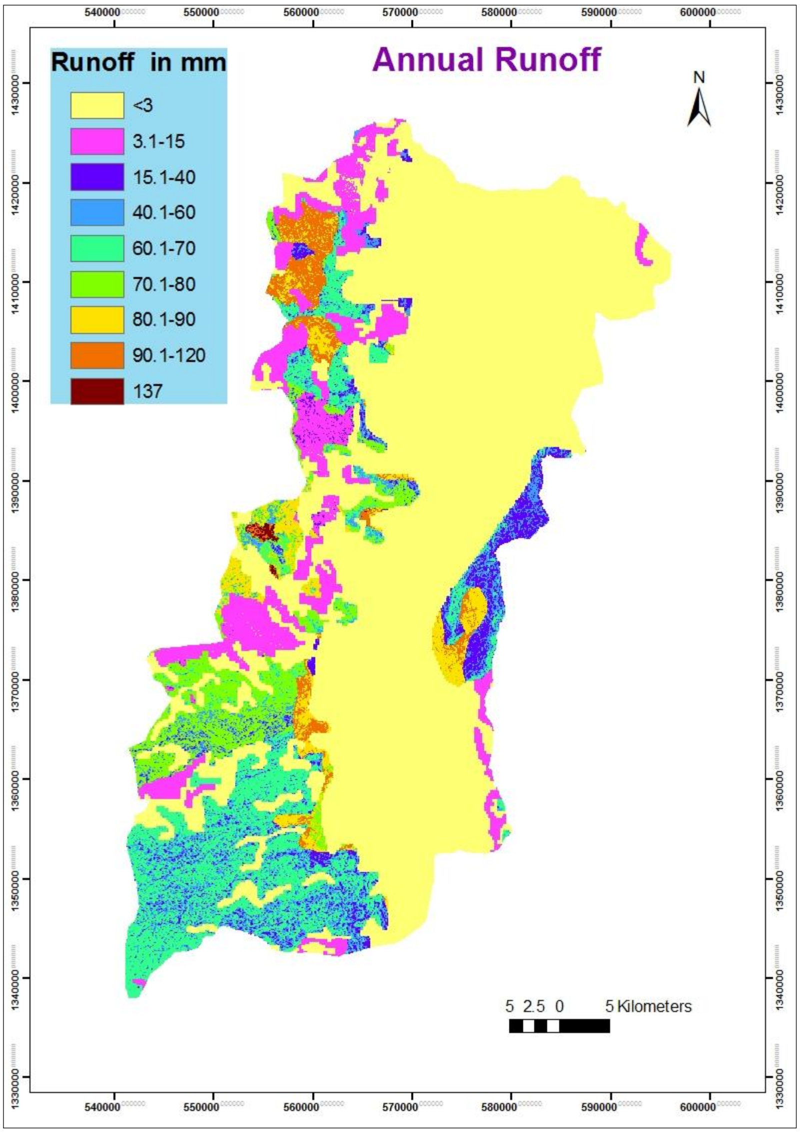

Figure 7.9 WetSpass simulated annual runoff

Groundwater recharge

The WetSpass model determines the long-term average spatially distributed recharge as a spatial variable dependent on the soil texture, land-use, slope, meteorological conditions etc. This is primarily to take into account the influence of the spatial variability of the land surface on the groundwater system (Batelaan O. and S.T. Woldeamlak, 2004). Recharge is promoted by natural vegetation cover, flat topography, permeable soils, a deep water table and the absence of confining beds. The resulting groundwater recharge from WetSpass, Figure 7.10, for the valley ranges from about 3.17 mm to 280, with an average value of 95mm, which is about 13% of the mean annual precipitation, and standard deviation of about 62.16.

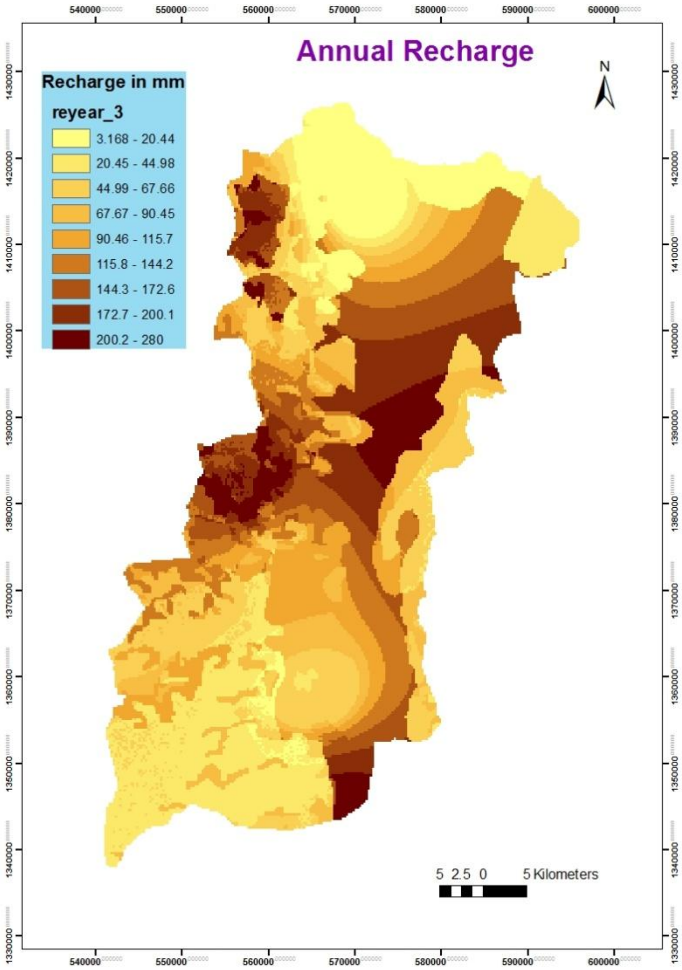

Figure 7.10 WetSpass simulated Annual recharge

7.3.2.7. WetSpass: Water balance results

The overall summary of water balance components of the Raya Valley is given in Table 7-13 Only about 13% and 6% of the mean annual precipitation is effective in producing groundwater recharge and surface runoff respectively, while the rest and the major part is lost as evapotranspiration. The very small error implies that the WetSpass model simulation is reasonably acceptable.

Table 7-13 Annual water balance (mm), based on the WetSpass results

	Min.	Max.	Average	Std. Dev.
Precipitation/P	597	865	733	
Evapotranspiration /ET	471	713	594	58.91
Surface Runoff/Ro	0.1	137	44	31.97
Groundwater Recharge/Re	3.17	280	95	62.16

7.4. CHLORIDE MASS BALANCE

According to (Abdulghaffar S. Bazuhair, Warren W. Wood, 1995), the method assumes that the chloride in the ground water is derived from precipitation and that chloride concentration occurs by evaporation prior to recharge. The assumptions necessary for successful application of the method are that (1) there is no source of chloride in the ground water other than that from precipitation, (2) chloride is conservative in the system, (3) steady-state conditions are maintained with respect to long term precipitation and chloride concentration in that precipitation, (4) precipitation is evaporated and/or recharged to ground water with no surface runoff leaving the aquifer area, (5) no recycling of chloride occurs within the basin, and (6) no evaporation of ground water occurs up gradient from the ground water sampling points.

(Bridget R. Scanlon, 2002), discussed that environmental tracers such as chloride (Cl) are produced naturally in the Earth's atmosphere and are used to estimate recharge rates. Chloride concentrations generally increase through the root zone as a result of evapotranspiration and then remain constant below this depth.

Therefore, based on the assumption stated above, the input is the chloride content of both the precipitation and the groundwater and hence is calculated as follows:

Analysis of consecutive rain water collected by the joint action of the IAEA and the Ministry of Water Resources of Ethiopia indicate that the average chloride concentration of rain water of the Raya Valley is 2.01mg., groundwater samples collected and analysed in this research and existing data of 2008 from WWDSE show the average chloride concentration is 21.1 mg. Hence, using the above formula, the recharge is calculated to be nearly 70mm/year.

8. CHAPTER VIII CONCEPTUAL MODEL and RESERVE ESTIMATION

8.1. CONCEPTUAL MODEL

A conceptual model is a suite of assumptions that summarizes the current understanding of "how water enters an aquifer system, flow though the aquifer system and leaves the aquifer system". Conceptual modeling should precede any attempt to mathematically model a groundwater system (Rushton 2003). They represent the current consensus on system behavior, whether this is informed by direct interpretation of field and laboratory data alone, or whether farther meaning has been extracted from these data by mathematical modeling. The following are key decisions that need to be made about any aquifer system when constructing conceptual model (Paul L. Younger, 2007).

- Specifying the mode of recharge to the aquifer and estimating their magnitude
- Specifying the magnitude of k or T and S and deciding the degree to which these vary from place to place within the aquifer is sufficiently great that ought to be considered.
- Defining the boundaries of the aquifer system, in terms of both their location and their properties.

The following observations and justification are made concerning the conceptual model of the Raya Valley:

- Three physiographic features dominate the area: the valley floor, chain of mountains and their sloping sides, and small portion of plateau. The elevation of the mountains ranges from about 1800 to over 3680 m.a.s.l. The plain areas are situated between 1353and 1800 m.a.s.l and the plateaus are mainly found in the high altitude between 2000 and over 2500 above mean sea level. The Raya Valley covers a total area of 2558 km^2.

- It is an alluvial graben running parallel to the western escarpment in a north-south direction. Description of the local geology and cross-sections along different orientations elucidate that the valley is mainly composed of basin fill deposits of varying degree of groundwater potential. This variation is attributed to the variation in thickness; proportion of soil type in the alluvial deposit and its sorting. Medium to coarse sand and gravel dominate the deposits. The thickness of the alluvial deposit is variable and ranges from about 18 to more than 311 meters. The minimum thickness is in the western and eastern flanks of the valley whereas the maximum thickness is obtained towards the eastern part of the valley center. Many boreholes are devoid of silt and clay while others contain silt and clay intercalations at various intervals.

- Over seventy percent of the boreholes drilled before 2007 and all boreholes drilled between 2007 and 2008 had penetrated the whole pile of the alluvial sediment and encountered mostly weathered and fractured basalt at their bottom.

- No significant impermeable layer that can act as a confining bed is observed. The presence of artesian wells is not attributed to the presence of considerable thickness of confining layers but due to their location along local depressions .

- The basalts occupy the second biggest portion of the valley and they do not only supply run off to the valley floor but, also because they are surfacially weathered and fractured, that allows water to percolate and replenish the groundwater of the alluvial aquifer through groundwater runoff.

This is evidenced by the presence of considerable quantities of water from boreholes pierced in the volcanic rocks; in which an attempt, (exploratory well in well field 6) to drill across the volcanic rocks beneath the alluvial sediment, failed due to the high buoyancy effect of the water rising up from the fractured volcanic rocks. As it is illustrated in the borehole log of the same borehole, the basalts are fractured even at depths below the surface. This could demonstrate the occurrence effect of the regional and local geological structures at depths. These structures could be conduits for both groundwater inflow and outflow in the area.

- The quaternary volcanic, sedimentary and metamorphic rocks cover small area and are more or less massive with no significant permeability.

- There is no any perennial flow of surface water during the dry period in all parts of the valley, except the minor seepages from Waja, Korem and Kisadgudo springs that die out within a short distance in the valley floor and another hot spring at the outlet in Selenber (the only surface water that drains out of the valley during dry season, about 2 liters per second). The surface flow through the outlet occurs only during heavy rains and after inundating local depressions.

- The hydraulic conductivity is variable both in lithology and space, thus it varies between 0.03-0.37 m/day in the volcanic rocks, and 0.11-26 m/day with mean value of 2.8m/day, in the alluvial sediments.

- The vertical hydraulic conductivity is less than the horizontal. The fluctuation in response to pumping and the presence of harmonic ups and downs in the pumping test data indicate that the thin clay horizons behave as vertical retarding layers that give rise to delayed yield to the boreholes under pumping condition.

- The gradient of the alluvial sediment is low (0.006 degree in a total length of over 60 kilometers along the flow direction) and the aquifer is inter-granular aquifer containing gravel, sand and with some intercalation of silt and clay. Hence the groundwater flow is laminar and Darcy’s law is applicable

- From a three years groundwater temperature observation; isotopic (oxygen 18 and deuterium) signature of water samples from boreholes and springs; and chemical analysis of water samples indicate that there are two sources of recharge to the valley. Consequently, the chemical, isotopic and water temperature properties of the water vary across the valley from west to east. The estimated recharge from precipitation is 74 mm per year when an average value of the water balance calculation methods are considered.

- The above investigations show that the groundwater boundary does not coincide with the surface water divide.

8.2 GROUNDWATER RESERVE ESTIMATION OF THE ALLUVIAL DEPOSIT

The alluvial sediment, covering above half of the study area (about 1300 km^2), is the main target of the groundwater exploitations so far.

The volume of the alluvial sediments is calculated using the depth of the alluvial sediments and surface of the static water level as inputs. By applying the spatial analyst manipulations in ArcGIS 9.3 and statistical methods in surfer 9.2 the volume of this unit is estimated to be and by multiplying it by the effective porosity (0.2), estimated from the pumping test, the total groundwater reserve in the alluvial sediment is . In order to estimate the volume of water available as a reserve, the following steps were followed:

1. The surface elevation of the static water level/piezometric level was extracted from the measured static water level measurements and was converted to an elevation data. These data were interpolated in Arc Gis as shown in Figure 8.1.

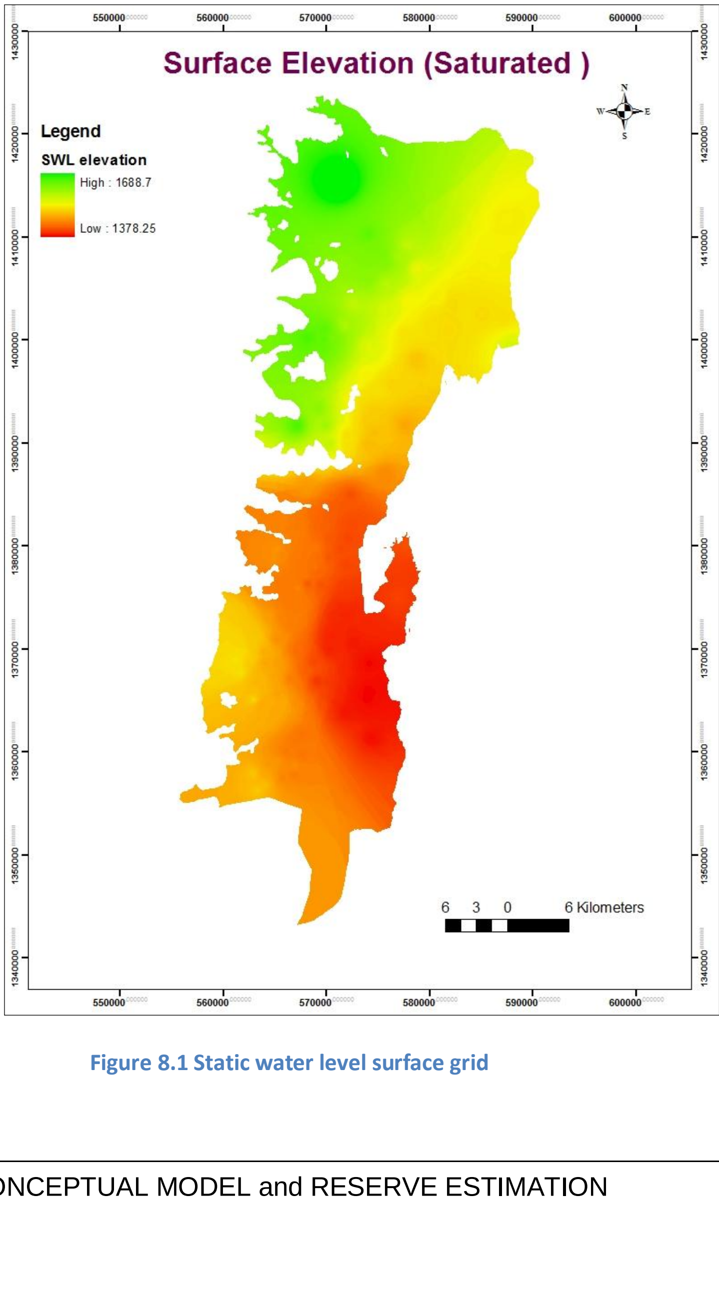

Figure 8.1 Static water level surface grid

2. The bottom elevation of the alluvial sediments was extracted from the lithologic logs of the existing boreholes (excluding the volcanic lithology, when encountered). Then the basal elevation was extrapolated in ArcGIS to obtain an elevation grid as shown in Figure 8.2.

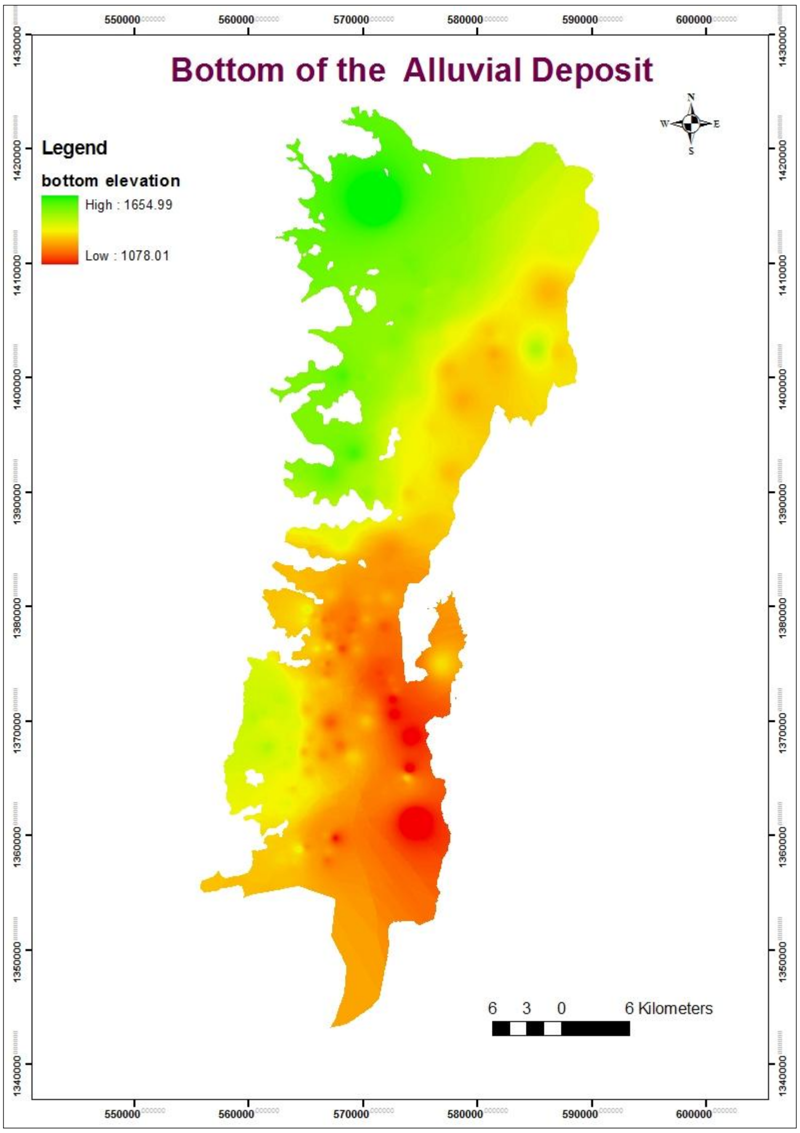

Figure 8.2 Grid map of the bottom of the alluvial sediments

3. The thickness of the alluvial sediments, derived from the lithologic logs of the 188 boreholes within the valley, was calculated by subtracting the bottom elevation grid map from the surface water level elevation grid map (Figure 8.3). The inverse distance weighting interpolation was applied to generate the grid of the alluvial layer with the grid size of 30 by 30 meters. Hence, the data of output grid map were statistically manipulated to obtain the volume stated above.

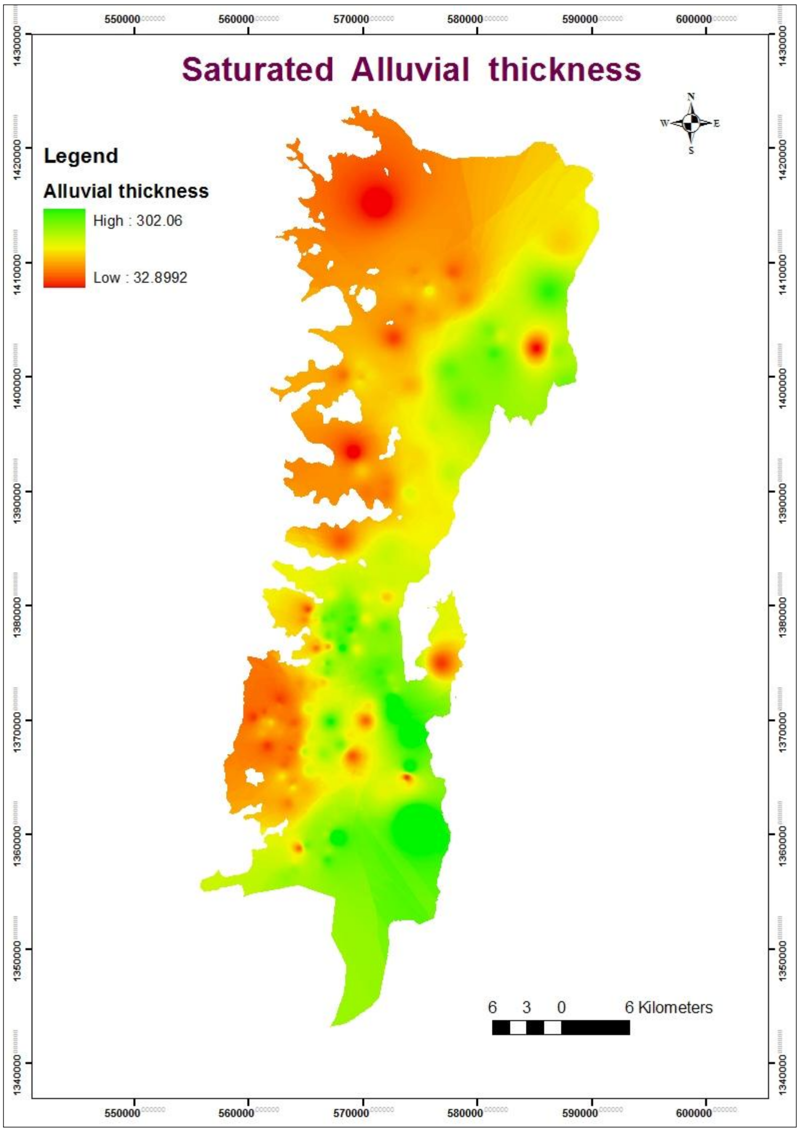

Figure 8.3 Alluvial saturated thickness

9. CHAPTER IX. AQUIFER INTRINSIC VULNERABILITY TO POLLUTION

9.1. INTRODUCTION

The inherent vulnerability assessment of an aquifer to pollution depends on various processes that occur within the hydrogeological system. The process of attenuation depends on the type and concentration of the pollutant and also by the geological characteristics of the system during its movement through the unsaturated zone. In this zone many interactions take place between soils and rocks on one hand and the pollutants on another. When a pollutant reaches the saturated zone further process of attenuation occurs due to dilution.

According to (Giorgio Ghiglieri, Giulio Barbieri, Antonio Vernier, 2006), researches for preventing groundwater from pollution have evolved since the 1980s; different methods of evaluation and representation of vulnerability of aquifers to pollution were developed. However, their poor adaptability to complex situations has triggered, in the 1990s, a new era of research to develop a method that somehow resolve this problems. Hence SINTACS [Civita 2000] model that consists of a system scores and weights was developed. In this method, the vulnerability is defined on the basis of reconstructing lithostratigraphic and subsurface hydrogeological conditions and therefore depends mainly on the permeability and thickness of material overlying the aquifer, and the type of groundwater movement.

The Raya Valley basin was discretised with a regular grid mesh of 100×100m. The weight strings have been prepared in order to satisfactorily describe the effective hydrogeological and impacting situation as set up by the sum of data. The SINTACS R5 presents five weight strings for normal impact, relevant impact, and drainage from the surface network, deep karstified terrain and fissured terrain. For each of the 2,554,800 grid squares, element normalized SINTACS index was calculated and different vulnerable areas were assessed using SINTACS R5 parametric methods (Civita M., De Maio M., SINTACS R5, 2000).

The method involves the determination and quantification of the following seven parameters:

- Depth to groundwater (S)
- Effective Infiltration (I)
- Effect of self-purification/attenuation of the unsaturated zone (N)
- Type of coverage (T)
- Hydrogeological characteristics of the aquifer (A)
- Hydraulic conductivity (C)
- Steepness of the surface topography/slope (S).

All ranges of rating and the procedures explained in chapter five of part two were followed in running the model. Parameters were synthesized in ArcGIS (Figure 9.1) and an overlay map was produced with vulnerability rates that range from very low to high as an output.

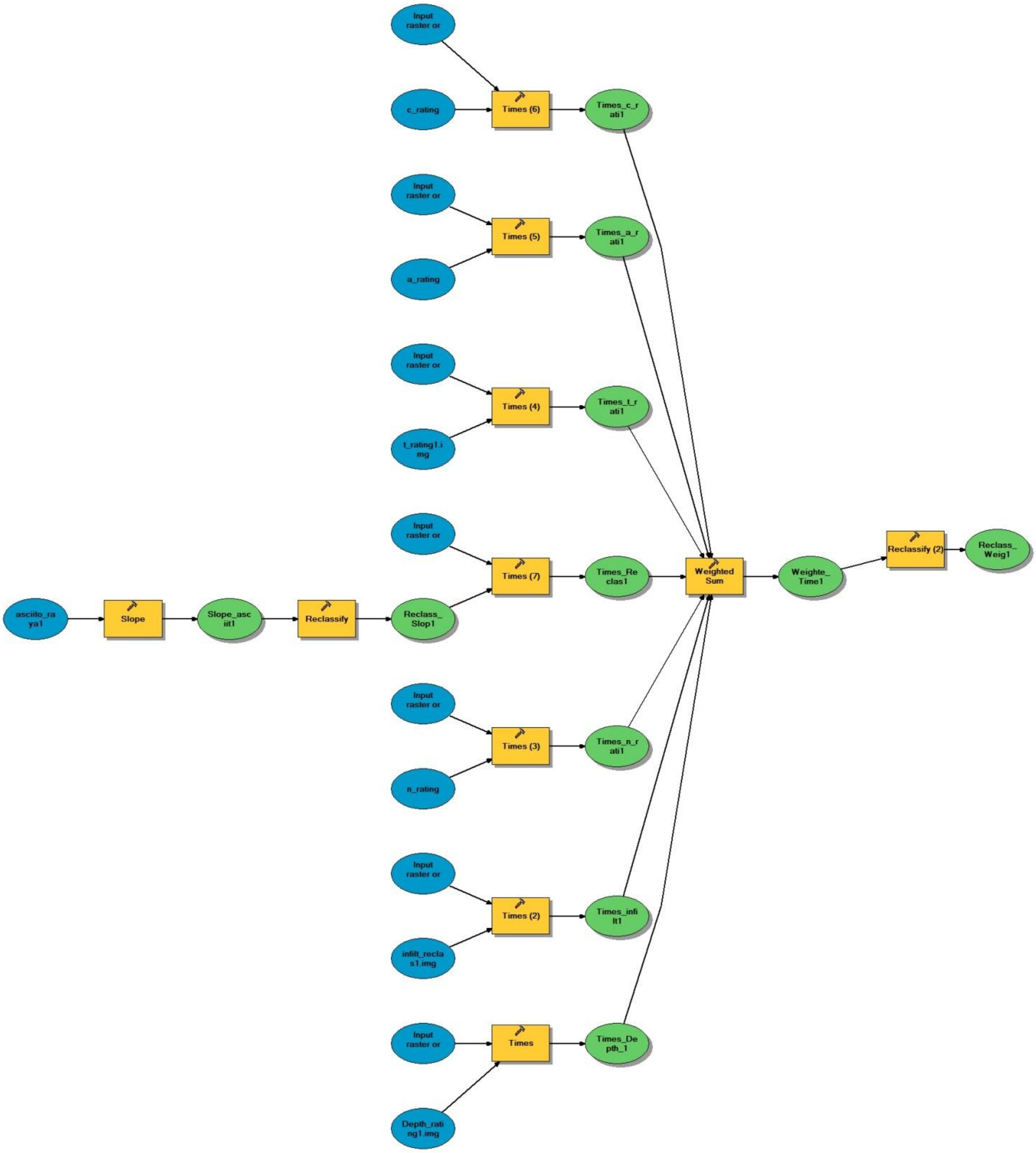

Figure 9.1 ARCGIS model structure for running SINTACS model

9.2. DEPTH TO GROUNDWATER SURFACE, PARAMETER (S)

The depth to groundwater grid map was created based on water level measurements of boreholes which were carried out in this research work (table 4.1) and secondary data. The values range between -2 meters to 61m meters. These points were converted into a grid map by interpolating them in ArcGIS (Figure 9.2). Then allocation of rating to the parameter S was made by reclassifying the grid map on the bases of Table 9-1.

Table 9-1 Depth to groundwater rating intervals, after Civita 2000

Depth to Groundwater Interval (in m)	SINTACS Rating
0-2	10
2-3	9
3-5	8
5-8	7
8-11	6
11-16	5
16-24	4
24-40	3
40-90	2
>90	1

Figure 9.2 Depth to groundwater grid map

9.3. THE INFILTRATION, PARAMETER (I)

This parameter requires calculation of corrected annual temperature (T_c), specific precipitation ( ), assigning the potential infiltration coefficient (χ), estimation of evapotranspiration and finally come up with the effective infiltration . The procedures are described in chapter five of part two as indicated before. The effective infiltration in the period 1996-2007 ranged between 20.6 mm and 219 mm. These values (Table 9-2) were interpolated and reclassified in ArcGIS to come up with the rated grid values (Figure 9.3)

Table 9-2 Infiltration rating intervals, after Civita 2000

Lithologic Units	Rates (I) Assigned
Acidic Volcanic rocks	0.4
Alluvial sediments	0.8
Basement rocks	0.2
Basic rocks	0.5
Sedimentary rocks	0.3
Volcanic rocks	0.6

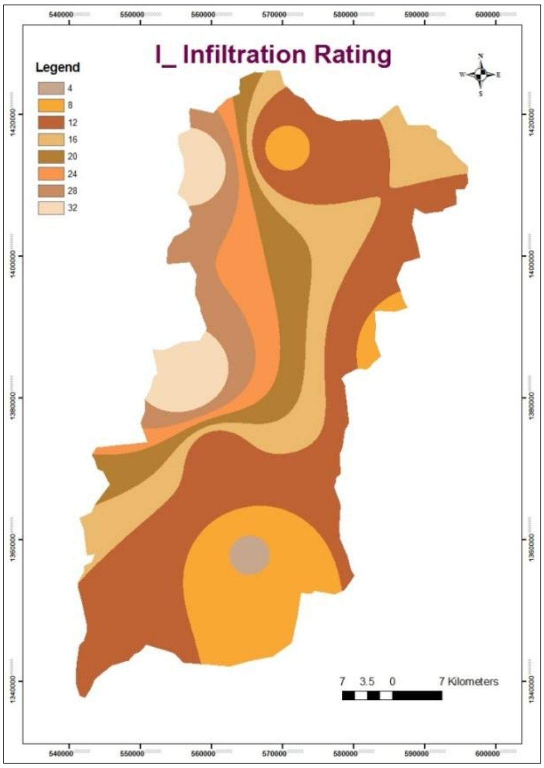

Figure 9.3 Infiltration grid map

9.4. ATTENUATION EFFECT OF THE UNSATURATED ZONE, PARAMETER (N)

The effect of self-purification of the unsaturated conditions is estimated from lithology, grain size, presence of clays and silts, to permeable rocks and fracturing. Rates are assigned to the lithologies that coincide with the width and height of the unsaturated zone Table 9-3 and Figure 9.4

Table 9-3 Attenuation effect rating intervals, after Civita 2000

Lithologic Units	Rates (N) Assigned
Acidic Volcanic rocks	3
Alluvial sediments	8
Basement rocks	1
Basic rocks	4
Sedimentary rocks	2
Volcanic rocks	5

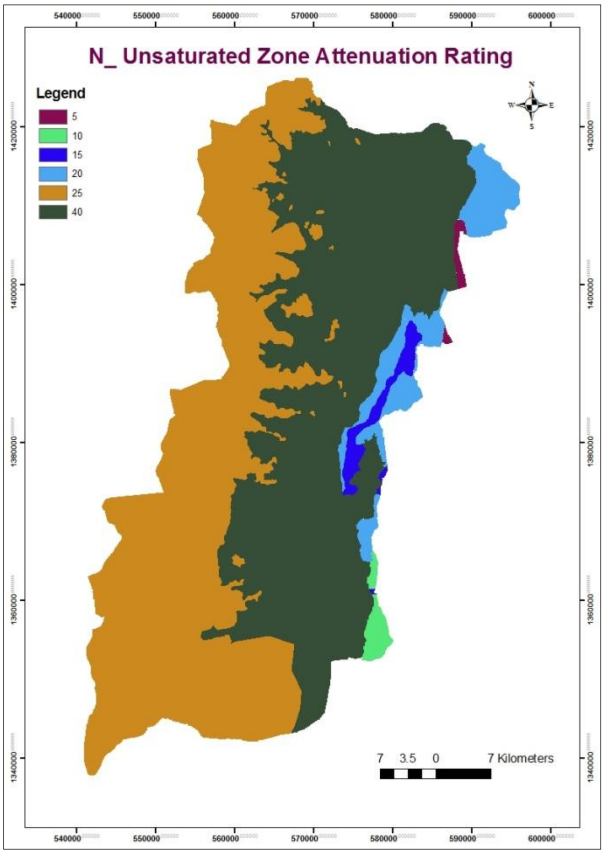

Figure 9.4 Unsaturated zone attenuation grid map

9.5. SOIL\OVERBURDEN ATTENUATION CAPACITY, PARAMETER T

Soils have a remarkable capacity to mitigate the impact of pollutants; it is the first line of defense of an aquifer system. Rates are assigned to the soils types of the area Table 9-4 and Figure 9.5.

Table 9-4 Soil/overburden rating, after Civita 2000

Soils	Rates (T) Assigned
Clay Loam	2
Sandy Clay Loam	5
Sandy	8
Sandy Loam	6
Silty Loam	4
Silty Clay Loam	3

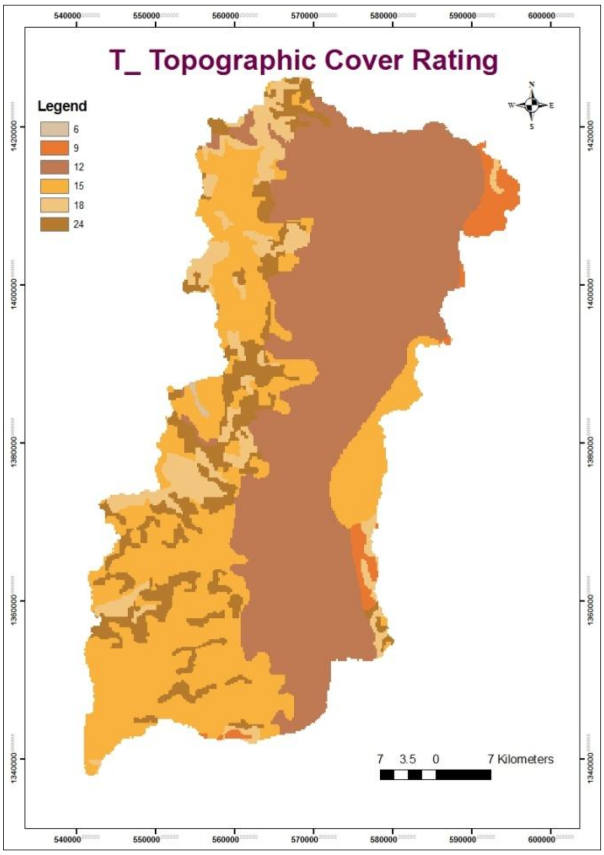

Figure 9.5 Topographic cover grid map

9.6. HYDROGEOLOGICAL CHARACTERISTICS OF THE AQUIFER, PARAMETER A

Aquifer characteristics describe the process that take place below the piezometric level when a contaminant becomes mixed with groundwater . The parameter A depends on the characteristics of the aquifer in which these processes are carried out. The following rates are assigned (Table 9-5 and Figure 9.6) for the different hydrogeological units.

Table 9-5 Aquifer characteristics rating intervals, Civita 2000

Lithologic Units	Rates (A) Assigned
Acidic Volcanic rocks	1
Alluvial sediments	8
Basement rocks	1
Basic rocks	2
Sedimentary rocks	1
Volcanic rocks	2

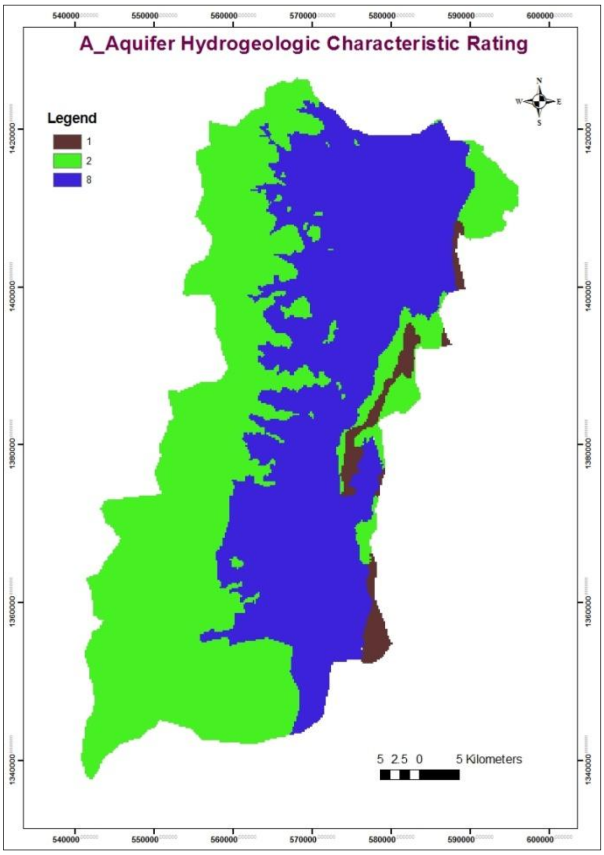

Figure 9.6 Hydrogeological characteristic of aquifers grid map

9.7. HYDRAULIC CONDUCTIVITY OF THE AQUIFER, PARAMETER (C)

Hydraulic conductivity is a processes that describes the ease with which water can move through pore spaces or fractures, thus, the potential mobility for a pollutant that has a density and viscosity value close to that groundwater. The values computed by pumping tests are assigned rates in a similar way to the other parameters (Table 9-6 and Figure 9.7)

Table 9-6 Hydraulic conductivity rating intervals, after Civita 2000

Lithologic Units	Rates (C) Assigned
Acidic Volcanic rocks	1
Alluvial sediments	6
Basement rocks	1
Basic rocks	2
Sedimentary rocks	1
Volcanic rocks	2

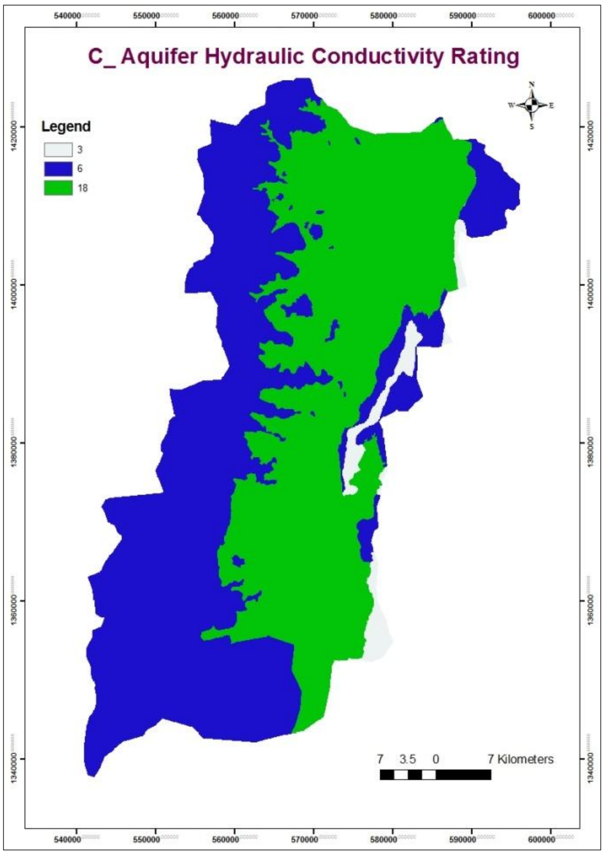

Figure 9.7 Hydraulic property grid map

9.8. STEEPNESS OF THE SURFACE TOPOGRAPHY, PARAMETER (S)

Slope is the percentage change of elevation over a certain distance. High rates are given to areas where the slope is very low or flat area, and high topographic gradient are rated low . Allocation of points was determined by the classes of slope between 0 and 30% (Table 9-7), obtainable through the construction of the steepness of classes derived from Digital Elevation model, and assigned the values by reclassification method in the ArcGIS special analyst tool, Figure 9.8.

Table 9-7 Slope rating intervals , Civita 2000

Value in %	Rating (S)
0-2	10
3-4	9
5-6	8
7-9	7
10-12	6
13-15	5
16-18	4
19-21	3
22-25	2
>26	1

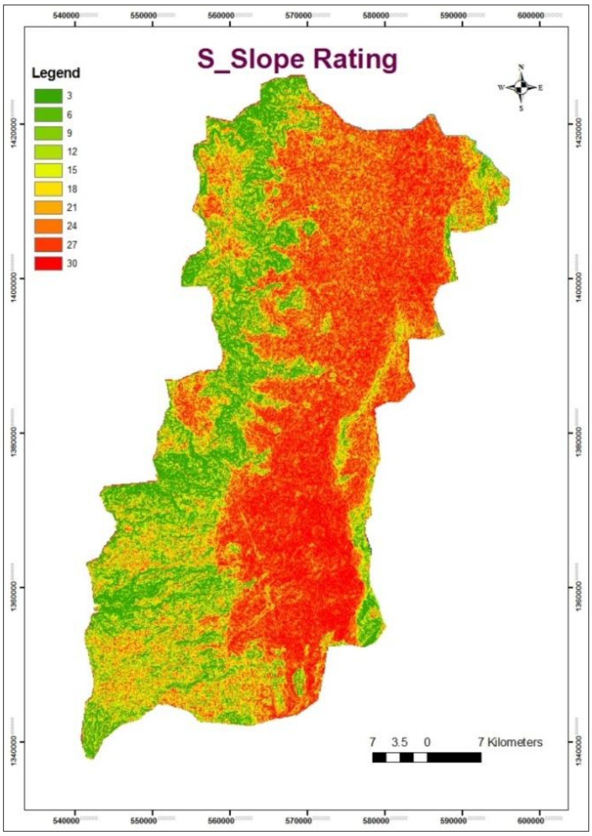

Figure 9.8 slope grid map

9.9. HYDROGEOLOGICAL SITUATIONS AND IMPACT

Once determined the rates for each of the parameters predicted by the model SINTACS which are discretized for each cell, it is necessary to identify strings of weight multipliers based on actual scenarios identified corresponding to particular situation. The possible strings of weights (W) will be as many scenarios as identified.

The values of these weights for each parameter are as follows (Table 9-8):

Table 9-8 String weights

Parameter	Normal Impact	Severe Impact	Seepage	Karst	Fissured
S	5	5	4	2	3
I	4	5	4	5	3
N	5	4	4	1	3
T	3	5	2	3	4
A	3	3	5	5	4
C	3	2	5	5	5
S	3	2	2	5	4

The normal impact was selected in calculating the vulnerability.

9.10. THE VULNERABILITY INDEX

After evaluating the seven parameters of the method and assigned weights on strings, the index of the intrinsic vulnerability SINTACS is given by the following table (
Table 9-9):

Table 9-9 Vulnerability Index rating intervals, after Civita 2000

Degree of vulnerability '	Values
Very low (Bb)	26-80
Low (B)	90-105
Medium (M)	110-140
High (A)	150-186
Very High (E)	190-210
Extremely High (Ee)	220-260

Finally, as an output of all the processes described above an intrinsic vulnerability map (Figure 9.9) is produced.

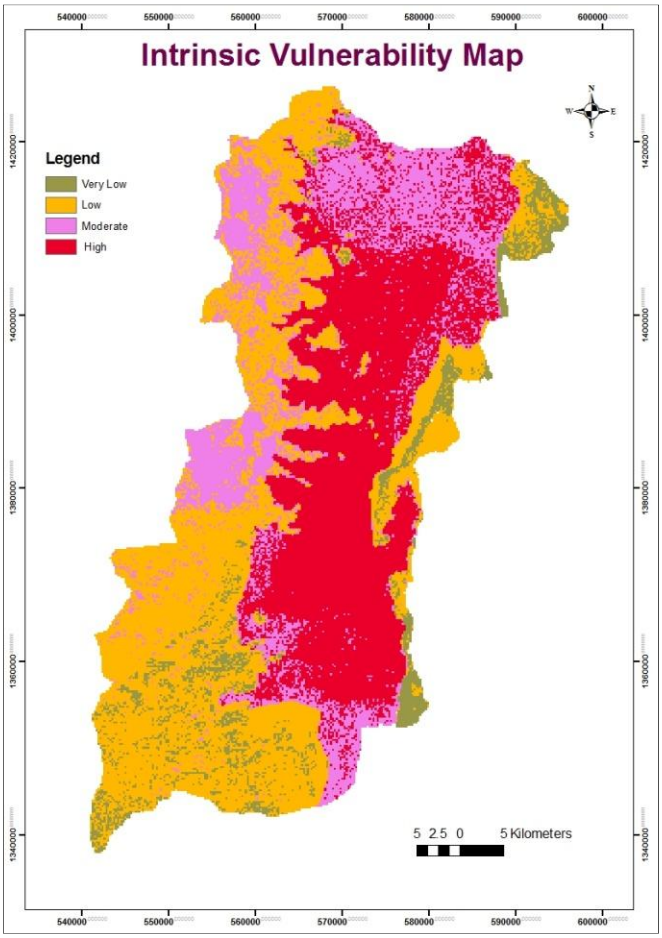

Figure 9.9 Rated intrinsic vulnerability map

10. CONCLUSIONS AND RECOMMENDATIONS

10.1. CONCLUSIONS

The Raya Valley is an alluvial graben running parallel to the western escarpment of the Afar Depression in a north-south direction, with no perennial stream. Description of the local geology and cross-sections along different orientations elucidate that the valley floor is mainly composed of basin fill deposits of varying degree of groundwater potential. The thickness of the alluvial deposit is variable and ranges from about 18 to more than 311 meters. The minimum thickness is in the western and eastern flanks of the valley whereas the maximum thickness is obtained towards the eastern part of the valley center.

The main conclusions are given below:

- The main target of the groundwater exploitations is the alluvial sediment and the fractured volcanic rocks beneath, but, based on pumping test data and appropriate reports, the dominant aquifer is alluvial phreatic type. By applying the spatial analyst manipulations in ArcGIS 9.3 and statistical methods in Surfer 9.2, the volume of the alluvial sediment, covering above half of the study area (about 1300 km^2) with an average alluvial saturated depth of 77.3 m, is estimated to be and by multiplying it by the effective porosity (0.2), estimated from the pumping tests, the total groundwater reserve in the alluvial sediment is .
- The hydraulic conductivity is variable both in lithology and space, thus it varies between 0.03-0.37 m/day in the volcanic rocks, and 0.11-26 m/day with mean value of 2.8 m/day~~,~~ in the alluvial sediments. The specific storage varies from 0.14 to 0.23 in the alluvial sediment and increases from the north to the south.
- Based on the measured data, an isopiezometric map was produced. This shows that the groundwater flows from the west, east and north toward the centre of the valley following the topography of the area. Then all groundwater flows in the north-south direction in a similar fashion to the surface water flow.
- The groundwater temperature in the Raya Valley increases to the east and the maximum temperature were recorded in the spring near the outlet of the basin, which is above the limit of the utilized measuring instrument, 50^0C. The lowest temperature is recorded in the springs of the highlands at Emba Hatsi (16.4^0C). Thus, a four time (September 2009, September 2010, February 2011 and August 2011) water temperature measurements have shown a distinct zonation of the water temperature.
- At least two types of waters were distinguished from hydrochemical analysis. These are the Ca-HCO_3 and Na-Cl-SO_4 types. Highland spring samples and most of the western borehole samples plot in the Ca-HCO_3 type field, while the eastern boreholes and the hot spring are grouped in the second category. The remaining central valley boreholes basically have a mixture of the two major types of water with considerable amount of magnesium. No detectable danger in groundwater quality for both domestic and agricultural use was found, except for the bit elevated hardness in some boreholes.
- Isotope analysis (stable isotope of oxygen and hydrogen) of rain water, borehole and spring samples showed that most of the borehole and spring samples plotted nearly along the Local Meteoric Water Line (LMWL). But, the eastern boreholes and the hot spring plotted away from the LMWL in the direction of higher water-rock interaction with a different regression equation. This implies that there is a different source for these points.
- Raya Valley is characterized by a bimodal rainfall, i.e. about 60% of the rain falls in the months from June to September and around 20% in the months from March to May. The weighted average rainfall in the valley is 733.6 mm per year.

- The amount of groundwater recharge was quantified using the following methods of water balance calculation :
  - Thornthwaite soil water balance method result indicated a total amount of 99 mm/y~~,~~ (13.5% of precipitation)~~,~~ of water as both recharge and as runoff. The highest amount, 634 mm/y (86.5%), is lost as evapotranspiration.
  - Results of WetSpass model pointed out that there are 95 m^{m} of recharge (13% of the total precipitation), 44 mm of runoff (6% of the total precipitation) and 594 m^{m} of evapotranspiration (81% of the total precipitation) annually.
  - In the Chloride Mass Balance method, the input is the chloride content of both the precipitation and the groundwater. The results of this calculation show 70 mm of recharge per year.
  - The effective infiltration value, obtained during the preparation of inputs of SINTACS model, is 64 mm. Therefore, the values obtained with the three methods, except WetSpass, are nearly similar.
- The intrinsic vulnerability output map, using SINTACS model, identified that the areas highly vulnerable to pollution are the alluvial deposits, indicating higher risk in the main target area of the valley.

In general, the groundwater in Raya Valley has two sources that can be identified by three independent parameters. The groundwater temperature increases from west to east, the stable isotopic signature of hydrogen and oxygen has two distinct zones (east and west) and the groundwater chemistry also follows similar trend. Therefore it can be concluded that the recharge to groundwater in the Raya Valley is not only the precipitation.

The origin of the hot water requires further investigation; however it can be postulated that the source of the chloride and sulfate of the hot spring and the eastern boreholes could be the upward movement of the hot water, probably originated beneath the Mesozoic sediments, which are expected to be overlain by the tertiary volcanic. Hence the hot water along its way to the surface has dissolved and captured the evaporitic sequence of the sediments.

10.2. RECOMMENDATIONS

- The outputs obtained in this study~~,~~ can be used as starting point for groundwater exploitation planning in the Raya Valley Basin.
- Continuous monitoring of groundwater level in wells and groundwater sampling, for chemical analysis, is recommended to understand time bound change in groundwater heads and water chemistry.
- There is no river gauging station in the area. Therefore, installing river gauging stations in the basin will improve data availability and better understanding of the basin water balance .
- Groundwater abstraction from public and private boreholes should be reported and recorded in the monitoring data base periodically to quantify seasonal and annual variations.
- Deepening the boreholes may provoke mixing up of the groundwaters and adversely affect the quality of the upper relatively fresh groundwater.
- The alluvial sediments are more vulnerable to pollution and hence continuous monitoring is recommended to maintain the present groundwater quality status.
- Detailed isotope hydrogeology is recommended to refine the conclusions made on the source of recharge and the amount of groundwater inflow and outflow to and out of the catchment.

PART TWO

RIO MANNU DI PABILLONIS BASIN

1. CHAPTER I: GENERALITIES

1.1. INTRODUCTION

Groundwaters are important renewable resources, in particular, in areas where high percentages of water developed for human consumption, agriculture and industry come from underground aquifers. In the last two decades, awareness of the need for sustainable use and protection of groundwater resources has been gradually extended by the scientific community and institutions responsible for protecting the environment. This has resulted in a worldwide attention of wise use and prevention of this important resource. Whilst groundwater play an important role, it is easy to understand how these resources will be subject to risks of over-exploitation that often are accompanied by periods of drought, local or diffuse pollution, which can compromise water quality on a temporary or permanent base.

According to the publication of INEA (Istituto Nazionale di Economia Agraria)“Status of irrigation in Sardinia" (INEA, 2001), the main source of water for almost all uses is surface water from dams. However, the scarcity of surface water resources has also contributed, indirectly, to the growing up of groundwater abstraction. The Sardinian climate is characterized by a rainy season (October to March), when both surface and groundwater are available, and a dry season (April to September). The significance of groundwater is evidenced in the dry period. Thus, while most of the need (some 81 %) is given by surface water, the contribution of wells and springs is fairly small (about 19 percent). However, the latter contribution is often quite important from the quality point of view.

The most significant phenomenon of the water quality degradation in Sardinia is represented by the eutrophication of many reservoirs. This problem primarily affects water use for drinking, industrial and irrigation purposes. The problems related to the eutrophication of water reservoirs in Sardinia were recognized in the early 1960s, when the phenomenon began to appear in Bidighinzu Lake. There were similar problems in other lakes, particularly in those that were within the direct discharge of untreated wastewater from civilian population centers located upstream. To address this, the Regional Government of Sardegna initiated an action plan to understand and to combat the problem, which was accomplished by preparing a Work Plan focused on the protection and conservation of water resources.

The fundamental aims of “Water Protection Plan” was to establish a comprehensive programmed instrumentation for a dynamic monitoring, planning, identification of the interventions and constraints intended at the protection of integrated quantitative and qualitative aspects of the water resources.

During the preparation of the plan, 37 major complex aquifers consisting of one or several hydrogeological units with substantially similar characteristics were identified. These complex aquifers have been classified based on their potential and their vulnerability. Regarding the second aspect, greater emphasis was given to Quaternary coastal aquifers (residential centers, tourist settlements, marine ingression, and area of intensive agriculture) that are more vulnerable compared to some deep aquifer sites in sparsely populated areas. Therefore, the Rio Mannu di Pabillons is one of these areas that require such type of studies in addition to its similarity to the Pabillonis basin because of its larger portion is covered by quaternary sediments and groundwater is an important resource for irrigation and livestock.

1.2.OBJECTIVE OF THE RESEARCH

The objective of this research work is, water balance evaluation and identification of the degree of vulnerability to contaminants of the Rio Mannu di Pabillonis basin using groundwater hydrogeology and hydrochemistry.

2. CHAPTER II: DESCRIPTION OF RIO MANNU DI PABILLONIS

2.1.LOCATION

Rio Mannu di Pabillonis is found in the central part of Sardinia, within the Campidano plain. It is located between UTM coordinates of 4365500 and 4394600 North and 457500 and 489000 East, Figure 2.1. The basin extends to about 600 square kilometers within the alluvial sediments which comprises around 320 square kilometers.

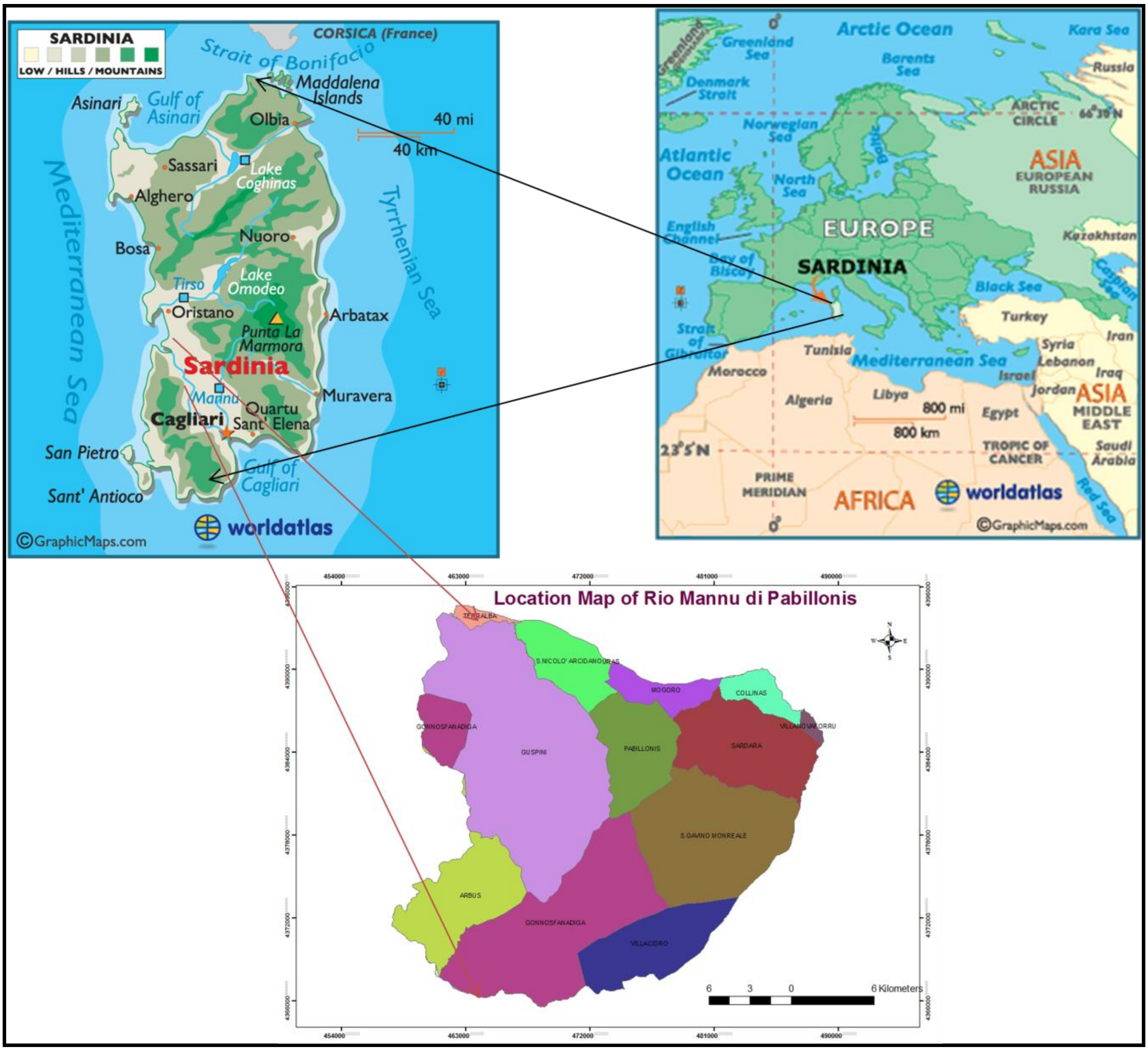

Figure 2.1 Location map of Rio mannu di Pabillonis

2.2.REGIONAL GEOLOGY

2.2.1. Paleozoic basement

The Paleozoic basement rocks are the oldest rock units in Sardinia. According to (Barca S. and Cherchi A., 2002), the Paleozoic Basement of Sardinia is part of the Southern European Hercynian Chain which is evidenced both by the stratigraphic and structural affinities with other Hercynian massifs of Southern Europe. From the stratigraphic point of view, the Sardinian Basement is constituted by a rather continuous Paleozoic succession which could be reconstructed based on paleo-environmental and paleo-geographic interpretations.

Furthermore, it is possible to distinguish in detail a “Caledonian Sedimentary Cycle” (from the Late Precambrian to the Early Ordovician) and a “Hercynian Sedimentary Cycle” (from the Late Ordovician to the Earliest Carboniferous). These important cycles are divided by a gap, Middle Ordovician in age (Barca S., Cocozza T., Del Rio M., Pillola G.L. and Pittau Demelia, P., 1987), substantiated by a strong angular unconformity due to the compressive movements known in the Iglesiente- Sulcis area as the “Sardic phase” (Stille H., 1939), and in the Sarrabus-Gerrei area as the “Sarrabese phase (Calvino F., 1972).

The oldest lithostratigraphic unit of the low grade metamorphic succession is known by the Bithia Formation (Upper Precambrian – Early Cambrian). The Bithia Formation is commonly formed by metasandstones, meta-argillites, metagreywackes, metalimestones and metaconglomerates (about 2000 m thick). These metasediments are related to slope and terrigenous shelf environments, placed along the north-Gondwana continental margin.

The Late Hercynian extensional movements were responsible for the birth and evolution of fluvio-lacustrine molassic basins, where terrigenous sediments, bearing a Stephanian- Autunian floristic association (Cassinis G., Durand, M. and Ronchi, A., 2002) and vertebrate remnant (Fondi R., 1980) amphibians, (Ronchi A. and Tintori A., 1997) accumulated.

2.2.2. Post-paleozoic covers

The Permo-Carboniferous continental deposits are unconformably overlain by Mesozoic-Cenozoic sequences (estimated thickness about 600 m), sometime associated with volcanites and volcanoclastics . The Mesozoic succession is built up by a complete Triassic transgressive-regressive facies, starting with terrigenous continental deposits (Buntsandstein) and ending, after a fossiliferous shallow marine carbonate level (Muschelkalk), with marly-clay sediments with gypsum. Both the distribution of outcrops and of the sedimentary facies supports a western provenance for the Triassic transgression (Cherchi A., 1983).

In Mesozoic time, Sardinia was undergoing regional extension, which favored shallow marine transgressions, starting from the west (Muschelkalk in Nurra and Sulcis) and heading east (Dogger in the Gulf of Orosei). Only in the Middle Jurassic did marine conditions prevail over the whole island. In the central part, the Jurassic cover horizontally lies above the Paleozoic basement, often with an intervening basal quartzitic conglomerate. Extensional tectonic features were also present during the Early and Middle Jurassic; some authors (Monleau C., 1986) support the idea of mainly NE-SW trending tensional tectonics in this chronostratigraphic interval, which would have been active in e Sardinia and the Maritime Alps.

During the Mesozoic and the Paleogene, Sardinia and Corsica formed an integral part of the southern margin of the European plate and were detached from it during the Burdigalian because of spreading and the anticlockwise rotation. Corsica and Sardinia shared the geological history of Western Europe (Iberian Peninsula – Southern France) up to the Early Burdigalian.

At the end of the Mesozoic Sardinia was completely emerged. The continental phase lasted until the Paleocene; marine fossil pebbles of the Dano- Mountain, Thanetian and Early Ilerdian ages are contained in the Tertiary conglomerate cropping out in Eastern Sardinia (Dieni I., Massari F. and Poignant A.F., 1979) and (Dieni I., Fischer J.C., Massari F., Salard-Cheboldaeff M. and Vozenin-Serra C., 1983). Deep wells in the Sulcis lignitiferous basin (Southwestern Sardinia) indicate the presence of the marine Ilerdian at the base of the Eocenic succession (Cherchi A., 1983).

The further compressive Middle Eocene tectonic phase (Barca S. and Costamagna L.G., 1997), is responsible for the basal unconformity of the Cixerri Formation (Middle- Upper Eocene), which truncates them from the Paleozoic to Lower Eocene beds.

A phase of very widespread tensional tectonics of Late Oligocene age seems to be the origin of the rift system affecting the Western Mediterranean area. The Sardinian Oligo-Miocene basin represents one of the eastern most branches of this tensile system (Cherchi, A. and Montadert, L., 1982). These movements began in a continental environment, before the marine transgression. Thick, clastic, syn-rift sediments (the Ussana Formation) emphasize the role of the faults in the Sardinian rift.

Upper Miocene deposits are very limited due to intensive erosion during the Messinian regression and the later Middle-Late Pliocene continental phase. The angular unconformity of the Lower Pliocene marine transgressive deposits on the Messinian substratum (Sinis) is related to the compressive movement of Late Miocene age, also evidenced by micro tectonic features (Cherchi A., and Trémolières P., 1984), Figure 2.2.

The superimposed Plio-Quaternary Campidano Graben, related to the opening of the Tyrrhenian Basin, contains more than 600 m of syntectonic continental deposits (the Samassi Formation). It consists of re-deposited Miocene and Lower Pliocene sediments, eroded from the eastern flank of the trough, thus emphasizing the importance of deep Middle – Late Pliocene erosion. The continental phase, which started during the Middle Pliocene, ended with the first marine deposits of the Upper Pleistocene.

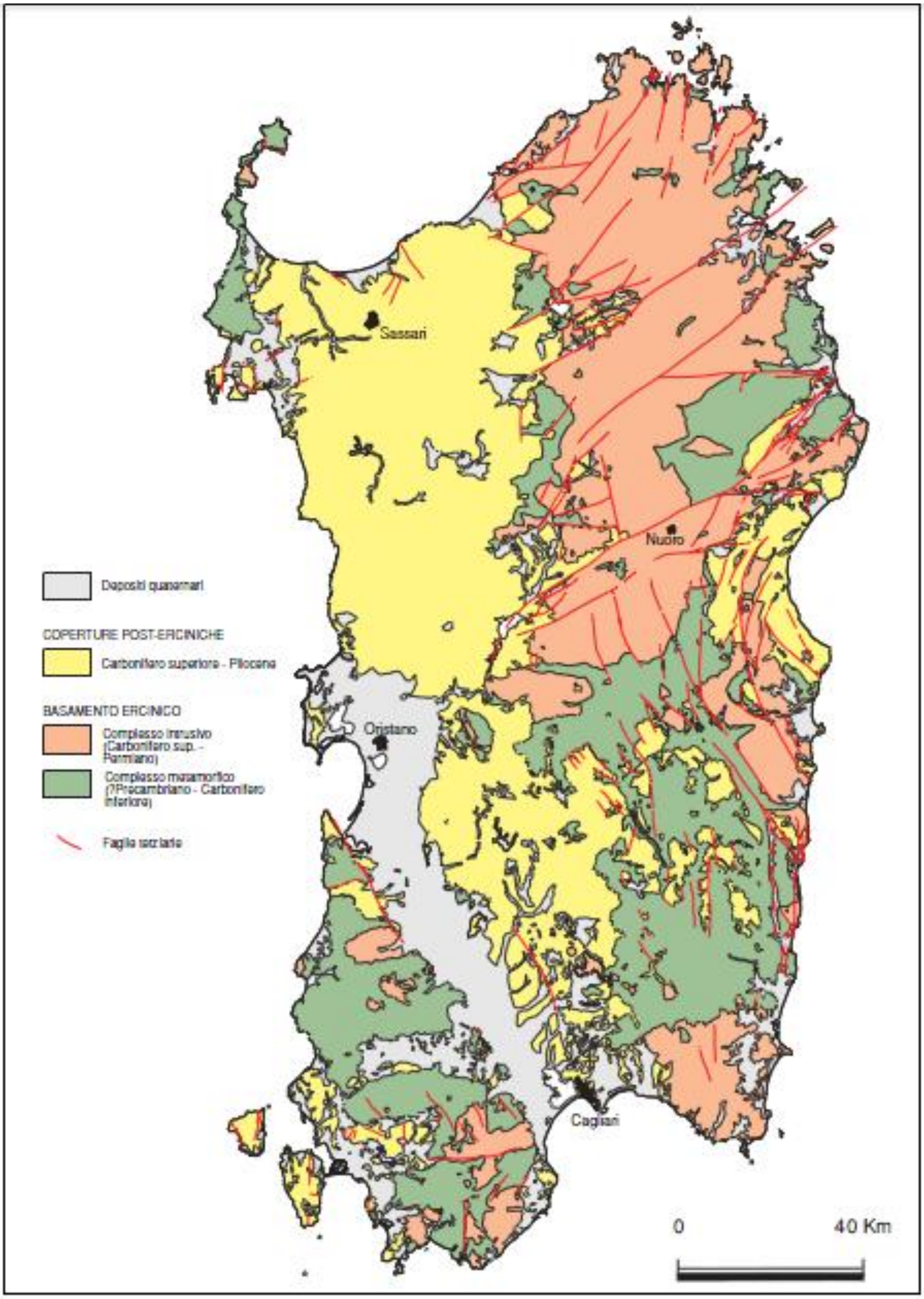

Figure 2.2 Main geological units of Sardinia, after (Carmignani L. and Pertusati P.C., 1977)

2.3.LOCAL GEOLOGY

The Geology of the study area has been reconstructed on the basis of existing bibliographic data (Figure 2.3). The current geological features are the result of a complex evolution of sedimentary, magmatic and tectonic activities that took place between the Upper Middle Cambrian to the Quaternary. Different tectonic deformation phases, which have had the greatest effects during the Hercynian orogeny in the Carboniferous, are almost entirely responsible for the current arrangement of the Paleozoic Basement (Carmignani L. and Pertusati P.C., 1977).

The basement rocks consist of primarily a complex metamorphic rocks and granite outcrops mainly exposed in the western half of the basin. They are overlain by the sediments mainly of Mesozoic limestone and dolomite.

The eastern part of the basin is characterized by hills covered by marine deposits of Miocene sandstones, marl, and Miocene sediments of continental conglomerates and sandstones.

The Cenozoic outcrops are mainly located at the central vast depression which is stretched from north to south. These consist of products of intense volcanism (andesites, ignimbrites, tuffs) and sediments of marine, lagoonal, and continental origin (sand, marl, limestone, conglomerates, and clays).

Basic (basalt) volcanism began at the end of the Cenozoic that has extended to quaternary during which basalt flows emerge in vast areas, particularly concentrated in central Sardinia. In the northern part of the basin lies the M. Archi, this was formed during post-Miocene eruptions which led to the huge volcanic outcrops of Sardinia. The lavas consist of intensified ignimbrite, rhyolite and dacite porphyritic to glassy and blistering of the Pliocene age. They are topped with transitional and alkaline basalts, andesitic basalts, trachytes and phonolites of the Plio-Pleistocene age.

Most of the Quaternary sediments are composed of sediments of the continental environment; represented mainly by alluvial plains located in the main island. They vary to a great extent in lithological nature, form and size of grains, in the nature of the fine fraction of cement and matrices, the degree of cementation and compaction.

The different morphological events and the wide variety lithological and structural frameworks dominated the subdivision in the Caledonian-Hercynian basement horst and the presence of the Great Rift Valley, Campidano.

The area is affected by systems of faults with NE-SW and NW-SE direction and the main drainage pattern is governed by these structures.

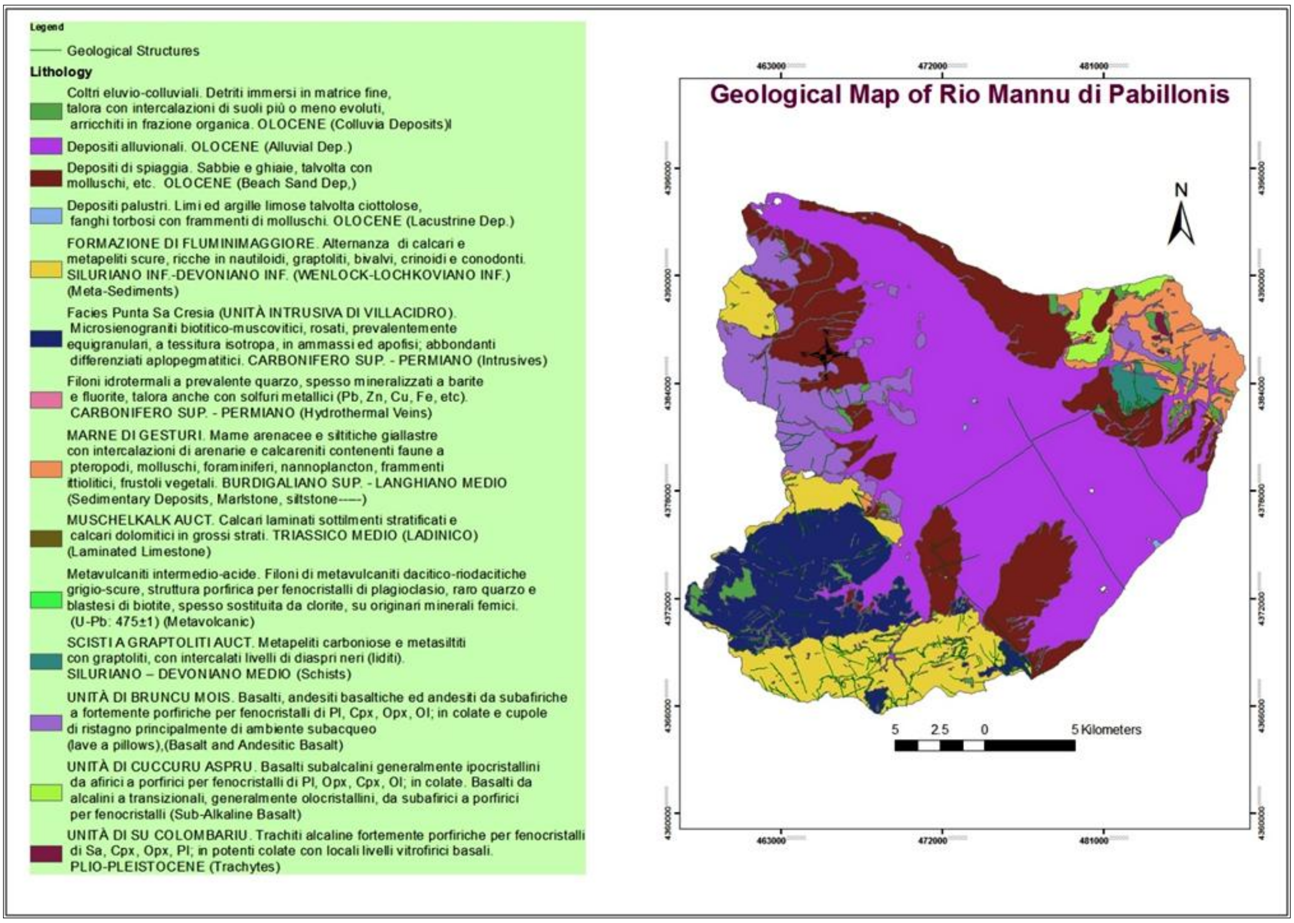

Figure 2.3 Geological map

2.4.GEOMORPHOLOGY and DRAINAGE

The Rio Mannu di Pabillonis is mainly situated on Holocene alluvial plain, the Campidano plain, which consists of gravel, sand, clay and silt, Figure 2.4. The plain has almost a uniform morphology and is intruded by some volcanic hills and ancient alluvial terraces that are sloping down toward its center.

The reliefs formed by the Carboniferous granite (Permian) and Paleozoic schist in the south-west, and andesitic extrusive rocks of Oligo-Miocene, in the west (volcanic complex of Mount Arcuentu) are sources of different tributaries of the Rio Mannu di Pabillonis. In both areas, the tectonic displacements have led to steep slopes so that the passage between the mountains and the plain is very abrupt, with no intermediate hills.

The granitic lithologies are highly weathered which gave rise to rounded morphologies, where the roughness of the terrain are masked by dense Mediterranean vegetation because of the presence of a considerable thickness of soil developed from weathering.

The volcanic morphology is rough and spiked with dense network of fractures created by volcanic effusions. The trend of fractures, which correspond to those identified in the Paleozoic, are evident at a distance, since the vegetation is mainly concentrated along these alignments, which offer less resistance to weathering and allow infiltration of water.

Pleistocene sedimentary rocks consisting of Eolithic sandstone cover areas between the hills and plains.

The eastern part of the basin is characterized by hills covered by marine deposits of Miocene sandstones, marl, and Miocene sediments of continental conglomerates and sandstones.

The more acidic lavas are deeply engraved and give rise to rugged mountains, while the basalts have tabular exposure.

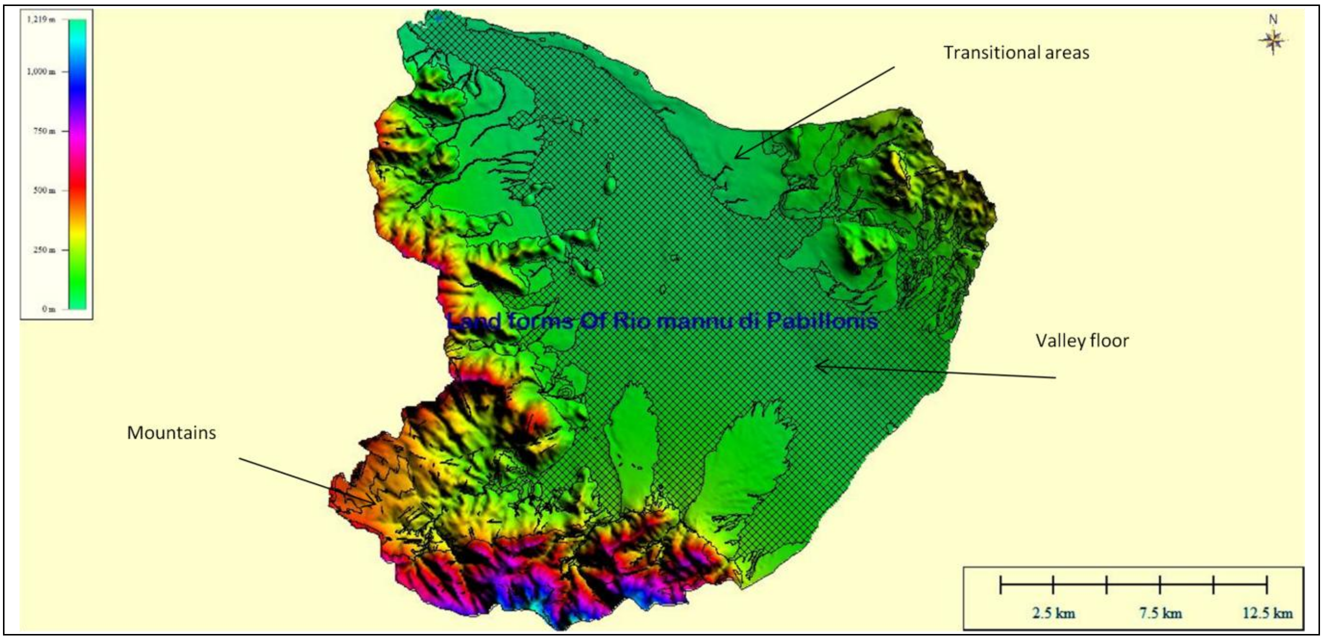

Figure 2.4 Geomorphological map

The Rio Mannu drains the basin in a south - north direction following the topography. Many tributaries feed the main stream both from the west and east with substantial amounts of water during the rainy season. The streams emanating from the western highlands are characterized by dendritic drainage pattern. They follow a nearly NE-SW and NW-SE flow direction, in concordance with one of the dominant geological structures and finally drain to east to join the other drainage patterns. The eastern streams tend to have a parallel type of drainage but less dense than the western part. The stream channels are well developed and protected with concrete pathways in most cases, Figure 2.5.

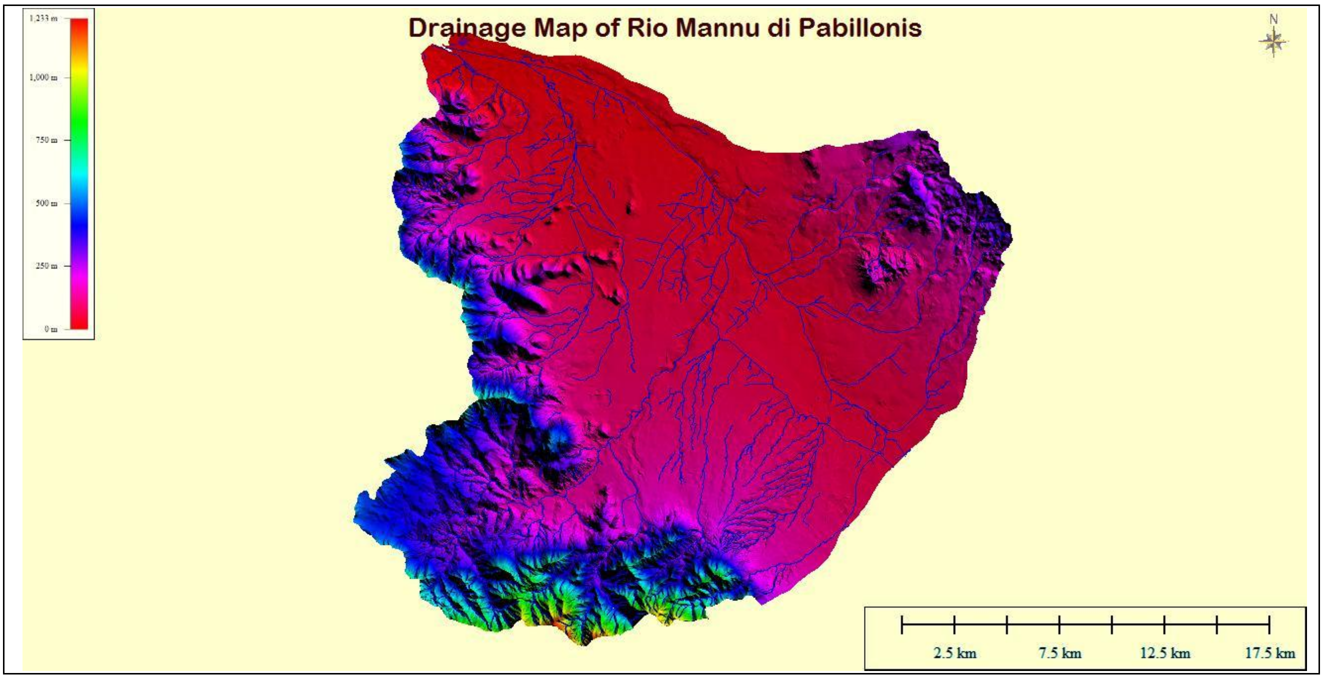

Figure 2.5 Drainage map

2.5. HYDROGEOLOGICAL CLASSIFICATION

The study area is a component of the northern part of the Campidano di Cagliari. Hydrogeological studies and cross sections made from existing borehole data indicate that the area is covered by thick alluvial sediment as shown in Figure 2.6 (Adopted from the study of the Groundwater Qualitative and Quantitative Monitoring Network of Sardinian aquifers, 2009). A study carried out by the monitoring network in the Campidano di Oristano, north of the area under consideration, indicates the presence of shallow water table aquifer set in the alluvial sandy gravel deposits with a thin layer, 1-2 meters, of clay and silt.

The lithologies have different permeability characteristics and the low permeability can be represented by volcanic and metamorphic lithologies. Even in these lithologies there is still some groundwater water circulation , manifested by the steams emanating from some of them.

The lithologies with medium-high permeability are represented by alluvial and detritus deposits that are found in flat area of the basin and on the slopes of the mountains.

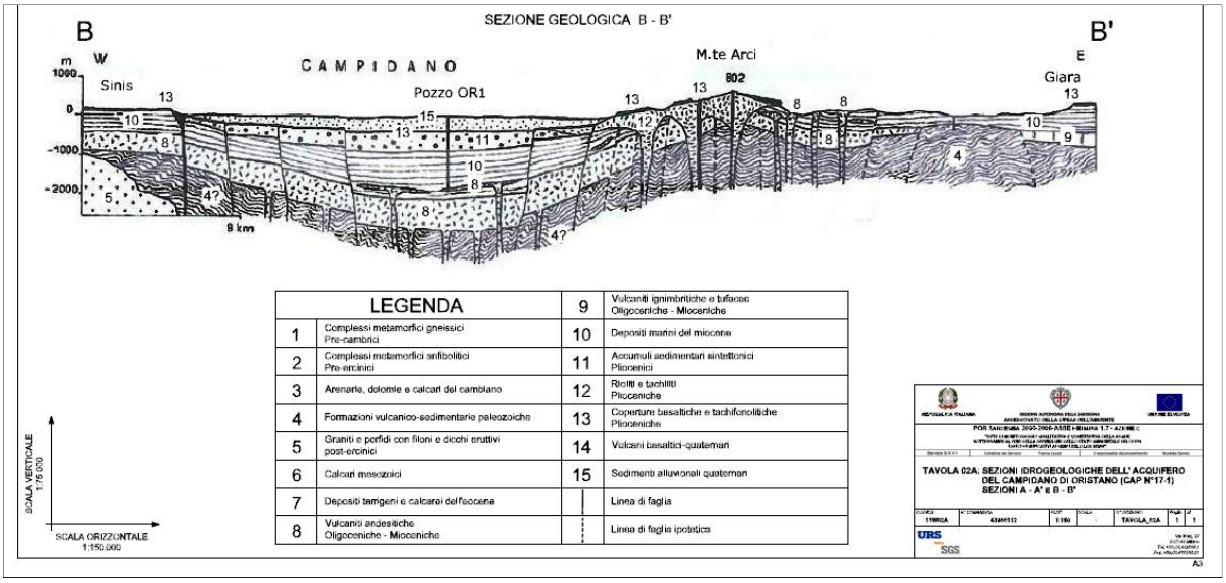

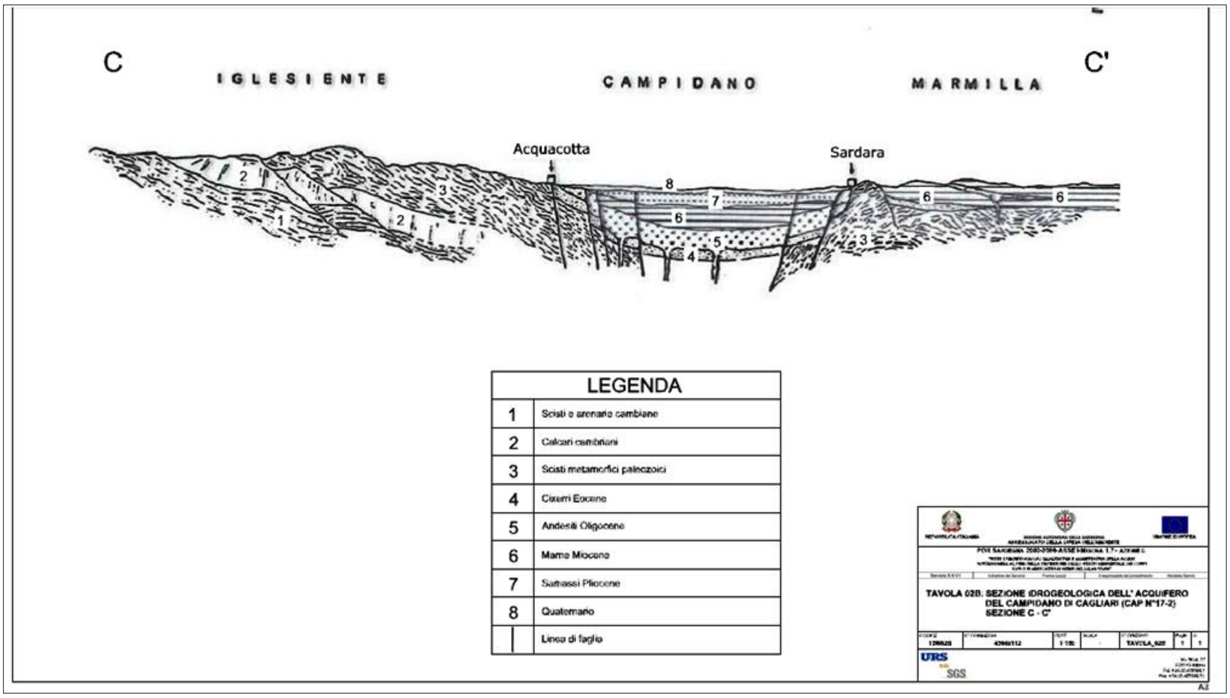

Figure 2.6 Cross-sections along part of the research area, adopted from URS,SGS

2.6. METEOROLOGY

Meteorological data of precipitation and temperature were downloaded from the SISS (**Nuovo Studio dell'Idrologia Superficiale della Sardegna)** for the seven stations inside and all around the basin. These data were scrutinized and used for the calculation of evapotranspiration. The later has been utilized as an input for the calculation of the water balance of the basin using Thornthwaite and Mather soil water balance method. Precipitation data of 1922 to 2007 were used for all stations (Gonnosfanadiga, Montevecchio, Pabillonis, San Gavino and Sardara) except for Uras (1922-1992).

2.6.1. Precipitation

It can be observed from Figure 2.7 that the rainy season in Rio Mannu di Pabillonis is an extended (October to March) and uni-modal rainfall type. The highest rainfall record for all the stations is in the month of December and decrease significantly in the month of April. The dry season begins in April and extends until the month of September.

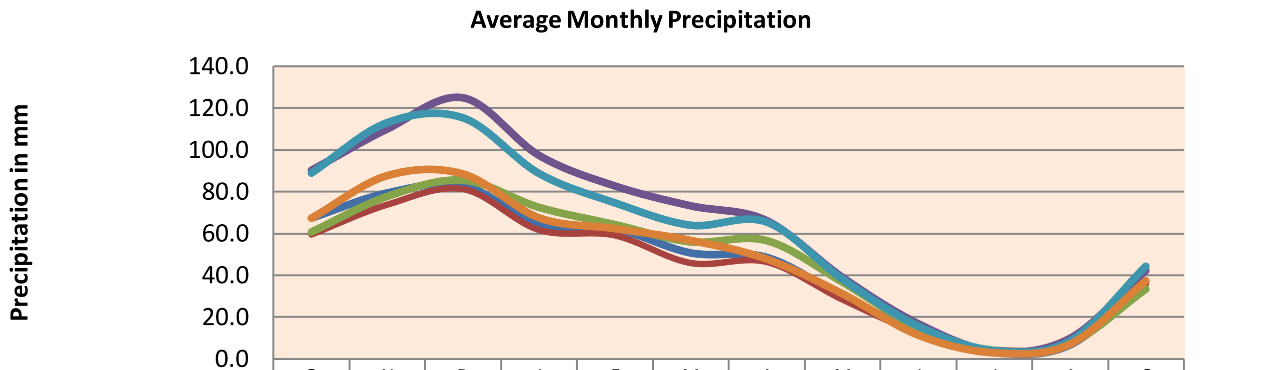

	O	N	D	J	F	M	A	M	J	J	A	S
PABILLONIS	67.4	79.4	82.9	64.5	62.3	50.8	48.7	30.2	13.0	3.1	6.8	37.1
SANGAVINO	59.5	73.7	81.2	61.7	59.1	45.9	46.4	28.5	12.6	4.4	8.1	35.8
SARDARA	60.8	77.9	85.6	72.7	64.4	56.1	56.7	36.8	14.9	4.0	7.4	33.5
GONNOSFANADIGA	90.1	109.9	124.8	97.3	82.7	73.2	66.2	39.0	16.8	3.7	9.8	42.2
MONTEVECCHIO	88.8	112.9	115.2	88.7	74.6	64.0	65.5	38.3	15.8	4.2	8.8	44.4
URAS	67.3	87.7	88.5	67.5	62.3	56.7	47.7	31.1	11.3	2.8	6.9	37.3

Figure 2.7 Average monthly precipitation

The weighted average maximum and minimum precipitation was calculated using the Thiessen polygons (Figure 2.8)as a method of Interpolating rainfall depths using the following equation :

$$P = \frac{A_1P_1 + A_2P_2 + A_3P_3 + \ldots.. + A_iP_i \ldots\ldots A_nP_n}{A_t}$$

Where:- p = Basin weighted mean precipitation

A_t = Total area of the basin

A_i = Area of the i^{th} Thiessen polygon

P_i = Precipitation on the i^{th} meteorological station

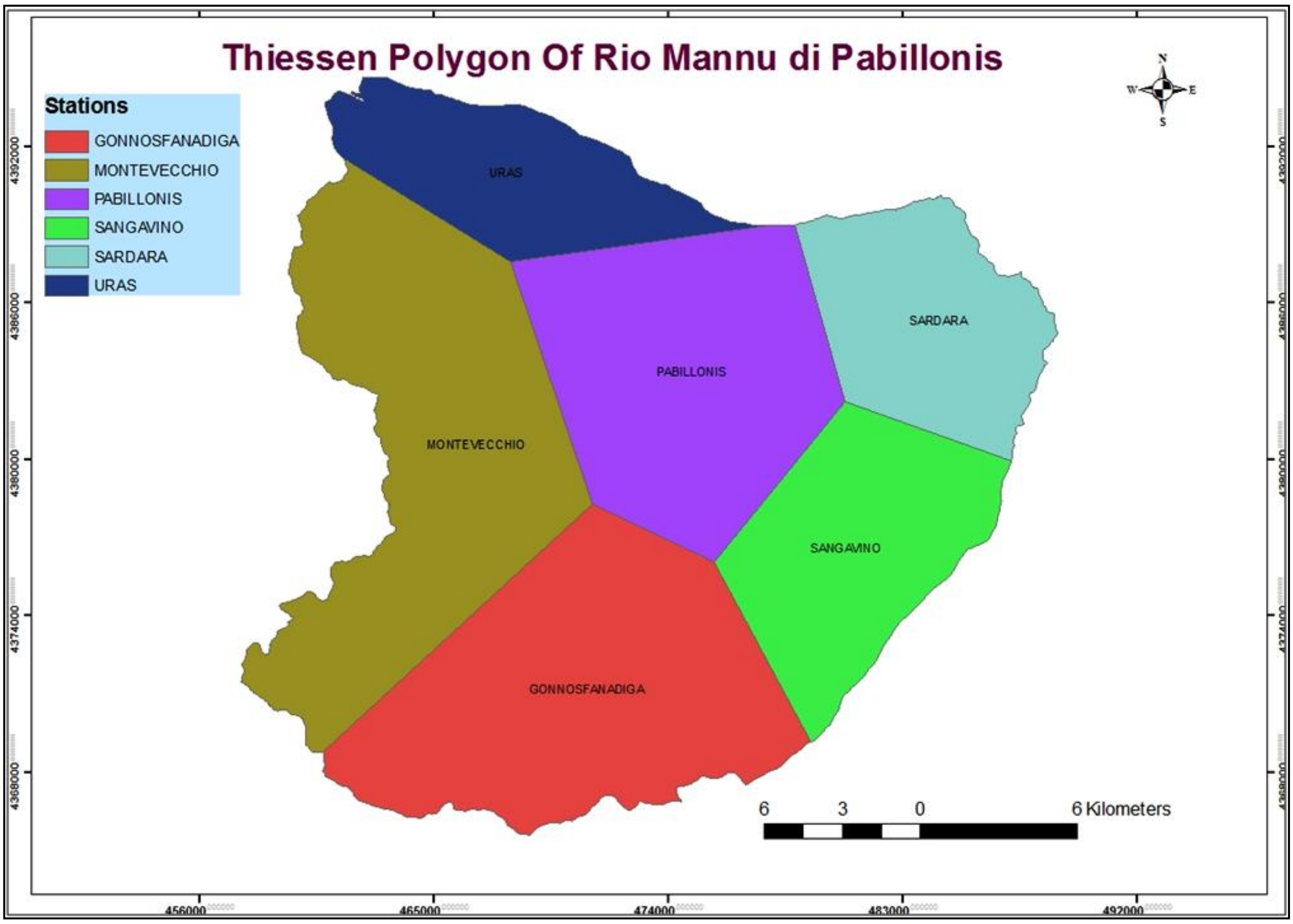

Figure 2.8 Thiessen polygon

Hence the amount of precipitation at highest precipitation period is 755.7mm per year while at the lowest precipitation period is 516.7mm per year. The five years moving average of the precipitation of the whole stations show that, precipitation from 1980’s to early 2000’s, there was decreasing trend while in the late 2000 the trend is in ascending direction. For simplicity of visualization the moving averages of only Montevecchio, Gonnosfanadiga and San Gavino are given in Figure 2.9.

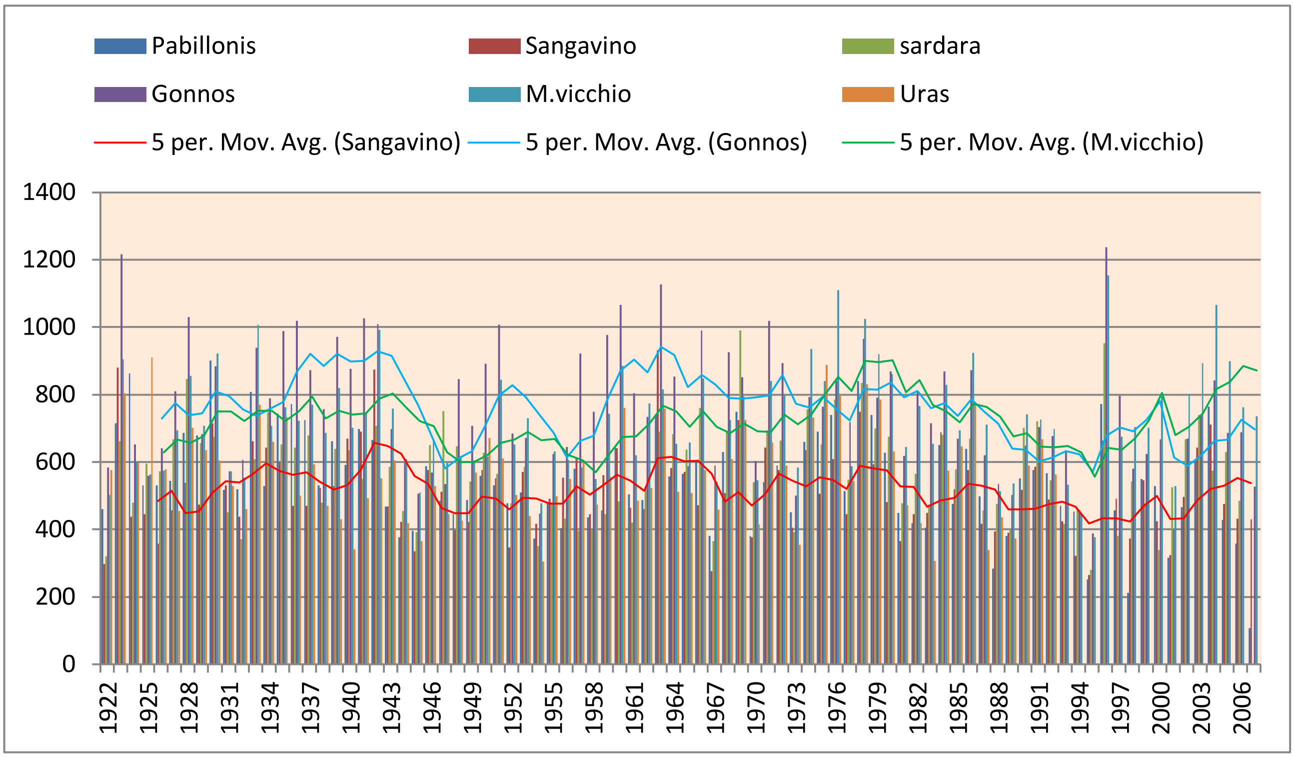

Figure 2.9 Five years moving average

2.6.2. Temperature

Temperature is an important variable in calculating the evapotranspiration of a basin. There are six meteorological stations in the basin and its surroundings with temperature recordings. The minimum average temperature is 9.5ºC in the month of January and the highest is 26.7ºc in the month August in Rio Mannu di Pabilonis, Figure 2.10. Data plot of average temperature versus altitude showed poor correlation, specially the data of the low altitude stations diverge from the general trend shown by the relatively high altitude stations of Montevecchio, Gonnosfanadiga and Sardara.

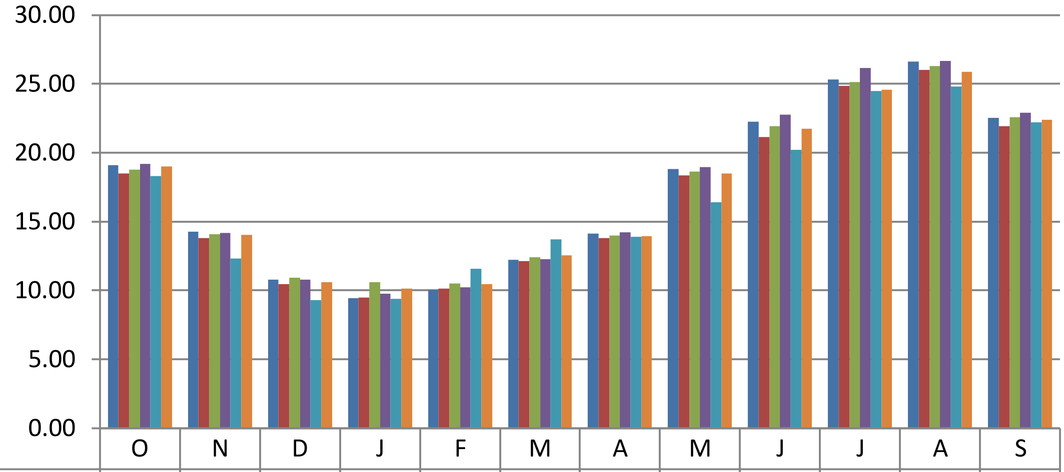

	O	N	D	J	F	M	A	M	J	J	A	S
PABILLONIS	19.12	14.25	10.81	9.42	10.03	12.23	14.13	18.81	22.27	25.31	26.64	22.53
SANGAVINO	18.48	13.83	10.47	9.47	10.15	12.15	13.82	18.34	21.15	24.84	26.01	21.93
SARDARA	18.76	14.08	10.92	10.60	10.53	12.41	14.00	18.61	21.94	25.13	26.28	22.57
GONNOSFANADIGA	19.20	14.20	10.80	9.78	10.25	12.29	14.21	18.95	22.78	26.17	26.69	22.90
MONTEVECCHIO	18.30	12.30	9.30	9.40	11.60	13.70	13.90	16.40	20.20	24.50	24.80	22.20
URAS	19.00	14.06	10.59	10.15	10.47	12.55	13.96	18.50	21.77	24.56	25.86	22.42

Figure 2.10 Monthly average temperature

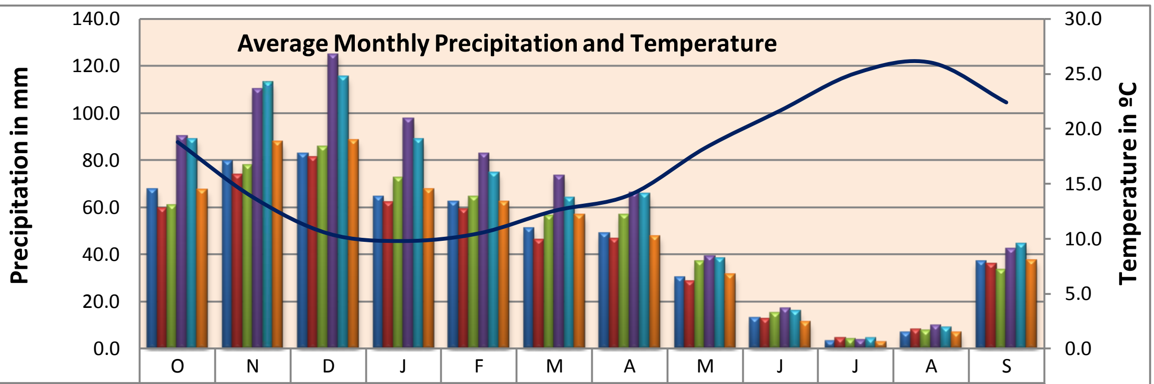

	O	N	D	J	F	M	A	M	J	J	A	S
PABILLONIS	67.4	79.4	82.9	64.5	62.3	50.8	48.7	30.2	13.0	3.1	6.8	37.1
SANGAVINO	59.5	73.7	81.2	61.7	59.1	45.9	46.4	28.5	12.6	4.4	8.1	35.8
SARDARA	60.8	77.9	85.6	72.7	64.4	56.1	56.7	36.8	14.9	4.0	7.4	33.5
GONNOSFANADIGA	90.1	109.9	124.8	97.3	82.7	73.2	66.2	39.0	16.8	3.7	9.8	42.2
MONTEVECCHIO	88.8	112.9	115.2	88.7	74.6	64.0	65.5	38.3	15.8	4.2	8.8	44.4
URAS	67.3	87.7	88.5	67.5	62.3	56.7	47.7	31.1	11.3	2.8	6.9	37.3
Temperature	18.8	13.8	10.5	9.8	10.5	12.6	14.0	18.3	21.7	25.1	26.0	22.4

Figure 2.11 Average monthly temperature & precipitation

2.7. GROUND WATER LEVEL AND FLOW DIRECTION

Primarily the area was subdivided in a three by three kilometer grid to carry out groundwater measurements for this research work. In addition to the borehole data that has being collected from **SIRA System of the Assessorato Difesa Ambiente of the Regione Sarda**., other boreholes that fall within each grid were targeted for the measurements, Figure 2.12. Hence 45 wells were monitored for static water measurements and water samples were collected for chemical analysis. Table 2-1 shows static water level measurements carried out in November 2010 and January 2011 and the variations observed during these measurement times. Most of the boreholes show reduction in the depth to groundwater (0.13-6.9meters), i.e. there was additional water entering the aquifer within the time gap. This change in groundwater level is attributed to the groundwater replenishment in concordance with the rainy season of the area. However, six boreholes showed an increase in static water level depth (0.05-2.2meters) because of probably of continuous abstraction.

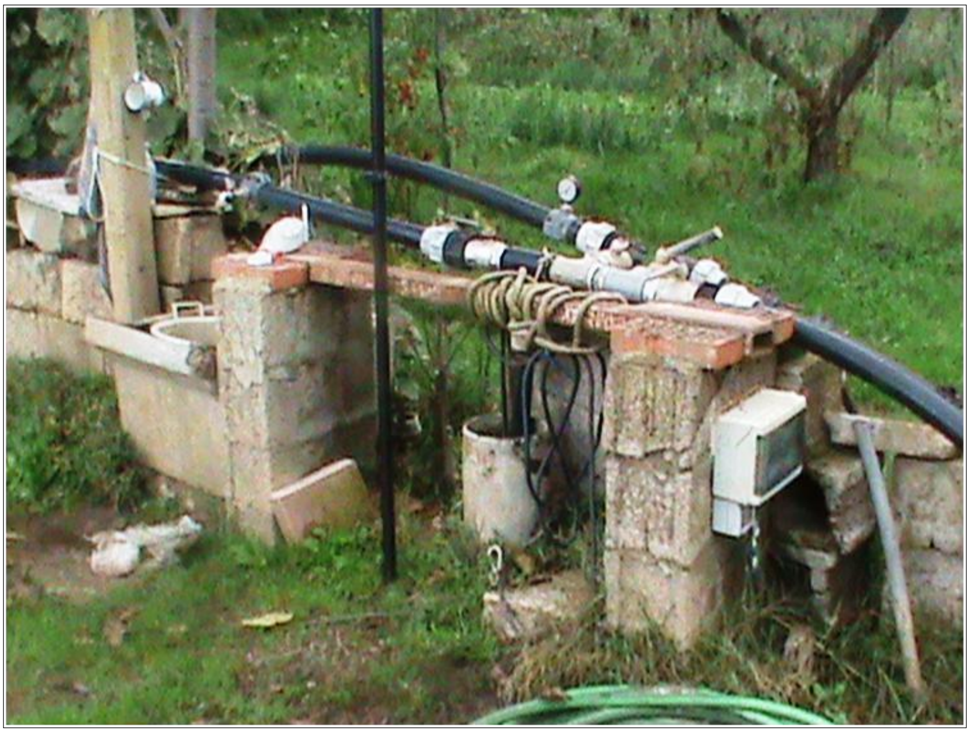

Figure 2.12 Shows one of the monitored wells

Table 2-1 Water level measurements

ID	X	Y	SWL, Nov. 2010	SWL Jan. 2011	Difference
17103PO0001	466379.3	4387291	6.32	2.68	3.64
17103PO0004	468007.5	4391628	2.8	2	0.8
17103PO0005	467033.1	4389769	3.3	1.3	2
17104PO0002	469834.8	4375831	3.01	3.3	-0.29
17104PO0004	476088.1	4382146	8.68	7.9	0.78
17104PO0006	470793.7	4386544	NO	NO	
17104PO0012	474270.1	4388792	9.95	9.3	0.65
17104PO0017	471529.5	4382311	0.93	0.8	0.13
17104PO0018	477424.5	4377906	4.59	1.14	3.45
17104PO0021	466707.5	4393373	1	0.7	0.3
17104PO0025	477883.9	4386629	14	13.82	0.18
17104PO0027	467425	4376575	12.52	10.72	1.8
17104PO0040	481901	4377039	4.05	1.2	2.85
17104PO0048	470209.4	4377455	3.58	1.82	1.76
17104PO0049	478846	4370469	6.35	5	1.35
17104PO0050	474503.4	4376187	7.31	4.72	2.59
17104PO0051	472188.2	4372581	15.2	13	2.2
17104PO0052	474980.8	4383078	9.6	8.2	1.4
17104PO0054	463817.3	4389299	2.28	0.8	1.48
17104PO0055	479636	4375949	1.83	1.25	0.58
17104PO0058	469962.2	4378558	2.37	0.4	1.97
24101PO0028	486653	4382519	2	2	0
24101PO0026	483529.8	4388805	12.72	5.82	6.9
28101PO0002	463813	4389306	22.23	20.48	1.75
28101PO0011	468595	4380195	70.74	63.9	6.84
28101SO0002	463871.3	4383905			0
PZ002	479531.3	4378509	0.78	0	0.78
BH 100	473165	4369820	1.7	1.78	-0.08
BH 500	460360.1	4370216	0.56	0.72	-0.16
BH 70	466964	4371193	1.3		1.3
BH 80	467768	4372610	1.8	1.85	-0.05
BH 90	473008.1	4372869	1.65	1.42	0.23
BH 101	470764.5	4372913	1.4	1.82	-0.42
BH 111	476290	4373115	23.15	23.02	0.13
BH 120	460967.8	4373146	2.45	1.32	1.13
BH 130	480395	4373300	2.52	0.52	2
BH 140	463819	4373843	0	0	00
BH 180	464716.9	4376671	6.68		
BH 230	473703	4376222	0.6	2.82	-2.22
BH 290	473055.7	4379831	10.57	10.11	0.46
BH 300	482917	4380123	2.53	0	2.53
BH 310	467327.7	4379904	47	44.3	2.7
BH 380	487000.3	4383460	1.3		

The data collected by this research work were plotted with help of ArcGIS 9.3. The isopiezometric map shows that the groundwater flow direction is to the centre of the basin and finally toward the north following the topographic gradient Figure 2.13.

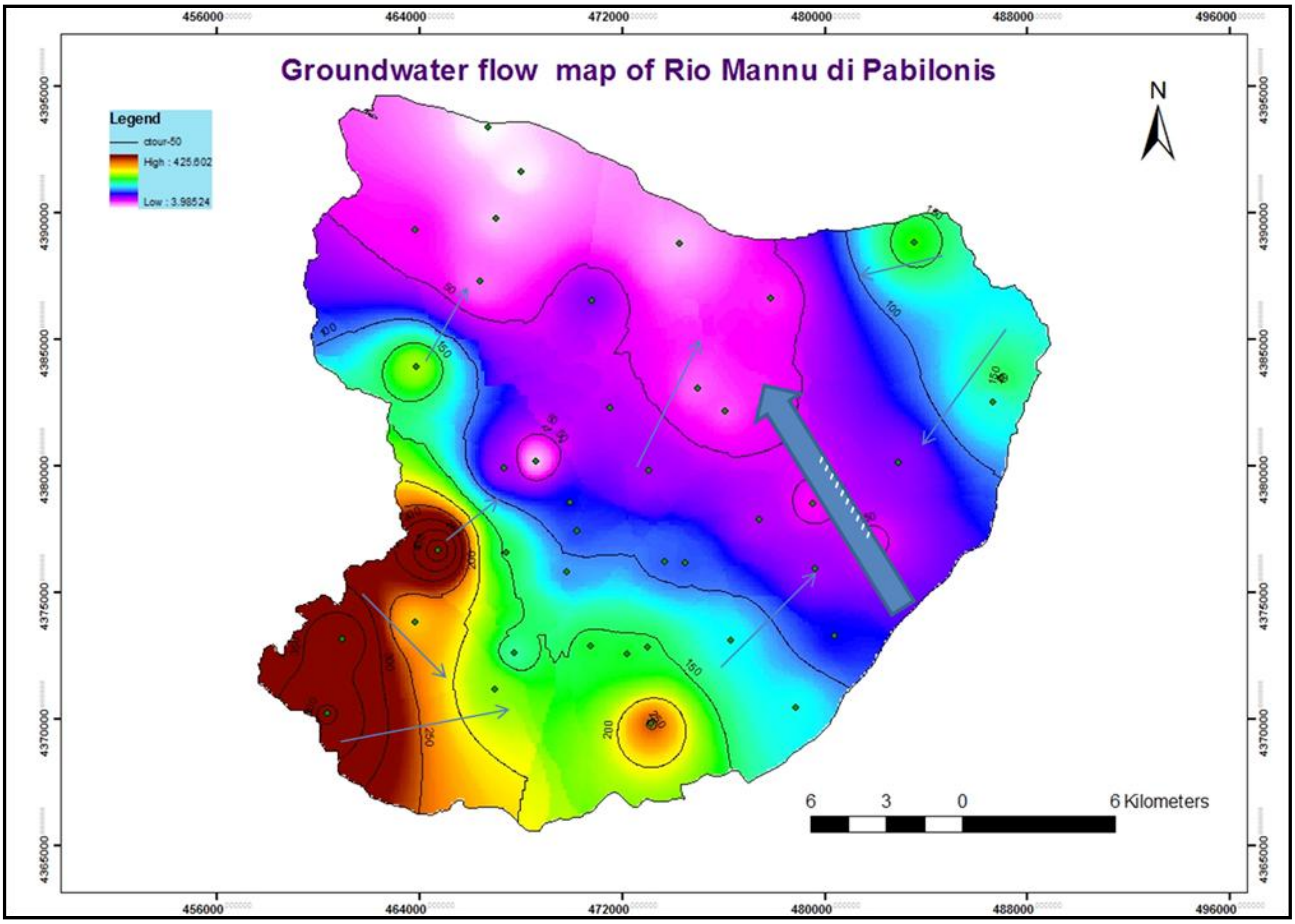

Figure 2.13 Map showing groundwater flow directions

2.8.WATER QUALITY

2.8.1. Sampling site selection

Water samples points were selected based on their location in the grid explained above. Boreholes of the regional groundwater monitoring system of Sardinian were the first choice to be sampled, because their previous works will contribute to compare and contrast the results of this work and/or vice versa. Where there are not these boreholes, do concentrate in the central zone, other alternative boreholes found within each grid were sampled for chemical analysis Figure 2.14.

Once on the sites, the location of a sampling point was recorded using the Global Positioning System (Differential GPS, WGS 84) for accurate measurements of elevation. The date and time of sampling was also noted. The measurement of static water level of the wells, using deep meters, was made (table 1). In all cases the boreholes were found to be under continuous pumping because of the need of water either for irrigation or other water supply before hours of sampling.

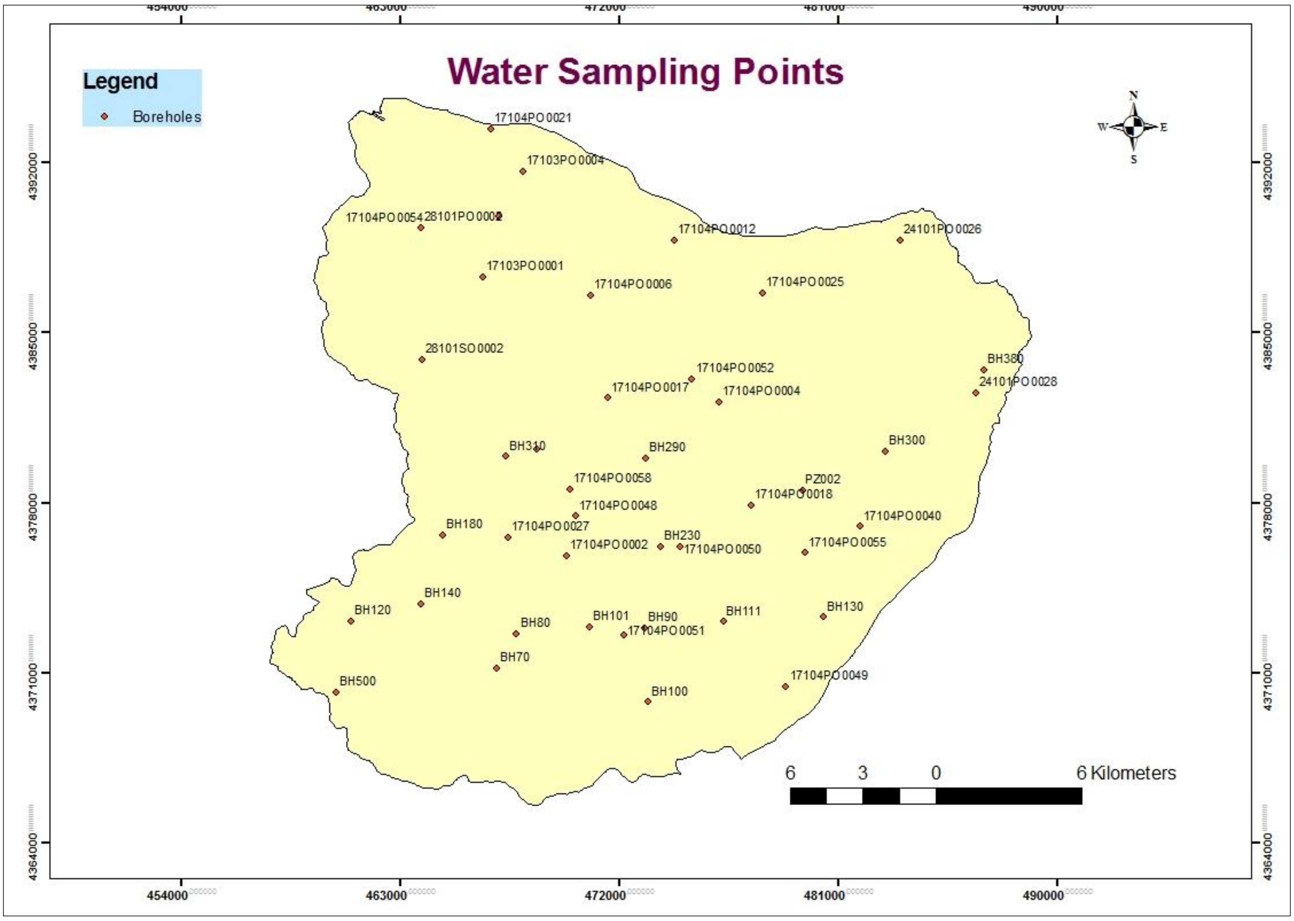

Figure 2.14 Water sampling and measurement points

2.8.2. In situ measurements

2.8.2.1. pH measurements

pH is the most common measure of acidity/alkalinity balance in a solution. It is defined as the negative logarithm (to base 10) of the hydrogen ion activity (in moles/liter) in water at 25°C. pH 7 is termed as neutral. The values above and below this values indicate the alkalinity and acidity of the water respectively. In practice few water have a pH of precisely equal to 7, and therefore refer to waters with a pH in the range between 6.5 and 8.5 as being circum-neutral, (Paul L. Younger, 2007).

Before the measurement the pH meter was calibrated according to the manufacturer's requirements, using a two point calibration with buffers of known concentration. The selection of the calibration standard was dependent on the anticipated nature of the water to be sampled and calibrated with standards appropriate to the anticipated range (pH 7 and 10). Calibration standards were stored appropriately to ensure their accuracy.

The pH of both borehole and spring samples ranges between 6.8 and 8.11. Generally the results are within the permissible limit of the drinking water quality according to the Italian law (D.L. 31/2001 (Italia) Acque destinate al consumo umano) which states the range as 6.5-9.5. Therefore, the pH values of water samples of the study indicate that there is no danger of extreme acidity or alkalinity of the water.

2.8.2.2. *Temperature measurements*

The temperature of the water to be sampled will generally be the mean temperature of the region where the monitored borehole is located. As temperature will move toward ambient upon sampling, it should be recorded as soon as a stable reading is obtained after collection.

The groundwater temperature of the boreholes and springs of the Rio Mannu di Pabillonis was measured twice in this work. No significant difference of temperature was observed temporally. The highest temperature measured is 27ºC in the borehole number 17104PO0006 and the lowest is 12.01ºC in BH-111 which is located far apart. Over 90% of the water samples have temperature values between 16-20ºC, indicating no significant difference between them.

2.8.2.3. *Total Dissolved Solids (TDS) and Electric Conductivity (Ec) Measurements*

The total dissolved solids measured during the field works vary from 89 to 2686 and 299 to 423 mg/l for boreholes and spring samples respectively. A plot of TDS concentration contours shows that there is high concentration of TDS in eastern part of the basin than the western part, Figure 2.15.

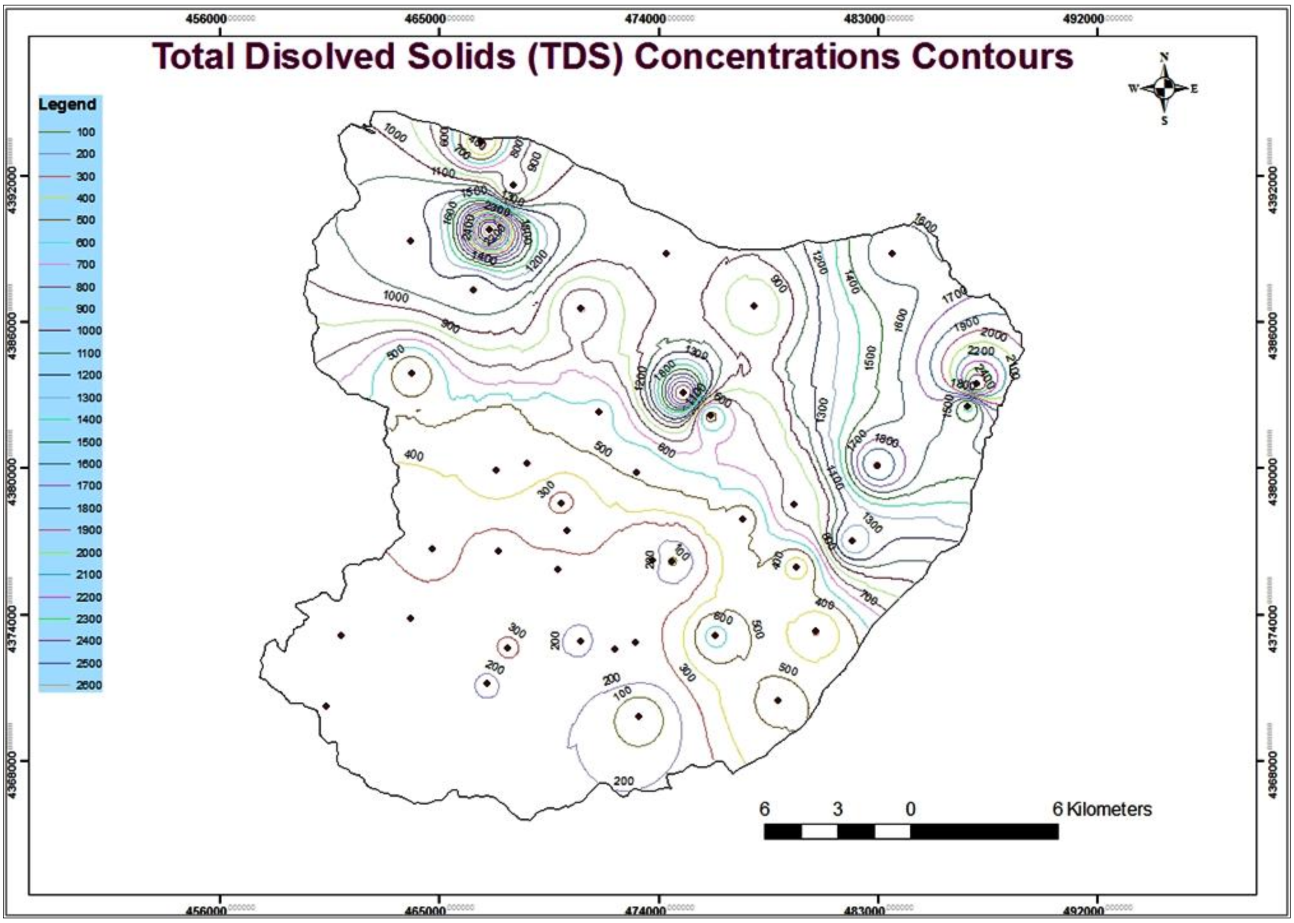

Figure 2.15 TDS concentration contour map

2.8.3. Filtration, acidification and labeling of samples for chemical analysis

Filtration of samples in the field is required for laboratory measurement of cations and anions. After disassembling the two-chamber filtering unit, a 0.45 µm membrane filter was placed onto the filter holder on the lower chamber of the filtration unit. After refitting the chamber units, water was injected through the upper opening of the chamber, using a 50ml syringe, slowly. Meanwhile the filtered water is collected in plastic bottle placed at the bottom end of the filtration unit. For cations, the filtered water sample was acidified using a few drops of concentrated nitric acid. Then was closed by double plastic lids and shacked for proper mixing. For anions, no need to add any chemicals. The bottles were labeled carefully with the relevant information about the sample.

3. CHAPTER III: HYDROCHEMICAL ANALYSIS

3.1. CHEMICAL COMPOSITION OF WATER SAMPLES

Groundwaters in unconsolidated aquifers are usually of excellent quality, being naturally filtered. The water is normally clear, colorless, and free from microbial contamination, and thus requires minimal treatment. As a consequence of the slow travel times in the flat plains and due to the long contact time with the sediment, the groundwater often contains significant quantities of minerals in solution. The solute content varies and depends on the residence time of water in the aquifer and the mineral composition of the aquifer itself.

Forty five water samples were collected for chemical analysis. The major constituents contained in the chemical analysis results include cations such as calcium, magnesium, sodium & potassium, and anions such as bicarbonate, sulfate, chloride & nitrate and both expressed in ionic form. The chemical composition of the waters from the area is variable but sodium dominates the cations and chloride dominates the anions (Table 3-1).

In addition to the major constituents, fluoride, Bromine, Nitrate and Nitrite were analyzed in the chemical laboratory of the Department of Earth Sciences of the University of Cagliari.

3.1.1. Cations

Sodium (Na) is the dominant cation and is followed by relatively low amounts of Calcium (Ca^{++}) and Magnesium (Mg^{++}). Sodium has a significant concentration in the wells located in the eastern part of the Rio Mannu di Pabillonis, in which the value goes up to 20.75milliequivalents per. The concentration of calcium varies between 0.5 to 12.78 milliequivalents per liter and that of magnesium varies between 0.25 and 15.64 milliequivalents per liter. The potassium value varies between 0.07 to 1.2 milliequivalents per liter. In most cases the highest values of the major cations correspond to the boreholes with high TDS values that are concentrated in the central and eastern part of the basin, Figure 3.1.

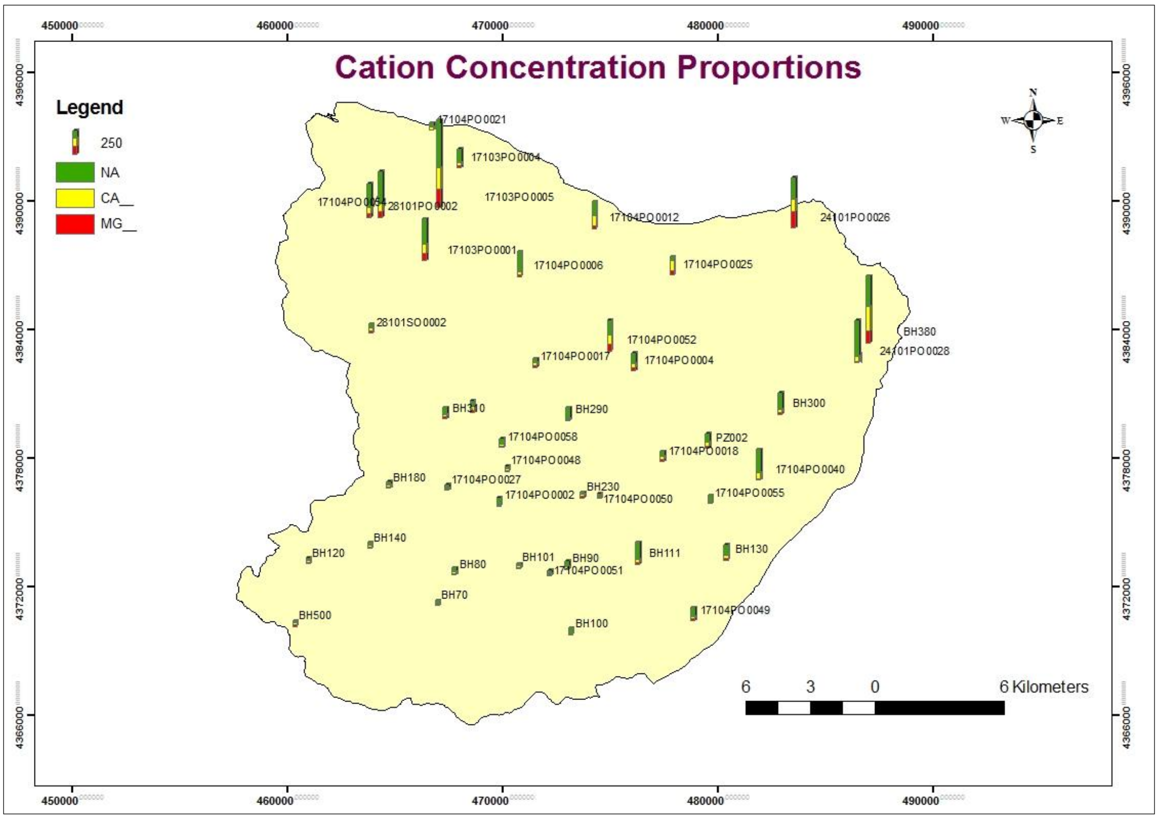

Figure 3.1 Cation proportions of water sampling points

3.1.2. Anions

The dominant anion is chloride in most boreholes and in the spring samples. The range of variation of chloride in the water samples is from 1.16 to 37.66 milliequivalents per liter. The sulfates and bicarbonates are with values ranging from 0.027to 13.37 and 0.58 to 9.59 milliequivalents per liter respectively.

In general the cations, anions and the TDS concentration follow the same trend with respect to their concentration. The dominant geology where these elements concentrate corresponds to the deposits of beach (Sand and gravel, sometimes with shellfish, etc.. Holocene in age) and to lithologic unit of Marne di Gesturi, which is also marine deposit. Therefore, the concentration of sodium and chloride is high because these lithologies, having marine origin, may have had contained evaporate sequences during their formation and governed the chemistry of the waters in these areas, Figure 3.2.

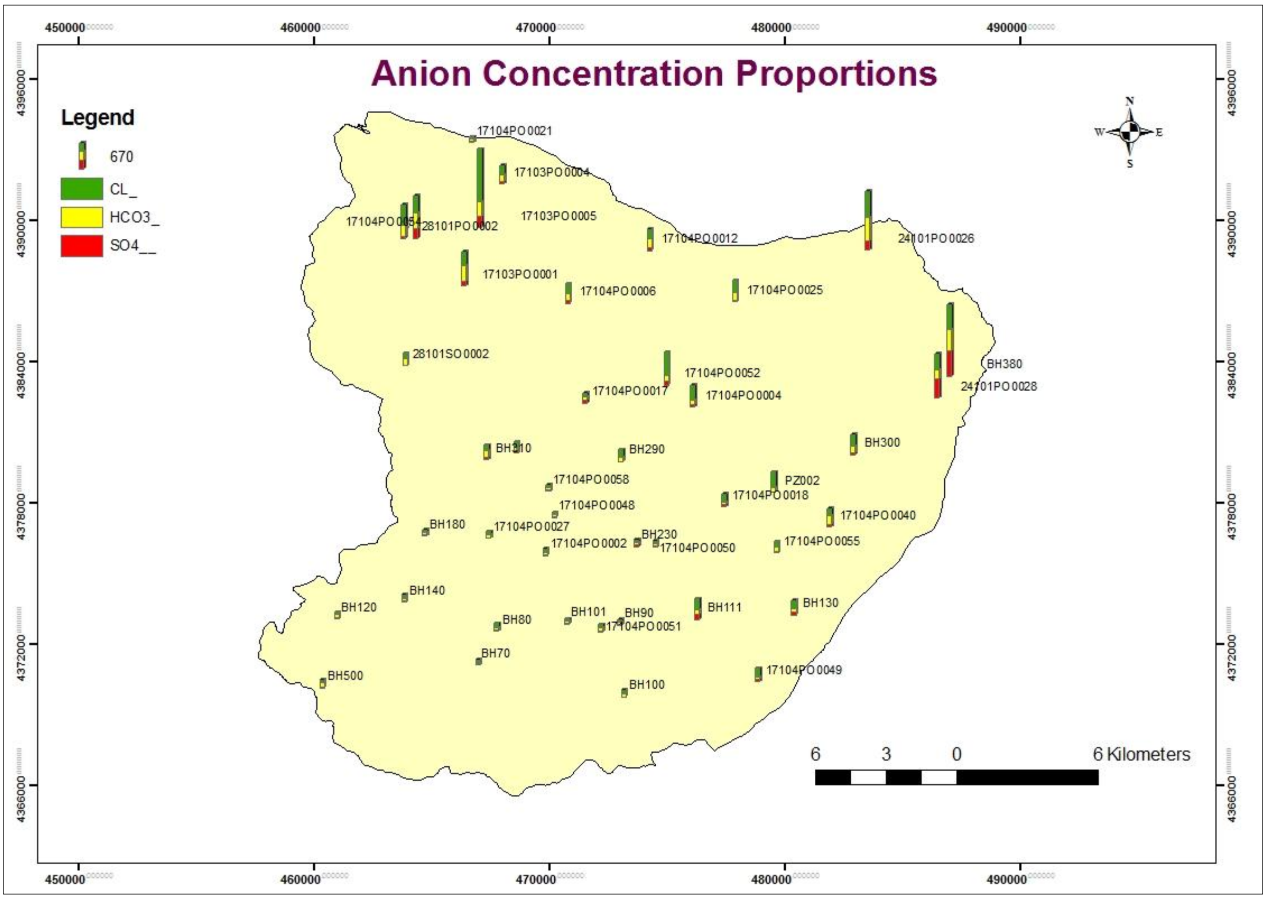

Figure 3.2 Anion proportion of water sampling points

Table 3-1 Chemical analysis results of water samples

Well-ID	Geology	X	Y	Z	pH	Eh	T(Wa)	Cond	TDS	Li	Na	K	Mg	Ca	F	Cl	Br	SO4	NO3	NO2	HCO3	WTYPE
24101PO0028	alluvial	486653	4382519	128	7.8	1.4	16.3	2631	1371	0.1	477	10.2	19	52	0.2	408	1.3	487.7	1	0.0	239	Na-Cl-SO4
BH100	sediments	473165	4369820	254	8.8	0.2	16.2	421	205	0.0	76	2.8	3	10	3.3	83	0.2	1.3	0	0.0	95	Na-Cl-HCO3
BH101	alluvial	470765	4372913	157	7.2	0.2	16.4	344	172	0.0	31	3.3	9	18	0.2	50	0.1	27.4	12	0.0	52	Na-Ca-Mg-Cl-HCO3
BH111	alluvial	476290	4373115	145	6.7	0.7	17.0	1314	635	0.0	212	14.4	22	25	0.1	269	1.0	125.9	23	0.0	129	Na-Cl-SO4
BH120	colluvial sediments	460968	4373146	394	7.3	0.2	16.2	427	214	0.0	41	3.6	8	23	0.1	50	0.2	27.7	19	0.0	85	Na-Ca-Cl-HCO3
BH130	alluvial	480395	4373300	84	7.4	0.3	20.4	595	297	0.0	131	4.6	23	31	0.3	193	0.7	67.3	37	0.0	109	Na-Cl
BH140	granitoid	463819	4373843	215	6.7	0.3	17.7	597	299	0.0	55	5.7	17	20	0.2	94	0.3	29.3	36	0.0	65	Na-Mg-Cl-NO3-HCO3
BH180	granitoid	464717	4376672	433	7.6	0.3	18.4	625	312	0.0	45	2.2	9	20	0.3	66	0.2	18.7	15	0.0	75	Na-Ca-Cl-HCO3
BH230	alluvial	473703	4376222	94	7.1	0.2	14.1	462	231	0.0	45	3.6	13	24	0.2	74	0.3	44.4	31	0.0	50	Na-Ca-Mg-Cl-NO3-SO4
BH290	alluvial	473056	4379832	69	8.8	0.5	18.5	999	500	0.1	140	5.4	12	7	0.1	207	0.7	2.9	1	0.0	91	Na-Cl
BH300	alluvial	482917	4380123	67	6.8	2.0	18.9	3867	1906	0.1	200	6.6	19	32	0.4	293	0.8	35.0	5	0.0	182	Na-Cl-HCO3
BH310	continental deposits	467328	4379904	106	7.3	0.5	18.6	922	461	0.0	133	6.5	19	24	0.1	148	0.4	73.1	37	0.2	155	Na-Cl-HCO3
BH380	continental deposits	487000	4383460	152		2.7	17.1	5029	2515	0.3	477	16.7	122	255	0.2	625	2.4	642.2	230	0.0	559	Na-Ca-Mg-Cl-SO4-HCO3
BH500	granitoid	460360	4370216	405	7.0	0.2	15.0	438	220	0.0	36	3.6	12	27	0.2	59	0.2	21.6	1	0.0	119	Na-Ca-Mg-HCO3-Cl
BH70	continental deposits	466964	4371193	176	7.2	0.2	14.4	377	188	0.0	36	2.5	10	15	0.1	58	0.2	22.2	29	0.0	37	Na-Mg-Ca-Cl-NO3
BH80	alluvial	467768	4372610	139	6.7	0.3	17.5	625	313	0.0	63	3.7	12	19	0.2	90	0.3	39.4	19	0.0	66	Na-Cl-HCO3
BH90	alluvial	473008	4372869	154	7.5	0.3	16.5	567	283	0.0	54	2.9	11	19	0.1	70	0.3	33.2	60	0.0	43	Na-Cl-NO3
PO000117103	continental deposits	466379	4387291	39	7.8	1.1	18.9	2247	1107	0.0	245	17.9	79	87	0.1	335	1.1	113.9	188	0.0	416	Na-Mg-Cl-HCO3-NO3
PO000217104	alluvial	469835	4375832	108	7.9	0.2	18.5	456	228	0.0	59	3.8	9	13	0.2	83	0.2	9.6	0	0.0	76	Na-Cl-HCO3
PO000228101	alluvial	463813	4389306	56	7.4	1.1	18.4	2067	1033	0.0	313	9.7	45	58	0.1	507	1.7	64.3	11	0.0	285	Na-Cl-HCO3
PO000417103	alluvial	468008	4391628	10	8.1	0.7	16.1	1443	722	0.0	167	7.6	27	33	0.1	225	0.7	64.9	26	0.0	179	Na-Cl-HCO3
PO000417104	alluvial	476088	4382146	46	7.6	0.5	17.8	931	466	0.1	207	10.3	30	43	0.1	384	1.2	51.8	13	0.0	113	Na-Cl
PO000517103	continental deposits	467033	4389769	20	7.1	2.9	19.9	5353	2686	0.0	591	27.4	190	227	0.1	1335	3.9	287.4	214	0.0	382	Na-Mg-Ca-Cl
PO000617104	volcanic	470794	4386544	65	7.9	0.7	27.5	1391	697	0.1	182	13.2	24	27	0.2	246	0.8	74.9	11	0.0	179	Na-Cl-HCO3
PO001128101	alluvial	468595	4380196	86	7.4	0.5	18.8	927	464	0.0	93	5.0	27	34	0.1	130	0.6	52.9	101	0.0	102	Na-Mg-Cl-NO3
PO001217104	continental deposits	474270	4388792	29	7.4	1.1	18.2	2110	1052	0.0	107	4.7	30	101	0.1	222	0.8	65.7	34	0.0	253	Ca-Na-Cl-HCO3

PO001717104	alluvial	471530	4382311	56	7.1	0.6	18.7	1155	578	0.0	52	49.3	18	35	0.1	75	0.3	84.9	82	0.0	90	Na-Ca-Mg-NO3-Cl-SO4
PO001817104	alluvial	477425	4377906	61	7.7	0.4	18.5	899	449	0.0	107	9.8	23	31	0.2	198	0.6	55.8	34	0.0	70	Na-Mg-Cl
PO002117104	continental deposits	466708	4393373	5	7.6	0.3	19.1	511	288	0.0	38	2.5	6	28	0.0	52	0.2	37.9	23	0.0	65	Na-Ca-Cl-HCO3-SO4
PO002517104	continental deposits	477884	4386629	55	7.6	0.8	18.2	1622	812	0.0	135	9.9	40	109	0.1	325	0.7	44.1	128	0.0	175	Na-Ca-Mg-Cl-NO3
PO002624101	sedimentary	483530	4388805	174	7.3	1.7	18.5	3275	1649	0.0	392	10.8	171	132	0.2	653	1.6	242.2	254	0.0	604	Na-Mg-Cl-HCO3-NO3
PO002717104	granitoid	467425	4376575	162	7.6	0.3	17.4	510	255	0.0	46	2.9	10	15	0.3	75	0.2	2.7	1	0.0	88	Na-Mg-Ca-Cl-HCO3
PO004017104	alluvial	481901	4377039	50	7.3	1.4	18.2	2779	1388	0.0	132	27.5	19	55	0.4	179	0.5	67.0	29	0.0	236	Na-Ca-Cl-HCO3
PO004817104	alluvial	470209	4377455	93	7.2	0.2	19.4	442	395	0.0	30	2.8	8	19	0.1	53	0.2	21.7	14	0.0	52	Na-Ca-Mg-Cl-HCO3
PO004917104	alluvial	478846	4370469	130	7.5	0.5	18.3	1082	541	0.0	137	7.3	21	25	0.1	223	0.7	51.7	40	0.0	68	Na-Cl
PO005017104	alluvial	474503	4376188	99	8.0	0.1	14.7	177	89	0.0	45	4.1	11	14	0.1	76	0.3	25.1	6	0.0	57	Na-Mg-Cl-HCO3
PO005117104	continental deposits	472188	4372581	172	7.1	0.3	18.0	568	283	0.0	72	3.0	9	13	0.2	82	0.3	29.9	24	0.0	78	Na-Cl-HCO3
PO005217104	alluvial	474981	4383078	44	6.8	2.2	18.4	3577	2016	0.1	239	16.0	69	100	0.3	598	2.1	111.9	14	0.0	130	Na-Mg-Ca-Cl
PO005417104	volcanic	463817	4389300	56	7.6	1.3	19.2	2591	1302	0.1	343	14.6	62	89	0.3	435	1.5	252.6	41	0.0	410	Na-Mg-Cl-HCO3-SO4
PO005517104	alluvial	479636	4375949	63	7.4	0.3	20.7	695	348	0.0	109	3.2	10	19	0.3	146	0.4	21.7	4	0.0	120	Na-Cl-HCO3
PO005817104	alluvial	469962	4378558	84	7.3	0.3	18.0	541	270	0.0	44	3.7	11	22	0.1	73	0.2	30.4	22	0.0	59	Na-Ca-Mg-Cl-HCO3
PZ002	alluvial	479531	4378509	44	8.0	0.9	16.8	1671	835	0.1	199	8.8	29	40	0.2	387	1.2	25.5	3	0.0	108	Na-Cl
SO000228101	volcanic	463871	4383906	180	7.6	0.4	20.9	849	423	0.0	81	6.7	20	32	0.0	125	0.5	17.4	4	0.0	173	Na-Mg-Ca-Cl-HCO3

3.2. OTHER PARAMETERS

3.2.1. Sodium Adsorption Ratio (SAR)

Sodium concentration is an important factor in classifying water for irrigation. Because sodium reacts with soils and reduce its permeability which makes cultivation difficult. The salinity laboratory of the United States Department of Agriculture recommended the SAR as an index (Table 3-2) for sodium hazard and defined it as:

$$SAR = \frac{Na}{\sqrt{\frac{Ca + Mg}{2}}}$$

Where, the concentrations of the constituents are expressed in milliequivalent per liter.

Table 3-2 Water classification for SAR, after (Todd, 2005)

Water class	Alkali Hazard (SAR)
Excellent	*up to 10*
Good	10-18
Fair	18-26
Poor	>26

9% of the water samples are of excellent, 37% are of good 9% of fair and the remaining 45% have poor quality with respect to the above standard.

3.2.2. Hardness

Hardness results from the presence of divalent metallic cations, of which calcium and magnesium are the most important once. Because of their adverse action with soap, hard waters are unsatisfactory for household cleaning purposes. Accordingly Hardness (H) is expressed as:

$$H = 2.5\,Ca + 4.1\,Mg$$

Where: Ca and Mg are measured in milligram per liter as the equivalent of calcium carbonate. In the present work this method has been used to determine the total hardness of the water samples (Table 3-3). For classification of range of hardness concentrations, (Todd, 2005) used the following classification.

Table 3-3 Classification of hardness values, after Todd 2005

Hardness, (mg/l as CaCO3)	water class
0-75	Soft
75-150	moderately soft
150-300	Hard
>300	Very hard

Based on the above classification, 10% are soft, 40% are moderately soft, 31% are hard and the remaining 19% fall in the very hard water class. Springs, are within the moderately soft to hard category as that of most of the boreholes.

3.2.3. Nitrate concentration

The nitrate concentration is low in most cases and the values vary between 0-254 mg per liter, Figure 3.4. Some 18% of the water samples analyzed have nitrate values greater than 50 mg/liter, which is the highest permissible limit for human use (D.L. 31/2001 (Italia) Acque destinate al consumo umano). The concentrations higher than 50mg per liter are usually associated in areas where the dominant activities are related to animal farming. As shown in Figure 3.3, the distance between the boreholes and the cattle troughs are too short for animal secrets to percolate into the well and pollute it.

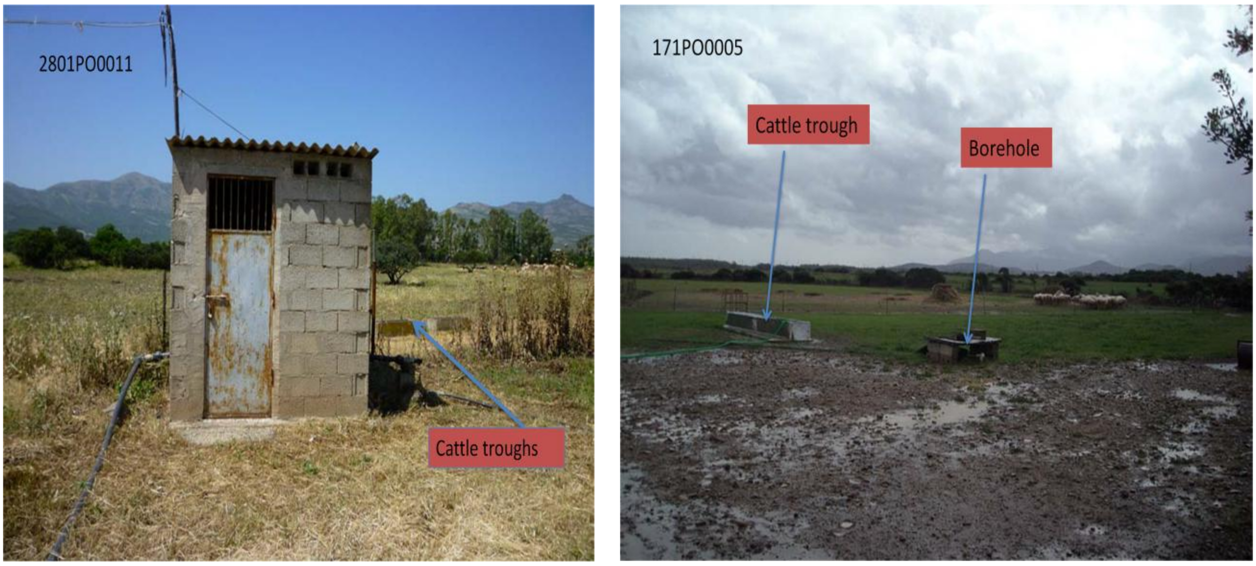

Figure 3.3 Shows examples of water wells with cattle troughs nearby to them

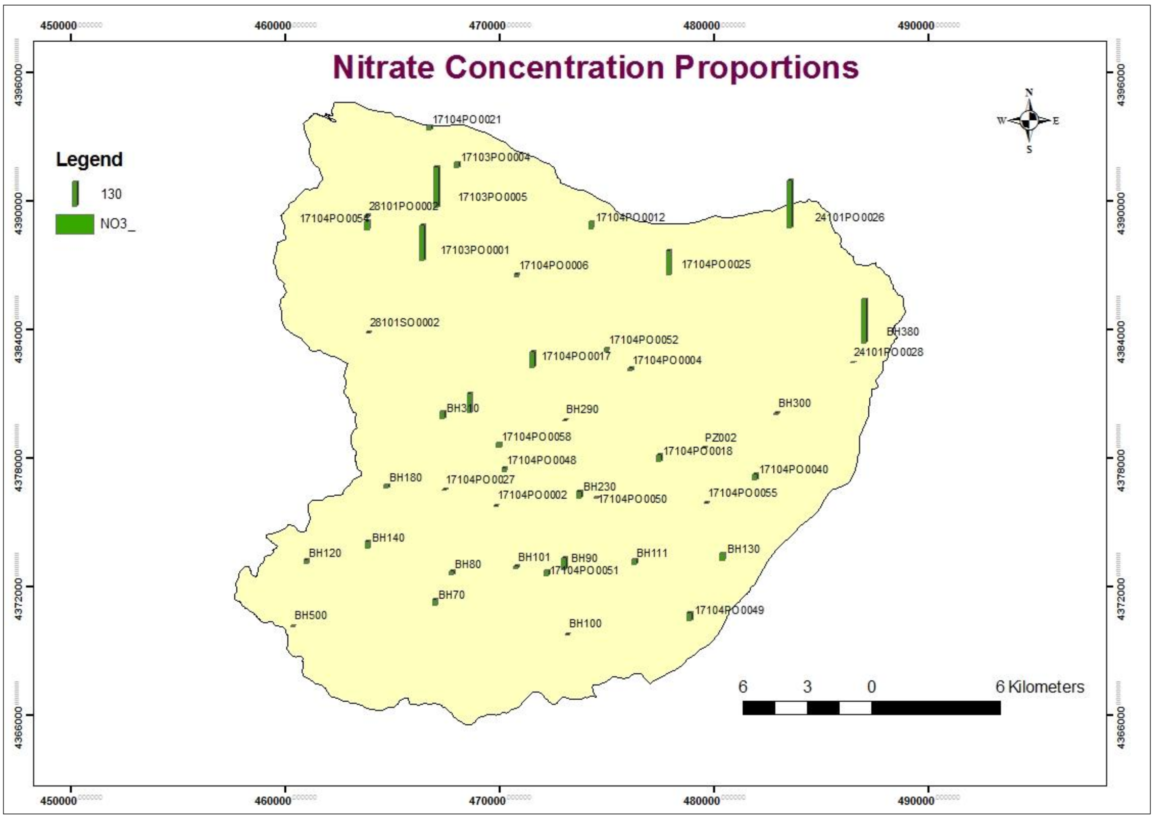

Figure 3.4 Nitrate proportion in water sampling points

3.2.4. Water type classification

An important task in groundwater investigation is the compilation and presentation of chemical data in a convenient manner for visual interpretation. Thus, the Pipers tri-linear diagram (Figure 3.5) and chemical variation plots (Figure 3.6) are used.

a) Pipers Tri-linear Plot

Here cations are expressed as percentages of total cations (Mg, Ca, Na, and K) and similarly anions are expressed as percentages of the total anions. These two points are then projected into the central diamond-shaped area parallel to the upper edges of the central area. This single point is thus uniquely related to the total ionic distributions. This diagram conveniently reveals similarities and differences among water samples because those with similar quantities will tend to plot together as groups.

The dominant groundwater type in the area is Na-Cl and Na-Cl-HCO_3 type except in few water samples incorporate Ca and Mg with Na in area where the geological units contain these elements in their composition, like in basalt.

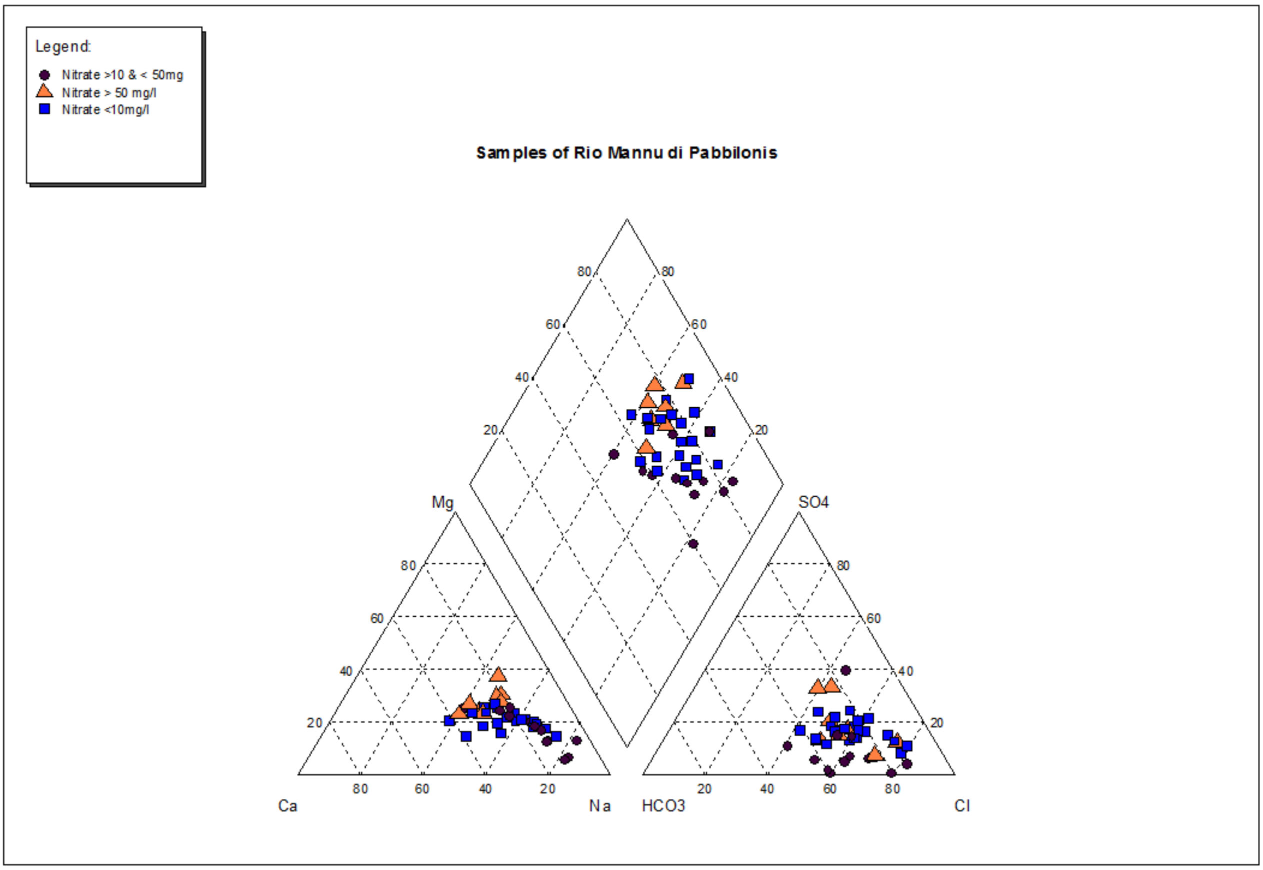

Figure 3.5 Piper trilinear diagram of water samples

b) Chemical Variation Plots

Chemical variation diagrams have been constructed in order to understand the evolution in groundwater chemistry. As it can be observed from Figure 3.6, though the dominant water type is Na-Cl type, but the water samples from the western and eastern parts of the study area contain significant amount of calcium and magnesium in the cations and bicarbonate in the anions. The direction of the groundwater movement is toward the center and the groundwater chemistry evolves in the same direction. The groundwater evolves from calcium bicarbonate to sodium chloride along its movement (Freeze R.A and Cherry, J.A., 1979)

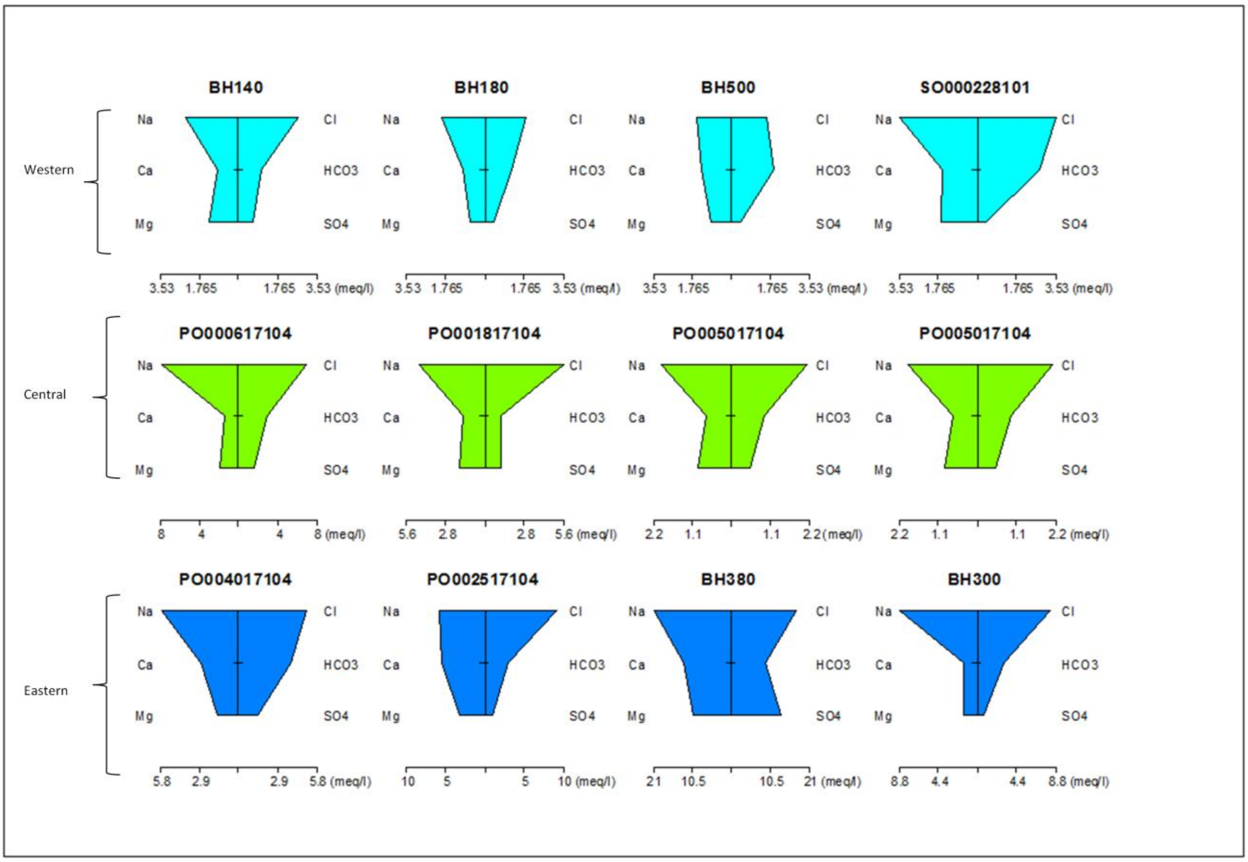

Figure 3.6 Stiff diagram of water samples

4. CHAPTER IV: GROUNDWATER RECHARGE EVALUATION

4.1.INTRODUCTION

Quantification of the rate of the natural groundwater recharge is a basic pre-requisite for efficient groundwater resource management. However, the rate of the aquifer recharge is one of the most difficult factors to measure in the evaluation of groundwater resources. The main techniques used to estimate the groundwater recharge rates are the Soil Water Balance approach, WetSpass, Chloride Mass Balance and the Groundwater Level Fluctuation approach etc. The Thornthwaite and WetSpass methods are employed in this research work and are presented as follows:

4.1.1. Thornthwaite and Mather method

Water balance calculations are required to know the amount of water available for ground water recharge and to indicate proper management of groundwater utilization. The water balance calculation is made using the following equation:

$$P = AET + Runoff + \mathrm{I}$$

where

P	=	Precipitation
AET	=	Actual evapotranspiration
Runoff	=	Overland flow
I	=	Infiltration

The estimation of the different hydrologic parameters involves different important considerations and assumptions. Water balance is done for the data of the years 1922-2007 for precipitation and 1922-1992 for temperature. (Thornthwaite and Mather, 1955)developed a simple “bookkeeping” model, which estimates the balance between the inflow and outflow of water.

The input parameters are mean monthly effective precipitation, mean monthly potential evapotranspiration of the considered months and water holding capacity of the soils. In addition to calculating the actual evapotranspiration of the catchment the model has been used to estimate the soil moisture deficit, detention, and runoff .The inputs of this model were derived as follows:

4.1.1.1. Soil map preparation

The Rio Mannu di Pabillonis soil map from the soil map of Sardegna and the textural classification was adopted from the explanation note of the soil map of Sardegna ‘Nota illustrativa alla carta dei suoli della Sardegna’, 1991. Seven major soil types were recognized from the map (Figure 4.1). Accordingly the areal coverage of each soil type is calculated using ArcGIS 9.3. An overlay of the soil map with the Thiessen polygons made it possible to get the proportion of each soil type in each polygon. Finally, the weighted average of each polygon was used in calculating the inputs to the method. And hence, the soil moisture content is considered to be 100mm as weighted average of the Rio Mannu di Pabillonis.

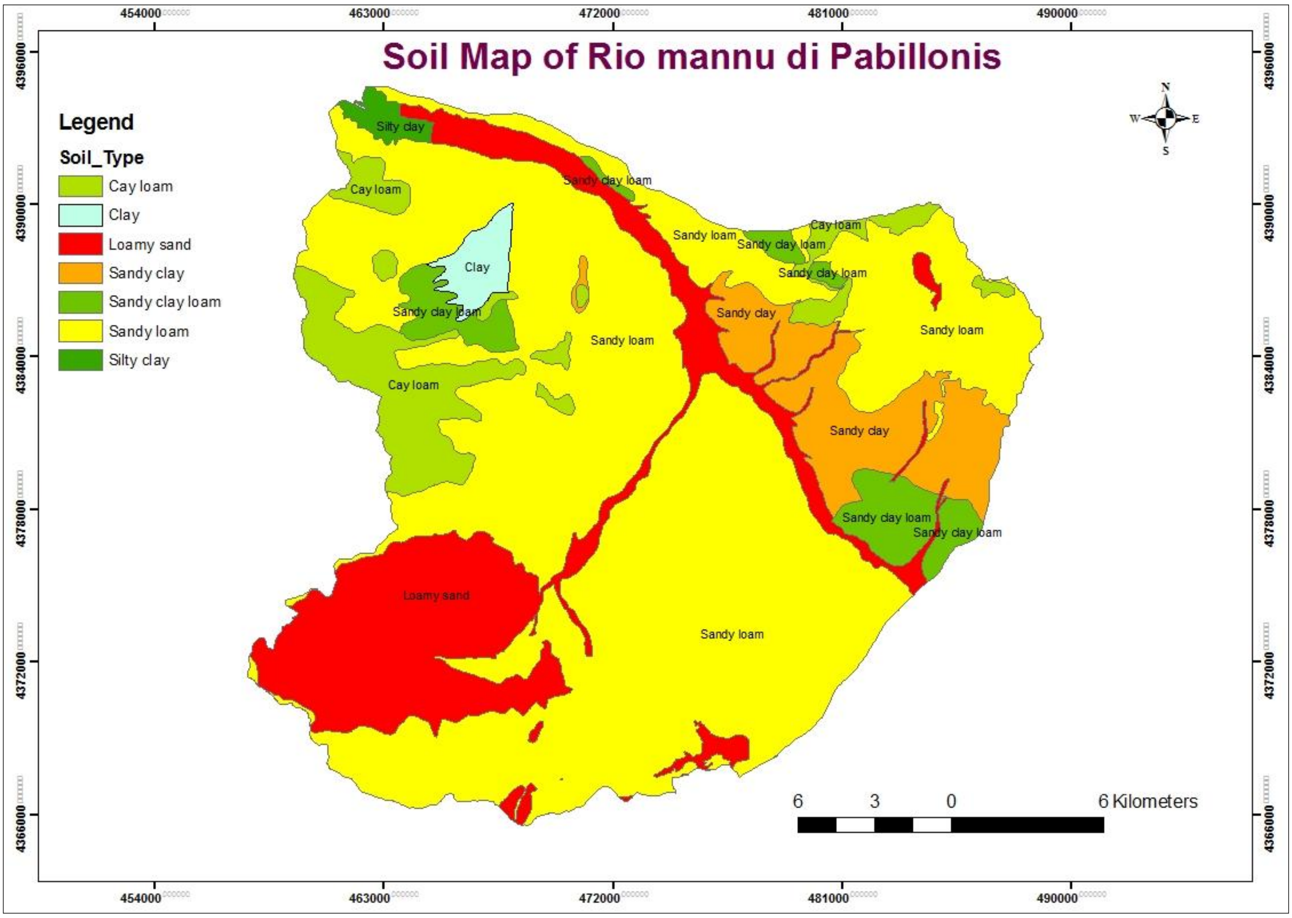

Figure 4.1 Classified soil map

4.1.1.2. *Potential evapotranspiration*

Potential evapotranspiration is defined as the amount of water that would be removed from the land surface by evaporation and transpiration processes if sufficient water were available in the soil to meet the demand. In order to calculate the potential evapotranspiration of the Rio Mannu di Pabillonis the Thornthwaite temperature based approach was utilized. The objective of calculating the potential evapotranspiration is to extract the actual evapotranspiration values using methods that make use of potential evapotranspiration.

The Thornthwaite methods requires only temperature data and the equation is given

ET_0 = Potential evapotranspiration in mm per month.

t = mean monthly temperature in ^{0} C .

i = monthly heat index

I = annual heat index obtained by summing the 12 monthly heat indices,

$$i = \left(\frac{t}{5}\right)^{1.514}$$

$$a = 675*10^{-9}I^3 - 771*10^{-7}I^2 + 1792*10^{-5}I + 0.49239$$

Meanwhile, the correction factor k, which is the day light length proportion as given by the equation

, was utilized to correct the input of Thornthwaite method for calculating potential evapotranspiration as defined by Roser Escuder et al 2009.

To observe the effect of precipitation on the amount of water available for both infiltration and runoff, analysis average precipitation of the years under consideration and of higher precipitation & lower precipitation than the average where employed in performing the water balance using Thornthwaite method. The out puts are presented in table (Table 4-2, Table 4-3 and Table 4-4) and the summary is given in Table 4-1.

Table 4-1 Comparison of output Thornthwaite method at different precipitation amounts

RIO MANNU BASIN									
Average PPT				High PPT 2003			Low PPT 2006		
PPT	613			709		15.7% incremnt of average PPT	574		6.4% reduction than average PPT
PET	878.5			878.5			878.5		
AET	450.3	73.5% of PPT		385.7	54.4% of PPT	14% reduction than average AET	475	82.8%of PPT	5.4 %increment than average AET
CAW	162.6	26.5% of PPT		322.9	45.6% of PPT increased from average	98.8% increment of Average CAW	98.7	17.2% of PPT decreased from average	39.3% reduction of average CAW
Runoff,R	72.6	11.9% of PPT	44.6% of CAW	144	20.3% of PPT increased from average	98.8% increment of average R	44	7.7% of PPT decreased from average	39.1% reduction of average R
Infiltration, I	90	14.7% of PPT	55.4% of CAW	178.9	25.2% of PPT increased from average	98.8% increment of average I	54.7	9.5% of PPT decreased from average	39.2% reduction of average I

where PPT is Precipitation, PET is Potential Evapotranspiration, AET is Actual Evapotranspiration and CAW is Cumulative Available Water that can be divided into both runoff and infiltration.

The following observations can drawn from the results in Table 4-1

- During higher precipitation (higher than average by 15.7%), there is reduction in the actual evapotranspiration (AET) by 14% and an increment of CAW (98.6%) than average PPT.
- During lower precipitation (lower than average by 6.4%), there is an increase in the actual evapotranspiration (AET) by 5.4% and a decrease of CAW (39.3%) than average PPT. The rise in

actual evapotranspiration could be due to the relatively extended daily sunshine hours caused by lack of cloud cover which exposed every drop of water for evaporation.

- The runoff and infiltration are affected by rainfall variability in a similar trend of CAW. Therefore it can be concluded that the CAW and its components are highly affected by rainfall variability than the actual evapotranspiration.

Table 4-2 Results of Thornthwaite method at higher precipitation

Higher PPT 2003													
	OCT	NOV	**DEC**	JAN	FEB	MAR	APR	MAY	JUNE	JULY	AUG	SEP	
Temperature	18.91	14.08	10.72	9.87	10.28	12.28	14.03	18.64	21.96	25.20	26.29	22.47	
Monthly index (i)	3.78	2.82	2.14	1.97	2.06	2.46	2.81	3.73	4.39	5.04	5.26	4.49	
PET not corrected	73.75	43.60	26.77	23.13	24.88	34.13	43.28	71.89	96.29	123.06	132.74	100.28	
K	0.96	0.83	0.81	0.84	0.82	1.03	1.11	1.24	1.25	1.27	1.18	1.04	
PET corrected	71.1	36.3	21.7	19.3	20.5	35.3	48.0	89.1	120.4	155.8	156.6	104.5	878.54
PPT	176.4	75.2	116.6	104.6	119.1	21.1	39.5	3.6	3.2	0.1	1.0	48.3	709
PPT-PET corrected	105.3	38.8	94.9	85.3	98.6	-14.1	-8.5	-85.5	-117.1	-155.7	-155.6	-56.2	
Soil Moisture	100.0	100.0	100.0	100.0	100.0	85.9	77.4	0.0	0.0	0.0	0.0	0.0	
Change in Soil moisture	100.0	0.0	0.0	0.0	0.0	-14.1	-8.5	-77.4	0.0	0.0	0.0	0.0	
AET	71.1	36.3	21.7	19.3	20.5	35.3	48.0	81.0	3.2	0.1	1.0	48.3	385.7
Surplus	5.3	38.8	94.9	85.3	98.6	0.0	0.0	0.0	0.0	0.0	0.0	0.0	322.9
Deficit	0.0	0.0	0.0	0.0	0.0	0.0	0.0	8.1	117.1	155.7	155.6	56.2	492.8

Table 4-3 Results of Thornthwaite method at average precipitation

Basin Average PPT													
	OCT	NOV	**DEC**	JAN	FEB	MAR	APR	MAY	JUNE	JULY	AUG	SEP	
Temperature	18.91	14.08	10.72	9.87	10.28	12.28	14.03	18.64	21.96	25.20	26.29	22.47	
Monthly index (i)	3.78	2.82	2.14	1.97	2.06	2.46	2.81	3.73	4.39	5.04	5.26	4.49	
PET not corrected	73.75	43.60	26.77	23.13	24.88	34.13	43.28	71.89	96.29	123.06	132.74	100.28	
K	0.96	0.83	0.81	0.84	0.82	1.03	1.11	1.24	1.25	1.27	1.18	1.04	
PET corrected	71.1	36.3	21.7	19.3	20.5	35.3	48.0	89.1	120.4	155.8	156.6	104.5	878.54
PPT	72.3	90.2	96.4	75.4	67.6	57.8	55.2	34.0	14.1	3.7	8.0	38.4	613
PPT-PET corrected	1.2	53.9	74.7	56.1	47.1	22.5	7.2	-55.2	-106.3	-152.1	-148.6	-66.1	
Soil Moisture	1.2	55.1	100.0	100.0	100.0	100.0	100.0	44.8	0.0	0.0	0.0	0.0	
Change in Soil moisture	1.2	53.9	44.9	0.0	0.0	0.0	0.0	-55.2	-44.8	0.0	0.0	0.0	
AET	71.1	36.3	21.5	19.3	20.5	35.3	48.0	89.1	58.9	3.7	8.0	38.4	450.3
Surplus	0.0	0.0	29.8	56.1	47.1	22.5	7.2	0.0	0.0	0.0	0.0	0.0	162.6
Deficit	0.0	0.0	0.2	0.0	0.0	0.0	0.0	0.0	61.5	152.1	148.6	66.1	428.2

Table 4-4 Results of Thornthwaite method at lower precipitation

	Lower PPT 2006												
	OCT	NOV	**DEC**	JAN	FEB	MAR	APR	MAY	JUNE	JULY	AUG	SEP	
Temperature	18.91	14.08	10.72	9.87	10.28	12.28	14.03	18.64	21.96	25.20	26.29	22.47	
Monthly index (i)	3.78	2.82	2.14	1.97	2.06	2.46	2.81	3.73	4.39	5.04	5.26	4.49	
PET not corrected	73.75	43.60	26.77	23.13	24.88	34.13	43.28	71.89	96.29	123.06	132.74	100.28	
K	0.96	0.83	0.81	0.84	0.82	1.03	1.11	1.24	1.25	1.27	1.18	1.04	
PET corrected	71.1	36.3	21.7	19.3	20.5	35.3	48.0	89.1	120.4	155.8	156.6	104.5	878.54
PPT	32.6	23.0	105.5	60.0	37.7	55.4	41.2	0.6	4.7	16.3	3.9	193.2	574
PPT-PET corrected	-38.5	-13.3	83.8	40.7	17.2	20.1	-6.8	-88.5	-115.7	-139.5	-152.7	88.7	
Soil Moisture	50.2	36.9	100.0	100.0	100.0	100.0	93.2	4.6	0.0	0.0	0.0	88.7	
Change in Soil moisture	-38.5	-13.3	63.1	0.0	0.0	0.0	-6.8	-88.5	-4.6	0.0	0.0	88.7	
AET	71.1	36.3	21.7	19.3	20.5	35.3	48.0	89.1	9.3	16.3	3.9	104.5	475.4
Surplus	0.0	0.0	20.7	40.7	17.2	20.1	0.0	0.0	0.0	0.0	0.0	0.0	98.7
Deficit	0.0	0.0	0.0	0.0	0.0	0.0	0.0	0.0	111.0	139.5	152.7	0.0	403.2

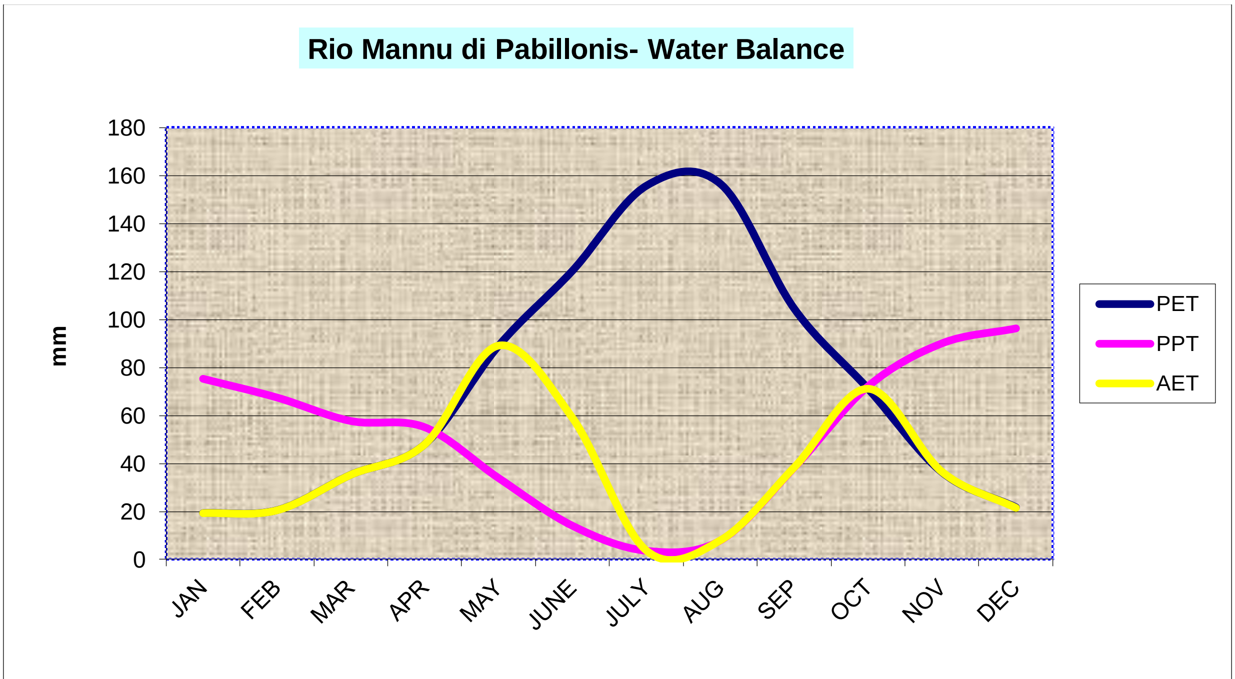

Figure 4.2 Thornthwaite results at average precipitation

The results obtained in the above method were compared with the out puts of an evaluation result for the period (1922-1992) at the outlet of the basin near San Nicola D'Arcidano. The surface area covered was 440 km^2 (Figure 4.3) and the value of runoff obtained is 50.1 mm/year; if this data is interpolated to include the whole basin of Rio Mannu di Pabillonis, a value of 67.4mm is obtained. This value is very close to the runoff value (72.6 mm/year) estimated from the average PPT using Thornthwaite method.

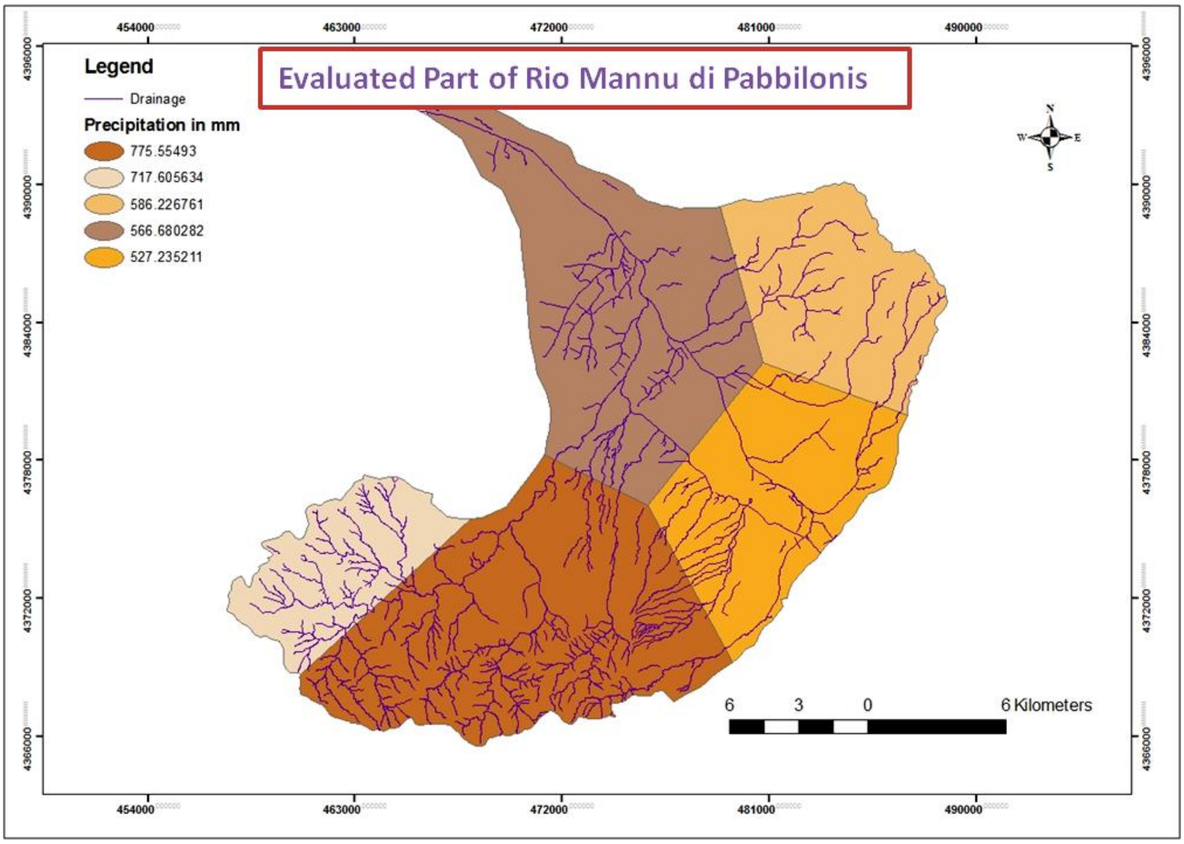

Figure 4.3 Gauged part of Rio Mannu di Pabillonis

4.1.2. WetSpass method

The WetSpass term stands for Water and Energy Transfer between Soil, Plants and Atmosphere under quasi-Steady State. It is a physically based model for estimation of the long term average spatial patterns of groundwater recharge, surface runoff and evapotranspiration from long term average meteorological data together with land use, soil, and groundwater level grid maps by employing physical and empirical relationships. The model treats a basin or region as a regular pattern of grid cells. Every grid cell can be subdivided in a vegetated and a non-vegetated part. For every grid cell a water balance will be maintained. Detail explanation of the concepts and calculations has been given in chapter 7.1.2 of part one. Here, the main inputs and outputs are presented as follows:

The input grid maps such as soil map Figure 4.1, slope map Figure 5.8, ground water level map interpolated from the data in Table 2-1 of part two, and the land use map which was downloaded from the Sardinian Regional Government data bank, were utilized.

Seasonal grid map of precipitation, temperature and wind are interpolated from the data in Table 4-6. Whereas winter and summer land use parameter tables are given in Table 4-7 and Table 4-8 respectively.

4.1.2.1. WetSpass model results

The outputs of WetSpass model are displayed on yearly and seasonal (summer and winter) basis. The total water balance per grid cell is calculated with the previously described (sub chapter 7.1.2)water balance components for vegetated and non-vegetated parts of a grid cell.

a) Groundwater recharge

The WetSpass model determines the long-term average spatially distributed recharge as a spatial variable dependent on the soil texture, land-use, slope, meteorological conditions etc. This is primarily to take into account the influence of the spatial variability of the land surface on the groundwater system (Batelaan et al., 2004). The resulting groundwater recharge from WetSpass for Rio Mannu di Pabillonis ranges from about 0 mm to 519mm, with an average value of 238 mm ,(Figure 4.4) which is about 38.8% of the mean annual precipitation, and standard deviation of about 144.4.

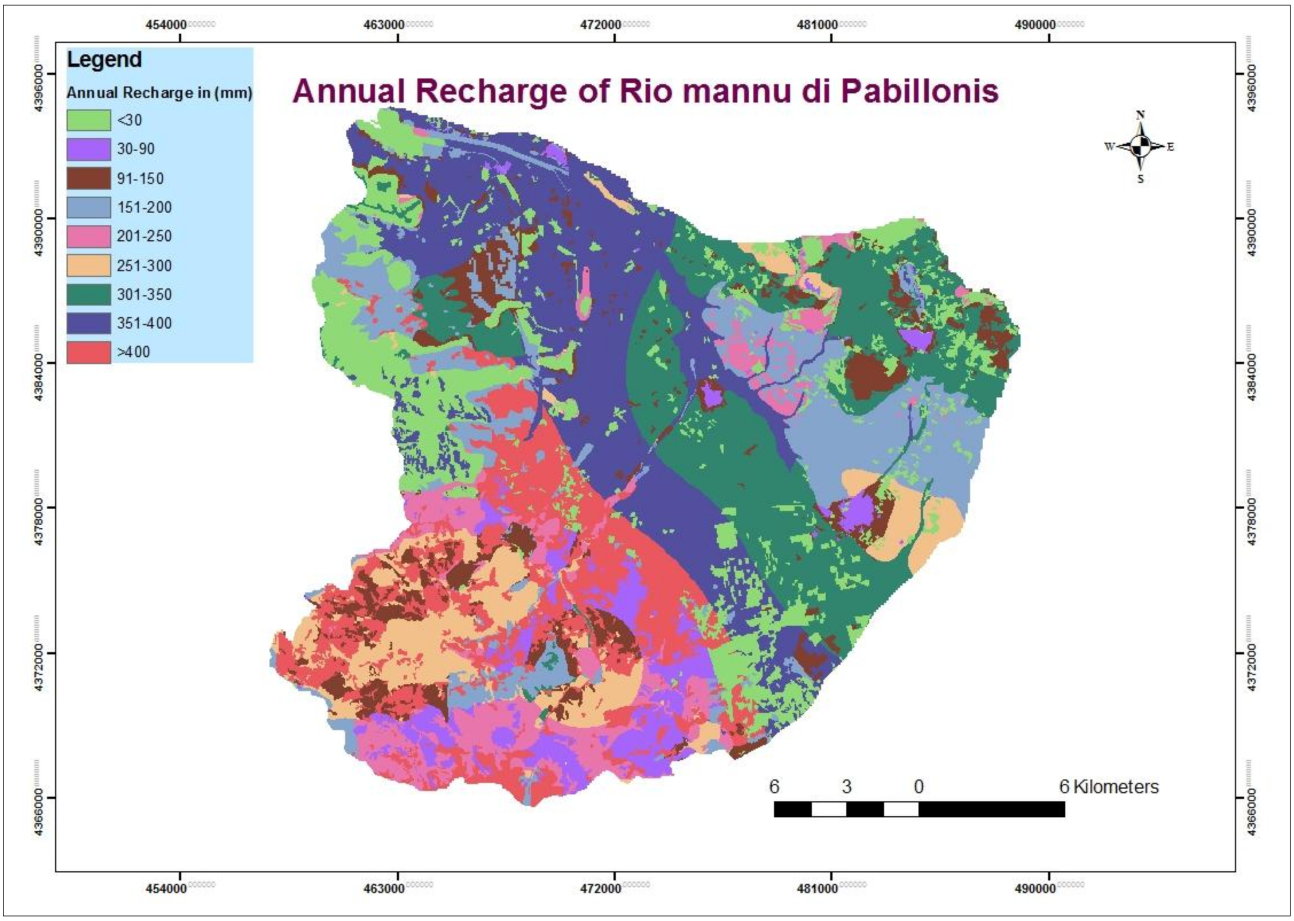

Figure 4.4 Recharge output of WetSpass model

b) Surface runoff

The WetSpass model uses the runoff coefficient method for the estimation of surface runoff. The surface runoff coefficient on the other hand is a function of vegetation type, soil texture and slope. Hence it is apparent that the surface runoff in Pabillonis basin does also vary spatially with topography and other catchment characteristics, Figure 4.5. The simulated runoff varies from less than a mm to a maximum of 392 mm with a mean and standard deviation of 42 mm and 76.95 mm respectively.

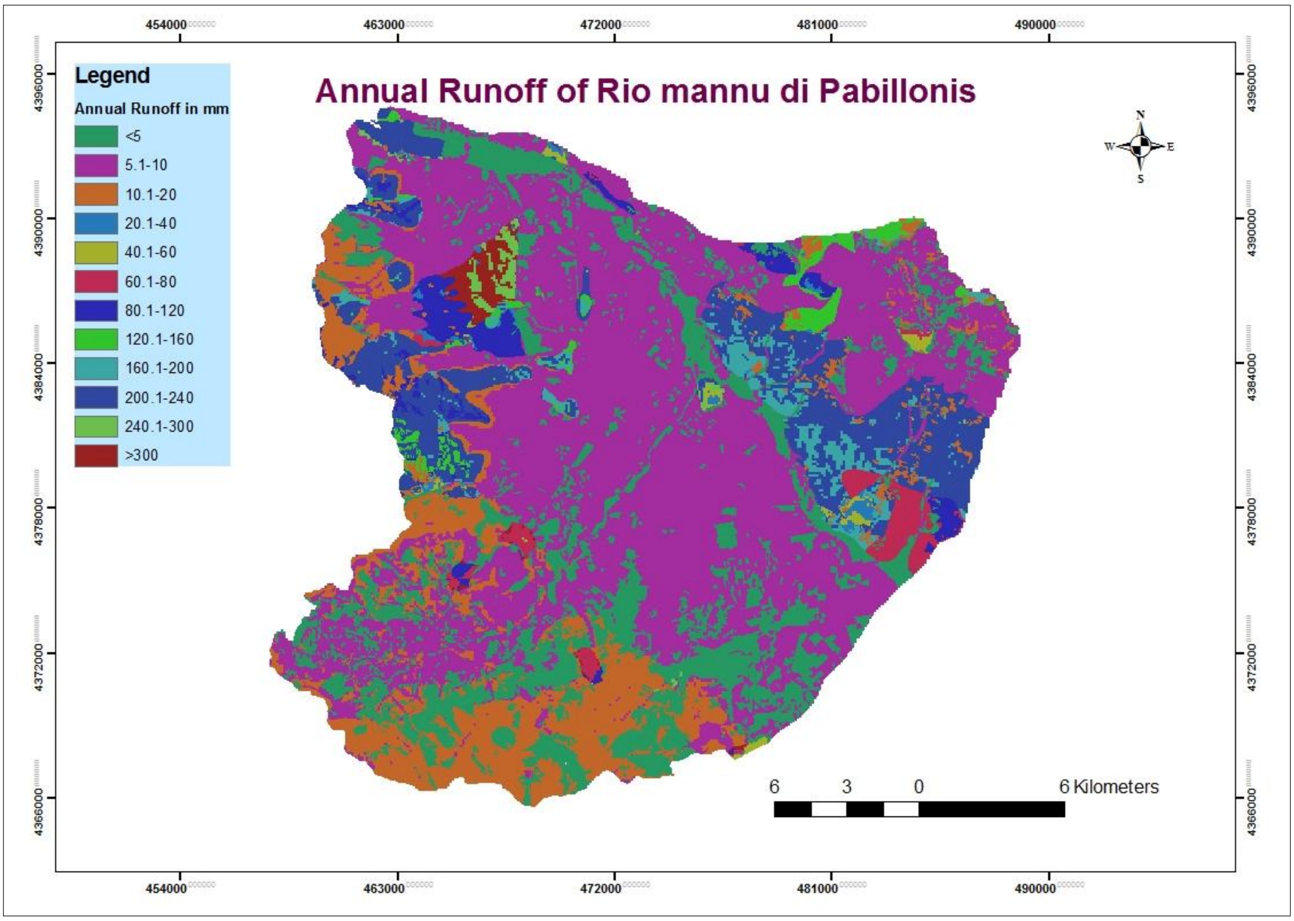

Figure 4.5 Runoff output of WetSpass model

a) Evapotranspiration

The simulated annual evapotranspiration of the Rio Mannu di Pabillonis basin is 145.4 mm and 1075mm as maximum and minimum values respectively, Figure 4.6. The mean and standard deviation of this distribution are 334 mm and 159.8 mm respectively. The average evapotranspiration is the largest portion of the mean annual rainfall accounting 54.4% of the precipitation. This shows that evapotranspiration is the main processes by which water is lost in the basin.

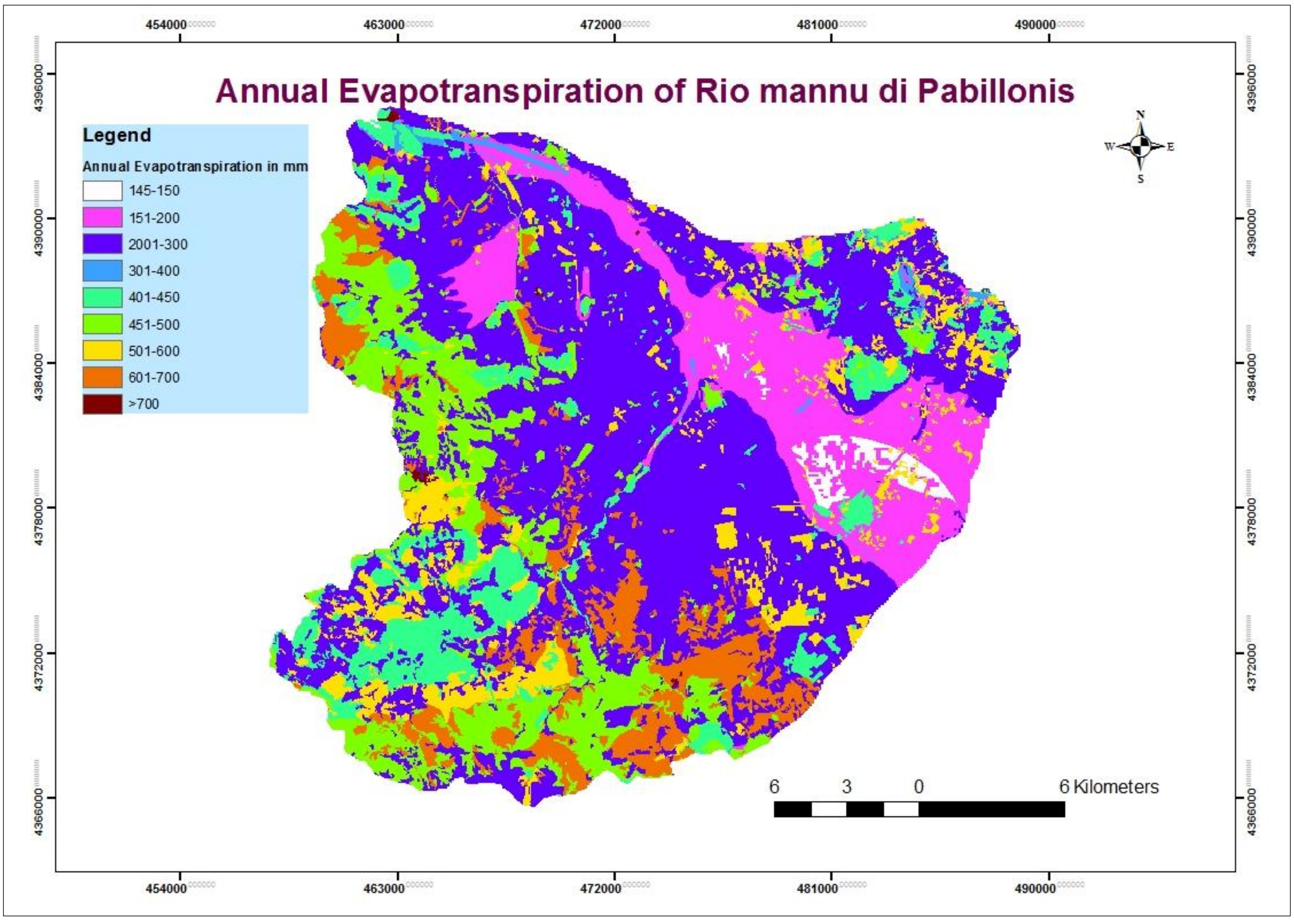

Figure 4.6 Evapotranspiration output map of WetSpass model

4.1.2.2. *WetSpass: Water balance results*

The overall summery of water balance components of the Rio Mannu di Pabillonis basin is given in Table 4-5. Only about 13% and 3.9% of the mean annual precipitation is effective in producing groundwater recharge and surface runoff respectively, while the rest and the major part is lost as evapotranspiration. The very small error implies that the WetSpass model simulation is reasonably acceptable.

Table 4-5 WetSpass water balance output

	Min.	Max.	Mean	Std.dev
Precipitation, P	544	754	614	
Evapotranspiration, ET	145.4	1075	334	159.8
Surface runoff, Ro	0	392.6	42	76.95
Groundwater recharge, Re	0	519	238	62.16

Table 4-6 meteorological data used in WetSpass

STATION	X	Y	Z	PPT Winter	PPT Summer	Temp Winter	Temp Summer	Wind Winter	Wind Summer	PET Winter	PET Summer
PABILLONIS	476079	4382539	40	407	138.9	12.6	21.6	0	0	310	689.8
SANGAVINO	482011	4377714	51	381	135.8	12.4	21	0	0	311	678.4
SARDARA	484586	4384910	138	417	153.3	12.9	21.4	3.03	3.06	280	769
GONNOSFANADIGA	470901	4371724	190	578	177.7	12.8	22	3.91	4.23	289	810
MONTEVECCHIO	464513	4378669	370	544	176.9	12.8	21.2	0	0	335	710.8
URAS	474377	4394692	20	430	137.2	12.8	21.2	0	0	309	661.3
Where PPT is Precipitation and PET is Potential Evapotranspiration											

Table 4-7 Winter land-use parameter table

NUMBER	LUSE TYPE	RUNOFF VEG	NUM VEG_RO	NUM IMP_RO	VEG AREA	BARE AREA	IMP AREA	OPENW AREA	ROOT DEPTH	LAI	MIN STOM	INTERC PER	VEG HEIGHT
12	Residential	grass	3.00	0.00	0.50	0.00	0.50	0.00	0.30	2.00	100.00	2.00	0.12
33	Bare land	bare soil	4.00	0.00	0.00	1.00	0.00	0.00	0.05	0.00	110.00	0.00	0.00
21	Agriculture	crop	1.00	0.00	0.80	0.20	0.00	0.00	0.40	4.00	120.00	2.00	0.60
31	Vegetation	forest	5.00	0.00	1.00	0.00	0.00	0.00	2.00	6.00	500.00	25.00	12.00
42	shrubs	grass	2.00	0.00	1.00	0.00	0.00	0.00	0.60	6.00	110.00	4.00	0.50
52	Water bodies	open water	0.00	0.00	0.00	0.00	0.00	1.00	0.05	0.00	110.00	0.00	0.00

Table 4-8 Summer land-use parameter table

NUMBER	LUSE TYPE	RUNOFF VEG	NUM VEG_RO	NUM IMP_RO	VEG AREA	BARE AREA	IMP AREA	OPENW AREA	ROOT DEPTH	LAI	MIN STOM	INTERC PER	VEG HEIGHT
12	Residential	grass	3.00	3.00	0.60	0.10	0.30	0.00	0.30	2.00	110.00	3.00	0.12
33	Bare land	bare soi	4.00	0.00	0.60	0.20	0.20	0.00	0.05	0.00	100.00	0.00	0.00
21	Agriculture	crop	1.00	0.00	0.90	0.10	0.00	0.00	0.35	0.00	180.00	0.00	0.60
31	Vegetation	forest	5.00	0.00	0.90	0.10	0.00	0.00	2.00	4.50	220.00	5.00	12.00
42	shrubs	grass	2.00	0.00	0.20	0.80	0.00	0.00	0.60	0.00	110.00	2.00	0.20
52	Water bodies	open wat	0.00	0.00	0.00	0.00	0.00	1.00	0.05	0.00	110.00	3.00	2.00

5. CHAPTER V: AQUIFER INTRINSIC VULNERABILITY TO POLLUTION

5.1.INTRODUCTION

The inherent vulnerability of an aquifer depends on various processes that occur within the hydrogeological system:-

- The movement of fluids (water or pollutants) through the unsaturated zone until it reaches the aquifer
- The underground dynamic flow in the saturated zone;
- The residual concentration of the pollutant in the saturated zone at the time of arrival with respect to the initial concentration (elimination or attenuation).

The process of attenuation depends on the type and concentration of the pollutant and also by the geological characteristics of the system during its movement through the unsaturated zone, because many interactions take place between soils and rocks, which make up the subsoil, and the pollutants. This can contribute to mitigate the effects of the latter. When a pollutant reaches the saturated zone further process of attenuation occurs due to dilution.

The valuation methods take into account the influence of the intrinsic vulnerability of these processes differently and use different systems for processing data base. For each type of evaluation adopted, the results are presented through cartographic processing of the cards or grids of vulnerability to pollution.

5.2.METHODOLOGY

Groundwater vulnerability represents the intrinsic geological and hydrogeological characteristics of the aquifer. Its concept has been widely used in assessing the likely impact of pollution pressures during the groundwater characterization process and in the regional groundwater protection strategy. The SINTACS scheme of aquifer pollution vulnerability mapping was established for hydrogeological, climatic and impacts settings, typical for the Mediterranean countries (Civita M., 1990).

The Rio Mannu di Pabillonis area was discretised with a regular mesh grid of 10×10 m. The weight strings have been prepared in order to satisfactorily describe the effective hydrogeological and impacting situation as set up by the sum of data. The SINTACS R5 presents five weight strings for normal impact, relevant impact, and drainage from the surface network, deep karstified terrain and fissured terrain. For each of the 9,098,910 grid squares, element normalized SINTACS index was calculated and different vulnerable areas were assessed using SINTACS R5 parametric methods (Civita, M., De Maio, M., SINTACS R5, 2000).

5.2.1. The SINTACS

The SINTACS stands for S= depth to groundwater table or piezometric surface, I= Effective Infiltration, N= pollutant attenuation capacity of the unsaturated zone, T= land cover, A= hydrologic characteristic of the aquifer, C= hydraulic conductivity of the aquifer and S=steepness of the slope of surface topography. Then the study area must be discretized, usually in square finite elements of a regular grid, and each grid cell should attain calculated values of these parameters.

5.2.1.1. *Depth to groundwater surface, parameter (S)*

This is defined as the *depth to* piezometric surface or static water level which is measured from ground surface. The influence of this factor to the vulnerability is due to the fact that the value determines the time required for a pollutant to traverse the unsaturated zone and the duration of self-cleaning action in that thickness. The maximum rate/weight in SINTACS is 10 for shallow depths, piezometric levels near the surface topography or aquifer outcrop areas, and tends asymptotically to the minimum value equal to 1 for values of depths greater than 60m. The depth is assessed on the basis of measurements made on water points in the area under consideration and data of 42 monitored boreholes were utilized in this respect (table 2.1). The values range between 0.6meters to 71m meters. These points were converted into a grid map by interpolating them in ArcGIS (Figure 5.2). Then allocation of the points to the parameter S was made by reclassifying the grid map on the bases of Figure 5.1.

* All ranges for rating the rock units for different SINTACS parameter values, indicated in tables 13,15,17,19 and 20, are adopted from Civita, 2000.

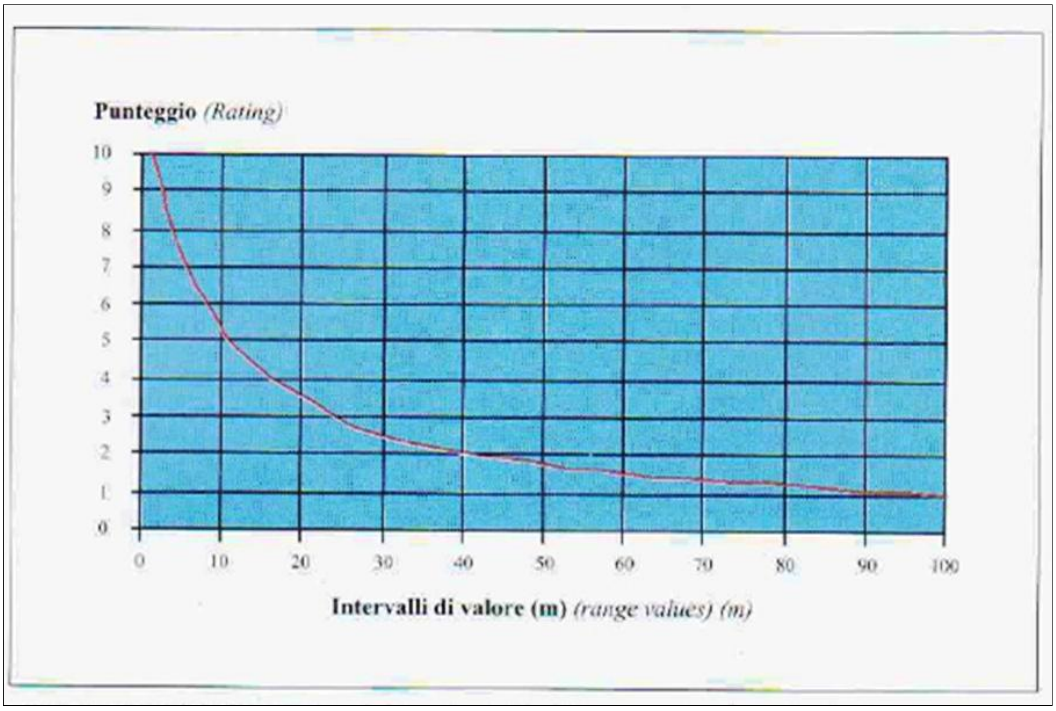

Figure 5.1Graph used for rating depth to groundwater, after Civita 2000

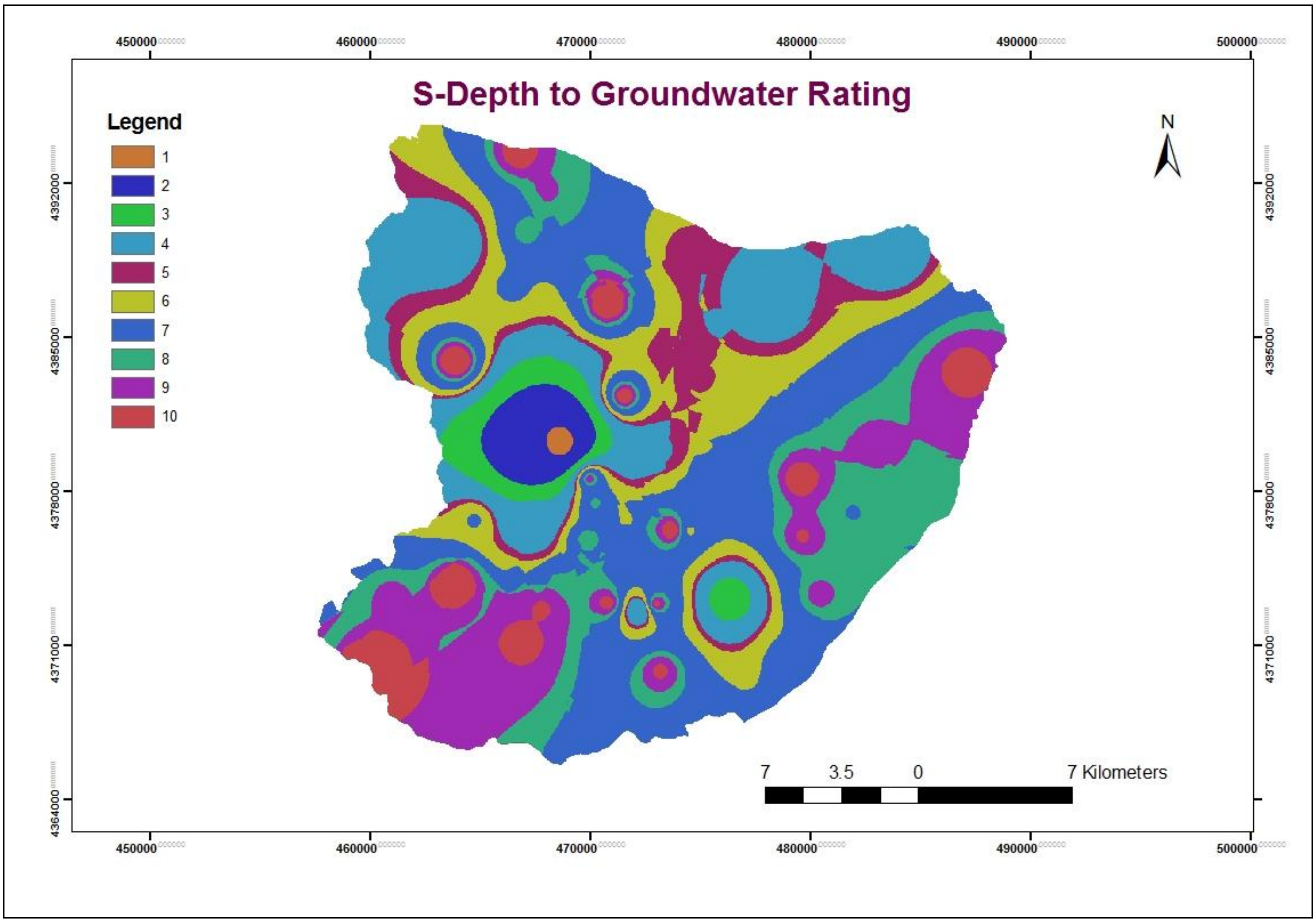

Figure 5.2 Depth to groundwater rated grid map

5.2.1.2. The Infiltration, parameter (I)

The calculation is based on the parameter values of effective rainfall and potential infiltration coefficient (χ). To determine and calculate the influence of each precipitation of every metrological station in the area, Thiessen polygon was made with ArcGIS fig.7. The rate of infiltration depends on the type of geological unit or on the type of soil encountered. Therefore, an overlay map of the geological map of the area and the Thiessen polygon made it possible to calculate the area influenced by each station. The potential infiltration coefficient was assigned for each unit from Table 5-1. Then the corrected annual temperature (T_c) was calculated using the following equation:

$$T_c = \frac{\sum_{i=1}^{12} P_i \cdot T_i}{P}$$

Where, P_i average monthly precipitation in mm, T_i average monthly temperature in ^{0}C and P is the annual precipitation in mm.

The specific precipitation ( ) was calculated in reference to the equations stated on page170-171 of Civita et al 2000. In the meantime, the evapotranspiration was estimated using the numerical model CALCO INFILTRAZIONE (Civita M., De Maio M., SINTACS R5, 2000) after (Turc, 1954).The effective infiltration in the period 1922-2007 ranged between 143.6 mm and 351.3 mm. Finally, the areal coverage of each lithologic unit (derived from Table 5-1) was multiplied by the specific precipitation of corresponding station times the coefficient of infiltration of each lithologic unit (Table 5-2) was interpolated and reclassified in ArcGIS to come up with the rated grid values (Figure 5.3).

Precipitation data of 1922 to 2007 were used for all stations (Gonnosfanadiga, Montevecchio, Pabillonis, Sangavino and Sardara) except for Uras (1922-1992).

Table 5-1 An index range for rocky outcrops or under low soil coverage

Complex hydrogeological	χ
Coarse alluvial deposit	0.65 to 1
Karstified limestone	0.75 to 1
Fractured limestone	0.5 to 0.85
Fissured dolomite	From 0.48 to 0.65
Medium-fine alluvial	0.15 to 0.48
Sand complex	0.75 to 0.88
Sandstones, conglomerates	0.3 to 0.5
Fissured plutonic rocks	0.05 to 0.35
Turbidic sequence	0.2 to 0.45
Fissured volcanic	0.75 to 1
Marl, shale	0.12 to 0.18
Coarse moraines	0.48 to 0.7
Medium-fine moraines	From 0.12 to 0.22
Clays, silts, peats	0 to 0.25
Pyroclastic rocks	0.2 to 0.65
Fissured Metamorphic rocks	0.2 to 0.28

Table 5-2 Assigned value of infiltration coefficient (χ) for each lithology

Lithology	Assigned χ
Alluvial deposits	0.8
Basalt	0.17
Basalt and Andesitic Basalt	0.1
Colluvial, Elluvial, Gravity and Slope deposits	0.7
Beach deposits	0.8
Granites	0.17
Hydro-thermal Veins	0.5
Lacustrine deposits	0.15
Laminated limestone	0.15
Meta-sediments	0.17
Meta-Volcanic	0.1
Schists	0.2
Sedimentary successions: Clay, Silt, Conglomerate	0.1

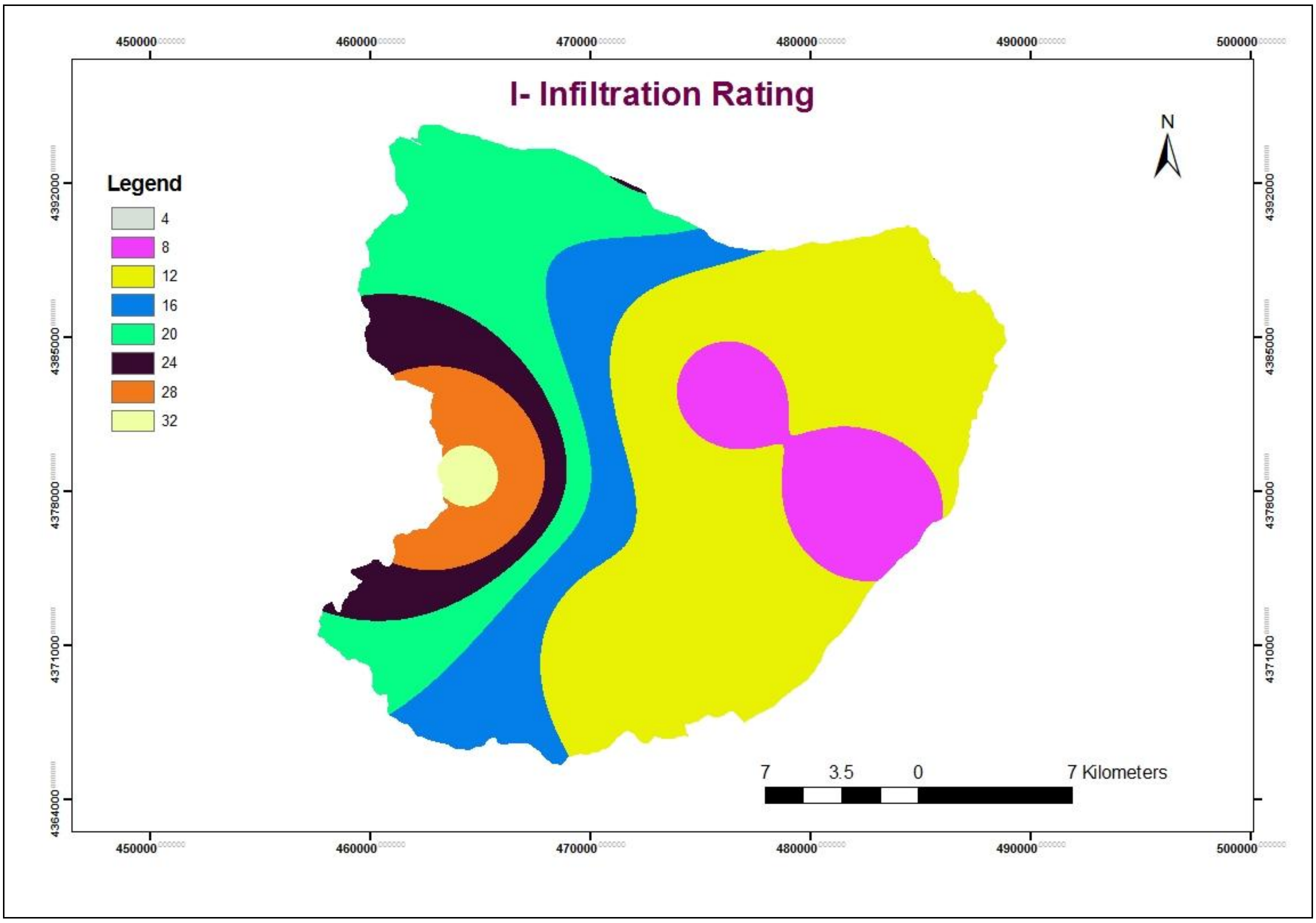

Figure 5.3 Infiltration rated grid map

5.2.1.3. Attenuation effect of the unsaturated zone, Parameter (N)

The unsaturated zone is the second defense line of the hydrogeological system against fluids or hydro vectored contaminants. Inside the unsaturated zone a four dimensional (including time) process takes place in which physical and chemical synergy work are involved in promoting the contaminant attenuation (Civita et al, 2000). The effect of self-purification of the unsaturated conditions is estimated from lithology, grain size, presence of clays and silts, to permeable rocks, fracturing and karstification in the case of hard rocks.

Rates are assigned to the discretized element based on lithology that coincides with the width and height unsaturated zone. If the thickness of the unsaturated consists of more than one lithologic type, it is necessary to calculate the rate as a weighted average in reference to the thickness of the individual lithologies.

The ranges of rating for the parameter N on the basis of lithology are shown below:

Table 5-3 Range of rating of attenuation effect for complex hydrogeological units

Complex hydrogeological	N
Coarse Alluvial deposit	6-9
karstified Limestone	8-10
Fractured Limestone	4-9
Fractured Dolomite	2-5
Medium-fine Alluvial deposit	3-6
Sand Complex	4-7
Sandstones, Conglomerates	5-8
Fissured Plutonic rocks	3-5
Turbidic sequence	2-5
Fissured Volcanic rocks	5-10
Marl, shale	1-2
Coarse moraines	4-6
Medium-fine Moraines	2-4
Clays, silts, peats	1-2
Pyroclastic Rocks	2-5
Fissured Metamorphic Rocks	2-6

Based on the The unsaturated zone is the second defense line of the hydrogeological system against fluids or hydro vectored contaminants. Inside the unsaturated zone a four dimensional (including time) process takes place in which physical and chemical synergy work are involved in promoting the contaminant attenuation (Civita et al, 2000). The effect of self-purification of the unsaturated conditions is estimated from lithology, grain size, presence of clays and silts, to permeable rocks, fracturing and karstification in the case of hard rocks.

Rates are assigned to the discretized element based on lithology that coincides with the width and height unsaturated zone. If the thickness of the unsaturated consists of more than one lithologic type, it is necessary to calculate the rate as a weighted average in reference to the thickness of the individual lithologies.

The ranges of rating for the parameter N on the basis of lithology are shown below:

Table 5-3 above, the rating for the lithological units of Rio Mannu di Pabillonis is given as Table 5-4 and was interpolated in Arc GIS as shown in Figure 5.4:

Table 5-4 Assigned rating values for each lithology

Lithology	N
Alluvial deposits	7
Basalt	3
Basalt and Andesitic Basalt	3
Colluvial, Elluvial, Gravity and Slope deposits	6

Beach deposits	8
Granites	2
Hydro-thermal Veins	5
Lacustrine deposits	2
Laminated limestone	2
Meta-sediments	2
Meta-Volcanic	3
Schists	1
Sedimentary successions: Clay, Silt, Conglomerate	2
Trachyte	3

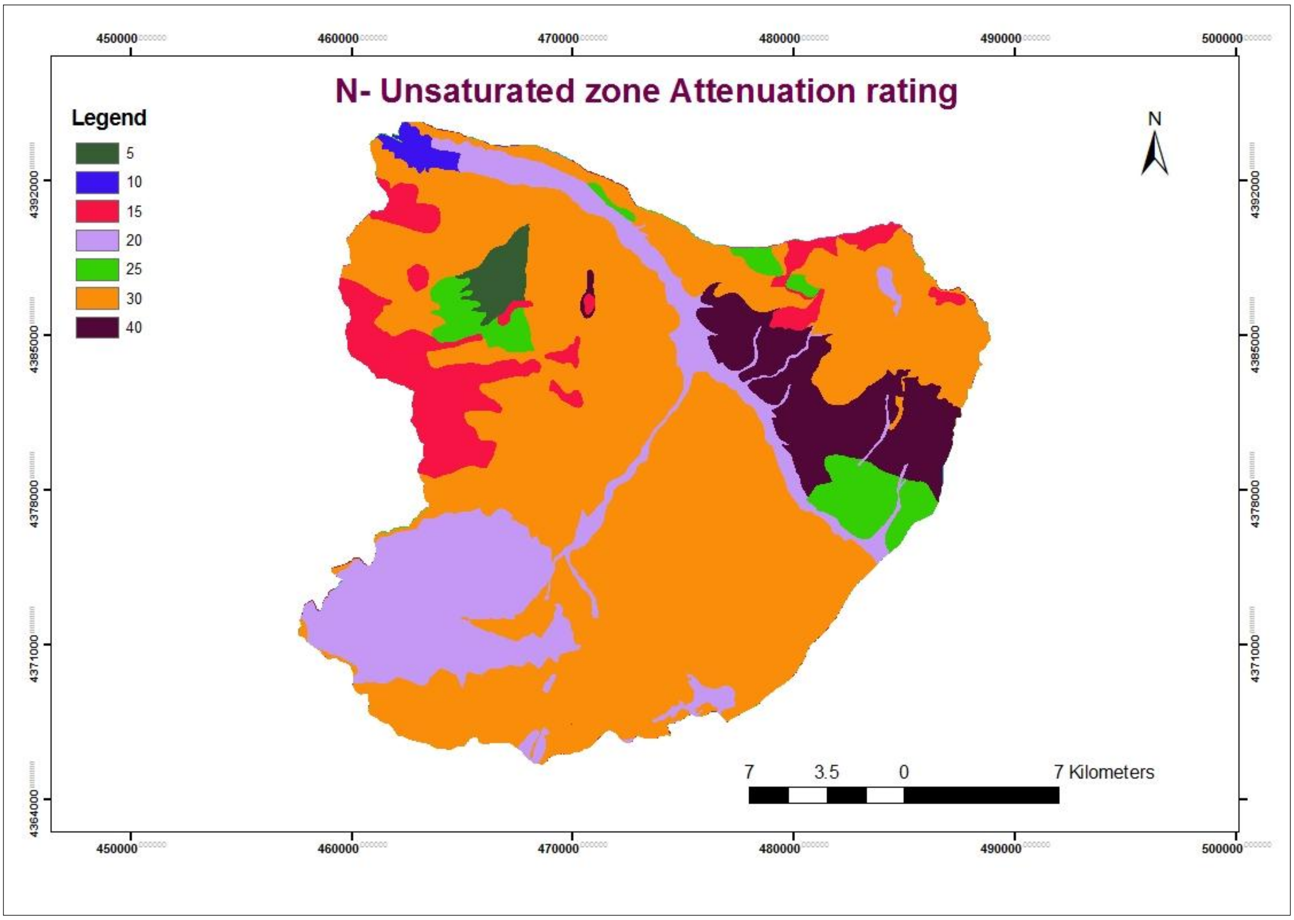

Figure 5.4 Attenuation effect of rated grid map

5.2.1.4. Soil\Overburden attenuation capacity, parameter T

The type of soil cover plays an utmost importance role in the assessment of vulnerability. Soils have a remarkable capacity to mitigate the impact of pollutants; it is the first line of defense of an aquifer system. The parameters that affect the mitigation potential of the soil can be divided into two groups: the first group consists of those parameters that characterize the processes of absorption, filtration, drainage capacity, moisture content, infiltration rate, and they are: grain size, texture, thinness, bulk density, total porosity, amount water available and hydraulic conductivity. The parameters of the second group instead affect the degree of adsorption of a chemical by the soil and are: The pH, the cation exchange capacity, organic matter content and clay content.

The following are the ranges of rates for the various textural classes of soil:

Table 5-5 Soil textural value ranges

Soils	T-Rating
Thin or absent	10
Clean gravel	9.5 to 10
Clean sand	8.9 to 9.5
Sandy	8 to 8.5
Peat	7.5 to 8.2
Sandy Clay	6.2 to 7
Sandy loam	5.5 to 6
Sandy clay loam	4.5 to 5.2
Loam	4-5
Silty-loam	3.5 to 4.2
Silty clay loam	3-4
Clay loam	2-3
Silty clay	1.4 to 2
Muck	1.2 to 2
Clay	1 to 1.3

Based on the The type of soil cover plays an utmost importance role in the assessment of vulnerability. Soils have a remarkable capacity to mitigate the impact of pollutants; it is the first line of defense of an aquifer system. The parameters that affect the mitigation potential of the soil can be divided into two groups: the first group consists of those parameters that characterize the processes of absorption, filtration, drainage capacity, moisture content, infiltration rate, and they are: grain size, texture, thinness, bulk density, total porosity, amount water available and hydraulic conductivity. The parameters of the second group instead affect the degree of adsorption of a chemical by the soil and are: The pH, the cation exchange capacity, organic matter content and clay content.

The following are the ranges of rates for the various textural classes of soil:

Table 5-5 above, the rating for the topographic cover of Rio Mannu di Pabillonis is given as Table 5-6 and was interpolated in Arc GIS as shown in Figure 5.5:

Table 5-6 Assigned textural value/rating

Topographic Cover	T
Cay loam	3
Clay	1
Loamy sand	4
Sandy clay	8
Sandy clay loam	5
Sandy loam	6
Silty clay	2

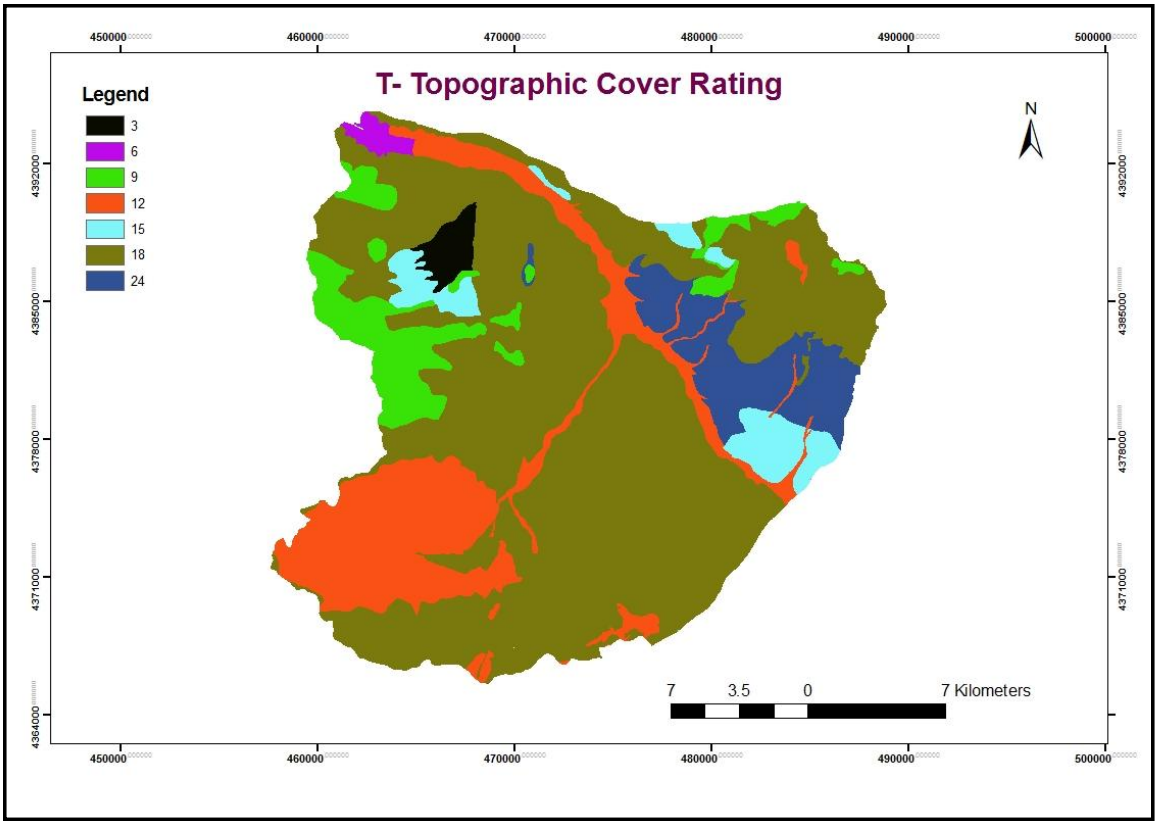

Figure 5.5 Topographic cover rated grid map

5.2.1.5. Hydrogeological characteristics of the aquifer, parameter A

In vulnerability assessment models the aquifer characteristics describe the process that take place below the piezometric level when a contaminant becomes mixed with groundwater after having lost a small or significant part of its original concentration while traveling through the soil and the unsaturated zone. The processes are dilution, dispersion, adsorption and chemical reactions. The parameter A depends on the characteristics of the aquifer in which these processes are carried out. The following are the ranges of rates for different hydrogeological complexes:

Table 5-7 Ranges of rates for different hydrogeological units

Complex hydrogeological	A-Rating

Coarse Alluvial deposit	8-9
karstified Limestone	9-10
Fractured Limestone	6-9
Fractured Dolomite	4-7
Medium-fine Alluvial deposit	6-8
Sand Complex	7-9
Sandstones, Conglomerates	4-9
Fissured Plutonic rocks	2-4
Turbidic sequence	5-8
Fissured Volcanic rocks	8-10
Marl, shale	1-3
Coarse moraines	6-8
Medium-fine Moraines	4-6
Clays, silts, peats	1-3
Pyroclastic Rocks	4-8
Fissured Metamorphic Rocks	2-5

Based on the In vulnerability assessment models the aquifer characteristics describe the process that take place below the piezometric level when a contaminant becomes mixed with groundwater after having lost a small or significant part of its original concentration while traveling through the soil and the unsaturated zone. The processes are dilution, dispersion, adsorption and chemical reactions. The parameter A depends on the characteristics of the aquifer in which these processes are carried out. The following are the ranges of rates for different hydrogeological complexes:

Table 5-7 above, the rating for the lithological units of Rio Mannu di Pabillonis is given as Table 5-8 and was interpolated in Arc GIS as shown in Figure 5.6:

Table 5-8 Assigned rates for each hydrogeological unit

Lithology	A
Alluvial deposits	8
Basalt	5
Basalt and Andesitic Basalt	5
Colluvial, Elluvial, Gravity and Slope deposits	8
Beach deposits	9
Granites	3
Hydro-thermal Veins	4
Lacustrine deposits	2
Laminated limestone	2
Meta-sediments	3
Meta-Volcanic	3
Schists	2
Sedimentary successions: Clay, Silt, Conglomerate	2
Trachyte	5

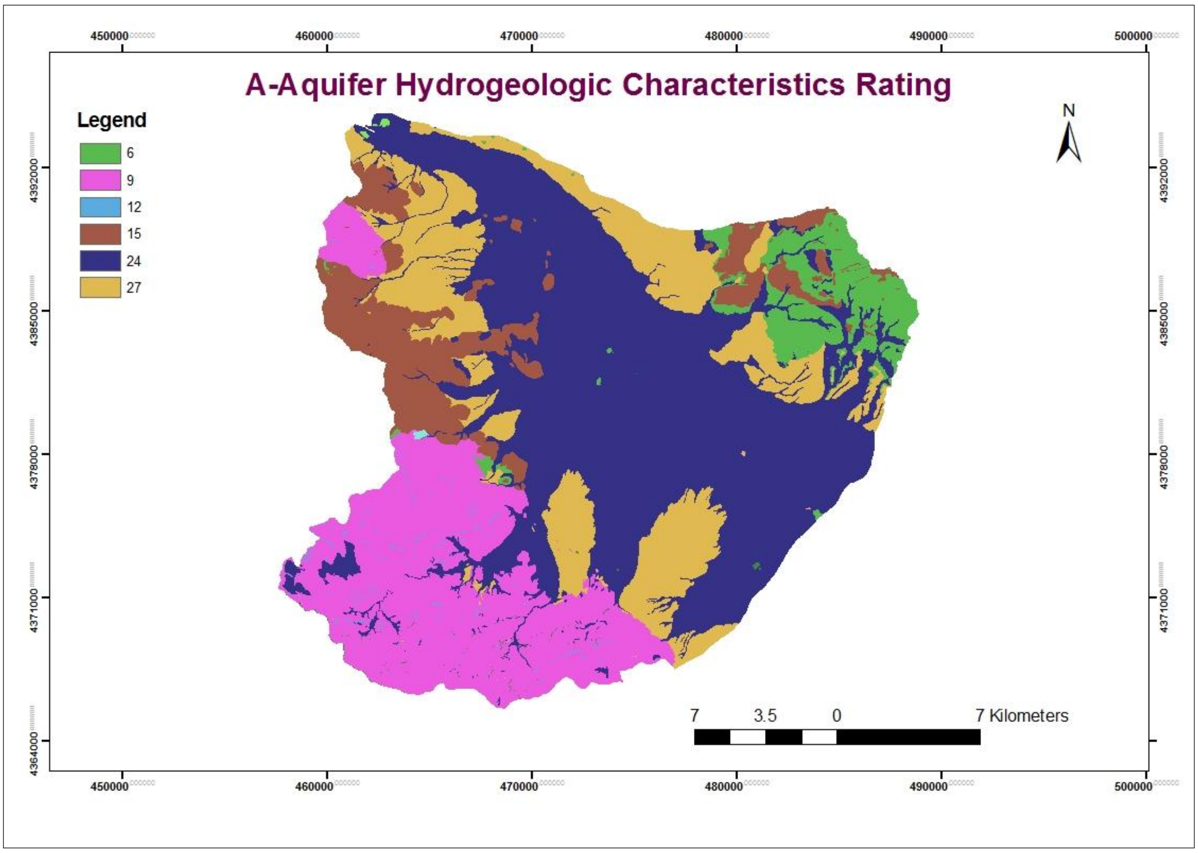

Figure 5.6 Rated aquifer grid map

5.2.1.6. Hydraulic conductivity of the aquifer, parameter (C)

The hydraulic conductivity indicates the ability of the groundwater to move in saturated zone, thus, the potential mobility for a pollutant that has a density and viscosity value close to that ground water. It is generally computed by pumping tests in which we determine the aquifer transmissivity T (m^2 / s) and given the value of H (thickness of the aquifer in m), we obtain the conductivity K = T / H (m / s).

If no data are available which distinguish reliably the hydraulic conductivity of aquifers, the model provides an estimation method SINTACS indirect, indicating the magnitude of hydraulic conductivity based on the complex hydrogeological that contains the aquifer. The rating for the parameter C is identified as follows:

Table 5-9 Ranges of hydraulic conductivity rating for different hydrogeological units

Complex hydrogeological	k(m / s)
Gravel	10^{-3} - 0
Sand	10^{-6} - 10^{-2}
Silty sand	10^{-7} -10^{-3}
Silt	10^{-10} -10^{-5}
Glacial deposit	10^{-12} -10^{-6}
Clay	$10^{-9\ -13}$ -10
Pyroclastic rocks	10^{-10} - 10^{-5}
Clay stone-Marl	$10^{-9\ -13}$ -10
Dolomite	10^{-9} -10^{-6}
Limestone and Marble	10^{-9} -10^{-2}
Sandstone	10^{-10} -10^{-6}
Volcanic rock	10^{-12} -10^{-2}
Crystalline rock	10^{-13} -10^{-4}

Based on the The hydraulic conductivity indicates the ability of the groundwater to move in saturated zone, thus, the potential mobility for a pollutant that has a density and viscosity value close to that ground water. It is generally computed by pumping tests in which we determine the aquifer transmissivity T (m 2 / s) and given the value of H (thickness of the aquifer in m), we obtain the conductivity K = T / H (m / s).

If no data are available which distinguish reliably the hydraulic conductivity of aquifers, the model provides an estimation method SINTACS indirect, indicating the magnitude of hydraulic conductivity based on the complex hydrogeological that contains the aquifer. The rating for the parameter C is identified as follows:

Table 5-9 above, the rating for the lithological units of Rio Mannu di Pabillonis is given as Table 5-10 and was interpolated in Arc GIS as shown in Figure 5.7:

Table 5-10 Assigned rates for each lithologic unit

Lithology	C
Alluvial deposits	6
Basalt	1
Basalt and Andesitic Basalt	1
Colluvial, Eluvial, Gravity and Slope deposits	6
Beach deposits	6
Granites	1
Hydro-thermal Veins	1
Lacustrine deposits	1
Laminated limestone	1
Meta-sediments	1
Meta-Volcanic	1
Schists	1
Sedimentary successions: Clay, Silt, Conglomerate	1
Trachyte	1

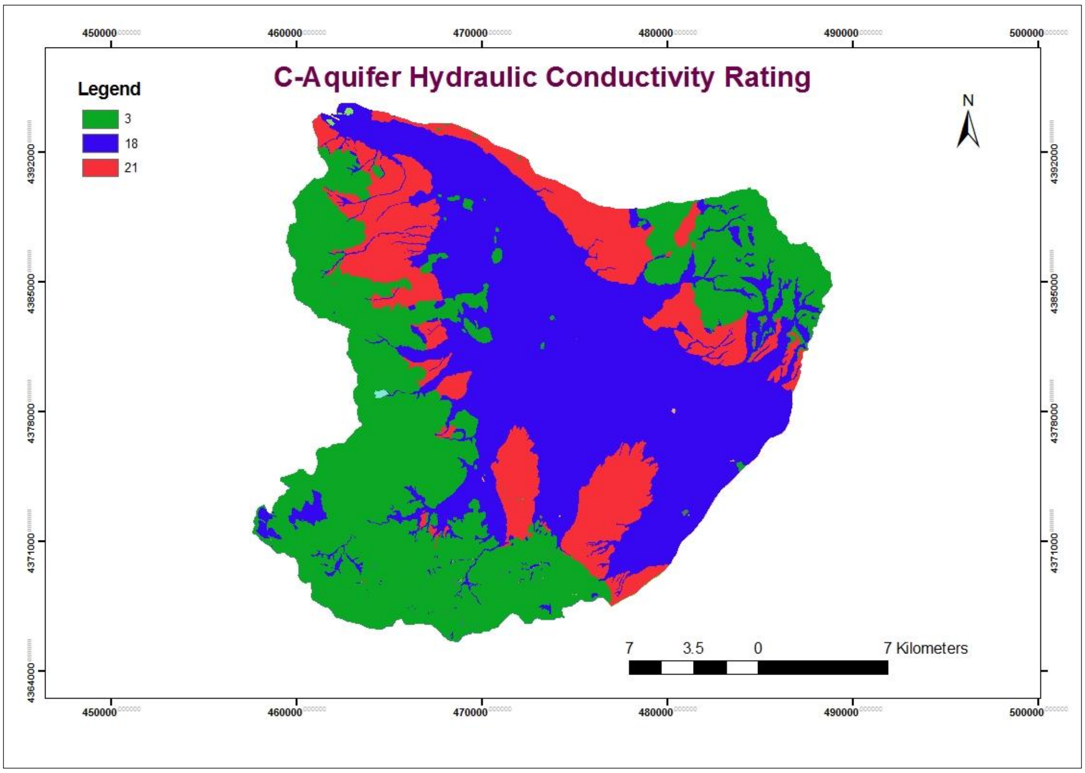

Figure 5.7 Hydraulic conductivity rated grid map

5.2.1.7. Steepness of the surface topography, parameter (S)

The topographic slope is an important factor in vulnerability assessment as it governs the amount of runoff, the precipitation rate and the displacement property of the water (fluid and hydro vectored contaminant) over an equal surface. High rates are given to areas where the slope is very low or flat area, and infiltration is favored by the limited ability of water (pollutants) to move on the surface, which may lead to stagnation. Areas with high topographic gradient are rated low due to the lack of these areas to absorb the fluids that are to be on the surface and are more easily carried by the force of gravity on the surface.

Allocation of points was determined by the classes of slope between 0 and 30%, obtainable through the construction of the steepness of classes derived from Digital Elevation model, and assigned the values according to Table 5-11. However in the present study, reclassification method in the ArcGIS special analyst tool was employed to achieve the results or classes stated below, Figure 5.8.

Table 5-11 Range of slope rating

Steepness of the surface topography	S-Rating
0-2	10
3-4	9
5-6	8
7-9	7
10-12	6
13-15	5
16-18	4
19-21	3
22-25	2
>26	1

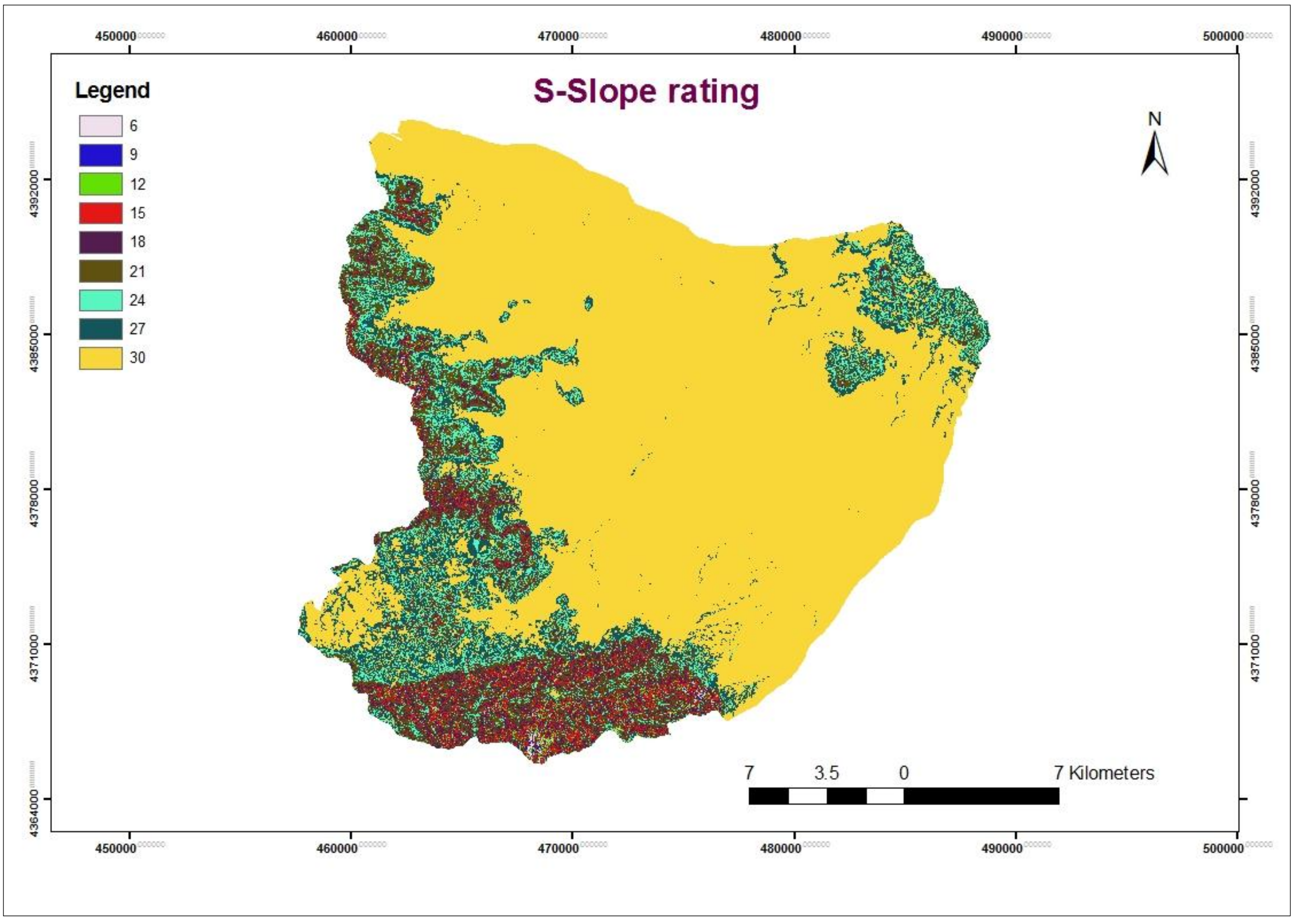

Figure 5.8 Rated slope

5.2.1.8. *Hydrogeological situations and impact*

Once determined the rates for each of the parameters predicted by the model SINTACS which are discretized for each cell, is necessary to identify strings of weight multipliers based on actual scenarios identified corresponding to particular situation. The possible strings of weights (W) will be as many scenarios as identified.

The values of these weights for each parameter are as follows (Table 5-12):

Table 5-12 String weights

Parameter	Normal Impact	Severe Impact	Seepage	Karst	Fissured
S	5	5	4	2	3
I	4	5	4	5	3
N	5	4	4	1	3
T	3	5	2	3	4
A	3	3	5	5	4
C	3	2	5	5	5
S	3	2	2	5	4

Areas subject to normal impact are those characterized by low topographic gradient, with predominantly unsaturated matrix permeability, are not subject to special situations of human impact or land-use content. Fall into this type areas in dry fallow or cultivated without the use of pesticides and fertilizers, in which the livestock breeding is also practiced with a limited number of animals. Hence the normal impact was selected in calculating the impact.

5.2.1.9. The vulnerability index

After evaluating the seven parameters of the method and assigned weights on strings, the index of the intrinsic vulnerability SINTACS is given in Table 5-13 and the final output map is, Figure 5.9:

Table 5-13 Vulnerability index

Degree of vulnerability '	Values
Very low (Bb)	**26-80**
Low (B)	**90-105**
Medium (M)	**110-140**
High (A)	**150-186**
Very High (E)	**190-210**
Extremely High (Ee)	**220-260**

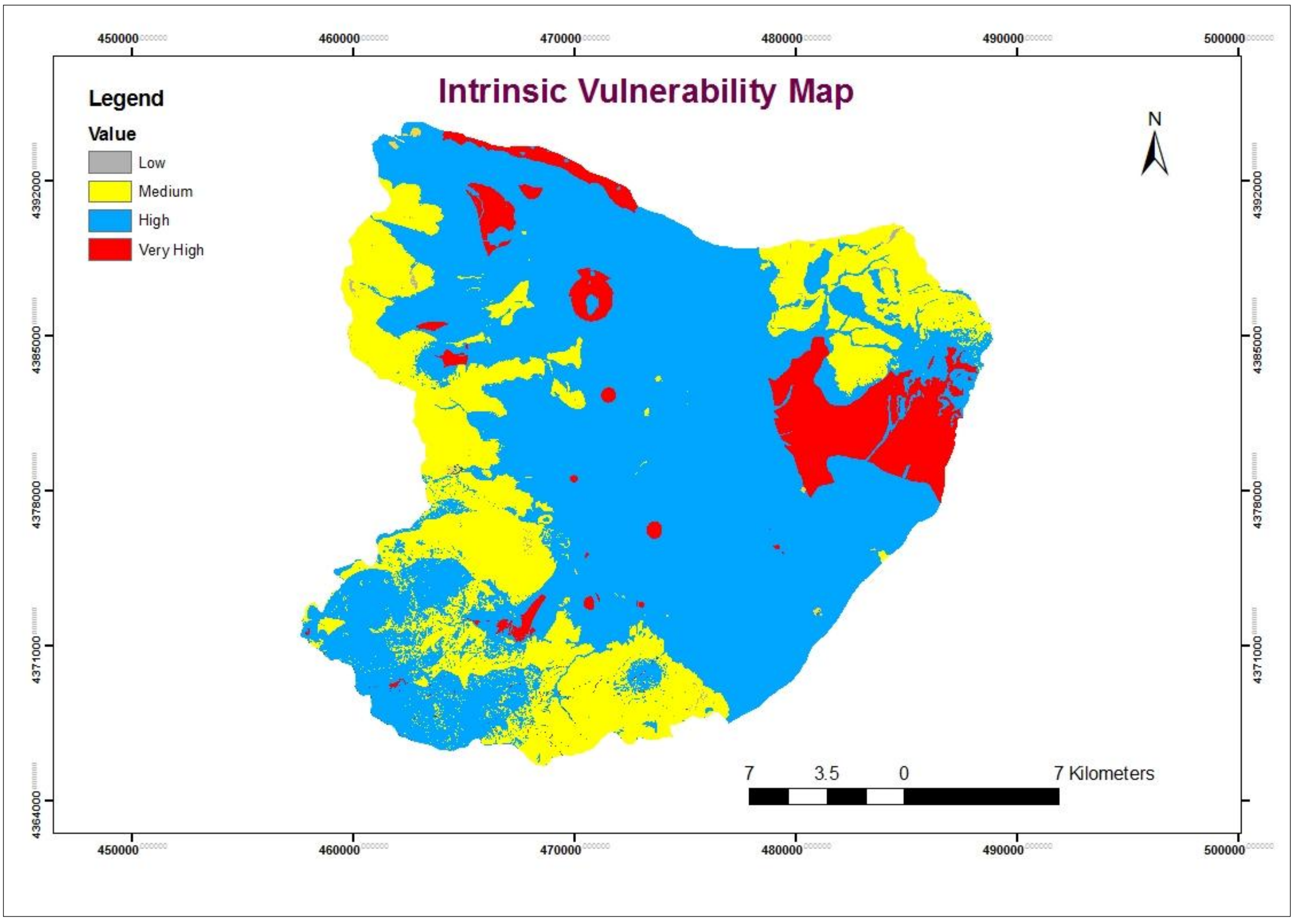

Figure 5.9 Intrinsic vulnerability map

6. CONCLUSIONS AND RECOMMENDATIONS

6.1. CONCLUSIONS

- Based on the measured data, an isopiezometric map was produced. This shows that the groundwater flow direction is to the centre of the basin and finally toward the north**,** following the topographic gradient.
- The weighted average rainfall in the basin is 614 mm per year. The amount of groundwater recharge was quantified using the following water balance calculation methods:
    - The Thornthwaite soil water balance method results indicated a total amount of 90 mm (14.7%) of water as recharge and 73mm (11.8%) as runoff per year. The highest amount, 451 mm/y (73.5%), is lost as evapotranspiration.
    - WetSpass model was applied to calculate the water balance components of the basin. The results pointed out that there is 238 mm of recharge (38.8% of the total precipitation), 42 mm of runoff (6.8% of the total precipitation) and 334 mm of evapotranspiration (54.4% of the total precipitation) annually.
    - SISS has carried out runoff evaluations or the period (1922-1992) at the outlet of the basin near San Nicola D'Arcidano. The surface area covered was 440 km^2 and the value of runoff obtained is 50.1 mm/year; if this data is interpolated to include the whole basin of Rio Mannu di Pabillonis, a value of 67.4 mm is obtained. This value is very close to the runoff value (73 mm/year) estimated from the average PPT using Thornthwaite method.
- The dominant groundwater type in the area is Na-Cl and Na-Cl-HCO_3 type**,** except in few samples located in the western highland**,** where the water type incorporates Ca and Mg with Na. Majority of the samples, 55%, have electrical conductivity values below 1000 µS/cm, while 20% of them have value above 3000 µS/cm and remaining fall between the two extremes.
- The water chemistry analysis results indicate the existence of elevated nitrate concentration, especially in areas where the dominant activities are livestock farming. However, majority of the water samples are within the limits of the WHO and the Italian standards.
- The intrinsic vulnerability output map, using SINTACS model, identified that the areas highly vulnerable to pollution are the alluvial deposits and associated sediments.

6.2.RECOMMENDATION

- The outputs obtained in this study, can be used as additional inputs to the monitoring efforts carried out by the Regional Government of Sardinia.

- Continuous monitoring of groundwater level in wells and groundwater sampling, for chemical analysis, is recommended to understand time bound change in groundwater heads and water chemistry.

- Groundwater abstraction from public and private boreholes should be reported and recorded in the monitoring data base periodically to quantify seasonal and annual variations.

SIMILARITIES AND DIFFERENCES OF THE TWO BASINS

The two basins, Raya Valley and Rio Mannu di Pabillonis, may be considered about similar from an hydrogeological point of view, because the alluvial sediment, which is the dominant hydrogeological formation, has about the same per cent area in both basins, Raya Valley, with 1302 km^2 of alluvial sediment on 2558 km^2 of total area (50.9 %), and Rio Mannu with 250 km^2 of alluvial sediment on 593 km^2 of total area (42.2 %).

The major activities in both areas are agriculture and livestock; hence the major risk of contamination could be attributed to these activities. However, in Rio Mannu di Pabilonis urbanization, mining and related industrialization could also contribute significantly.

The rainy season in Rio Mannu di Pabilonis is an extended (October to February) uni-modal rain while the rain in the Raya Valley is bimodal with short durations. The weighted average precipitation is 614 and 730 mm per year respectively.

The evapotranspiration is higher in the Raya Valley than in Pabillonis, this can be due the coexistence of high temperature and /or solar radiation and PPT. that is, at this time the AET is equal to the PET, while in Pabillonis basin the period of higher precipitation and the higher solar radiation differ significantly. The differences in meteorological and climatic conditions of the two basins, especially the higher monthly average temperatures of the lowlands of the Raya Valley (between 12.2 and 34.7 °C), compared to those of the lowlands of the Rio Mannu di Pabillonis Basin (between 9.5 and 26.7 °C), result in a higher Actual Evapotranspiration (AET) and consequently in a much lower Cumulative Available Water (CAW) in the Raya Valley than in the Rio Mannu di Pabillonis Basin. With reference to the Annual Average Precipitations (733.6 mm in the Raya Valley and 613.0 mm in the Rio Mannu Basin), the Actual Evapotranspiration (AET) accounts for 86.5% and 73.5% respectively . Though rainfalls in the Raya Valley are higher by 20% on average than the Rio Mannu Basin, the Raya Valley suffers from a much lower availability of cumulative water, CAW = 99.1 mm / year, as compared to CAW = 162.6 mm / year for the Rio Mannu Basin. The Cumulative Available Water value of the Raya Valley represents little more than half of that of the Rio Mannu Basin (13.5% vs. 26.5%) when expressed in terms of percentage.

Because of its particular morphological shape and sedimentary lithostratigraphy, the Raya Valley, has much less Surface Runoff (R) and consequently much higher Infiltration ~~(~~ I) than the corresponding values of the Rio Mannu Basin. The annual water balance estimation shows that the Surface Runoff, amounts to scarcely 4.3% of Average Annual Precipitation and 32.0% of the ~~C~~AW in the Raya Valley against corresponding values of 11.8% and 44.6% in the Rio Mannu Basin. Conversely, by considering the amount of CAW, there is much higher Infiltration (I) on percentage in the Raya Valley Basin as compared to the Rio Mannu Basin, with values equal to 68.0% and 55.4 % respectively. The Groundwater resource , as the main source of water supply in the Raya Valley, is also confirmed by the results of water balance with a value of Infiltration, I =67.4 mm / year, more than twice the Surface Runoff, R =31.7 mm / year. However, both in absolute and in percentage terms of total Average Annual Precipitation, the recharge is significantly lower in the Raya Valley as compared to the Rio Mannu Basin, with values of I = 67.4 mm / 9.2% and I = 90.0 mm / 14.7% respectively.

The Raya Valley is characterized by strong variation in the Annual Rainfall Indices (Precipitation of a given year divided by the Average Yearly Precipitation), in which the values range from a minimum of 0.72 in 2002 up to a maximum of 1.22 in 2000, with corresponding maximum reduction and increment of 28.2%

and 21.8% to the Weighted Yearly Average Precipitation (733.6 mm). Thus, higher variations are observed in the Raya Valley as compared to Rio Mannu Basin, especially with regard to the major components of the hydrogeological balance~~:~~ , such as Surface Runoff and Aquifer Recharge The Raya Valley Basin is much more sensitive than the Rio Mannu Basin particularly when precipitation decreases to below average values. Thus, taking into account the years 2003 for the Raya Valley Basin and 2006 for the Rio Mannu Basin, in which both have the same reduction of about 6%, from their respective Weighted Yearly Precipitation, it can be observed that the both Surface Runoff and Infiltration are reduced by 65% in the Raya Valley against a more modest 39.4% in Rio Mannu Basin, when compared with the corresponding average values. The strong decrease of the Cumulative Available Water (CAW) is essentially due to the elevated high value of Actual Evapotranspiration (AET), which remains constant and, indeed, presents also a feeble growth in the years of drought, which strongly affects the water balance by having higher percentage values, consequently restricting the proportion of Cumulative Available Water (CAW) to lower values.

This fact explains how recurrent severe droughts and acute shortage of water resources, both surface and groundwater, occurs in the Raya Valley Basin more than in the Rio Mannu Basin. It is apparent that the Raya Valley is highly affected by droughts even in years when rainfall is a bit smaller than the average, but still with considerable amount of rainfall (in absolute terms), as in 2002 (PPT = 526. 4 mm).

REFERENCES

Abdulghaffar S. Bazuhair, Warren W. Wood. (1995). Chloride mass-balance method for estimating ground water recharge in arid areas: examples from western Saudi Arabia. *Journal of Hydrology 186 (1996)* , 153-159.

Alebachew Beyene, Mohamed G. Abdelsalam. (2005). Tectonics of the Afar Depression: A review and synthesis. *Journal of African Earth Sciences 41 (2005) 41–59*, 41-59.

Asefa T, Wang Z, Batelaan O, De Smedt F. (1999). Open integration of a spatial water balance model and GIS to study the response of a catchment. *Nineteenth Annual American Geophysical Union Hydrology Days,*, (pp. 11-22). Fort Collins, Colorado,.

Awulachew S. B.; Merrey D. J.; Kamara A. B.; Van Koppen B.; Penning de Vries, F.; Boelee, E.; Makombe, G. (2005). *Experiences and opportunities for promoting small–scale/micro irrigation and rainwater harvesting for food security in Ethiopia. Colombo, Sri Lanka: IWMI. v. 86p. (Working paper 98).* Colombo, Sri Lanka:: IWMI.

Ayalew D., Ebinger C., Bourdon E., Wolfenden E., Yirgu G., & Grassineau N. (2006). Temporal compositional variation of early syn-rift rhyolites along the western Red Sea margin and northern Main Ethiopian rift, in The Afar Volcanic Province within the East African Rift System. *Geological Society of London, Special Pub. 259,*, pp. 121-130.

Ayele A., Jacques E., Kassim M., Kidane T., Omar A., Tait S.,Nercessian, A., de Chabalier, J. B. & King, G. (2007). The volcano-seismic crisis in Afar, Ethiopia, starting September 2005. *Earth and Planetary Science Letters 255*, 177-187.

Ayenew T., D. M. (2008). Hydrogeological framework and occurrence of groundwater in the Ethiopian aquifers. *Journal of African Earth Sciences.52*, 97-113.

B. Awulachew S.; D. Yilma A.; M. Loulseged; Loiskandl W. Ayana M.; T. Alamirew. (2007). *Water Resources and Irrigation Development in Ethiopia.* Colombo, Sri Lanka: International Water Management Institute. 78p. (Working Paper 123).

Baker J., Snee J., Menzies L. (1996). A brief Oligocene period of flood volcanism in Yemen: Implication for the duration and rate of continental flood basalt volcanism at the Afro-Arabian triple junction. *Earth and Planetary Science Letters 138*, 39-55.

Barca S. and Cherchi A. (2002). Introduction to the geology of Sardinia. *Rend. Soc. Paleont. Ital. 1*, 11-34.

Barca S. and Costamagna L.G. (1997). Compressive “Alpine” tectonics in Western Sardinia (Italy): geodynamic consequences. *C. R. Acad. Sci. Paris, 325*, 791-797.

Barca S., Cocozza T., Del Rio M., Pillola G.L. and Pittau Demelia, P. (1987). Datation de l’Ordovicien inférieur par Dictyonema fl abelliforme et Acritarches dans la partie supérieure de la formation “Cambrienne” de Cabitza (SW de la Sardaigne, Italie): conséquences géodynamiques. *C.R. Acad. Sci. Paris 305 (2),*, 1109-1113.

Batelaan O. and De Smedt F. (2001). “WetSpass: a flexible, GIS based, distributed recharge methodology for regional groundwater modelling”Gehrels, H., Peters, J., Hoehn, E., Jensen, K., Leibundgut, C., Griffioen, J., Webb, B. and Zaadnoordijk, W-J. (Eds.), Impact of Human Activity on Ground. *IAHS Publ. No. 269, 2001,*, pp. 11-17.

Batelaan O. and S.T. Woldeamlak. (2004). ArcView Interface for WetSpass, User Manual. Version 1-1-2003. *Vrije Univerisity, Brussel, Belgium.*

Batelaan O. and Woldeamlak S.T. (2003). *ArcView Interface for WetSpass, User Manual, Version 1-1-2003.* Vrije Universiteit Brussel, 50 pp. + app.: Department of Hydrology and Hydraulic Engineering.

Batelaan O., Wang Z. M. & de Smedt F. (1996). An adaptive GIS toolbox for hydrological modelling. In: Application of Geographic Information Systems in Hydrology and Water Resources Management. *IAHS Publ. no. 235.*, 3-9.

Belcher W.R., ed. (2004). *Death Valley regional ground-water flow system, Nevada andCalifornia - Hydrogeologic framework and transient ground-water flow model:.* p.408: U.S. Geological Survey Scientific Investigations Report 5205.

Blair T. C., and McPherson J. G. (2009). *Alluvial fan processes and forms. In: Geomorphology of Desert Environments (2nd Edn).* A. D. Abrahams and A. J. Parsons (eds.).

Blanford W.T. (1870). Report on .the Geology of a Portion of Abyssinia. *Assoc. J. Geol.Soc.London Q.Jl, v.25, (cited in the explanatory note of the geological map of Ethiopia)*, p.401-406.

Bosellini A., Russo A., Fantozzi P.L., Getaneh A., and Solomon T.,. (1977). The Mesozoic succession of the Mekelle Outlier (Tigre Province, Ethiopia). *Mem. Sci. Geol. 49,*, 95-116.

BRAJA M. DAS. (2006). *Principles of Geotechnical Engineering, FIFTH EDITION.* Ontario, Canada: Nelson, a division of Thomson Canada Limited.

Bridget R. Scanlon, ·. R. (2002). Choosing appropriate techniques for quantifying groundwater recharge. *Hydrogeology Journal10:*, 18–39.

Calvino F. (1972). *Note Illustrative della Carta Geologica d’Italia, Foglio 227 - Muravera.* Roma: Geol. d’It., 60 pp.

Carmignani L. and Pertusati P.C. (1977). *Analisi strutturale di un segmento della catena ercinica: il Gerrei (Sardegna sud-orientale).* 339-364.: Boll. Soc. Geol. It.96.

Cassinis G., Durand, M. and Ronchi, A. (2002). The Permian and Triassic continental framework of Nurra (NW Sardinia). *Rend. Soc. Paleont. Ital.1*, 297-305.

Central Statistical Agency, C. (2008). *Summary and statistical report of the 2007 population and housing census.* Addi Ababa.

Cherchi A. (1983). Presenza di Ilerdiano a Alveolinidae ed Orbitolitidae nel bacino paleogenico del Sulcis (Sardegna sud-ovest),. *Boll. Soc. Sarda Scienze Nat. 22,*, 107-119.

Cherchi A. (1985a). Introduction to the Geology of Sardinia. *In “Guidebook of the 19th European Micropalentological Colloquium” Sardinia Oct.*

Cherchi A., and Trémolières P. (1984). Nouvelles données sur l’évolution structurale au Mésozoique et au Cénozoique de la Sardaigne et leurs implications géodynamique dans le cadre méditerranéen. *C.R. Acad Sc. Paris 298 (20),*, 889-894.

Cherchi, A. and Montadert, L. (1982). The Oligo-Miocene rift of Sardinia and the early history of the western mediterranean basin. . *Nature 298*, 736-739.

Chorowicz J., Collet B., Bonavia F., Korme T. (1999). Left lateral strike-slip tectonics and gravity-induced individualization of wide continental blocks in the west Afar margin. *Eclogae Geologicae Helvetiae 92*, 149–158.

Civita M. (1990). La valutacione della vulnerabilita degli aquiferi all’inquinamento. *Proc. 1st Con.Naz. »Protezione E Gestione delle Acque Sotterranee: Metodologie, Technologie e Obiettivi sul Panaro*, 39-86.

Civita M., De Maio M., SINTACS R5. (2000). *A New Parametric System for the Assessment and Automatic Mapping of Groundwater Vulnerability to Contamination.* Bologna,: Pitagora Editrice.226 p.

Collins W. D. (1925). Temperature of water available for industrial use in the United States:. *U.S. Geological Survey Water-Supply Paper 520-F*, 97-104.

COMISIÓN DOCENTE CURSO INTERNACIONAL DI HIDROLOGÌA SUBTERRÁNEA. (2009). *HIDROGEOLOGIA.* Barcelona: FUNDACIÓN CENTRO INTERNACIONAL DI HIDROLOGÌA SUBTERRÁNEA.

Dainelli G. (1943). Geologia dell' Africa Orientale:4 vols. *Academia d'Italia, Centro Studi A. O. L,Roma.*

Dessie Nedaw. (2003). *Aquifer characterisation and hydrochemical investigation in the Raya Valley, Northern Ethiopia. PhD thesis.* Boku, Vienna.: University of Natural Resources and Applied Life Sciences, Department of Applied Geology,p248.

Desta, B. (1978). *Preliminary Regional geological Report on the Dodola Area (NB 37-7) 1:250.000 scale.* Addis Ababa, Ethiopia: Ethiopian Institute of Geological Surveys.

Dieni I., Fischer J.C., Massari F., Salard-Cheboldaeff M. and Vozenin-Serra C. (1983). La succession de Genna Selole (Baunei) dans le cadre de la paléogéographie mésojurassique de la Sardaigne orientale. *Mem. Soc. Geol. It. 36,*, 117-148.

Dieni I., Massari F. and Poignant A.F. (1979). Testimonianze di Paleocene marino in Sardegna. *Riv. It. Paleont. 85*, 481-516.

Dingman, S. (2002). *Physical Hydrology.* New Jersey: Prentice Hall: Upper Saddle River.

Dupuit. J. (1863). *Etudes théoriques et pratiques sur le mouvement des caus dans les canaux découverts et a travers les terrains permables. 2éme edition.* Paris: Dunot.

Federer C. A. (1979). A soil–plant–atmosphere model for transpiration and availability of soil water. *Wat. Resour. Res.1 5(3),*, 555–562.

Fondi R. (1980). Orme di microsauri nel Carbonifero superiore della Sardegna. *Mem. Soc. Geol. It. 20 (1979),*, 347-356.

Freeze R.A and Cherry, J.A. (1979). *Groundwater.* New Jersey: Prentice Hall.

Gemechu, D. (1977). *Aspects of climate and water budget in Ethiopia.* p.71: Addis Ababa University Press.

German Agency for Technical Cooperation LTD. (1977). *Kobo-Alamata Agricultural Development Program. Volume II: Annexes Pedology and Water Development.* ESSEN, GERMANY: German consults.

Gholam H. Karami, & Paul L. Younger. (2002). Analysing step-drawdown tests in heterogeneous aquifers. *Quarterly Journal of Engineering Geology and Hydrogeology, 35,*, pp. 295-303.

Giorgio Ghiglieri, Giulio Barbieri, Antonio Vernier. (2006). *STUDIO SULLA GESTIONE SOSTENIBILE DELLE RISORSE IDRICHE: DALL'ANALISI CONOSCITIVA ALLE STRATEGIE DI SALVAGUARDIA E TUTELA.* Roma: Ente per le Nuove Tecnologie L'Energia e l'Ambiente.

Harbaugh J.W., Banta E.R., Hill M.C., and McDonald M.G. (2000). MODFLOW-2000 The U.S. Geological Survey' s modular ground-water flow model—User guide to modularization concepts and the ground-water flow process. *U.S. Geological Survey Open-File Report 00–92*, p.121.

Hartley A., Mather A. E., Jolley E., and Turner P. (2005). Climatic controls on alluvial-fan activity, Coastal Cordillera, northern Chile. In: Alluvial fans: Geomorphology, sedimentology dynamics A. M. Harvey, A. E. Mather and M. Stokes (eds.). *Geological Society Special Publications 251, London*, pp. 95–115.

Isaak Gervshanovich. (2000). *Report on examination, verification and appraisal of hydrogeological feasibility study report by RVADP.* Mekele,Ethiopia: REST.

Kazmin V. (1972). *The geology of Ethiopia.* Addis Ababa: Ethiopian Institute of Geological Surveys. Note No. 821-051-12, 208 pp.

Kazmin V. (1975). *Explanatory Note to the Geology of Ethiopia.* Addis Ababa, Ethiopia: Ethiopian Institute of Geological Surveys.Bull. no. 2,.

Kazmin V., Alemu Shiferaw and Tilahun Balcha,. (1978). The Ethiopian Basement: Stratigraphy and Possible Manner of Evolution. *Geol. Rund.,67 (2),*, p. 531-546.

Kruseman G.P. and de Ridder N.A. (1994). *Analysis and Evaluation of Pumping Test Data.* Wageningen, The Netherlands: International Institute for Land Reclamation and Improvement,.

Leeder M. R., Harris T., and Kirkby M. J. (1998). Sediment supply and climate change: implications for basin stratigraphy. *Basin Research 10*, 7-18.

Leopold, Thomas Dunne and Luna B. (1998). *Water in Environmental Planning.* W.H. Freeman and Company.

Luigi Beccaluva, Gianluca Bianchini,Claudio Natali and Franca Siena. (2009). Continental Flood Basalts and Mantle Plumes: a Case Study of the Northern Ethiopian Plateau. *JOURNALOF PETROLOGY VOLUME 00 NUMBER 0 doi:10.1093/petrology/egp024*, 1-27.

M. Macdonald, and Partners. (1974-75). *Central Tigre Development Study Tigre Province Ethiopia. Working Paper 1: Soils and Land Classification.* Addis Ababa, Ethiopia: Hunting Technical Services Ltd. in association with Sir M. Macdonald and Partners.p56.

Malmstrom V.H.,. (1969). A new approach to the classification of climate. *Journal of Geography 68*, 351-357.

Me'ge D. & Korme T. (2004). Dyke swarm emplacement in the Ethiopian Large Igneous Province: not only a matter of stress. *Journal of Volcanology and Geothermal Research 132*, 283-310.

Mengesha T.,Tadiwos C. and Workineh H. (1996). *Explanation of the Geological Map of Ethiopia, Scale 1:2,000,000 second edition.* Addis Ababa: THE FEDERAL DEMOCRATIC REPUBLIC OF ETHIOPIA.

Merla G., Abbate E., Canuti P.,Sagri M. and Tacconi P. (1973). Geological Map of Ethiopian and Somalia1:2,000.000 Scale. *Consiglio Nazionale delle Ricerche, Italy*.

MoFED. (2006). *Ethiopia: Building on Progress, A Plan for Accelerated and Sustained Development to End Poverty (PASDEP) 2005/06-2009/10.* Addis Ababa, Ethiopia: Federal Democratic Republic of Ethiopia, Ministry of Finance and Economic Development.

Mohr P.A. (1962). *The Geologyof Ethiopia.* Addis Ababa, Ethiopia, p268: University. Coll. of Addis Ababa Press.

Mohr, P. (1983). The Ethiopian Flood Basalt Province. *Nature, v. 303*, p.577-584.

Monleau C. (1986). Le Jurassique inférieur et moyen de Provence, Sardaigne et Alpes maritimes: correlations, essai de synthèse paléogéographique. *Rev. Géol. dynam. Géol. phys. 27 (1)*, 3-11.

Morton W.H., Rex D.C., Mitchell J.G., Mohr P.,. (1979). Rift- ward younging of volcanic units in the Addis Ababa region,Ethiopian rift valley. *Nature 280*, 284-288.

MoWR. (2001). *ETHIOPIAN WATER SECTOR STRATEGY.* Addis Ababa: Federal democratic republic of Ethiopia, Ministry of Water Resources, 37 pp.

MoWR. (2001). *ETHIOPIAN WATER SECTOR STRATEGY.* Addis Ababa, Ethiopia: MINISTRY OF WATER RESOURCES.

MoWR. (2005). *Irrigation (Potential) in Ethiopia.* Addis Ababa: Irrigation and Drainage Development Studies Department, Federal Democratic Republic of Ethiopia, Ministry of Water Resources.

Parker F. L., and Krenkel P. A. (1969). *Thermal Polution Status of art.* Nashville, Tenn.: Vanderbilt University, Dep. of Environmental and Water Resources Eng. No.3 p.430.

Paul L. Younger. (2007). *GROUNDWATER in the Environment.* Oxford, UK: Blackwell Publishing.

Priestely C.H.B., and Taylor R.J. (1972). On the assessment of surface heat flux and evaporation using large-scale parameters. *Monthly Review 100*, 81-92.

R. Scanlon,Ian Jolly, Marios Sophocleous and Lu Zhang. (2007). Global impacts of conversions from natural to agricultural:Quantity versus quality. *WATER RESOURCES RESEARCH, VOL. 43, W03437, doi:10.1029/2006WR005486*, 18.

Raya Valley Agricultural Development Project . (1998). *Feasibility study report.Volume II, Water Resources. Annexes:Hydrology and Hydrogeology.* Mekele, Ethiopia: REST.

Raya Valley Development Study Project . (1997). *Phase I: Reconnaissance Report, Volume II Water Resources Engineering-Annexes Hydrology, Hydrogeology and Geology.* Mekelle, Ethiopia: REST (Relief Society of Tigray).

Roberts J. (1983). Forest transpiration: a conservative hydrological process? *J. Hydrol. 66*, 133.141.

Ronchi A. and Tintori A. (1997). First Amphibian fi nd in Early Permian from Sardinia (Italy). *Riv.Ital. Paleont. Strat. 103*, 29-38.

Rubin J. (1966). Theory of rainfall uptake by soils initially drier than their field capacity and its applications. *Wat. Resour.Res. 2(4),*, 739–749.

Sileshi, M. (2007). *Hydrogeology, Hydrogeochemistry and Isotope Hydrology of Raya and Kobo Valleys, Adjacent Plateau, Escarpment and Part of Afar Rift, Ethiopia: Hydrogeological Mapping, Recharge Evaluation and Water Quality Assessment.* Addia Ababa, Ethiopia: MINISTRY OF MINES AND ENERGY, GEOLOGICAL SURVEY OF ETHIOPIA.

Smedema L. K. & Rycroft D. W. (1988). Land Drainage. *Batsford, London, UK.*

Stille H. (1939). Bemerkungen betreffend die “Sardische” Faultung und den Ausdruck “Ophiolitisch”. *Z. Dt. Geol. Ges. 91,*, 771-773.

Tesfaye S., Harding D.J., Kusky T.M. (2003). Early continental breakup boundary and migration of the Afar triple junction, Ethiopia. *Geological Society of America Bulletin 115*, 1053–1067.

Tesfaye, K. (2003). *Field comparison of resource utilization and productivity of three grain legumes under water stress. Ph.D. thesis in Agrometeorology.* University of the Free State, South Africa.: Department of Soil, Crop and Climate Sciences. .

Theis C.V. (1935). The relation between the lowering of the piezometric surface and the rate and duration of discharge of a well using groundwater storage. *Transactions of the American Geophysical Union, 16*, 519-524.

Thiem G. (1906). *Hydrologische Methoden.* Leipzig 56 pp.: Gebhardt.

Thornthwaite and Mather. (1955). “The Water Balance,”. *Climatology VIII (1)*, Laboratory of Climatology, Centerton NJ.

Tirusew Asefa, Z. W. (August 16 – 20, 1999). OPEN INTEGRATION OF A SPATIAL WATER BALANCE MODEL AND GIS TO STUDY THE RESPONSE OF A CATCHMENT. *Proceedings of the Nineteenth Annual American Geophysical Union Hydrology Days*, (pp. 11-22). Fort Collins, Colorado, USA.

Todd, D. K. (2005). *Groundwater Hydrology.* John Wiley and Sons, Inc.

Turc, L. (1954). Le bilan d'eaux des sols: relation entre les precipitations l'evaporation et l'ecoulement. *Annales Agronomiques.; Vol. 5,*, 491-595.

UNESCO. (2004). *National Water Development Report for Ethiopia.* Addis Ababa: UNESCO, World Water Assessment Program .

Van der Beken, A. and Huybrechts, W. (1990). The water balance of Flamish Region: A rational water management via the knowledge of the water balance. *Water, 50,* , pp. 88-92.

Vandewiele G. L., Xu C.-Y. & Ni-Lar-Win. (1991). Methodology for constructing monthly water balance models on basin scale. *VUB-Hydrologie 20. Free University Brussels, Brussels, Belgium.*

Vandewiele G.L., Xu C-Y. and Ni-Lar-Win,. (1993). “Methodology forconstructing monthly water balance models on basin scale”. *VUB-Hydrologie,20, VUB, Brussel,.*, 57p.

Vukovic M., and Soro A. (1992). *Determination of Hydraulic Conductivity of Porous media from Grain-Size composition.* Littleton, Colorado: Water Resources Publications.

Walton W.C. (1962). Selected analytical methods for well and aquifer evaluation. *Illinois Water Survey Bull, No 49*, 81 pp.

Waterloo Hydrogeology. (2006). *Visual MODFLOW v. 4.2 User’ s Manual: For Professional Application in three-Dimensional Groundwater Flow and Contaminant Transport Modeling.* Waterloo Ontario. 632pp.

WHO. (2011). *Guidelines for Drinking-water Quality, Fourth Edition.* Malta: Gutenberg.

Zanettin B., Justin-Visentin, E.Nicoletti M., Piccirillo E.M. (1980). *Correlation among Ethiopian Volcanic formations with Special References to the Chronological and Stratigraphic Problems of the "Trap Series" in GeodynamicEvolution of the Afro-Arabian Rift System.* p.231-252.: Atti dei convegni Lincei,v. 47,.

APPENDIXES

A. Raya Valley

A-1: Precipitation records of different stations in the Raya Valley, in mm

					Maichew PPT							
	Jan	*Feb*	*Mar*	*Apr*	*May*	*Jun*	*Jul*	*Aug*	*Sep*	*Oct*	*Nov*	*Dec*
1993	51.2	35.1	75.9	135.2	125.5	3.0	57.7	125.6	33.7	44.9	0.0	**1.3**
1994	0.0	0.0	53.4	83.6	42.2	28.9	234.1	311.3	136.2	5.0	20.0	**4.3**
1995	0.0	59.7	26.6	122.7	72.8	21.2	211.6	195.6	55.1	15.7	0.0	**61.0**
1996	8.8	1.2	123.5	146.4	141.2	66.6	117.2	246.5	42.1	4.1	57.3	**10.4**
1997	15.8	0.0	51.7	59.3	38.4	58.9	166.5	64.2	63.8	206.1	80.8	**0.0**
1998	65.1	33.3	35.0	39.4	116.5	0.0	151.2	214.7	223.5	10.3	0.0	**0.0**
1999	45.4	0.0	10.8	21.9	15.9	12.7	176.7	252.5	77.8	110.3	0.4	**1.9**
2000	0.0	0.0	5.9	17.7	65.1	12.0	196.8	194.4	114.3	123.3	61.7	**74.9**
2001	0.0	2.0	92.9	9.2	34.5	26.6	252.2	283.2	83.7	25.9	0.0	**11.0**
2002	83.7	0.0	34.3	67.5	40.9	21.3	67.4	188.6	92.9	50.3	0.0	**33.5**
2003	24.4	38.2	92.8	193.6	13.1	13.7	106.8	316.0	31.5	4.7	2.3	**17.9**
2004	12.7	5.3	19.7	128.6	0.9	59.6	140.8	247.2	27.4	37.7	3.2	**0.0**
2005	6.4	2.6	51.2	61.4	98.0	18.1	119.9	219.2	22.7	21.5	29.0	**0.0**
2006	0.0	0.1	56.6	80.4	47.5	23.8	179.5	292.2	83.7	64.4	11.3	**116.6**
2007	33.0	41.4	9.6	55.5	5.9	48.1	297.9	212.8	48.1	9.7	3.8	**0.0**
2008	35.8	0.0	0.0	13.5	68.6	28.5	83.9	135.4	100.7	91.7	47.9	**0.0**
					Alamata PPT							
	Jan	*Feb*	*Mar*	*Apr*	*May*	*Jun*	*Jul*	*Aug*	*Sep*	*Oct*	*Nov*	*Dec*
1993	49.4	99.1	52.7	160.5	96.6	6.2	96.0	52.9	113.2	36.9	0.0	**5.7**
1994	0.0	0.0	143.1	57.7	14.4	0.0	150.2	282.9	77.8	0.0	20.6	**0.5**
1995	0.0	69.2	120.6	211.8	30.6	12.5	126.9	201.4	51.7	11.0	0.0	**97.4**
1996	132.9	0.0	69.2	123.4	115.0	19.0	76.5	250.0	36.3	8.0	58.2	**0.0**
1997	46.1	0.0	125.1	26.7	28.5	22.0	87.0	54.4	72.0	191.6	139.0	**0.0**
1998	179.0	23.4	25.5	35.2	10.0	0.0	348.0	271.9	63.5	17.6	0.0	**0.0**
1999	44.3	0.0	20.8	9.0	7.0	0.0	211.4	431.8	66.7	54.5	0.0	**0.0**
2000	0.0	0.0	10.0	43.5	74.0	6.0	246.2	448.1	68.4	14.8	83.3	**72.8**
2001	0.0	0.0	136.8	12.8	29.5	16.8	225.1	244.3	24.8	10.0	10.0	**2.5**
2002	72.4	0.0	18.0	112.3	8.0	3.5	72.6	213.5	46.1	3.5	0.0	**89.5**
2003	75.8	69.8	41.9	94.2	24.5	12.7	111.8	234.2	22.8	0.0	0.0	**66.9**
2004	32.9	16.3	39.6	168.1	13.5	49.5	116.5	243.0	41.1	8.2	21.0	**20.2**
2005	21.0	1.4	110.3	131.6	65.8	23.5	141.5	167.0	33.1	6.0	0.0	**0.0**
2006	0.0	0.0	215.5	176.1	4.5	0.0	123.2	192.0	54.0	2.4	0.0	**23.5**
2007	12.3	46.3	8.4	109.0	9.6	9.6	164.8	214.7	50.9	0.0	7.8	**0.0**
2008	21.9	2.9	0.0	6.6	21.1	11.0	84.2	211.6	60.8	53.1	55.0	**0.0**
					Korem PPT							
	Jan	*Feb*	*Mar*	*Apr*	*May*	*Jun*	*Jul*	*Aug*	*Sep*	*Oct*	*Nov*	*Dec*
1993	54.5	45.1	46.0	217.2	54.0	5.6	101.8	98.1	85.3	30.6	0.0	**23.9**
1994	0.0	0.0	33.3	25.5	29.3	6.3	203.7	329.4	86.3	0.0	34.5	**0.0**
1995	0.0	118.9	35.7	95.4	79.5	30.8	226.7	402.9	55.4	13.1	0.0	**80.4**
1996	35.9	0.6	98.1	241.8	165.3	67.9	136.6	281.4	63.1	4.4	72.7	**0.0**
1997	9.9	2.0	99.7	52.7	92.9	63.6	172.1	55.9	58.8	322.6	xx	**1.1**
1998	159.6	38.5	26.7	27.8	80.2	12.4	398.6	355.8	212.3	45.6	0.2	**0.0**
1999	65.8	0.0	2.8	49.8	12.8	32.1	234.9	350.1	112.2	44.5	2.2	**0.4**
2000	0.0	0.0	3.5	48.2	76.2	9.3	317.6	304.8	90.8	133.2	65.6	**93.8**
2001	1.9	3.2	130.1	22.1	36.1	50.9	282.8	380.1	62.4	13.2	8.7	**13.3**
2002	65.3	0.7	34.1	107.7	15.6	3.0	137.2	228.6	90.2	8.0	0.0	**92.6**

2003	13.0	24.0	74.2	74.8	23.7	20.1	168.0	377.1	77.5	1.8	3.9	30.1
2004	13.9	6.0	40.9	56.0	1.9	54.0	143.6	249.1	65.5	4.1	25.7	9.9
2005	8.3	0.0	34.5	223.4	163.4	28.1	253.0	297.6	39.7	36.5	48.1	0.0
2006	0.0	1.0	182.2	96.2	44.6	6.9	149.0	307.4	51.7	60.1	10.2	172.2
2007	58.1	21.0	68.8	152.6	13.2	76.6	313.4	388.5	32.6	29.4	27.5	0.0
2008	64.2	0.0	0.0	16.6	70.4	42.6	187.1	143.3	103.4	29.5	137.0	0.0
2009	2.2	0	44.2	49.3	4.7	6.5	330.6	176.2	32.2	66.9	38.6	55.1

Kobo PPT

	Jan	Feb	Mar	Apr	May	Jun	Jul	Aug	Sep	Oct	Nov	Dec
1996	79	0	31	75	133	53	147	205	67	18	64	0
1997	0	0	43	58	48	52	111	94	37	169	49	0
1998	54	32	24	39	12	4	326	312	51	6	0	0
1999	316	226	2	12	48	34	0	20	107	25	0	0
2000	1	0	2	76	42	5	227	268	49	88	24	83
2001	0	0	71	19	16	2	231	220	98	8	4	2
2002	5	0	0	0	13	3	100	296	117	16	0	67
2003	41	33	35	66	33	11	138	248	42	0	0	43
2004	30	0	28	88	3	26	116	162	9	74	36	10
2005	0	8	17	134	88	7	148	169	21	1	0	0

Waja PPT

Year	Jan	Feb	Mar	Apr	May	Jun	Jul	Aug	Sep	Oct	Nov	Dec
1996	20.0	0.0	83.0	121.0	166.0	26.0	94.0	195.0	54.0	15.0	48.0	5.0
1997	10.0	0.0	90.0	20.0	27.0	4.0	60.0	55.0	7.0	230.0	79.0	0.0
1998	76.0	31.0	47.0	27.0	38.0	0.0	311.0	345.0	92.0	8.0	0.0	0.0
1999	41.0	0.0	71.0	36.0	4.0	40.0	92.0	324.0	47.0	0.0	1.0	43.0
2000	74.0	0.0	0.0	56.0	19.0	7.0	154.0	259.0	7.0	37.0	30.0	8.0
2001	0.0	0.0	60.0	20.0	26.0	23.0	150.0	197.0	37.0	10.0	0.0	0.0
2002	62.0	0.0	22.0	64.0	0.0	7.0	65.0	158.0	55.0	0.0	0.0	82.0
2003	0.0	61.0	42.0	93.0	0.0	8.0	113.0	329.0	51.0	0.0	1.0	43.0
2004	32.0	44.0	31.0	88.0	6.0	22.0	50.0	113.0	25.0	4.0	43.0	8.0
2005	0.0	8.0	17.0	134.0	88.0	7.0	148.0	169.0	21.0	1.0	0.0	0.0
2006	0.0	0.0	74.3	131.4	27.9	23.1	181.7	181.7	73.5	31.8	7.9	9.2
2007	21.2	17.5	26.8	95.7	0.0	8.4	276.5	276.5	56.0	6.9	4.4	0.0
2008	12.9	0.0	0.0	3.5	35.2	7.2	164.4	164.4	99.7	6.8	58.5	0.0

Mehoni PPT

	Jan	Feb	Mar	Apr	May	Jun	Jul	Aug	Sep	Oct	Nov	Dec
1992	2	3	83	8	52	27	3	6	6	65	92	10
1993	0	8	14	251	54	83	9	88	2	1	0	0
1994	0	0	25	49	28	0	11	116	25	3	3	6
1995	0	39	59	217	61	14	71	58	39	0	0	0
1996	13	0	8	152	45	12	0	90	27	1	87	0
1997	162	0	44	9	28	64	189	99	0	66	56	0
1998	1	17	20	15	33	1	7	229	25	0	0	6
1999	32	0	107	3	36	1	36	237	22	22	0	0
2000	0	0	29	32	30	16	271	283	4	0	176	23
2001	30	0	27	1	4	65	152	126	27	0	25	1
2002	1	0	16	41	8	1	12	150	14			2
2003	48	36	35	51	15	0	22	150	100	0	0	0
2004	18	1	91	188	0	33	0	139	92	95	3	5
2005	34.7	17.6	83.7	128	64	20	88.6	102	10.5	0	18.5	7
2006	0	0	211.6	131.2	5.3	32.8	62	282.2	7	6.5	98.7	0
2007	25.7	60.4	38	91.3	43	71	190.3	145.2	6	0	0	0

					Chercher PPT							
	Jan	Feb	Mar	Apr	May	Jun	Jul	Aug	Sep	Oct	Nov	Dec
1996	143.0	14.0	48.0	25.0	93.0	370.0	91.0	116.0	46.0	7.0	67.0	**0.0**
1997	6.0	0.0	111.0	67.0	32.0	5.0	112.0	50.0	23.0	198.0	79.0	**0.0**
1998	21.0	55.0	4.0	37.0	62.0	265.0	91.0	207.0	53.0	3.0	0.0	**1.0**
1999	22.0	180.0	0.0	63.0	42.0	1.0	105.0	511.0	74.0	13.0	0.0	**1.0**
2000	1.0	10.0	7.0	96.0	96.0	0.0	116.0	329.0	57.0	71.0	36.0	**2.0**
2001	0.0	6.0	40.0	26.0	26.0	2.0	114.0	315.0	112.0	4.0	8.0	**1.0**
2002	11.0	1.0	14.0	20.0	20.0	0.0	114.0	98.0	63.0	25.0	0.0	**8.0**
2003	45.0	1.0	21.0	46.0	46.0	100.0	128.0	199.0	42.0	0.0	0.0	**2.0**
2004	50.0	1.0	44.0	28.0	28.0	60.0	100.0	95.0	24.0	18.0	17.0	**2.0**
2006	xx	xx	xx	xx	xx	xx	57.1	177.1	46.3	22.2	7.8	**23.2**
2007	8.4	23.3	2.0	56.7	0.0	21.3	168.3	229.1	51.1	7.7	3.4	**0.0**
2008	**1.4**	**0.0**	**0.0**	**31.9**	**33.7**	**21.7**	**107.8**	**80.0**	**82.6**	**42.1**	**104.7**	**0.0**

A-2: Average Sun shine hours, relative humidity and wind speed in the Raya Valley

	Average Sunshine Hours											
	Jan	Feb	Mar	Apr	May	Jun	Jul	Aug	Sep	Oct	Nov	Dec
Maichew	7.0	8.0	8.2	7.9	8.9	6.8	5.0	5.2	6.2	7.4	8.1	7.5
Chercher	8.5	8.9	9.6	9.1	8.8	6.2	5.4	6.5	6.2	8.9	8.7	8.8
Kobo	8.0	7.7	8.5	8.3	8.6	6.8	5.6	6.2	6.7	8.5	9.2	8.5
				Average Relative Humidity in %								
	Jan	Feb	Mar	Apr	May	Jun	Jul	Aug	Sep	Oct	Nov	Dec
Maichew	64	53	54	54	44	42	61	65	58	55	56	59
Chercher	68	58	42	45	38	33	51	57	55	50	55	59
Kobo	60	56	52	56	44	34	46	59	62	52	45	53
				Average Wind Speed in kilometers/day								
	Jan	Feb	Mar	Apr	May	Jun	Jul	Aug	Sep	Oct	Nov	Dec
Maichew	93	104	110	111	118	193	282	204	109	96	110	94
Chercher	200	220	238	235	198	211	244	198	146	162	186	195
Kobo	164	178	182	167	148	170	170	140	111	132	149	162

A-3: Record of solar radiation and sensible heat, after Macdonald (1975)			
Months	Solar radiation including Albedo allowance mm/day	Back radiation from the earth mm/day	Dynamic diffusion process (mm/day)
O	6.563	1.968	0.752
	6.816	2.287	1.318
	6.571	2.373	1.381
N	6.419	2.47	1.635
	5.941	2.378	1.42
	5.719	2.421	1.634
D	5.533	2.225	1.28
	5.526	2.246	1.468
	5.517	2.257	1.432
J	5.573	2.488	1.82
	5.695	2.317	1.581
	5.123	1.734	1.492
F	4.973	1.517	1.246
	6.011	1.914	1.343
	6.84	2.542	2.141
M	7.179	2.409	1.858
	7.363	2.198	1.314
	6.152	1.669	1.911
A	7.62	2.257	1.427
	7.596	2.377	1.758
	6.769	1.965	1.945
M	7.929	2.774	2.979
	7.341	2.265	1.605
	6.539	1.855	1.547
J	5.475	1.201	0.819
	5.95	1.486	1.085
	5.063	1.088	0.569
J	5.063	0.995	0.575
	5.07	0.987	0.444
	4.981	0.976	0.334
A	3.781	0.542	0.137
	5.002	1.006	0.239
	4.726	0.879	0.214
S	4.988	0.984	0.178
	5.229	1.196	0.357
	6.1	1.606	0.639

A-4: Analysis results of water sample, after WWDSE 2008

Sample index	Site name	X	Y	Z	TDS	COND	Ph	NH3	Na	K	Ca	Mg	Fe	F	Cl	No3	HCo3	So4	Po4	Water Type
RPW-002-08	Laelay wargeba	574080	1410165	1661	410	613	7.4	0.3	31.0	1.0	106.4	11.0	0.0	0.4	30.8	40.3	343.3	10.3	0.2	Ca-HCO3
RPW-004-08	Mohoni	587866	1399382	1607	370	529	9.6	1.3	114.0	2.5	6.1	0.9	1.0	0.7	34.2	9.6	78.1	108.1	1.1	Na-SO4-HCO3-CO3
RPW-005-08	Aid Mohoni	577889	1409202	1607	360	606	7.4	0.8	32.0	1.2	92.7	8.3	0.0	0.2	15.2	13.5	361.6	5.9	0.8	Ca-Na-HCO3
RPW-012-08	Adi Tela	581052	1404035	1549	274	464	7.6	0.9	44.0	2.1	38.0	13.8	0.0	0.5	15.2	18.6	255.0	8.1	0.9	Na-Ca-Mg-HCO3
RPW-013-08	Kushere	572677	1403437	1613	374	570	8.1	0.2	87.0	10.0	41.2	4.1	0.0	6.5	37.1	3.1	269.0	45.9	0.1	Na-Ca-HCO3
RPW-014-08	Adi Tela	582104	1403603	1529	286	438	7.8	0.9	43.0	1.9	15.2	27.6	0.0	0.4	15.2	12.9	243.4	9.0	0.9	Mg-Na-HCO3
RPW-017-08	Sulula,Mohoni	571732	1375106	1406	396	558	7.8	0.3	75.0	2.7	55.0	9.8	0.1	0.7	13.3	2.8	283.0	86.4	0.2	Na-Ca-HCO
RPW-018-08	Fachagama	579972	1401424	1534	270	414	7.8	0.2	55.0	2.3	39.5	8.3	0.0	0.4	13.9	26.9	230.6	6.8	0.1	Na-Ca-HCO3
RPW-019-08	Adi Tela	581768	1400964	1520	280	449	7.8	0.9	42.0	2.7	39.5	18.9	0.0	0.4	13.3	10.0	261.9	4.5	0.9	Ca-Na-Mg-HCO3
RPW-020-08	Mohoni	577596	1400661	1548	330	508	7.7	0.3	51.0	2.4	38.0	17.5	0.0	0.3	15.2	13.5	289.8	2.9	0.8	Na-Ca-Mg-HCO3
RPW-021-08	Gotu, Alamata	571906	1363793	1404	638	929	7.6	0.5	71.0	2.8	116.0	32.9	0.0	0.6	62.7	31.6	380.6	118.8	0.2	Ca-Na-Mg-HCO3-SO
RPW-022-08	Mohoni	576837	1374986	1489	318	493	7.7	0.1	30.0	1.0	60.8	12.9	0.0	0.2	10.4	14.2	301.3	5.8	0.3	Ca-Na-HCO3
RPW-023-08	Genda ago	568247	1400186	1661	384	594	7.4	0.2	34.0	0.6	73.1	10.2	0.0	0.3	9.3	18.5	358.7	4.6	0.2	Ca-Na-HCO3
RPW-024-08	Hugera	574055	1399330	1575	368	562	7.6	0.2	34.0	0.9	76.4	16.8	0.0	0.6	11.3	5.6	384.3	10.3	0.2	Ca-Na-Mg-HCO3
RPW-025-08	Mohoni	574144	1368595	1397	460	705	8.3	0.4	86.0	2.6	49.4	29.0	0.0	0.3	15.2	2.1	365.5	74.5	0.2	Na-Ca-Mg-HCO3
RPW-026-08	Tseada meda	570329	1389923	1575	356	548	7.5	0.7	49.0	1.0	63.8	12.9	0.0	0.6	12.9	21.7	338.2	0.8	0.1	Ca-Na-HCO3
RPW-028-08	Kushere	574055	1399330	1575	328	499	7.7	0.2	63.0	2.5	40.3	15.3	0.0	0.5	14.4	6.7	333.1	6.7	0.5	Na-Ca-Mg-HCO3
RPW-030-08	Bale,Mohoni	578718	1398109	1515	354	539	7.3	0.4	44.0	1.0	62.2	18.4	0.0	0.3	15.5	0.2	335.6	10.0	0.1	Ca-Na-Mg-HCO3
RPW-032-08	Delbo, Mohoni	573856	1396696	1542	352	539	7.2	0.2	39.0	1.4	68.0	17.9	0.0	0.9	11.3	2.0	351.0	0.3	0.4	Ca-Na-Mg-HCO3
RPW-033-08	Delbo, Mohoni	576189	1395698	1527	332	509	7.4	0.1	40.0	1.0	74.8	11.2	0.0	0.8	11.3	6.0	320.2	5.3	0.2	Ca-Na-HCO3
RPW-034-08	Delbo, Mohoni	575022	1395075	1528	334	512	7.1	0.2	43.0	1.8	60.5	12.2	0.0	0.9	13.4	3.1	297.2	2.9	0.3	Ca-Na-HCO3
RPW-035-08	Gerjele, Alamata	576332	1394432	1514	352	532	7.8	0.2	22.0	1.0	84.8	20.9	0.0	0.6	10.9	20.6	340.7	4.0	0.2	Ca-Mg-HCO3
RPW-036-08	Tseada meda	566991	1377439	1430	396	604	7.3	0.1	55.0	1.2	75.6	11.2	0.0	0.6	21.6	3.2	351.0	7.8	0.1	Ca-Na-HCO3
RPW-037-08	Genda ago	574094	1392035	1517	348	533	7.8	0.1	56.0	1.3	48.7	15.3	0.0	0.5	26.8	14.2	302.3	5.3	0.2	Na-Ca-Mg-HCO3

RPW-038-08	Tseada meda	574690	1390976	1515	330	505	7.5	0.0	63.0	1.2	53.8	10.7	0.0	1.0	21.6	6.2	289.5	11.7	0.3	Na-Ca-HCO3
RPW-039-08	Kalina, Mohoni	571901	1389798	1547	444	676	7.1	0.5	30.0	1.1	87.4	20.7	0.0	0.5	30.7	58.2	345.9	8.4	0.1	Ca-Mg-HCO3-NO3
RPW-040-08	Kalina, Mohoni	569910	1391794	1599	366	558	7.6	0.2	41.0	0.7	60.8	20.2	0.0	0.4	10.9	31.4	345.9	0.2	0.5	Ca-Na-Mg-HCO3
RPW-041-08	Beru, Mohoni	567155	1391738	1659	412	629	7.2	0.2	41.0	0.7	87.4	14.7	0.0	0.7	15.4	37.7	384.3	0.4	0.4	Ca-Na-HCO3
RPW-042-08	Mohoni	572853	1372716	1402	406	615	8.0	0.1	79.0	3.3	34.2	18.9	0.0	0.7	22.8	2.0	301.3	63.7	0.2	Na-Ca-Mg-HCO3
RPW-043-08	Tao	574039	1389891	1509	312	492	7.8	0.2	48.0	1.4	52.1	14.8	0.0	0.9	16.5	7.4	286.9	4.7	0.5	Ca-Na-Mg-HCO3
RPW-046-08	Tao	572436	1382113	1435	440	676	7.4	0.2	42.1	2.1	69.7	21.4	0.0	0.9	45.3	27.6	322.8	24.1	0.4	Ca-Na-Mg-HCO3
RPW-048-08	Alamata	572052	1380755	1426	338	505	7.7	0.1	53.0	1.2	55.1	14.8	0.0	0.8	31.0	22.4	248.5	28.3	0.1	Ca-Na-HCO3
RPW-049-08	Gerjal	570343	1380681	1430	269.6	378	6.8	0.6	43.3	3.2	51.2	5.7	2.4	3.8	0.0	9.7	231.7	48.3	17.1	Ca-Na-HCO3
RPW-051-08	Gerjele	571429	1379689	1422	396	600	7.5	0.3	22.0	1.0	92.2	27.7	0.0	0.5	23.8	39.0	340.7	15.3	0.2	Ca-Mg-HCO3
RPW-052-08	Gerjele	568031	1379400	1439	279.79	425	6.6	-0.1	68.5	2.6	48.8	2.1	1.0	0.5	0.0	17.0	270.0	2.0	7.4	Na-Ca-HCO3
RPW-053-08	Gerjele	570263	1378912	1421	355.8	499	6.7	0.0	42.5	3.3	89.9	12.3	2.6	3.8	0.0	170.5	292.7	67.2	16.2	Ca-NO3-HCO3
RPW-054-08	Gerjele	568862	1377910	1433	396	573	7.9	0.3	21.0	1.0	94.3	28.4	0.1	0.6	15.9	38.4	363.8	12.3	0.2	Ca-Mg-HCO3
RPW-055-08	Kersele	567333	1378232	1450	320	446	7.8	0.1	68.0	1.7	42.4	6.5	0.0	0.4	20.8	34.3	215.2	36.8	0.2	Na-Ca-HCO3
RPW-056-08	Gerjele	571864	1378166	1422	280	430	7.8	0.1	32.0	1.1	58.3	14.8	0.0	0.4	7.9	8.3	281.8	1.5	0.1	Ca-Na-Mg-HCO3
RPW-058-08	Gerjele	569431	1376222	1417	454.25	637	6.6	0.3	49.8	4.5	69.3	24.4	2.9	0.9	0.0	22.1	359.8	6.6	15.1	Ca-Na-Mg-HCO3
RPW-059-08	Gerjele	571642	1376249	1411	396	575	7.9	0.2	26.0	1.0	92.2	24.5	0.0	1.0	15.9	32.7	353.6	14.2	0.3	Ca-Mg-HCO3
RPW-060-08	Alamata	565861	1379159	1469	320	487	7.2	0.1	30.0	1.2	63.0	17.3	0.0	0.4	12.4	2.6	286.9	11.4	0.3	Ca-Mg-Na-HCO3
RPW-061-08	Alamata	566917	1374980	1425	272	415	7.7	0.2	33.0	1.4	46.6	18.1	0.0	0.8	6.0	1.3	279.2	0.3	0.1	Ca-Mg-Na-HCO3
RPW-063-08	Mohoni	567200	1375899	1439	444	674	7.1	0.1	81.0	3.1	52.1	20.4	0.0	0.3	19.6	0.3	338.2	83.6	0.3	Na-Ca-Mg-HCO3-SO4
RPW-064-08	Alamata	571462	1374198	1399	434	664	6.8	0.3	20.0	0.9	85.7	31.6	0.0	0.6	30.9	3.7	379.2	13.0	0.2	Ca-Mg-HCO3
RPW-065-08	Alamata	565658	1373049	1457	588	888	7.7	0.5	27.0	1.0	121.6	29.9	0.0	0.1	51.3	53.9	426.5	52.1	0.2	Ca-Mg-HCO3
RPW-066-08	Alamata	564467	1373141	1476	514	789	7.2	0.3	34.0	1.1	83.2	43.9	0.2	0.7	31.9	12.1	435.5	24.0	0.1	Ca-Mg-HCO3
RPW-067-08	Mohoni	566444	1372391	1444	422	645	7.5	0.1	85.0	3.6	47.0	12.2	0.1	0.2	18.5	0.3	307.4	99.9	0.3	Na-Ca-HCO3-SO4
RPW-068-08	Mohoni	571726	1373354	1400	410	617	7.3	0.2	81.0	2.7	40.3	25.0	0.0	0.4	21.0	0.4	345.9	46.1	0.4	Na-Mg-Ca-HCO3
RPW-069-08	Adi-bore, Alamata	572613	1371922	1407	598	847	7.6	0.4	38.0	1.0	141.0	28.7	0.0	0.7	25.7	112.6	451.4	24.4	0.3	Ca-Mg-HCO3-NO3
RPW-070-08	Mohoni	565204	1371005	1459	486	744	7.1	0.3	74.0	1.9	58.8	31.6	0.0	0.5	18.5	0.3	471.4	53.7	0.3	Na-Ca-Mg-HCO3
RPW-071-08	Alamata	570481	1371229	1408	604	938	7.6	0.5	32.5	1.1	121.6	29.9	0.0	0.7	32.3	38.6	473.4	50.4	0.7	Ca-Mg-HCO3
RPW-072-08	Mohoni	565705	1372178	1453	422	640	7.4	0.2	74.0	3.1	42.0	21.5	0.0	1.3	20.6	0.2	379.2	49.1	0.3	Na-Ca-Mg-HCO3

RPW-074-08	Alamata	564898	1367281	1474	524	800	7.7	0.3	50.0	2.7	95.0	23.0	0.1	0.7	56.1	40.6	370.9	33.9	0.1	Ca-Na-Mg-HCO3
RPW-075-08	Alamata	572671	1370616	1400	422	648	7.7	0.3	58.0	2.0	58.8	30.6	0.0	0.9	16.5	9.4	397.1	5.9	0.2	Ca-Na-Mg-HCO3
RPW-076-08	Alamata	561215	1368924	1530	412	627	7.3	0.8	47.0	1.9	50.4	31.6	0.1	0.5	29.9	4.7	335.6	23.5	0.3	Mg-Ca-Na-HCO3
RPW-077-08	Alamata	567162	1369865	1438	710	1084	6.9	0.9	38.0	1.7	103.3	70.1	0.0	0.6	44.3	29.8	525.2	70.7	0.2	Mg-Ca-HCO3
RPW-078-08	Limat	565483	1368490	1465	528	809	7.1	0.2	87.0	2.4	58.8	35.7	0.1	0.9	18.5	2.3	476.5	69.3	0.3	Na-Mg-Ca-HCO3
RPW-079-08	Limat	569076	1366877	1424	497	755	6.7	0.0	48.0	35.0	32.0	30.0	0.0	0.8	27.6	30.0	274.4	37.0	2.2	Mg-Na-Ca-HCO3
RPW-081-08	Limat	566566	1367059	1450	460	703	7.4	0.2	86.0	1.7	49.6	27.0	0.0	0.6	31.9	10.3	374.1	26.9	0.2	Na-Ca-Mg-HCO3
RPW-082-08	Addis kighn	574045	1365777	1388	352	538	7.5	0.2	32.0	4.3	57.1	24.5	0.0	0.7	11.3	11.2	312.6	5.7	0.2	Ca-Mg-Na-HCO3
RPW-085-08	Ayer Marefia	564906	1363929	1479	390	598	8.0	0.2	37.0	1.6	91.0	17.7	0.0	0.8	16.2	42.3	348.9	7.5	0.3	Ca-Na-HCO3
RPW-086-08	Alamata	563445	1362750	1503	652	999	7.3	0.6	77.0	1.5	82.3	45.9	0.0	0.5	100.9	40.7	420.0	70.9	0.3	Ca-Mg-Na-HCO3-Cl
RPW-087-08	Alamata	567591	1361714	1438	604	925	7.5	0.5	81.0	2.7	77.3	41.8	0.0	0.9	43.3	3.2	479.1	64.6	0.1	Ca-Na-Mg-HCO3
RPW-088-08	Timuga	567019	1360930	1443	1134	1740	7.4	0.6	164.0	3.0	151.2	90.8	0.0	0.6	151.0	43.1	589.3	281.8	0.4	Ca-Mg-Na-HCO3-SO4
RPW-090-08	Alamata	563934	1356825	1473	420	640	7.7	0.5	37.0	1.3	55.4	40.3	0.0	0.6	16.5	13.8	399.7	0.5	0.3	Mg-Ca-Na-HCO3
RPW-093-08	Babo-korma	567588	1359766	1427	430	657	7.6	0.3	80.0	3.2	47.0	25.2	0.1	0.8	16.5	2.5	420.2	11.2	0.2	Na-Ca-Mg-HCO3
RPW-095-08	Timuga	565153	1359042	1459	416	636	7.3	0.3	28.0	0.8	77.3	29.1	0.0	0.6	22.7	13.2	343.3	18.2	0.5	Ca-Mg-HCO3
RPW-096-08	Babo-korma	566902	1358605	1447	512	783	7.1	0.5	57.0	2.2	53.8	53.6	0.0	0.9	19.6	7.2	507.3	6.9	0.4	Mg-Ca-Na-HCO3
RPW-097-08	Alamata	564016	1357876	1478	318	484	7.4	0.2	31.0	7.2	48.7	19.4	0.0	1.1	8.2	6.9	302.3	1.3	0.4	Ca-Mg-Na-HCO3
RPW-098-08	Babo-korma	562933	1357904	1492	420	646	7.4	0.3	46.0	1.0	67.2	31.6	0.0	0.7	21.6	6.6	381.7	13.0	0.3	Ca-Mg-Na-HCO3
RPW-099-08	Alamata	566904	1357791	1450	514	791	7.7	0.8	36.0	1.9	60.5	57.6	0.0	0.2	16.5	30.7	538.0	0.3	0.3	Mg-Ca-HCO3
RPW-100-08	Alamata	565838	1357528	1457	504	776	7.7	0.5	41.0	1.5	58.8	54.6	0.0	0.3	13.9	34.1	507.3	5.5	0.4	Mg-Ca-HCO3

B) Rio Mannu di Pabillonis Basin

B-1: Annual precipitation in mm at different stations

Year	Gonnosfanadiga	Montevecchio	Pabbilonis	Sangavino	Sardara	Uras
1922	583	502.7	460.9	297.8	319	**576.5**
1923	1215	903.7	714.5	878.9	661	**804.6**
1924	651.5	600.5	862.5	436.8	479	**597**
1925	559.5	562.1	530.7	445.5	595.5	**910**
1926	640	573.7	530.5	358	572	**577**
1927	810	693.3	542.9	456.5	667	**455**
1928	1030	854.3	686.1	538.8	845	**702.1**
1929	683	707.3	678	472.8	655	**634**
1930	883	920.8	900.5	714.1	675.3	**604**
1931	572.6	572.7	518	529.8	451	**529**
1932	606.5	553.8	519.6	437.6	370.5	**461.1**
1933	938.5	1007	807.8	660.8	607.6	**769.5**
1934	788	706.6	528.3	642.1	747.8	**659.5**
1935	988.5	762.7	742.8	599.7	652.1	**733**
1936	1018.6	722.3	770.7	470.4	641.7	**499.6**
1937	871.7	770	723.7	470.2	678.4	**594**
1938	757.1	686.3	530.3	522.5	478.7	**469.4**
1939	970.1	819.9	661.9	528.6	638.2	**429.3**
1940	876.3	700.9	591.6	669.8	635.3	**340.3**
1941	1025.7	744.6	697.6	690.5	550.2	**491.9**
1942	1008.5	991.3	664.9	874.7	706.8	**550.4**
1943	697.3	757.9	466.9	468.6	585.4	**605.1**
1944	597.1	608.3	377.2	422.8	455	**418**
1945	505.7	508.8	396.5	334.4	391.2	**364.6**
1946	569	668.2	587.7	576.5	651	**528.9**
1947	534.6	596.4	485	512	751	**445.1**
1948	846.4	616.9	445.5	397	647.2	**426.8**
1949	707.2	605	486.1	421.6	541.5	**567.7**
1950	891.2	616.3	558	576	627.5	**671.2**
1951	1007.8	844.3	529.6	552	564.5	**609.6**
1952	683.7	651.9	477.6	347	478	**502.3**
1953	671.4	730.4	510.5	570.3	586.3	**439.1**
1954	447.3	478.2	372.9	416.9	350.1	**304**
1955	624	631.9	479.1	491.4	480.1	**498.8**
1956	643.5	606.2	404.1	553.8	431.7	**549.4**
1957	921.5	584.3	580.2	609.8	396	**606.2**
1958	749.5	549.3	436.2	445	397.1	**472.8**
1959	976.7	743.8	456.7	561.2	444.4	**554.9**
1960	1065.5	885.5	644.6	641.5	483.8	**759.3**
1961	804.6	619.1	504.4	463.6	420.5	**484.8**
1962	734	774.2	487.2	459.8	519.9	**522.5**
1963	1127.2	815.8	737.9	930.8	689.6	**758.6**
1964	852.7	653.2	557.3	581.6	682.2	**511.8**

1965	587.7	658.2	564.8	569.5	637.1	**507.6**
1966	989.8	847.7	604.3	471.6	760.4	**576.4**
1967	589.7	542.3	380.7	276.3	364.5	**458**
1968	924.8	724	629.7	508.4	691.8	**607.8**
1969	851.3	794.3	749.5	723.7	989.1	**724.5**
1970	602.3	546.4	379.6	376.6	540.7	**415.5**
1971	1018.8	839.6	540.8	643.1	693.8	**656.8**
1972	893.2	797.6	589.6	575.7	663.2	**590**
1973	500.7	582.9	450.1	405.9	390.9	**353.6**
1974	792.9	935.1	659	635.4	756.7	**732.3**
1975	763.4	840.3	690	506.5	652.2	**887.4**
1976	839.9	1109.9	738.5	608.3	784.3	**800.7**
1977	717.9	587.9	514	445.6	548	**543.3**
1978	964.6	1024.3	839.2	748.1	834.5	**830.9**
1979	790.1	920.6	740	592.7	699.3	**785.8**
1980	867.8	860.9	627.4	481	674.3	**631.4**
1981	618.5	644	448	366	476.4	**471.8**
1982	808	765.2	419	445	565	**419**
1983	714	653.8	405	449.4	472.8	**307**
1984	867.8	829	651	688.2	680	**574.4**
1985	669.4	694.2	475.2	520	577	**645.8**
1986	873	923.6	638.6	576	668.8	**777.4**
1987	619.6	711.4	498.4	416.4	456.4	**339.4**
1988	534.8	513.2	283.8	393.4	476	**436.4**
1989	502.4	536.8	380.6	390	400	**373.2**
1990	647.4	741	551.4	517	701.4	**589.4**
1991	703	726.6	575.4	586	720.6	**667.2**
1992	676.6	696.8	565.7	488.4	545.8	**563.6**
1993	629.8	531.6	469.2	424.8	416	
1994	455.6	446.2	453.4	321	460.8	
1995	388.4	376.4	251.4	265.4	279.8	
1996	1236.2	1154	772.4	664	951.8	
1997	796.8	674.8	455.8	490.8		
1998	580.4	702.8	210.8	373.8	380	
1999	622.6	700.4	550.2	546.2	542.2	
2000	666.8	794.3	529.4	423.2	477.4	
2001	400.6	528.6	316.2	323.2	338.8	
2002	668.4	798.4	466.2	496	525.2	
2003	738	894	602.7	641.8	666.6	
2004	841.6	1065.2	764.2	711.4	738.6	
2005	687	898.4	427.9	475.6	573.2	
2006	689	762.6	357.9	432	628.4	
2007	526.4	736	106.2	429.3	485.6	

B-2: Average monthly temperature in ^{0}C

Average Monthly Temperature												
Stations	Oct.	Nov.	Dec.	Jan	Feb	Mar	Apr	May	Jun	Jul	Aug.	Sep
Gonnofanadiga	19.2	14.2	10.8	9.8	10.3	12.3	14.2	19.0	22.8	26.2	26.7	22.9
Pabbilonis	19.1	14.3	10.8	9.4	10.0	12.2	14.1	18.8	22.3	25.3	26.6	22.5
Sangavino	18.5	13.8	10.5	9.5	10.2	12.2	13.8	18.3	21.2	24.8	26.0	21.9
Sardara	18.8	14.1	10.9	10.5	10.5	12.2	14.0	18.6	21.8	25.1	26.3	22.6
Uras	19.0	14.1	10.6	10.2	10.5	12.6	14.0	18.5	21.8	24.6	25.9	22.4

B-3: Summer potential evapotranspiration used in WetSpass model

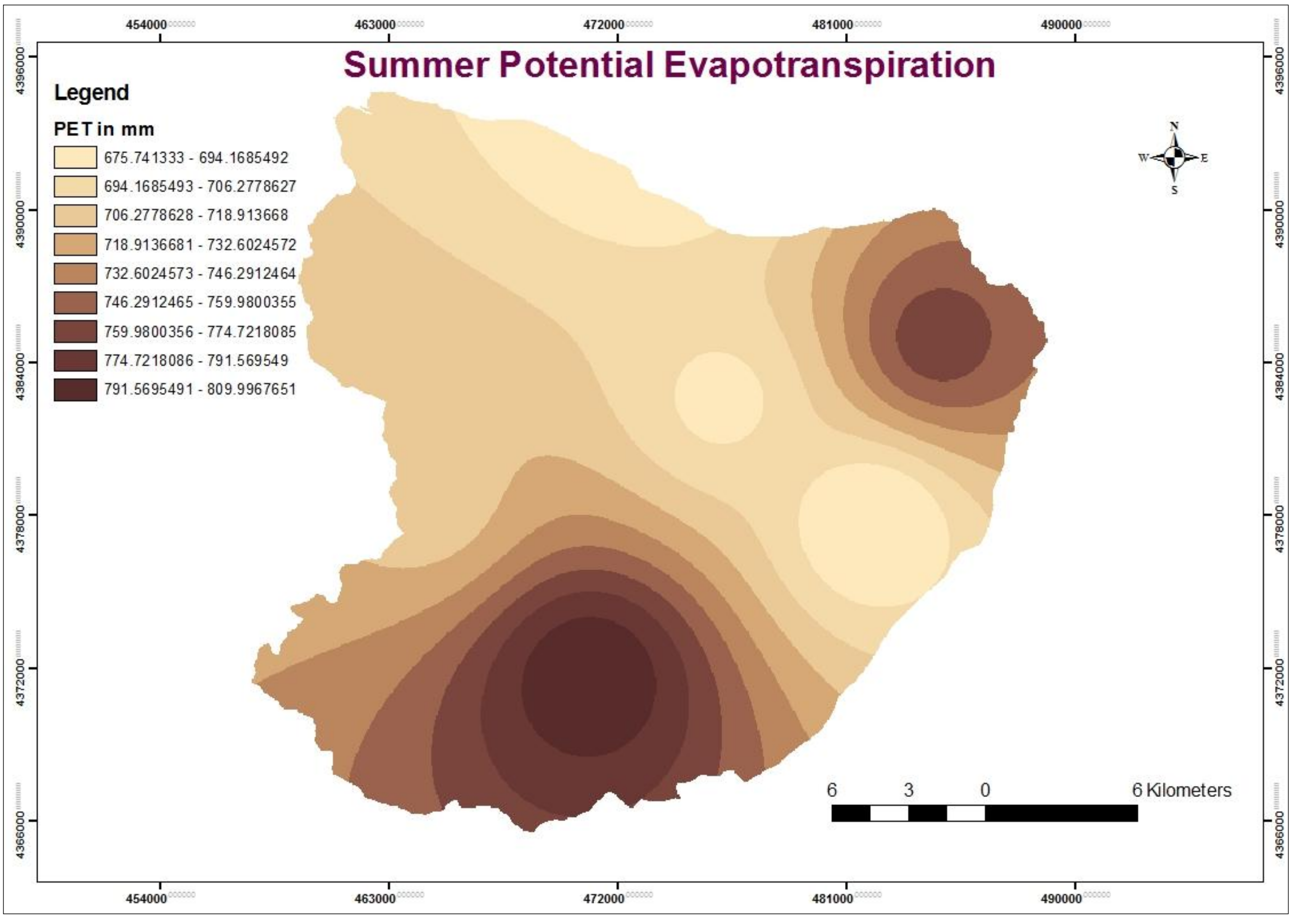

B-4: Winter potential evapotranspiration used in WetSpass model

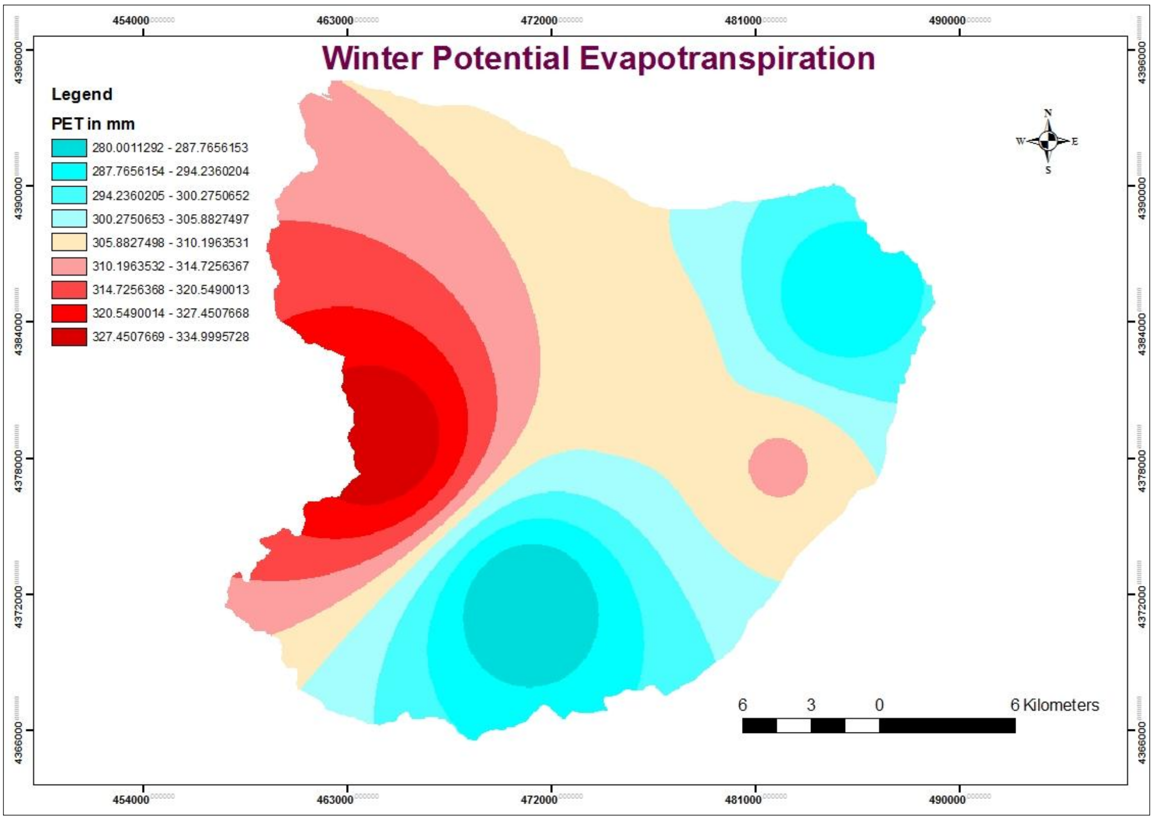

B-4: Summer temperature used in WetSpass model

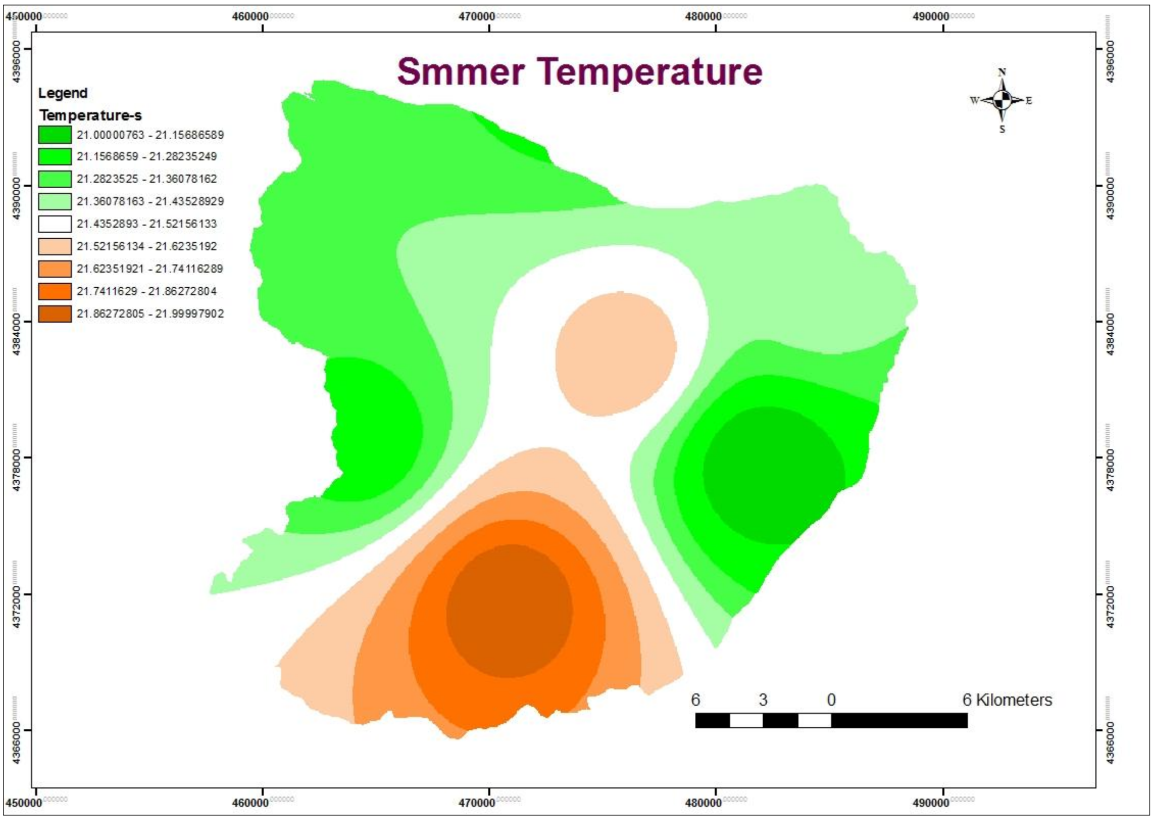

B-4: Winter temperature used in WetSpass model